

Stormwater Infiltration in Highway Embankments – Saturated Hydraulic Conductivity Estimation for Uncompacted and Compacted Soils

WA-RD 872.1

Tony M. Allen

October 2017



**Washington State
Department of Transportation**

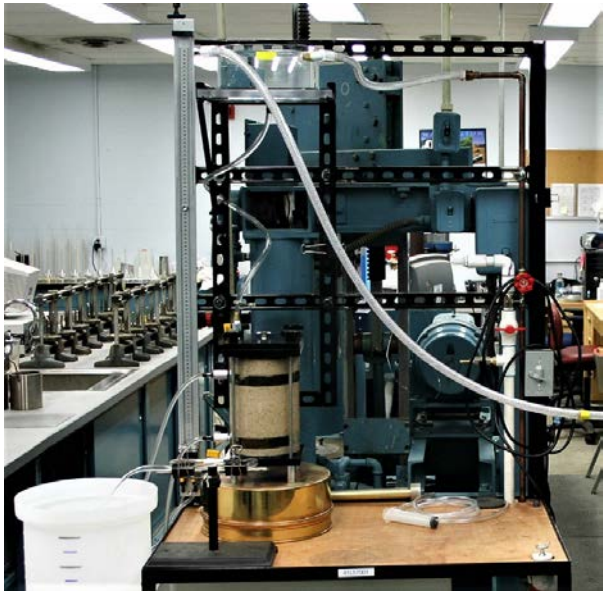
Office of Research & Library Services

WSDOT Research Report

Research Report

WA-RD 872.1

**STORMWATER INFILTRATION IN HIGHWAY
EMBANKMENTS – SATURATED HYDRAULIC
CONDUCTIVITY ESTIMATION FOR UNCOMPACTED
AND COMPACTED SOILS**



by

Tony M. Allen, P.E.

Washington State Department of Transportation
HQ Geotechnical Office
Olympia, Washington

Prepared for

The State of Washington
Department of Transportation
Roger Millar, Secretary

And in cooperation with
U.S. Department of Transportation
Federal Highway Administration

October 2017

1. REPORT NO. WA-RD 872.1	2. GOVERNMENT ACCESSION NO.	3. RECIPIENT'S CATALOG NO.	
4. TITLE AND SUBTITLE STORMWATER INFILTRATION IN HIGHWAY EMBANKMENTS – SATURATED HYDRAULIC CONDUCTIVITY ESTIMATION FOR UNCOMPACTED AND COMPACTED SOILS		5. REPORT DATE October 2017	
		6. PERFORMING ORGANIZATION CODE	
7. AUTHOR(S) Tony M. Allen		8. PERFORMING ORGANIZATION REPORT NO.	
9. PERFORMING ORGANIZATION NAME AND ADDRESS Washington State Department of Transportation State Materials Laboratory 1655 South Second Avenue Tumwater, WA 98512-6951		10. WORK UNIT NO.	
		11. CONTRACT OR GRANT NO.	
12. SPONSORING AGENCY NAME AND ADDRESS Research Office Washington State Department of Transportation Transportation Building, MS 47372 Olympia, Washington 98504-7372 Project Manager: Lu Saechao, 360-705-7260		13. TYPE OF REPORT AND PERIOD COVERED Final Research Report	
		14. SPONSORING AGENCY CODE	
15. SUPPLEMENTARY NOTES This study was conducted in cooperation with the U.S. Department of Transportation, Federal Highway Administration.			
16. ABSTRACT: The estimation of hydraulic conductivity (K_{sat}) is a key step to assess the rate of infiltration, whether that estimate is for an infiltration pond or trench, if it is for a highway embankment, or if it is for natural dispersion in general. The focus of this research is to assess available methods for estimating K_{sat} , especially with regard to the ability of various methods to assess K_{sat} in both a loose, uncompacted state as well as in a compacted state for embankments. K_{sat} prediction for natural soils is also considered. To accomplish this, a series of relatively large diameter (i.e., 6 to 9 inch) saturated hydraulic conductivity tests were conducted both in a loose state and in a compacted state. Existing K_{sat} prediction equations such as those developed by Hazen (1892), Slichter (1898), Terzaghi (1925), Chapuis (2004), and Massmann (2003) were evaluated and, using the K_{sat} laboratory measurements gathered in this study, were empirically optimized to improve prediction performance. Those equations that included soil porosity, η , or void ratio, e , were given preference for further development, since η or e were determined to be the best parameters to address the effects of compaction on K_{sat} . The empirically optimized Slichter, Terzaghi, and Chapuis equations were found to provide the most accurate prediction performance. Since it may be difficult to obtain a measured porosity or void ratio at design time, a method to estimate the soil porosity using grain size parameters plus degree of soil compaction, or for natural soils, degree of over-consolidation, was developed, and could be used in the optimized equations with only minimal reduction in K_{sat} prediction accuracy. The optimized Slichter Equation was used for several example infiltration facilities as was done by Massmann (2003) to determine what effect the use of this new equation would have on infiltration design and infiltration rate prediction accuracy.			
17. KEY WORDS Infiltration, Hydraulic conductivity, embankments		18. DISTRIBUTION STATEMENT No restrictions. This document is available to the public through the National Technical Information Service, Springfield, VA 22616	
19. SECURITY CLASSIF. (of this report) None	20. SECURITY CLASSIF. (of this page) None	21. NO. OF PAGES	22. PRICE

DISCLAIMER

The contents of this report reflect the views of the author, who is responsible for the facts and the accuracy of the data presented herein. The contents do not necessarily reflect the official views or policies of the Washington State Department of Transportation, Federal Highway Administration, or U.S. Department of Transportation. This report does not constitute a standard, specification or regulation.

TABLE OF CONTENTS

EXECUTIVE SUMMARY	12
THE PROBLEM.....	16
BACKGROUND and Review of Previous Work.....	17
Use of Air Conductivity Test Results to Obtain Soil K_{sat} Values	18
Recommended K_{sat} Correlations from Previous WSDOT Infiltration Research	19
Previous Work on the Estimation of K_{sat} and the Effect of Compaction	20
OBJECTIVE AND SCOPE OF THE CURRENT RESEARCH.....	27
RESEARCH APPROACH	28
Materials Tested	29
Test Procedures and Equipment Used	33
Rigid Wall Permeameter Testing:	34
Flexible Wall Permeameter Testing	37
TEST RESULTS.....	42
K_{sat} PREDICTION ANALYSIS.....	47
Effect of Grain Size Parameters on K_{sat}	47
Assessment of Outliers and Data Set Differences	49
Analysis of K_{sat} Prediction Equation in the WSDOT Highway Runoff Manual.....	52
Analysis Using Other Historical K_{sat} Predictive Equations	55
Improvements to Existing Predictive Equations	59
Estimating Porosity Based on Grain Size Parameters and Compaction Level.....	68
Using Estimated η and e with Optimized K_{sat} Prediction Methods	77
STATISTICAL ANALYSIS AND METHOD PERFORMANCE	79
APPLICATION TO INFILTRATION DESIGN.....	90
CONCLUDING REMARKS AND RECOMMENDATIONS	98
ACKNOWLEDGMENTS	101
REFERENCES	102
Appendix A Laboratory Summaries of Soils Used for 2008 Testing.....	A.1
Appendix B Laboratory Summaries and Close-Up Photos of Soils Used for 2013 Testing.....	B.1
Appendix C Laboratory Summaries of Soils Used for 2014 Testing	C.1

Appendix D Compaction Test Laboratory Summaries for Soils Used for 2013 Testing.....	D.1
Appendix E Compaction Test Laboratory Summaries for Soils Used for 2014 Testing.....	E.1
Appendix F Grain Size Parameters of Soils Tested.....	F.1
Appendix G Additional Analyses for the Data and Equation by Massman (2003).....	G.1
Appendix H Assessment of the Cozeny-Carmen Equation.....	H.1

FIGURES

Figure 1. Measured K_{sat} values as a function of $d_{10}^2e^3/(1+e)$ (after Chapuis 2004).....	25
Figure 2. K_{sat} predictive accuracy of various methods (after Chapuis 2004).....	25
Figure 3. Effects of void ratio and clay content on hydraulic conductivity of compacted tills (from Leroueil et al., 2002).....	26
Figure 4. Close-up of soil as placed in the rigid wall test cell for soil used in the 2008 testing.....	30
Figure 5. Close-up of test soil grains used for 2013-2014 testing – 0.75 inch (19 mm) size.	32
Figure 6. Close-up of test soil grains used for 2013-2014 testing – 0.017 inch (0.425 mm) size.....	32
Figure 7. Close-up of test soil grains used for 2013-2014 testing – 0.003 inch (0.075 mm) size.....	33
Figure 8. Test equipment setup for rigid wall permeameter testing.	36
Figure 9. Close-up of rigid wall permeameter.	37
Figure 10. Flexible wall permeameter testing system.	38
Figure 11. Software input screen for flexible wall permeameter.....	39
Figure 12. Specimen mold with rammer and test soil.	39
Figure 13. Test specimen being compacted with rammer.	40
Figure 14. Measured hydraulic conductivity values as a function of the soil d_{10} size for uncompact and compacted specimens (outliers included).....	48
Figure 15. Measured hydraulic conductivity values as a function of the soil C_u for uncompact and compacted specimens (outliers included).....	48
Figure 16. Grain size characteristics of the K_{sat} data sets evaluated (outliers included).	52
Figure 17. Measured versus predicted K_{sat} using Eq. 1 developed by Massmann (2003): (a) All data, (b) only data in which K_{sat} (predicted and measured) is between 0.0001 and 10 cm/second.	54
Figure 18. K_{sat} predictions using the Hazen Equation (with outliers removed).	57
Figure 19. K_{sat} predictions using the Slichter Equation (with outliers removed).....	57
Figure 20. K_{sat} predictions using the Terzaghi Equation (with outliers removed).	58
Figure 21. (a) Measured K_{sat} as a function of the Chapuis grain size – void ratio parameter, (b) K_{sat} predictions using the Chapuis (2004) equation (with outliers removed).	59

Figure 22. K_{sat} predictions using the optimized Slichter Equation, with outliers removed.	62
Figure 23. Method bias as a function of d_{10} size for (a) original Slichter Equation, but for 20° C, with outliers removed, and (b) optimized Slichter Equation at 20° C, with outliers removed (note: linear functions used for regressions).	63
Figure 24. K_{sat} predictions using the optimized Terzaghi Equation, with outliers removed.....	64
Figure 25. Method bias as a function of d_{10} size for (a) original Terzaghi Equation with outliers removed, and (b) optimized Terzaghi Equation with outliers removed (note: linear functions used for regressions).	65
Figure 26. K_{sat} prediction for the optimized Chapuis Equation (i.e., Eq. 11), with outliers removed: (a) measured K_{sat} vs. optimized Chapuis parameter, (b) K_{sat} predictions using the optimized Chapuis Equation, (c) method bias as a function of d_{10} size for original Chapuis Equation, and (d) method bias as a function of d_{10} size for optimized Chapuis Equation (power functions used for regressions in parts a and b, and linear functions used in part d).	67
Figure 27. Porosity prediction bias for Vucovic and Soro (1992) method as a function of: (a) d_{10} size, and (b) coefficient of uniformity, C_u (outliers removed).	69
Figure 28. Effect of compaction on porosity as a function of: (a) the d_{10} size, and (b) the coefficient of uniformity, C_u (outliers removed).	70
Figure 29. Porosity prediction bias as a function of the d_{10} size when: (a) the soil d_{10} size is not considered, and (b) the soil d_{10} size is considered.	74
Figure 30. (a) Predicted versus measured porosity considering compaction effects (i.e., using equations 13 and 14), and (b) porosity prediction bias (i.e., measured/predicted value) as a function of the soil d_{10} size (outliers removed for both plots).	75
Figure 31. Porosity prediction bias versus the soil coefficient of uniformity, C_u (outliers removed).	76
Figure 32. Optimized Slichter Equation, but using Eq's. 13 and 14 to estimate porosity (outliers removed).	77
Figure 33. Optimized Terzaghi Equation, but using Eq's. 13 and 14 to estimate porosity (outliers removed).	78
Figure 34. Optimized Chapuis Equation, but using Eq's. 13, 14, and 16 to estimate porosity and void ratio (outliers removed).	78
Figure 35. Porosity prediction bias as a function of porosity prediction value.	83
Figure 36. Bias distributions for the original and optimized equations with lognormal data fit and adjusted lognormal data fit to improve match the lower distribution tail	

(outliers removed): (a) Slichter Method, (b) Terzaghi Method, and (c) Chapuis Method.	86
Figure 37. Bias distributions for datasets analyzed using the optimized K_{sat} equations with adjusted lognormal data fit to match the lower distribution tail (outliers removed): (a) Slichter Method, (b) Terzaghi Method, and (c) Chapuis Method.	87
Figure 38. Ratio of optimized Slichter Equation (Eq. 9) to Massmann Equation (Eq. 1) K_{sat} predictions as a function of d_{10} size.	91
Figure 39. Comparison of full scale pond infiltration rates to infiltration rates from grain size analysis, assuming hydraulic gradient of 1.0, and from double-ring infiltrometer measurements just below pond bottoms for case histories in Western Washington.	93
Figure 40. Comparison of estimated and measured full scale pond infiltration rates using the Massmann (2003) equation (Eq. 1) and the optimized Slichter Equation (Eq. 9) to estimate K_{sat}	97
Figure B.1. Close-up of 1.0 in. (25 mm) soil particles used in 2013 and 2014 K_{sat} testing.	B.4
Figure B.2. Close-up of 0.75 in. (19 mm) soil particles used in 2013 and 2014 K_{sat} testing.	B.5
Figure B.3. Close-up of 0.0167 in. (0.425 mm) soil particles used in 2013 and 2014 K_{sat} testing.	B.6
Figure B.4. Close-up of 0.0098 in. (0.25 mm) soil particles used in 2013 and 2014 K_{sat} testing.	B.7
Figure B.5. Close-up of 0.0071 in. (0.18 mm) soil particles used in 2013 and 2014 K_{sat} testing.	B.8
Figure B.6. Close-up of 0.0059 in. (0.15 mm) soil particles used in 2013 and 2014 K_{sat} testing.	B.9
Figure B.7. Close-up of 0.003 in. (0.075 mm) soil particles used in 2013 and 2014 K_{sat} testing.	B.10
Figure B.8. Close-up of 0.003 in. (0.075 mm) minus soil particles used in 2013 and 2014 K_{sat} testing.	B.11
Figure D.1. Compaction test for 2013 WSDOT manufactured soil with 26% Gravel, 64%, Sand, and 10% fines.	D.1
Figure D.2. Compaction test for 2013 WSDOT manufactured soil with 23% Gravel, 57%, Sand, and 20% fines.	D.2
Figure D.3. Compaction test for 2013 WSDOT manufactured soil with 19% Gravel, 51%, Sand, and 30% fines.	D.3

Figure E.1. Compaction test for 2014 WSDOT manufactured soil – extreme fine end with target d_{10} of 0.02 mm.....	E.1
Figure E.2. Compaction test for 2014 WSDOT manufactured soil –fine end sand with target d_{10} of 0.26 mm.....	E.2
Figure G.2. K_{sat} prediction bias for equation by Massman (2003) – all data except data from Chapuis (2004).....	G.2
Figure G.3. CDF of K_{sat} prediction bias for equation by Massman (2003) – all WSDOT specimen data.....	G.3
Figure G.4. CDF of K_{sat} prediction bias for equation by Massman (2003) – all WSDOT specimen data with $d_{10} < 1.0$ mm.	G.4
Figure G.5. CDF of K_{sat} prediction bias for equation by Massman (2003) – all uncompacted WSDOT specimen data with $d_{10} < 1.0$ mm.....	G.4
Figure G.6. CDF of K_{sat} prediction bias for equation by Massman (2003) – all compacted WSDOT specimen data with $d_{10} < 1.0$ mm.....	G.5
Figure H.1. K_{sat} predictions using the Cozeny-Carmen Equation, with outliers removed.....	H.2
Figure H.2. Method bias as a function of d_{10} size for the Cozeny-Carmen Equation with outliers removed.....	H.3
Figure H.3. Bias distributions for datasets analyzed using the Cozeny-Carmen equation with lognormal fit to data and adjusted lognormal data fit to match the lower distribution tail (outliers removed).....	H.3

TABLES

Table 1. Soil gradation Standard Specifications (WSDOT 2008) for soils tested.....	30
Table 2. Summary of compaction test results, and their comparison to measured specimen unit weights, conducted for representative soil gradations.....	44
Table 3. Comparison of uncompacted and compacted specimen properties for tests conducted in this study.....	45
Table 4. Comparison of uncompacted and compacted specimen measured K_{sat} values.	46
Table 5. Bias statistics for all historical methods investigated (outliers removed).	80
Table 6. Bias statistics for all optimized methods investigated, using measured porosity or void ratio (outliers removed).	80
Table 7. Summary of bias statistics (without consideration of data distribution) for prediction of soil porosity.	80

Table 8. Bias statistics comparing the use of measured versus estimated porosity values as input for the optimized (a) Slichter, (b) Terzaghi, and (c) Chapuis methods..... 81

Table 9. Bias statistics for all original K_{sat} prediction methods, using measured porosity or void ratio, comparing standard lognormal fit to lognormal fit adjusted to match lower distribution tail..... 88

Table 10. Bias statistics for all optimized K_{sat} prediction methods, using measured porosity or void ratio, comparing standard lognormal fit to lognormal fit adjusted to match lower distribution tail. 88

Table 11. Measured K_{sat} values for typical WSDOT fill materials. 97

Table F.1. Measured index properties for soils tested in current study, sorted by degree of compaction and then by the d_{10} size..... F.1

EXECUTIVE SUMMARY

The estimation of saturated hydraulic conductivity (K_{sat}) is a key step to assess the rate of infiltration, whether that estimate is for an infiltration pond or trench, a highway embankment, or for natural dispersion in general. The focus of this research is to assess available methods for estimating K_{sat} , especially with regard to the ability of various methods to assess K_{sat} in both a loose, uncompacted state as well as in a compacted state for embankments. K_{sat} prediction for natural soils is also considered. The existing K_{sat} prediction equation in the WSDOT Highway Runoff Manual (WSDOT 2016a) and WSDOE Stormwater Management Manual for Western Washington (WSDOE 2014), as well as other historical K_{sat} prediction equations, were evaluated, especially with regard to their ability to account for the effects of compaction. To accomplish this, a series of relatively large diameter (i.e., 6 to 9 inch diameter) saturated hydraulic conductivity tests were conducted both in a loose state and in a compacted state. A range of soil types were tested which include typical embankment soils as well as synthetically created soils reconstituted from natural soils. Rigid wall constant head permeability tests and flexible wall permeability tests were conducted as appropriate depending on gradation of the soil being tested. A total of 73 tests were conducted to assess the effect of compaction. In addition, 137 saturated hydraulic conductivity tests were obtained from the literature as summarized by Chapuis (2004) to use as a basis for comparison to the tests from the current study to ensure that the current test results are reasonably consistent with similar test results obtained by others.

For all of the data sets considered, including the ones developed specifically for this study, the measured K_{sat} appeared to be moderately to strongly correlated to the soil d_{10} size and moderately correlated to the soil uniformity coefficient, C_u . Considering that most K_{sat} prediction equations developed to date include d_{10} as an equation parameter, the strong correlation to d_{10} was expected. C_u has not been used much in K_{sat} prediction formulations, though logically, it should be expected that the soil uniformity would affect the soil K_{sat} .

Existing K_{sat} prediction equations evaluated include Eq. 1 (Massmann 2003, WSDOE 2014, and WSDOT 2016a), Eq. 2 (Hazen 1892), Eq. 3 (Slichter 1898), Eq. 4

(Terzaghi 1925), Eq. 5 Cozeny-Carmen (as reported in Chapuis 2012), and Eq. 6 (Chapuis 2004). Of these, only the Slichter, Terzaghi, Cozeny-Carmen, and Chapuis equations are directly capable of addressing the effects of compaction or over-consolidation through the porosity or void ratio. All of these equations have, for the most part, been empirically developed, and their accuracy is dependent on the empirical data used to develop them.

The soils used in the current study are characterized as consisting of subangular to angular particles that are irregular in shape. An exception to this is that the coarsest particles used were more rounded. Additionally, the soils tested are more well graded than soils used in previous studies. The majority of the soils encountered by WSDOT, especially for embankments, are glacial in origin, which tend to consist of well graded subangular to angular soil particles. Some of these historical K_{sat} equations were more affected by the difference in these soil characteristics than others. Of course the Hazen Equation is only a function of d_{10} , and it was clear that the measured K_{sat} values for the compacted soils were consistently smaller than predicted by that equation, which was developed for loose soils.

All of the historical K_{sat} equations needed some empirical adjustment to more accurately fit the measured K_{sat} measurements. Recalibration of those equations was accomplished through a combination of using regression and optimization tools in Excel (i.e., the SOLVER function) as well as final adjustments conducted without those tools. The difference in the data set soil characteristics for the tests conducted within the current study versus the soils and materials tested by others (e.g., Chapuis 2004) did effect the accuracy of the historical K_{sat} prediction equations. The Terzaghi, Slichter, and Chapuis equations were least affected by this, and it was possible to obtain a reasonably consistent accuracy for all of the data sets considered. After the historical equations were optimized, the optimized Slichter (Eq. 9), Terzaghi (Eq. 10), and Chapuis (Eq. 11) equations provided the most accurate K_{sat} predictions over the widest range and could also account for the effect of compaction on K_{sat} through the porosity (or void ratio).

Regarding the application of these results in infiltration design practice, the estimation of soil porosity can be a hindrance, especially for new compacted embankments, since even the specific soil characteristics of the embankment fill may not

be known during design. However, the fill material specifications are likely known, and the potential material sources that could be used for the fill may be known. Therefore, if the soil gradational property ranges can be determined, then the range in K_{sat} values for the proposed fill could be estimated, if the porosity of the compacted fill can be estimated using soil gradation parameters.

Porosity cannot be estimated with soil gradation properties alone. Using the data gathered in this study, as well as data gathered by others reported in the literature, the effect of soil gradation parameters on how well a given soil can be compacted was assessed. The effect of compaction on porosity, considering the soil gradational parameters, was only developed crudely (i.e., the effect of compaction is either on or off in the current study). Based on the available data, use of a porosity estimated from gradational parameters considering compaction effects in the optimized Slichter, Terzaghi, and Chapuis equations had only a minimal effect on their K_{sat} prediction accuracy.

The full scale infiltration pond examples provided in Massmann (2003) were used to assess the ability of the optimized Slichter Equation (Eq. 9) and the original equation (Eq. 1) by Massmann (2003) to predict full scale field infiltration rates. To estimate infiltration rates, the hydraulic gradient as well as other factors that may the infiltration rate must be determined. Therefore, the estimated K_{sat} values were used in combination with calculated hydraulic gradients for those ponds, and correction factors to account for the pond bottom conditions (i.e., in a well maintained condition, or in a poor condition due to siltation and biofouling), to assess infiltration rate prediction accuracy. From this analysis, it was observed that at the largest soil d_{10} values for the case histories evaluated, the estimated infiltration rates using both the optimized Slichter and historical Massmann (2003) equations to estimate K_{sat} , the predicted and measured infiltration rates are fairly close together. However, at smaller d_{10} values (i.e., high silt content soils), the scatter in the predictions increases, and infiltration estimates using the optimized Slichter Equation for K_{sat} are consistently lower (i.e., more conservative) than when the Massmann (2003) Equation is used to determine K_{sat} . It was also observed that the predicted infiltration rates when using either K_{sat} method are mostly less than the measured rates. In one of the cases when using the optimized Slichter Equation, the prediction was very conservative,

and in a couple of cases when using the Massmann (2003) Equation the prediction was slightly unconservative. Based on these observations, it appears that the siltation/biofouling reduction factor is overly conservative for finer grained soils (i.e., when the soil d_{10} is less than about 0.01 mm).

The report concludes with the recommendation that that current K_{sat} prediction equation in the WSDOT Highway Runoff Manual (WSDOT 2016a) be replaced with the optimized Slichter Equation (Eq. 9) since it is the simplest of the three optimized equations (i.e., Slichter, Terzaghi, and Chapuis). However, any of these three equations should be considered acceptable and equally accurate, and therefore should be acceptable to use for design. If only grain size data is available for estimation of K_{sat} for an embankment soil or for subsurface natural soil strata, the porosity can be estimated using eq's. 13 and 14, which use the soil d_{10} size, C_u , and the degree of compaction or over-consolidation (i.e., either it is compacted or loose, or for natural subsurface soil strata it is either over-consolidated or normally consolidated) as input parameters.

THE PROBLEM

Storm water infiltration facilities are used routinely by the Washington State Department of Transportation (WSDOT), local agencies, and private developers to reduce the hydrologic and environmental impact of storm water runoff from constructed facilities. Typically, the size of facilities designed to infiltrate storm water runoff is determined assuming that all of the runoff is captured by the infiltration facility. However, for the transportation facilities there can be significant infiltration of this runoff in the slopes below the paved roadway surface through natural dispersion processes before it can be collected and transported to storm water runoff infiltration and retention facilities adjacent to the transportation facility.

In many cases, the slope below the transportation facility (e.g., highway) is the surface of a compacted embankment. Previous infiltration research has primarily been focused on infiltration of storm water into natural soils that have not been subjected to compaction (e.g., Massmann 2003, 2008). However, a rather common situation is that the stormwater could infiltrate into embankment soils that have been compacted or into natural soils that have become relatively dense due to natural processes such as the historical, or prehistorical, loading due overburden soils, or even glacial loading.

The rate of infiltration into soils is determined through a two-step process: (1) estimate the hydraulic conductivity of the soils to be infiltrated, and (2) estimate the hydraulic gradient considering the depth to the ground water surface. Since the tools available to estimate the hydraulic conductivity of soils considering the effect of compaction are limited (Massmann 2008), improved tools to accomplish estimation of hydraulic conductivity of compacted soils are needed. To extend the work conducted by Massmann (2003, 2008), the present study focuses on saturated hydraulic conductivity (i.e., K_{sat}) laboratory testing of uncompacted and compacted granular soils typically used as embankment materials, as well as which occur naturally in the soils below the embankments. Development of any modifications needed to estimate the hydraulic gradient within and below embankments (i.e., Step 2) is beyond the scope of this research.

BACKGROUND AND REVIEW OF PREVIOUS WORK

Saturated hydraulic conductivity (K_{sat}) is a key property needed for the assessment of infiltration rates in soils. In previous WSDOT sponsored research on infiltration design, Massmann (2003) developed correlations between K_{sat} and the grain size distribution of the soil using laboratory air conductivity testing, but converted to saturated hydraulic conductivity values. Massmann (2008) later extended that research to coarser grained soils, such as those found in Eastern Washington. Massmann (2003) considered both laboratory hydraulic conductivity test results and back analysis (i.e., hindcasting) of measurements from full scale infiltration facilities to develop and evaluate K_{sat} correlations. Both studies were focused on infiltration rates of natural soils rather than compacted embankment soils.

Furthermore, the correlations developed were based on saturated hydraulic conductivity, not partially saturated hydraulic conductivity values. Massmann (2003) developed and evaluated models considering both saturated and unsaturated flow, and concluded that using a saturated flow model was a reasonable and usually conservative approximation to the more complex unsaturated flow model. With regard to infiltration, infiltration rates tend to be higher in unsaturated conditions because the hydraulic gradient is higher due to greater ground water table depth. The saturated flow infiltration rate gets more conservative relative to the unsaturated flow infiltration rate for the following situations:

- as the depth to the water table gets deeper,
- as the soil permeability values get lower (i.e., for finer grained soils), and
- earlier in the wet season when the soils are drier (Massmann 2003).

In such cases, the saturated flow infiltration rate may be 2 to 3 times lower, or at most less than an order of magnitude lower, than the unsaturated flow infiltration rate. Hence, use of K_{sat} as the key design parameter to characterize the soil is reasonable and conservative, as well as practical with regard to computational effort and site characterization needs. Massmann (2003) should be reviewed for more details on the

analyses conducted and the differences observed for saturated and unsaturated flow conditions.

Use of Air Conductivity Test Results to Obtain Soil K_{sat} Values

The specific procedures used to measure air conductivity values for the range of soils tested in the previous research are described in Massmann (2003). Soils used in the experiments included soils with synthetically created gradations as well as natural soils taken from actual infiltration sites in western Washington. Synthetic soils were created from various sizes of silica sand (No. 16, No. 50, and No. 125), and rock flour to provide the fines. Since these soils were manufactured in a dry state, further drying to make them ready to create the synthetic soils was not necessary. The natural soils taken from various sites were air-dried to make them ready for placement into the air permeameter, as residual moisture in the specimens can contribute to error in the measured air permeability (Massmann 2003).

Massmann (2003) indicates that translation of air conductivity to K_{sat} can become more inaccurate as the soil becomes finer grained, especially when swelling clays are present that can reduce conductivity of the soil upon wetting, causing air conductivity measurements to be too high relative to the saturated hydraulic conductivity values. Since no expansive clays appeared to be present in the natural soil samples, Massman (2003) assumed no correction for this was needed. However, for the finer natural soils tested, a significant percentage of the soil particles were fine enough to be considered clay (Massmann 2003). The nature of the clay present (i.e., from plasticity index test results or other data) was not provided.

Massmann (2003) also summarized work by others (Weeks, 1978; Blackwell et al., 1990; Loll et al., 1999; Iverson, et al., 2001) in which air conductivity values were compared to in-situ hydraulic recharge tests for the same soil or to laboratory scale hydraulic conductivity tests. The studies conducted by Weeks (1978) indicated that the measured air conductivity values converted to saturated hydraulic conductivity were 2 to 3 times higher than the saturated hydraulic conductivity values from the recharge tests, especially for tests conducted at shallower depths. In the tests conducted by Loll, et al. (1999), when comparing air conductivity test results converted to saturated hydraulic

conductivity with hydraulic conductivity test values, the K_{sat} values derived from both test types were generally within ± 0.7 orders of magnitude of one another. Greater scatter in the comparisons was observed when the hydraulic conductivity values were less than 0.001 cm/s. Iverson, et al. (2001) conducted air and hydraulic conductivity tests in “textured” soils and found that the 95% prediction interval was ± 1.7 orders of magnitude (i.e., a factor of 50) for loamy samples and ± 0.4 orders of magnitude (i.e., a factor of 2.5) for the sandy soils.

It must be recognized that K_{sat} values range over many orders of magnitude for the typical soils found in practice. Therefore, the amount of scatter in K_{sat} measurements, both in the laboratory and in-situ, should be expected to be significant. Massmann (2003) indicated that the advantage air conductivity tests is they can be run quickly at relatively low cost, allowing more experiments to be conducted to better capture the variability in the measurements. He concluded that this advantage outweighed the disadvantage of additional error that could occur relative to hydraulic conductivity tests, considering that the hydraulic conductivity tests themselves can also have significant variability.

However, it is also desirable to reduce the potential error in the measured K_{sat} values as much as possible. Therefore, hydraulic conductivity measurements should be given more weight when assessing correlations with grain size parameters. This appears to be especially important as the soil gradation becomes finer since the error incurred by using air conductivity measurements to determine K_{sat} tends to increase significantly.

Recommended K_{sat} Correlations from Previous WSDOT Infiltration Research

The correlation developed from this previous research applies to silty to clean sands (Massmann 2003):

$$\text{Log}_{10}(K_{sat}) = -1.57 + 1.90d_{10} + 0.015d_{60} - 0.013d_{90} - 2.08F_{\text{fines}} \quad (1)$$

where, d_{10} , d_{60} , and d_{90} are the grain sizes for which 10%, 60% and 90% of the sample by weight, respectively, is finer, and F_{fines} is the fraction of soil (by weight) that passes the No. 200 sieve. This equation is units specific, and the grain sizes must be in mm, and

K_{sat} is in cm/sec. This equation is also specified in the Washington State Department of Transportation (WSDOT) Highway Runoff Manual (WSDOT 2016a) and the Washington State Department of Ecology (WSDOE) Stormwater Management Manual for Western Washington (WSDOE 2014). Massmann (2008) also suggested some refinements to Eq. 1 to extend its range of applicability, but those refinements were never adopted by WSDOT.

Previous Work on the Estimation of K_{sat} and the Effect of Compaction

Chapuis (2012) provided an extensive summary on the determination of K_{sat} for soils. It is not the intent of this report to re-summarize what is already summarized quite well in that paper. However, key features of that summary, as well as information found in other publications, are provided to help set the stage for the current study.

The soil d_{10} size (typically in mm) has been used for over 100 years as a key parameter for the prediction of K_{sat} . For example, Hazen (1892) recommended the following empirical relationship for loose, uniform sands:

$$K_{sat} = Cd_{10}^2 \quad (2)$$

in which $C = 1.16$ for loose sand up to 1.5 for very uniform loose sand, K_{sat} is in cm/s and d_{10} , the grain size at which 10% of the material passes by weight, is in mm. In long-term practice, C has ranged from 0.4 to 1.5 , ranging from 0.4 to 0.8 for fine, high fines content, well graded silty sands, 0.8 to 1.2 for medium coarse poorly graded to clean coarse well graded sands, and 1.2 to 1.5 for very coarse, very poorly graded, clean gravelly sand (Bowles 1979). This range is sometimes further simplified to a value of 1.0 for typical field applications. $C = 1.0$ is used for this method in the analyses that follow.

A short-coming of the Hazen equation is that it cannot be directly applied to soils in a dense (i.e., compact, over-consolidated) state, though extending the equation empirically may be possible (Chapuis 2004). A contemporary of Hazen (1892) was Slichter (1898), who included porosity as a key property to assess K_{sat} , in addition to an effective grain size diameter. However, it was derived from a more theoretical standpoint, assuming the soil to be uniform spheres (Terzaghi 1925). The form of

Slichter's equation is similar to Hazen, but with the addition of a porosity term (as simplified and reported in Vukovic and Soro 1992, but corrected for the units provided below):

$$K_{sat} = 10.2 \eta^{3.287} d_{10}^2 \quad (3)$$

where,

η = porosity, and

K_{sat} is in cm/s, and d_{10} is in mm.

The coefficient in Equation 3 reported by Vukovic and Soro (1992) of 5.74 corresponds to the water viscosity at 0° C. To represent the equation at 20° C, the coefficient increases to approximately 10.2 (i.e., increasing the temperature from near 0° C to 20° C decreases the viscosity by a factor of approximately 1.78, increasing K_{sat}). Since this equation is likely the earliest method that incorporates soil porosity, an evaluation of this method can be instructive in understanding the role porosity plays in the prediction of K_{sat} , and the feasibility of using soil porosity to account for the density of the soil.

Terzaghi (1925) also used porosity as a key property to include in a K_{sat} prediction method, enabling the prediction to include the effect of soil density. The Terzaghi equation is as follows:

$$K_{sat} = C_0 \frac{\mu_{10}}{\mu_t} \left(\frac{\eta - 0.13}{\sqrt[3]{1 - \eta}} \right)^2 d_{10}^2 \quad (4)$$

where,

$C_0 = 8$ for smooth grains and 4.6 for grains of irregular shape

μ_{10} = water viscosity at 10° C

μ_t = water viscosity at the soil temperature "t" (usually 20° C)

η = porosity

For laboratory conditions, the ratio μ_{10}/μ_t can usually be taken as 1.30.

To develop this semi-empirical equation, Terzaghi started with theoretical considerations developed by Slichter (1898) and empirical developments by Hazen (Eq. 2) for clean loose sands. The result related the permeability to the square of the effective grain size, defined as the d_{10} size. Furthermore, Terzaghi's formulation assumed that the widest parts of the capillary channels through which the water flows have at least five times the cross-section of the narrowest ones. This means that the loss of head per unit length of the narrowest channels is at least 25 times greater than the loss per unit length of the widest ones. He then treated the percolation of water through the soil (a sand was in view here) like a series of sieves in series, in which the resistance to percolation is confined to the sieves while in the spaces between the sieves the resistance is negligible. This semi-empirical model was then adjusted empirically from experimental data using the C_0 coefficient, within the limits of void ratio of 0.352 to 0.905. However, it was not clear in Terzaghi (1925) how the 0.13 value subtracted from η was derived, but appeared to be the result of both theoretical and empirical considerations.

Taylor (1948), Kozeny (1927), and Carmen (1937, 1939) independently developed K_{sat} prediction methods that included the void ratio instead of porosity, also enabling the prediction of K_{sat} for soils with different degrees of compaction or consolidation. A common scalar in their equations to characterize the effect of void ratio, e , is $e^3/(1+e)$. So if the void ratio can be determined, then the K_{sat} prediction can be extended to soils that are in a compact or dense state. From this work, the Cozeny-Carmen Method as shown in Eq. 5 below was developed, as reported in Chapuis (2012):

$$K_{sat} = C \frac{g}{\mu_w \rho_w} \left(\frac{e^3}{S_s^2 G_s^2 (1+e)} \right) \quad (5)$$

where,

C = a constant that depends on the porous space geometry

g = gravitational constant (m/s^2)

μ_w = dynamic viscosity of water (Pa-s)

ρ_w = density of water (kg/m^3)

G_s = specific gravity of solids

S_s = specific surface of solids (m^2 /mass of solids in kg)

e = void ratio

While the method can be used with a reasonable degree of accuracy for non-plastic soils, e.g., one-third to 3 times the measured K_{sat} value, due to the difficulty of determining S_s , this method is not commonly used (Chapuis 2012).

Chapuis (2004) developed a method using the same void ratio scalar, but simplified the approach using d_{10} rather than S_s . Since this method includes the void ratio, it provides a potentially useful approach to dealing with the compaction effect on K_{sat} , providing a relationship between K_{sat} , d_{10} , and void ratio. His method was based on 100 rigid wall permeameter hydraulic conductivity tests on sands with void ratios that varied from 0.4 to 1.5, with an effective grain size diameter, d_{10} , of 0.13 to 1.98 mm. Based on this work, Chapuis (2004) provided the following equation to estimate K_{sat} :

$$K = 2.4622 \left[d_{10}^2 \frac{e^3}{1+e} \right]^{0.7825} \quad (6)$$

Where “e” is the void ratio, and other variables are as defined previously. Chapuis (2004) concluded that this equation provides a reasonably accurate prediction for K_{sat} values for soils with d_{10} size of 0.003mm to 3 mm, provided the soil is not from crushed rock (due to particle angularity), tills, or clays. The effect of angularity on K_{sat} values has been recognized for many years, in that Terzaghi (1925) reduced the K_{sat} value of soil with angular grains predicted from his equation to 60% of the K_{sat} value for rounded grains. However, Chapuis (2004) found for Eq. 6 that the scatter in the K_{sat} predictions relative to the measured values for crushed (i.e., angular) materials was large and the prediction overall was poor.

Figure 1 illustrates the range of test results considered by Chapuis (2004) in the development of Eq. 6, and Figure 2 shows predicted and measured K_{sat} values for several K_{sat} prediction methods. All test results provided in the figure are from laboratory hydraulic conductivity tests. With regard to Figure 2, the power law equation is Eq. 6 (referred to as Eq. 17 in Figure 2). The extended Hazen equation referred to in Figure 2 (Chapuis 2004) is approximately equal to:

$$K_{sat} \text{ (in cm/s)} = 1.5d_{10}^2e^3(1+e_{max})/[e_{max}^3(1+e)] \quad (7)$$

where,

e = the void ratio

e_{max} = the void ratio for the soil's loosest state

The NAVFAC equation referred to in Figure 2 (as reported and extended in Chapuis 2004) is:

$$K_{sat} \text{ (in cm/s)} = 10^{1.291e-0.6435} [d_{10} \text{ (mm)}]^{10^{0.5504-0.2937e}} \quad (8)$$

Where, all variables are as defined previously.

As can be observed from these figures, both Eq. 6 as proposed by Chapuis (2004) and Eq. 4 as proposed by Terzaghi (1925) produce reasonably accurate predictions for K_{sat} values ranging from 0.01 to approximately 1 cm/s. Based on Figure 2, the Terzaghi equation appears to over-predict the K_{sat} value at relatively high values of K_{sat} and under-predict the K_{sat} value at relatively small values of K_{sat} , and that trend appears to be consistent throughout the range shown in the figure.

The use of void ratio in the Chapuis (2004) equation, or porosity as used in the Terzaghi (1925) equation, makes them potentially useful in that compaction, at least theoretically, should affect the soil void ratio and porosity, i.e., the greater the compaction, the smaller the void ratio and porosity.

Massmann (2008) summarized work conducted by Leroueil et al. (2002) and Watabe et al. (2000) for compacted tills with at least some clay content (i.e., greater than approximately 2 to 4%) over a range of void ratios from 0.2 to 0.3. Figure 3 provides an example of the results, in which hydraulic conductivity is plotted as a function of void ratio. Note that the hydraulic conductivity value at the right end of the horizontal axis in Figure 3 is 0.001 cm/sec. For soils near the upper end of the range evaluated (i.e., 0.001 to 0.0001 cm/sec), changes in void ratio have an even stronger effect on hydraulic conductivity than indicated by the Chapuis (2004) equation. This suggests that as soils become finer and more well graded, compaction effects may be significantly greater than

is the case for relatively clean coarse grained soils. Watabe et al. (2000) also show data that indicate the degree of saturation during compaction can affect the K_{sat} values for till soils (see Watabe et al. 2000 for additional details).

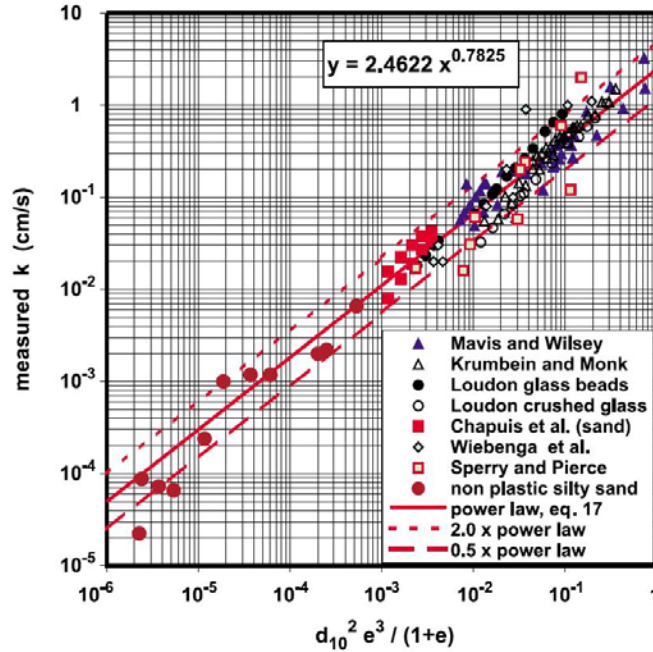


Figure 1. Measured K_{sat} values as a function of $d_{10}^2 e^3 / (1+e)$ (after Chapuis 2004).

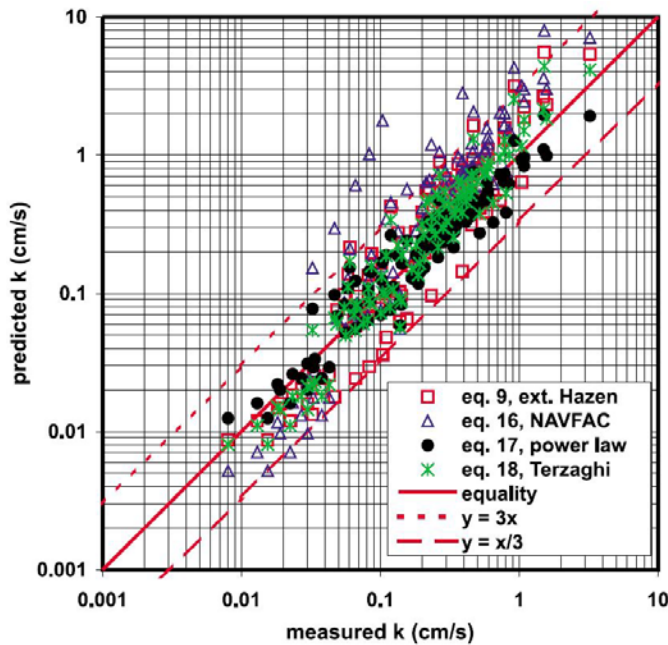


Figure 2. K_{sat} predictive accuracy of various methods (after Chapuis 2004).

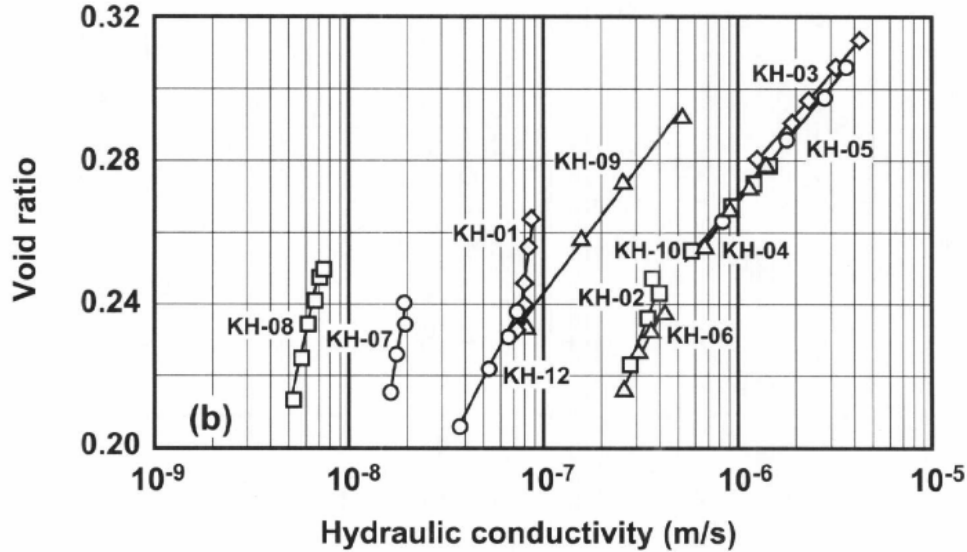


Figure 3. Effects of void ratio and clay content on hydraulic conductivity of compacted tills (from Leroueil et al., 2002).

Massmann (2008) also provided a preliminary evaluation of the effects of compaction on granular noncohesive soils through a literature review. In general, based on this preliminary evaluation, Massmann found that the effect of compaction on K_{sat} is sensitive to factors such as grain size distribution, moisture content, and degree of saturation during compaction. Massmann (2008) concluded that the available data in the literature provides a good starting point for evaluating the effect of compaction on saturated hydraulic conductivity, but that more test data are needed to quantify the effect of compaction on the estimation of K_{sat} . In the interim, Massmann (2003) and WSDOT (2016a) recommend K_{sat} for uncompacted soils be reduced by a factor of 0.2 for clean uniformly graded sands and gravels, 0.1 for well-graded soils with moderate to high silt content, or 0.067 for clayey soils due to compaction.

OBJECTIVE AND SCOPE OF THE CURRENT RESEARCH

To extend the work conducted by Massmann (2003, 2008), the present study is focused on laboratory saturated hydraulic conductivity (i.e., K_{sat}) testing of granular soils, obtaining measurements of K_{sat} for various soil gradations, both naturally and synthetically derived, in which the samples are prepared in an uncompacted and in a compacted state. The K_{sat} values obtained from the samples tested in an uncompacted state are used to relate the new data obtained from the current study to previous tests obtained and analyses conducted by Massmann (2003, 2008) and others (e.g., Chapuis 2004). These test results are then compared to the K_{sat} values obtained from the compacted soils to assess the effects of compaction on K_{sat} .

The objective of this research is to improve upon the K_{sat} correlations developed by Massmann, if possible, to account for the effects of compaction on K_{sat} , and reassess the K_{sat} correlations for uncompacted (i.e., loose) soils as needed based on the new hydraulic conductivity data. The scope of this study is limited to a laboratory investigation of saturated hydraulic conductivity of typical WSDOT embankment soils, both in a compacted and an uncompacted state.

RESEARCH APPROACH

The infiltration and K_{sat} research conducted by Massmann (2003, 2008) is used as a starting point for the current research. However, for the current study, saturated hydraulic conductivity (i.e., K_{sat}) tests were conducted rather than air conductivity tests to assess the effects of compaction on K_{sat} , as the water content of the soil during compaction (i.e., during specimen preparation) is important. Proper, adequately controlled, specimen compaction would be difficult to achieve using an air permeameter, since the specimens would have to be dry in that case. The overall approach used is to perform a series of large diameter, saturated hydraulic conductivity tests on a range of soils with various fines contents and two levels of compaction to obtain measured K_{sat} values. The two levels of compaction are:

- uncompacted (i.e., placed in layers and very lightly tamped only for maintaining uniformity), and
- fully compacted to represent embankments compacted to WSDOT standards (e.g., 90 to 95 percent of standard or modified proctor, AASHTO T99 or AASHTO T180, respectively, depending on soil type, per Section 203.3(14)C of the WSDOT Standard Specifications for Road, Bridge, and Municipal Construction).

Soil typical of embankment materials used by WSDOT was obtained for this laboratory testing. Both naturally occurring granular soils, and natural granular soils mixed with various amounts of fines (i.e., non-plastic silt) to obtain the range of soil gradations needed for this study, are used. For the coarse soils, a rigid wall permeameter is used, and for the higher fines content soils, a flexible wall permeameter is used.

It was originally intended to primarily conduct rigid wall permeameter testing, focusing on relatively low fines content soils (i.e., with less than 10% passing the No. 200 sieve), as the test procedures available for rigid wall permeameters limit the fines content to 10%. The rigid wall permeameter testing was conducted in 2008 as the first phase of this investigation. For higher fines content soils, a flexible wall permeameter is

needed. Testing primarily using the flexible wall permeameter was conducted as the second phase of this investigation, completed in 2013 and 2014. Only the coarsest soils tested in 2013 and 2014 used a rigid wall permeameter due to limitations of the flexible wall permeameter with regard to maximum flowrate. Test results from both phases of the testing are combined and analyzed in the current study.

Materials Tested

Two sets of soils were used for the testing conducted. The testing conducted in 2008 focused on actual materials typically used for WSDOT embankments. The testing conducted in 2013 and 2014 focused on extending that initial work to a wider range of soils, especially higher fines content soils, by artificially mixing natural soils to produce other gradations.

Some of the soils used for the rigid wall permeameter testing conducted in 2008 were obtained from pit sites that have been used to supply WSDOT projects with embankment materials. The Glacier NW, Inc., pit in Dupont, WA was used as one of the sources for the soils used in the experiments. In this case, materials meeting the WSDOT Standard Specifications (2008), Sections 9-03.14(1) and 9-03.14(3) for Gravel Borrow and Common Borrow, respectively, were obtained from these pit sites. For the Gravel Borrow, two samples were obtained: one that had a very low fines content, and one that had a fines content that was close to the upper range allowed for Gravel Borrow (i.e., 7% fines maximum). The specification requirements for these materials are summarized in Table 1. The soils obtained from these pits were not crushed, but they were sieved by the pit owner from naturally occurring gravels and sands to obtain the gradations needed to meet the specification requirements. The remaining soils tested in 2008 were naturally occurring. One of the soils used met the WSDOT Standard Specifications (2008) for Select Borrow, Section 9-03.14(2). This soil was obtained from a pit site located in Grand Mound south of Olympia, Washington. A naturally occurring glacial outwash soil from the Grand Mound pit was also obtained and tested. Glacial outwash soils can be used to meet select or even gravel borrow Standard Specification requirements for embankments, or could simply be an infiltration receptor stratum below the embankment. Glacial outwash soils tend to be coarse grained, well graded, and have high permeability,

and the soil used for this study was no exception to that characterization. For all the soils tested, the gravel portion of the soil appeared to be subrounded. However, the sands were typically subangular, with some angular and some subrounded particles, which is typical for glacial soils in Western Washington. Figure 4 shows an example of the soil tested in 2008. Soil descriptions and laboratory test summaries for the 2008 testing are provided in Appendix A.

Table 1. Soil gradation Standard Specifications (WSDOT 2008) for soils tested.

Material	Property/Sieve Size	Requirement
Gravel Borrow	4 inch	99 to 100 % passing
	2 inch	75 to 100% passing
	No. 4	50 to 80% passing
	No. 40	0 to 30% passing
	No. 200	0 to 7% passing
	Sand Equivalent	50 minimum
Select Borrow	6 inch	99 to 100 % passing
	3 inch	75 to 100% passing
	No. 40	0 to 50% passing
	No. 200	0 to 10% passing
	Sand Equivalent	30 minimum
Common Borrow	Plasticity	Must be “non-plastic”, defines as no test requirement if have less than 15% passing the No. 200 sieve, or if the soil fraction passing the No. 40 sieve cannot be rolled into a thread per Section 4 of AASHTO T90
	Organic content by weight	Less than 3%



Figure 4. Close-up of soil as placed in the rigid wall test cell for soil used in the 2008 testing.

For the 2013 hydraulic conductivity testing, different gradations of material were artificially constructed, with each gradation including 10, 20, and 30 percent fines for a total of 9 different gradations. In 2014, additional samples were prepared to fill gaps in the data and to extend the upper and lower ranges of soil gradation, and permeability. A combination of four sources, all of which contained materials that were geologically similar, was used to get the range of grain sizes needed. These sources are as follows:

- The Grand Mound pit site mentioned previously (provided coarser sands and gravels for the 2013 and 2014 testing),
- Two embankment sites near the Mellen Street Interchange project on I-5 north of Centralia, Washington (provided sands and silts for the 2013 and 2014 testing),
- A site along SR-502 near Battle Ground in southwest Washington (provided finer sands and silts for the 2013 and 2014 testing), and
- A site near the Rock Creek Bridge on SR-6 (provided fine silts and clays for only the 2014 testing).

To develop the various gradations needed, all the soil used was dried and sieved using the 3 inch, 1.5 inch, 0.75 inch, No. 4, No. 10, No. 40, No. 60, No. 80, No. 100, and No. 200 sieves. The soil retained on each sieve was placed in a separate bucket. The weight of each soil fraction needed to artificially produce the desired gradation for each test specimen was determined and the test specimen produced (plus about 10% more to make sure enough soil would be available). Then the soil fractions for each specimen were blended together in a bowl and thoroughly mixed, being careful not to lose any soil. The mixed soil was then placed into the specimen mold for each test. For soils that contained more than 10% fines (i.e., particle sizes smaller than the #200 sieve), hydrometer analyses were conducted so that the d_{10} size could be more accurately determined.

Close-up photos of the soils used, at least for the 2013-2014 testing, are provided in Figures 5 through 7 to illustrate the angularity and particle shape. Based on visual observations from the 2008 testing, those soils also followed a similar pattern with regard to particle angularity (e.g., Figure 4). Considering that much of the hydraulic

conductivity testing conducted by others has been on soils with more rounded soil particles, some differences between the test results from previous studies and the test results from the current study which were conducted on soils with greater angularity should be expected, such as due to the effect of increased tortuosity (Chapuis 2004). Additional photos of the soils included in the 2013-2014 testing, as well as detailed laboratory test summaries and soil descriptions, are provided in appendices B and C.



Figure 5. Close-up of test soil grains used for 2013-2014 testing – 0.75 inch (19 mm) size.



Figure 6. Close-up of test soil grains used for 2013-2014 testing – 0.017 inch (0.425 mm) size.



Figure 7. Close-up of test soil grains used for 2013-2014 testing – 0.003 inch (0.075 mm) size.

Test Procedures and Equipment Used

Both rigid wall and flexible wall permeameter testing was conducted to obtain K_{sat} values. In addition to the permeameter testing, soil gradation testing of each sample was conducted in accordance with ASTM C-136-06. The unit weight of the specimens was determined in accordance with ASTM D7263-09. For both the rigid and flexible wall permeameter testing, test specimens reflect the gradation of the material sampled for the 2008 testing. However, for the 2013 and 2014 testing, test samples were constructed artificially using gradations that targeted different values of d_{10} as described in the previous section. Post-test gradations were performed on all samples to obtain the gradations used for further analysis and to assess any changes in the soil gradation relative to the pretest gradation. To help determine target densities and moisture content needed to compact the specimens in the permeameter, compaction tests were conducted in accordance with AASHTO T180 for the well graded sandy soils and in accordance with the WSDOT T606 Max Density Test (WSDOT 2016b) for the poorly graded gravels. Additional details regarding the compaction tests are provided in appendices D and E.

Specimen densities were determined based on the as placed dimensions of the specimens in the permeameter mold after saturation and testing were completed. The

specimen diameter was fairly accurate as a result of the mold rigidity; however, the specimen height was based on the average of several dimension readings taken on the top of the specimen. Those readings varied by no more than 0.25 inches, and considering that the average height from several readings was used, the accuracy of the height was estimated to be approximately $\pm 2\%$, which translates to a unit weight accuracy of approximately ± 2.5 pcf. Specimen height was also measured as placed before saturation and testing. In most cases, the difference in specimen height between the before test and after test measurement was less than 0.1 inch (3 mm). However, a few of the specimens had a rather large difference in specimen heights – 0.5 to 1.0 inch (13 to 25 mm). Based on observations made by the testers, most, if not all, of this change in height occurred during the saturation phase. These bigger changes only occurred for some of the fine sand specimens placed without compaction. This was likely the result of angular sand particles hanging up on each other during placement, and the saturation process enabled the particles to move past one another under their own weight to form a more stable soil matrix. However, since specimen unit weight and porosity were determined based on specimen measurements taken at the end of the test, and since all the compaction occurred before the permeability testing, this problem should have a minimal influence on the test results.

Rigid Wall Permeameter Testing:

The Standard Test Method for Permeability of Granular Soils (Constant Head), AASHTO T215, was used for all test samples with a d_{10} of 0.1 mm or greater. A 6 inch cell was used for all tests with d_{10} from 0.12 to 1.2 mm. A 9 inch cell was used for all tests with d_{10} of 1.55 mm and greater. Tests conducted on the coarse gravel borrow (2008 testing) and samples with a d_{10} of 5.8 and 8.4 mm (the 2014 testing) deviated from the standard test method in that they contained particles with grain sizes larger than 19 mm. Furthermore, based on the calibration of the test equipment used, the permeability of these very coarse specimens appears to be near the upper limits that the rigid wall permeameter can measure. Figures 8 and 9 illustrate the rigid wall permeameter test set-up.

For uncompacted samples, material was placed into the cell as described in AASHTO T215 and lightly tamped by hand using a rod with a 2 inch diameter tamping foot. No compaction hammer was used. For compacted samples, material was also placed into the cell as described AASHTO T215, but each layer was compacted using the same tamping foot and a 2.25 lb (1.02 kg) sliding weight with a drop of 12 inches (0.3 m). Compaction continued until no further deformation could be detected (no set number of blows was used, but typically from 12 to 20 blows/layer), based on measurements of depth to the top of the compacted soil surface. The goal of the compaction process was to achieve at least 90 to 95% of maximum density, based on either a WSDOT Maximum Density Test (WSDOT T606) for the coarsest soils or a modified Proctor Test (AASHTO T180) for the rest of the soils tested. For the material as placed in the permeameter, the target moisture content was approximately 6%. However, for the coarser specimens, the moisture content had to be significantly reduced to approximately 1%, as more moisture than this resulted in water pooling at the bottom of the permeameter, providing no usefulness for compacting the specimen in the permeameter.

For saturation of all samples, a minimum vacuum of 25 inches Hg (847 millibars) was applied to the top of the cell for 15 minutes or more. De-aired water was then slowly drawn into the bottom of the cell until the cell was full. The vacuum was released, and any air bubbles were removed from the cell and hose lines. Once this was accomplished, testing commenced. Most samples tested had a saturation of over 90%, and in most cases was in the 95% to 97% range. On average, the compacted soil specimen saturation was 89%, versus 92% for the uncompacted specimens. Note that this saturation problem did not occur for the flex-wall tests.

Test data and measurements were entered into an Excel spreadsheet where corrections for temperature were applied, all necessary calculations were performed, and plots of k (permeability) and laminar flow (velocity vs hydraulic gradient) were produced. Lateral manometers were used to measure head loss through the specimen.



Figure 8. Test equipment setup for rigid wall permeameter testing.



Figure 9. Close-up of rigid wall permeameter.

Flexible Wall Permeameter Testing

For the flexible wall permeameter testing, ASTM D5084 using Method C – Falling Head Rising Tailwater, was used for all testing. A GEOTAC (Geotechnical Acquisition & Control) system from Trautwein Testing Equipment was used. See Figure 10 for the test set-up. This system consists of three servo-controlled pumps to control cell pressure (effective stress), influent (headwater), and effluent (tailwater). The triaxial

pressure cell was 8 inches in diameter by 18 inches in height. Figure 11 illustrates the software screen used to control the test.

The test specimens were 6 inches in diameter by 6 inches in height. For each of the sample gradations, uncompacted and compacted specimens were constructed. For the un-compacted specimen, material was placed into a split mold in 2 inch thick layers. Each layer was lightly tamped with a tamping rod and the process repeated until the desired height was reached, as shown in figures 12 and 13. This was done to achieve as uniform a placement as possible, and to minimize the potential for localized soil movement (i.e., piping) during the saturation process. For the compacted specimens, a slide hammer (2.25 lb rammer with a 12 inch drop) was used to compact each layer to an unyielding condition, achieving higher densities. The goal of the compaction process was to achieve at least 90 to 95% of maximum density as described for the rigid wall permeameter testing. For the material as placed in the split mold for the permeameter, the target moisture content was approximately 8%.



Figure 10. Flexible wall permeameter testing system.

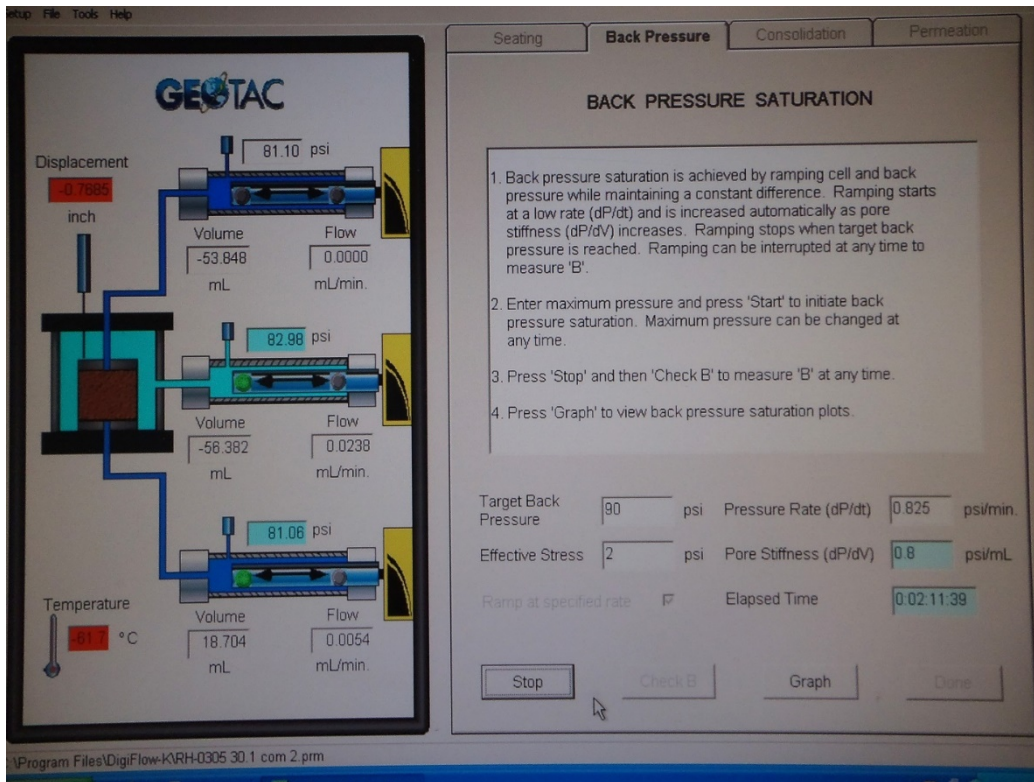


Figure 11. Software input screen for flexible wall permeameter.



Figure 12. Specimen mold with rammer and test soil.



Figure 13. Test specimen being compacted with rammer.

Specimens were tested in accordance with the ASTM procedure noted above. A 2 psi seating pressure was applied. For saturation of the specimen, ASTM D5084 calls for a non-pressurized water source to be connected at the bottom of the test cell and a small vacuum applied to the top of the cell to “pull” water into the specimen. Every attempt to follow this procedure resulted in piping of the water through the specimen, thus not achieving saturation and creating non-uniformities in the specimen. Instead a pressurized water source was applied to the bottom of the specimen, with an open drainage path from the top of the specimen, limiting the volume of water entering the specimen to 0.5 ml per minute. After approximately 50 ml of water had discharged from the top of the specimen, the water introduction process was halted and back pressure saturation was initiated. After back pressure saturation (at least 85 to 90% saturation was achieved for all specimens tested), the specimens were subjected to one additional psi for an effective stress of 3 psi for the consolidation phase (no consolidation was expected and none was observed). For permeation, the headwater pressure was increased 2 psi while the

tailwater pressure was held constant. On average, over 200 ml of water flowed through each specimen. For all tests conducted, the ratio of outflow to inflow was between 0.75 and 1.25 for much of the test. Based on observations during the tests, very little, if any, fines were washed through the specimen during testing, as the water was observed to be mostly clear.

TEST RESULTS

The soil specimens tested were characterized with regard to gradation, moisture content, unit weight, and saturated hydraulic conductivity, K_{sat} . Compaction properties and as placed specimen unit weights for selected soil gradations are provided in Table 2. Gradation parameters were evaluated before and after the hydraulic conductivity testing. Key gradation parameters needed for estimating K_{sat} for these soils, based on the post-hydraulic conductivity test gradations, are summarized in Appendix F (i.e., Table F.1). Both pre- and post-hydraulic conductivity test gradation test results for all soils for each specimen tested are provided in appendices A through C. In most cases the differences between the gradations taken before the hydraulic conductivity sample placement in the test device and the gradations performed after the hydraulic conductivity testing were minor. However, in some cases (mostly with regard to the natural soils tested in 2008) the differences were significant. This may simply be the result of gradation variations within the bigger sample used as the source for the test specimen (the 2008 test specimens were taken directly from the materials source “as is” rather than recreated to specific gradations as was done for the 2013/2014 testing). When larger differences in the gradation did occur, the differences tended to be in the sand sized particles rather than the silt sized particles. It should also be noted that water coming from the specimens during the test was generally clear, indicating little, if any, soil was being washed through the specimens.

The compaction tests were conducted to gain a better understanding of the degree of compaction achieved in the as placed permeameter specimens relative to typical compaction standards. Note that a reduced hammer size and drop had to be used to avoid damaging the membrane and crushing the soil particles (Chapuis 2012). Furthermore, compaction tests were conducted on representative soil gradations used in the K_{sat} tests. Therefore, a direct correlation to compaction in terms of percent of maximum density could not be achieved for all test specimens. Since the specimen compaction procedures used were consistent for all specimens tested (i.e., in 2008, 2013, and 2014), the compaction test results should be considered representative of all the specimens tested with regard to relative degree of compaction.

As can be seen in Table 2, 95 to 100% of the maximum density at the specimen moisture content was typically achieved for the compacted soil tests. However, a couple of the compacted soil test results only achieved 90% of the maximum density. For the specimens that were slightly above 100% compaction, test variability is likely the reason they are over 100%. In any case, the level of compaction achieved in the specimens was consistent with typical embankment construction for WSDOT. For the “uncompacted” specimens, the percent of maximum density observed was more variable, but typically in the range of 80 to 85 percent. The two exceptions to this were a very coarse specimen in which it was expected that compaction would have little effect anyway, and the other case was likely due to the specimen consolidation that took place during saturation. This specimen consolidation likely occurred due to the following:

- The sample was prepared to target a loose, uncompacted state.
- The soil particles were relatively angular, allowing the soil structure as initially placed to be somewhat unstable with particles hanging up on one another.
- During the saturation process, the friction between particles was reduced enough to allow them to slip past one another under their own weight.

The porosity and void ratio were also determined for each specimen tested, both for the uncompacted and compacted specimens. These properties are shown in Table 3. These properties, as well as the specimen unit weights, were determined after specimen saturation to account for the potential effect of specimen consolidation during saturation, especially for the uncompacted specimens.

To obtain the porosity and void ratio, the specific gravity of solids, G_s , for the source soils used is needed. For soil samples in which G_s was not measured, a typical G_s of 2.67 was assumed to estimate the void ratio and porosity. For the testing conducted in 2013 and 2014, the soils (No. 200 sieve or larger) were artificially created using soils that were for the most part from the same source. The finer fraction of the soil, however, was obtained from a couple of sources. For the coarser soil specimens, which were tested using the rigid wall permeameter, specific gravity measurements were obtained as part of the compaction tests conducted on representative samples, with G_s ranging from 2.67 to

2.68. G_s was determined for all flexible wall permeameter tests as part of the hydrometer test conducted in conjunction with the permeameter test. For these tests, the finer (i.e., No. 10 sieve minus) component of the soil had a measured G_s that ranged from 2.71 to 2.77.

Table 2. Summary of compaction test results, and their comparison to measured specimen unit weights, conducted for representative soil gradations.

¹ Soil	Uncompacted Dry Unit Weight (pcf)	Compacted Dry Unit Weight, γ_m (pcf)	² Maximum Dry Unit Wt. at Moisture Content for Sample from AASHTO T180 Compaction test, γ_{max} (pcf)	% of Max. Density, Uncompacted	% of Max. Density, Compacted
Extreme Fine End - 0.01 mm	107	111	109 (117 at optimum)	98	101
Fine End Sand - 0.26 mm (rigid wall)	96	106	119 (127 at optimum)	81	89
Coarse Sand/Gravel – 1.55 mm (rigid wall)	117	124	135*	87	92
Coarse Sand/Gravel – 5.8 mm (rigid wall)	117	119	125*	94	95
Gravel = 19%, Sand = 51%, Silt = 30%	104	132	128	83	103
Gravel = 23%, Sand = 57%, Silt = 20%	117	138	136	86	101
Gravel = 26%, Sand = 64%, Silt = 10%	110	135	134	82	101

¹Tests were conducted in flexible wall permeameter, except where noted.

²As compacted specimen moisture content was 8% for flex wall tests and 6% for rigid wall tests, except the coarser rigid wall specimens, in which the moisture content was as low as 1%.

*Based on WSDOT T606 Max Density Test (WSDOT 2016b).

Table 3 also contains data for two fine grained, natural, normally consolidated, alluvial silt specimens obtained using a Shelby tube sampler for a project in the Chehalis River valley south of Olympia, Washington, located just south of the terminus of the continental glaciers that carved out the Puget Sound region. The samples had a G_s value of 2.76, which is reasonably consistent with the values obtained from the fine-grained portion of the soils used to create the “artificial soil” test gradations. The samples taken were tested for permeability in the axial direction. Therefore, the permeability measured in those two specimens is for the vertical direction. It is also possible there could be some soil structure issues that could affect the measured permeability relative to the remolded test specimens that make up most of the soils tested in this study. Since that soil was normally consolidated, the test results for those samples will be considered as “uncompacted.”

Table 3. Comparison of uncompacted and compacted specimen properties for tests conducted in this study.

¹ Soil	Uncompacted Dry Unit Weight (pcf)	Compacted Dry Unit Weight, γ_m (pcf)	Specific Gravity, G_s^3	Uncompacted Porosity, n	Compacted Porosity, n	Uncompacted Void Ratio, e	Compacted Void Ratio, e
Natural alluvial soil (silt) – Chehalis River	118	--	2.76*	0.55	--	1.24	--
Natural alluvial soil (silt) – Chehalis River	114	--	2.76	0.55	--	1.23	--
Extreme Fine End - 0.005 mm	114	113	2.73*	0.33	0.34	0.493	0.52
Extreme Fine End - 0.01 mm	107	111	2.67*	0.37	0.34	0.59	0.52
Fine End Sand - 0.12 mm (rigid wall)	108	--	2.67	0.36	--	0.55	--
Fine End Sand - 0.12 mm (rigid wall)	113	119	2.67	0.33	0.29	0.49	0.41
Fine End Sand - 0.12 mm	--	122	2.67	--	0.27	--	0.37
Fine End Sand - 0.17 mm (rigid wall)	111	117	2.67	0.34	0.30	0.52	0.43
Fine End Sand - 0.17 mm (rigid wall)	111	--	2.67	0.34	--	0.52	--
Fine End Sand - 0.17 mm	--	123	2.67	--	0.26	--	0.35
Fine End Sand - 0.23 mm (rigid wall)	116	127	2.67	0.31	0.25	0.45	0.33
Fine End Sand - 0.26 mm (rigid wall)	96	102	2.67*	0.43	0.39	0.75	0.64
Fine End Sand - 0.26 mm (rigid wall)	--	106	2.67	--	0.36	--	0.56
Fine End Sand - 0.26 mm	--	120	2.67	--	0.29	--	0.41
Coarse Sand/Gravel – 1.2 mm (rigid wall)	113	115	2.67	0.32	0.31	0.47	0.45
Coarse Sand/Gravel – 1.55 mm (rigid wall)	117	124	2.67*	0.30	0.26	0.43	0.35
Coarse Sand/Gravel – 2.18 mm (rigid wall)	113	120	2.67	0.32	0.28	0.47	0.39
Coarse Sand/Gravel – 2.9 mm (rigid wall)	109	119	2.68	0.35	0.29	0.54	0.41
Coarse Sand/Gravel – 3.9 mm (rigid wall)	107	111	2.68	0.36	0.34	0.56	0.52
Coarse Sand/Gravel – 5.8 mm (rigid wall)	117	119	2.68*	0.29	0.32	0.41	0.52
Coarse Sand/Gravel – 8.4 mm (rigid wall)	--	113	2.68	--	0.32	--	0.47
Gravel = 4%, Sand = 66%, Silt = 30%	92	121	2.71	0.45	0.28	0.83	0.40
Gravel = 4%, Sand = 66%, Silt = 30%	-	128	2.71	--	0.23	-	0.30
Gravel = 19%, Sand = 51%, Silt = 30%	104	132	2.71*	0.39	0.22	0.63	0.28
Gravel = 19%, Sand = 51%, Silt = 30%	-	134	2.71	--	0.21	-	0.26
Gravel = 45%, Sand = 25%, Silt = 30%	102	130	2.71	0.40	0.23	0.66	0.30
Gravel = 45%, Sand = 25%, Silt = 30%	-	136	2.71	--	0.20	-	0.24
Gravel = 5%, Sand = 75%, Silt = 20%	96	129	2.76	0.44	0.25	0.79	0.33
Gravel = 49%, Sand = 31%, Silt = 20%	120	130	2.76	0.30	0.25	0.43	0.33
Gravel = 23%, Sand = 57%, Silt = 20%	117	138	2.76*	0.32	0.20	0.48	0.25
Gravel = 55%, Sand = 35%, Silt = 10%	125	137	2.77	0.28	0.20	0.38	0.26
Gravel = 26%, Sand = 64%, Silt = 10%	110	135	2.77*	0.36	0.22	0.57	0.28
Gravel = 26%, Sand = 64%, Silt = 10%	104	128	2.77	0.40	0.26	0.67	0.35
Gravel = 6%, Sand = 84%, Silt = 10%	103	125	2.77	0.40	0.27	0.67	0.38
Fine End Gravel Borrow (rigid wall)	102	118	2.67	0.39	0.29	0.63	0.42
Fine End Gravel Borrow (rigid wall)	100	120	2.67	0.40	0.28	0.66	0.39
Fine End Gravel Borrow (rigid wall)	102	121	2.67	0.39	0.27	0.63	0.37
Select Borrow (rigid wall)	113	123	2.68*	0.32	0.26	0.48	0.36
Select Borrow (rigid wall)	107	122	2.68	0.36	0.27	0.56	0.38
Select Borrow (rigid wall)	113	122	2.68	0.33	0.27	0.48	0.37
Common Borrow (rigid wall)	110	126	2.67	0.34	0.24	0.51	0.32
Common Borrow (rigid wall)	110	121	2.67	0.34	0.27	0.51	0.38
Common Borrow (rigid wall)	107	124	2.67	0.36	0.26	0.56	0.35
Sandy Glacial Outwash (rigid wall)	113	123	2.67*	0.32	0.26	0.48	0.35
Sandy Glacial Outwash (rigid wall)	111	122	2.67	0.33	0.27	0.50	0.37
Sandy Glacial Outwash (rigid wall)	110	122	2.67	0.34	0.27	0.52	0.37
Course Gravel Borrow (rigid wall)	108	115	2.67	0.35	0.31	0.53	0.45
Course Gravel Borrow (rigid wall)	108	114	2.67	0.35	0.31	0.53	0.45
Course Gravel Borrow (rigid wall)	108	114	2.67	0.36	0.32	0.55	0.46

¹Tests were conducted in flexible wall permeameter, except where noted.

²As compacted specimen moisture content was 8% for flex wall tests and 6% for rigid wall tests.

³Specific Gravity, G_s , assumed to be 2.67 for soils with no measurement of G_s (typical for glacially derived soils in the Puget Sound region), or was assumed to be the same as measured G_s for a similar soil (same source with approximately the same gradation).

*Measured G_s for soil.

Table 4 summarizes the measured K_{sat} values for the soil specimens tested, with and without compaction. The effect of compaction can be seen in the data presented in Tables 2, 3 and 4. In Table 4, the hydraulic conductivity (K_{sat}) also drops due to compaction, but the drop is greater for higher fines content soils than for relatively clean coarse grained soils.

Table 4. Comparison of uncompacted and compacted specimen measured K_{sat} values.

Soil	Uncompacted K_{sat} (cm/s)	Compacted K_{sat} (cm/s)	Ratio Compacted to Uncompacted K_{sat}
Natural alluvial soil (silt) – Chehalis River	0.000057		
Natural alluvial soil (silt) – Chehalis River	0.000009		
Extreme Fine End – $d_{10} = 0.005$ mm	0.00018*	0.0000553*	0.307*
Extreme Fine End – $d_{10} = 0.01$ mm	0.00133*	0.00681*	5.12*
Fine End Sand – $d_{10} = 0.12$ mm (rigid wall)	0.0127	0.00393	0.309
Fine End Sand – $d_{10} = 0.12$ mm (rigid wall)	0.0072		0.546
Fine End Sand – $d_{10} = 0.12$ mm (flex wall)		0.00263	
Fine End Sand – $d_{10} = 0.17$ mm (rigid wall)	0.0112	0.00839	0.534
Fine End Sand – $d_{10} = 0.17$ mm (rigid wall)	0.0112		0.749
Fine End Sand – $d_{10} = 0.17$ mm (flex wall)		0.00438	
Fine End Sand – $d_{10} = 0.23$ mm	0.051	0.00883	0.173
Fine End Sand – $d_{10} = 0.26$ mm (rigid wall)	0.125	0.0196	0.157
Fine End Sand – $d_{10} = 0.26$ mm (rigid wall)		0.0507	0.406
Fine End Sand – $d_{10} = 0.26$ mm (flex wall)		0.00355*	
Course Sand/Gravel – $d_{10} = 1.2$ mm (rigid wall)	1.04	0.786	0.756
Course Sand/Gravel – $d_{10} = 1.55$ mm (rigid wall)	1.97	0.95	0.482
Course Sand/Gravel – $d_{10} = 2.18$ mm (rigid wall)	3.98	2.45	0.616
Course Sand/Gravel – $d_{10} = 2.9$ mm (rigid wall)	10.1	4.48	0.444
Course Sand/Gravel – $d_{10} = 3.9$ mm (rigid wall)	13.9	9.61	0.691
Course Sand/Gravel – $d_{10} = 5.8$ mm (rigid wall)	10.9	11.0	1.010
Course Sand/Gravel – $d_{10} = 8.4$ mm (rigid wall)		14.4*	
Gravel = 4%, Sand = 66%, Silt = 30%	0.000532	0.000268	0.504
Gravel = 4%, Sand = 66%, Silt = 30%		0.000235	0.442
Gravel = 19%, Sand = 51%, Silt = 30%	0.00101	0.000584	0.578
Gravel = 45%, Sand = 25%, Silt = 30%	0.00168	0.000441	0.263
Gravel = 5%, Sand = 75%, Silt = 20%	0.00136	0.000189	0.139
Gravel = 49%, Sand = 31%, Silt = 20%	0.00193	0.00161	0.884
Gravel = 23%, Sand = 57%, Silt = 20%	0.00299	0.000495	0.166
Gravel = 55%, Sand = 35%, Silt = 10%	0.00115	0.00111	0.965
Gravel = 26%, Sand = 64%, Silt = 10%	0.0012	0.000776	0.647
Gravel = 26%, Sand = 64%, Silt = 10%	0.0019	0.00256	1.347
Gravel = 6%, Sand = 84%, Silt = 10%	0.00217	0.00126	0.581
Fine End Gravel Borrow	0.067	0.022	0.328
Fine End Gravel Borrow	0.032	0.020	0.625
Fine End Gravel Borrow	0.046	0.021	0.457
Select Borrow	0.13	0.021	0.162
Select Borrow	0.07	0.059	0.842
Select Borrow	0.07	0.052	0.743
Common Borrow	0.15	0.023	0.153
Common Borrow	0.25	0.026	0.104
Common Borrow	0.13	0.017	0.192
Sandy Glacial Outwash	0.047	0.035	0.745
Sandy Glacial Outwash	0.54	0.026	0.048
Sandy Glacial Outwash	0.18	0.066	0.367
Course Gravel Borrow	28*	16*	0.57*
Course Gravel Borrow	49*	29*	0.59*
Course Gravel Borrow	36*	11	0.31*

*Considered as outliers. See Section entitled “*Assessment of Outliers and Data Set Differences*” for additional explanation.

K_{SAT} PREDICTION ANALYSIS

Effect of Grain Size Parameters on K_{sat}

The d_{10} size has been a key soil gradation parameter used for correlation to K_{sat} for over 100 years. The measured results for the current study, as well as the K_{sat} values from the studies conducted by Massmann (2003) and gathered by Chapuis (2004) are plotted against the soil d_{10} size in Figure 14 to provide a common assessment for the all of the data considered in this study and to also help identify possible outlier values. Figure 14 illustrates that there is a fairly strong relationship between the soil d_{10} size and the measured K_{sat} values for the hydraulic conductivity tests conducted for the present study as well as those gathered by Chapuis (2004), with the exception of a few possible outlier measurements. However, for the air permeability tests conducted by Massmann (2003) which were converted to hydraulic conductivity using theoretical means, the scatter in the measurements is much greater, especially for finer grained soils. There also appears to be a distinction between the K_{sat} values for the soils subjected to compaction and the soils that were not subjected to compaction, but primarily for d_{10} sizes less than approximately 1.0 mm.

The effect of the uniformity of the gradation, as characterized by the coefficient of uniformity, C_u , defined as d_{60}/d_{10} , was also investigated for potential use in the current study to develop an improved prediction methodology (Figure 15). To more clearly see the trends, only tests in which saturated hydraulic conductivity was directly measured are included. Data gathered by Chapuis (2004) are also included, at least for those cases in which both the d_{10} and d_{60} size were available (i.e., 107 of the 137 data points from Chapuis 2004). While there appears to be a moderate relationship between C_u and K_{sat} , in which K_{sat} decreases as C_u increases (i.e., as the gradation becomes less uniform and more well graded), the data exhibit significant scatter. Note that the test results reported by Chapuis (2004) at K_{sat} values near or less than 0.0001 cm/sec. are for natural till soils, which Chapuis (2004) indicated were difficult to predict K_{sat} accurately.

Other parameters investigated for direct correlation with K_{sat} include the soil porosity and void ratio, as well as the coefficient of curvature. None of these parameters exhibited a direct correlation with the measured K_{sat} values. Considering that several of

the historical K_{sat} equations use porosity and void ratio, this means that the equation formulation using this parameter must be more complex for porosity or void ratio to be of use – more on this later in this report.

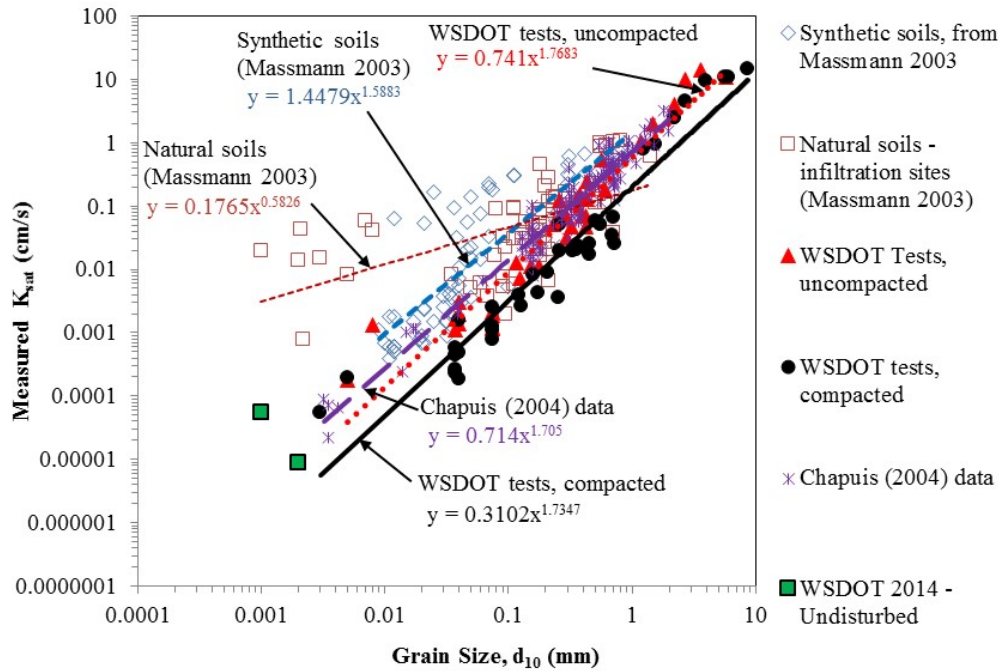


Figure 14. Measured hydraulic conductivity values as a function of the soil d_{10} size for uncompacted and compacted specimens (outliers included).

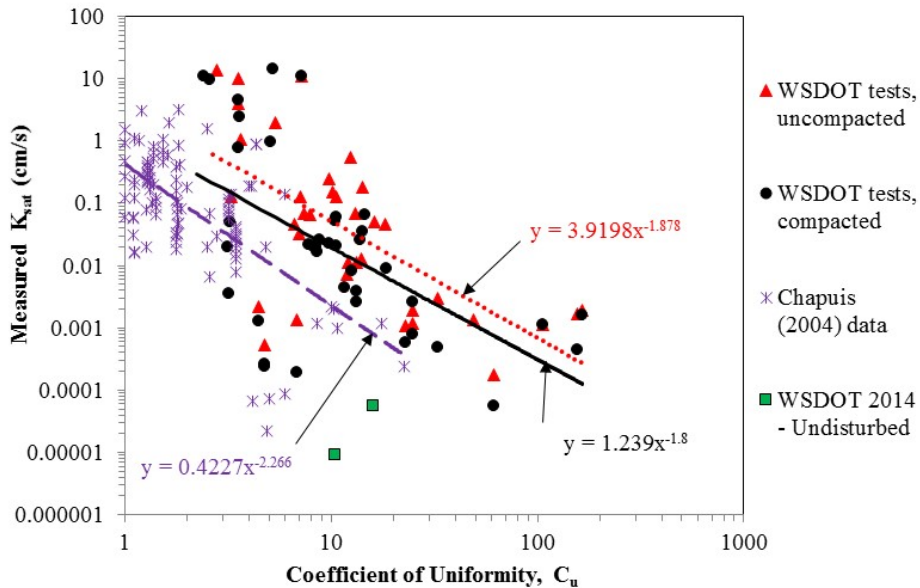


Figure 15. Measured hydraulic conductivity values as a function of the soil C_u for uncompacted and compacted specimens (outliers included).

Assessment of Outliers and Data Set Differences

Before making a detailed assessment of the historical methods and developing empirical adjustments to improve the prediction accuracy of selected methodologies, a careful assessment of the data was made to remove any outlier data that could skew the results. Allen et al. (2005) state that outlier removal should be done with consideration to the following:

1. a different criterion is used to establish the value of a given point or set of points (e.g., a different failure criterion),
2. a different measurement technique is used,
3. data from a source that may be suspect,
4. data that are affected by regional factors (e.g., regional geology effects on soil or rock properties), or
5. any other issues that would cause the data within a given data set to not be completely random in nature.

Table 4 identifies the specific K_{sat} test results that are considered as outliers. The specific explanations as to why these test results are considered as outliers are provided in the paragraphs that follow.

From the list above, only bullets 2 through 5 are potentially applicable to the current study. With the possible exception of K_{sat} test results obtained using rigid versus flex wall permeameters, the measurement techniques used can be considered reasonably consistent for all the test data obtained from the current test program. With regard to rigid versus flex wall permeameter testing, no systematic difference in the data obtained using these two types of permeameters could be detected. Furthermore, tests using both the rigid wall and flex wall permeameter on the same soil and amount of compaction were conducted for three cases, all of which were fully compacted, with d_{10} values ranging from 0.12 mm to 0.25 mm. With the exception of the specimens with a d_{10} of approximately 0.25 mm, the test results using both the flex wall and the rigid wall permeameter are reasonably close. For the comparison using the specimens with a d_{10} of approximately 0.25 mm, there was almost an order of magnitude difference. For the flex

wall test of the specimen with a d_{10} of approximately 0.25 mm, the density was significantly higher, and porosity and void ratio significantly lower, than the specimens with the same gradation tested in the rigid wall permeameter. This may explain why the bias (i.e., measured/predicted value) was unusually low (i.e., in the range of 0.1 to 0.2 for the various existing prediction methods), indicating that this flex wall test (d_{10} of 0.25 mm) could be an outlier and should be removed from the data set.

Another possible cause for consideration as an outlier that is related to bullet 2 are tests conducted on soils that are beyond the limits of the test device used. Specifically, 5 of the 6 coarse gravel borrow specimens had K_{sat} values that were at the limit of the rigid wall testing device with measured K_{sat} values of 15 to 50 cm/s. Therefore, these 5 test results were considered as outliers and excluded from further analysis.

For the finest soils (i.e., the WSDOT soils with a d_{10} of less than 0.01 mm), the water content used to prepare the specimens was unfortunately less than the optimum water content for compaction (e.g., 8% versus 13 to 14%). As reported in Holtz and Kovaks (1981), K_{sat} tends to increase rapidly with decreasing water content when more than 2 to 3% below optimum, but K_{sat} only gradually increases as water content increases above optimum. Holtz and Kovaks (1981) explain that the void ratio increases significantly as water content decreases due to the flocculated structure of the soil grains. However, near and above optimum, the soil grains tend to become more oriented (i.e., dispersed) with increasing water content. Additionally, as the compactive effort increases, even dry of optimum the soil structure tends to become more oriented (Holtz and Kovaks 1981). This may explain why the measured K_{sat} values for such specimens exhibited more scatter and tended to have high bias values of 5 to 10, especially for the lightly compacted (identified as “uncompact” in this report) test specimens. While this flocculated structure concept has platy clay particles in view, similar behavior with regard to K_{sat} could also occur for angular soils, especially for very light compaction. Therefore, the WSDOT test specimens reconstituted from natural soils in the laboratory with a d_{10} less than 0.01 mm are considered as outliers with regard to further analysis.

One additional test must also be considered an outlier. The coarse sand and gravel specimen in which the d_{10} value was 8.6 mm did not have laminar flow during the K_{sat} test. So it must be removed from the data set for further analysis, as the K_{sat}

prediction methods assessed and developed further in this study apply to, and have been developed for, laminar flow conditions.

For the remaining bullets, the third and fourth bullets are not likely to apply to the data, since any questionable sources were never incorporated in this study, and for the WSDOT tests, the source of the materials used was from sites in western Washington that have a generally consistent geologic history. Since the data gathered by Chapuis (2004) are from different sources and are not necessarily geologically similar to the WSDOT data, it is reasonable to treat the WSDOT and Chapuis (2004) data as separate data sets. Therefore, the Chapuis (2004) data are treated as a separate source in the analysis for comparison purposes to the WSDOT data.

In addition, Figure 16 illustrates the differences between these data sets regarding their gradation characteristics. In general, for the same d_{10} size, the soils used for the K_{sat} test data gathered by Chapuis (2004) were more uniformly graded than the soils tested in the current study. The effect of these gradational characteristics must be considered before combining the data sets together to develop improved K_{sat} prediction method formulations.

When merging different data sets together, pervasive differences in those data sets may affect the outcome of empirical adjustments made to existing empirically based methods. For example, in the Terzaghi Equation (Eq. 4), C_0 is set equal to 8 for smooth grains and 4.6 for grains of irregular shape. These particle shape differences, which could affect the tortuosity of the drainage paths through the soil, could be the result of differences in the geologic history that produced the soil grains (outlier reason No. 4 above). Smooth, rounded grains would be characteristic of soils that have been water or wind transported significant distances (e.g., beach or wind-blown sands), and irregular shaped soils grains could apply to glacial soils (e.g., typical sands in Western Washington).

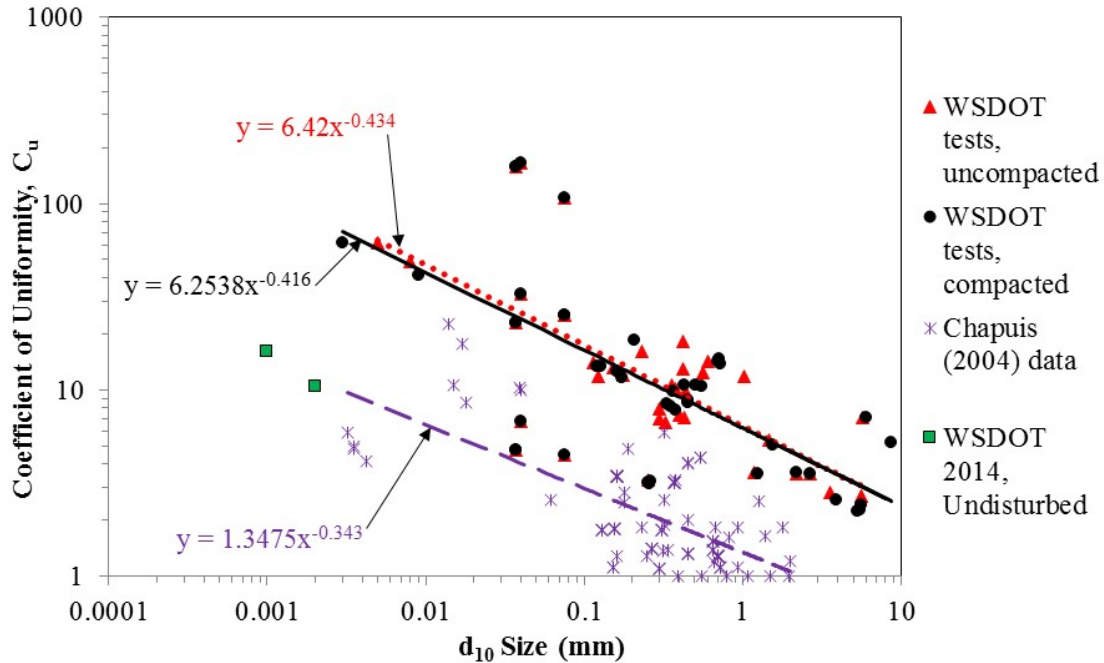


Figure 16. Grain size characteristics of the K_{sat} data sets evaluated (outliers included).

Analysis of K_{sat} Prediction Equation in the WSDOT Highway Runoff Manual

One of the anticipated outcomes of this study was to develop a modification to the K_{sat} equation in the Highway Runoff Manual (WSDOT 2016a) to account for the K_{sat} reducing effects of soil compaction. Therefore, this analysis begins with an assessment of that method. The K_{sat} prediction Method in the current Highway Runoff Manual (WSDOT 2016a) is the one developed by Massmann (2003), shown as Eq. 1.

As presented previously, Massmann (2003) developed a multi-grain size parameter equation for predicting K_{sat} (Eq. 1) based on the K_{sat} values converted from air permeability laboratory test results. Figure 17 (a and b) illustrates the prediction accuracy of that equation. Figure 17a shows the full range of the data (but with outliers identified in the previous section removed), and Figure 17b shows only the main group of data points. Only data for which all the grain size parameters were available are shown in this figure, which includes the WSDOT data obtained from the current study and the data developed by Massmann (2003). Note that the K_{sat} data gathered by Chapuis (2004) could not be included here since all the grain size data for those tests that are needed to

use Eq. 1 were not available. However, both data sets could be considered if one of the other historical prediction equations is used. See Appendix G for a plot comparing the air permeability data from Massmann (2003) to the rest of the data sets using the Chapuis (2004) prediction equation. In that plot it is clear that the air permeability data sets over-predict the K_{sat} value, especially as the soils become finer grained.

As can be seen in this figure, it appears, based on the trend lines, that the equation was developed as a best fit to the converted air permeability data obtained for the 2003 study. The saturated hydraulic conductivity test results obtained for the present study, however, fit poorly to this equation, both in the general regression trends and at the extremes, especially for coarse gravelly soils. The K_{sat} values from the hydraulic conductivity tests were over-predicted by several orders of magnitude at the very coarse end (approximately, a $d_{10} > 0.8$ mm) and to a lesser extent at the finer-grained end (approximately, a $d_{10} < 0.04$ mm) of the range (see Appendix G for plots illustrating this). At the fine end of the range, this over-prediction should be expected since air permeability tests tend to measure permeability values that are higher than they should be for finer grained soils. At the coarse end, since the regression has been forced to fit the high conductivity values at the fine end, the coarse end predicted values will also be much too high, as can be observed in Figure 17a.

While not specifically mentioned in Massmann (2003), the difference in how the soil specimens are prepared in air permeability tests versus saturated hydraulic conductivity tests may also have contributed to the differences between the permeability values obtained by Massmann (2003) relative to those obtained in the current study. Since the soils tested in the current study have angular or irregular soil particles and in addition are well graded (due to their glacial origin), specimen preparation in a completely dry state for the air permeability tests is potentially problematic, especially for natural soils in the Puget Sound Region. As can be observed in Figure 17, it is the natural soils from the Massmann (2003) study that have the greatest scatter, especially for the finer grained soils. This issue of as placed moisture content is especially important for compacted soils, as the moisture content of the soil has a significant effect on the as compacted soil structure (Holtz and Kovacs 1981). In the current study, the soil

specimens are compacted in a moist condition and then saturated, which may improve uniformity of the as prepared specimens and provide more consistent results.

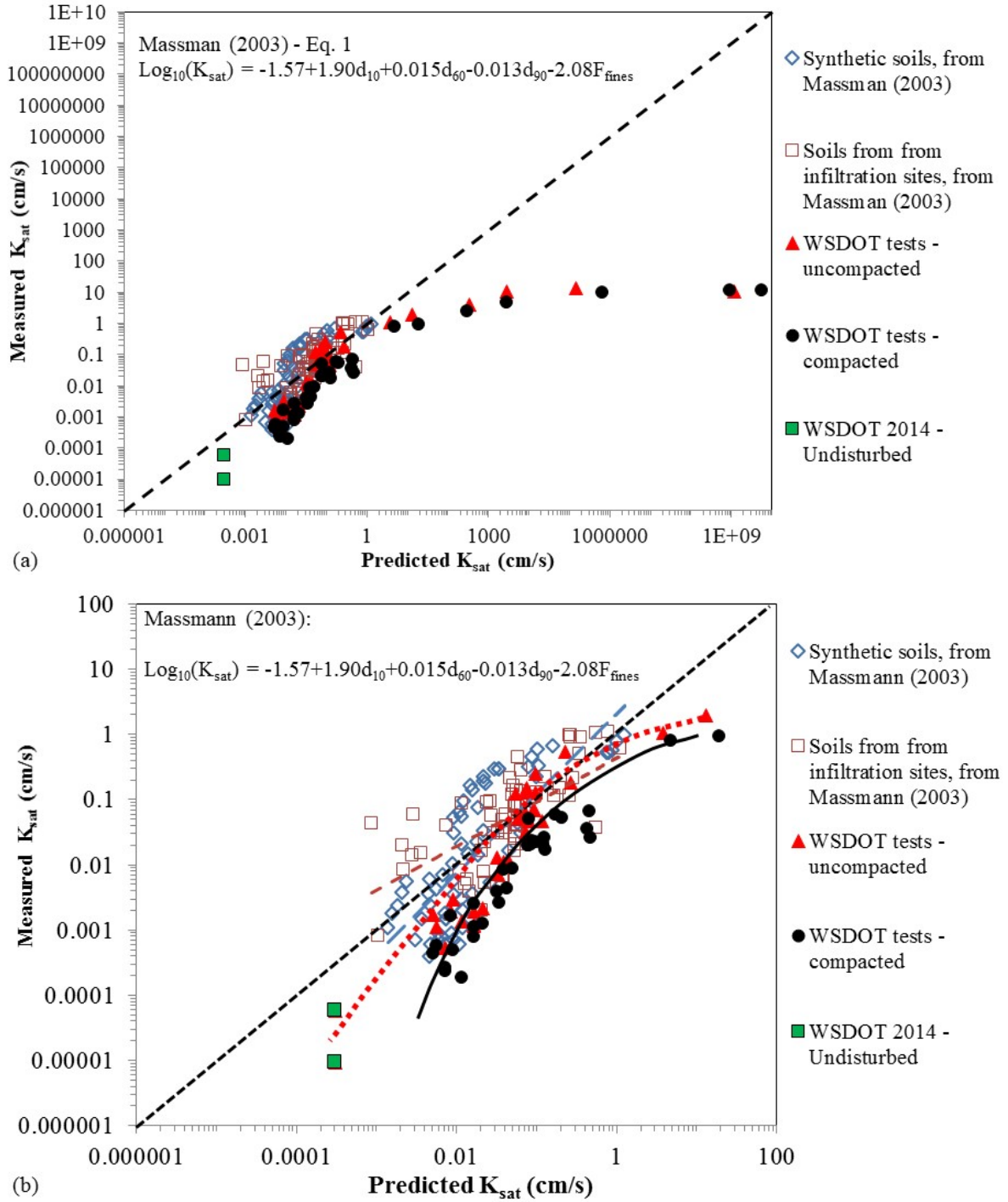


Figure 17. Measured versus predicted K_{sat} using Eq. 1 developed by Massmann (2003): (a) All data, (b) only data in which K_{sat} (predicted and measured) is between 0.0001 and 10 cm/second.

Considering the data shown in Figure 17, and the Eq. 1 analysis results provided in Appendix G, the mean and Coefficient of Variation (COV) of the bias of the WSDOT test results are 0.36 and 158%, respectively. If data with d_{10} values that are greater than 1.0 mm are excluded, the mean and Coefficient of Variation (COV) of the K_{sat} prediction bias (i.e., measured/predicted value) for all of the WSDOT test results are 0.43 and 142%, respectively. For the compacted WSDOT soils, excluding test results for soils with a d_{10} greater than 1.0 mm, the mean and COV of the K_{sat} prediction bias are 0.16 and 78%, respectively, and for the uncompacted soils, 0.69 and 110%, respectively. Therefore, in general, Eq. 1 tends to over-predict K_{sat} , especially for the compacted soils.

Analysis Using Other Historical K_{sat} Predictive Equations

To select or develop an improved predictive methodology to estimate K_{sat} , existing K_{sat} prediction methods available in the literature are considered first. From this point forward, only saturated hydraulic conductivity test results are considered. Furthermore, only methods applicable to granular soils with little or no cohesion are considered. Most prediction methods available in the literature for granular soils use one or more characteristic grain sizes. However, other parameters such as the soil porosity (η) or void ratio (e), are considered by the more reliable predictive methods. In fact, K_{sat} prediction methods should consider porosity or void ratio, as the density of the soil matrix (i.e., whether the soil is in a loose or dense state) can have a big effect on the saturated hydraulic conductivity of the soil (Chapuis 2012). This is also important to the current study if the effect of soil compaction is to be properly assessed.

The Hazen (1892), Slichter (1898), Terzaghi (1925), and Chapuis (2004) equations are investigated in more detail in this section. The Cozeny-Carmen equation (i.e., Eq. 5) is also investigated, but the results of that investigation are reported in detail in Appendix H for the interested reader.

Figure 18 illustrates the prediction performance of the Hazen Equation, assuming $C = 1.0$ in Eq. 2. The coefficient of 1.0 has been identified as being applicable to loose (i.e., uncompacted or normally consolidated) clean sands with a d_{10} value between 0.1 mm and 3 mm, a coefficient of uniformity C_u of less than 5. The data gathered by Chapuis (2004), as well as the uncompacted K_{sat} test results from the current study, plot

reasonably close to the one-to-one correspondence line. The compacted soils from the current study, however, plot below the one-to-one correspondence line, indicating that the Simplified Hazen Equation provides a larger prediction of K_{sat} than was measured. This is not surprising considering that the Hazen equation was originally developed for loose sands. This does point to the need for some type of correction to account for the effects of compaction on the soil K_{sat} value, such as decreased porosity or void ratio.

Figure 19 illustrates the prediction performance of the Slichter Equation (Eq. 3), adjusted to reflect a laboratory temperature of 20° C. Vucovic and Soro (1992) indicated that the Slichter Equation is applicable to a d_{10} size range of 0.01 mm to 5 mm. For all the data (i.e., both compacted and loose soil), the data trend does not follow the one-to-one correspondence line very well for finer grained soils with lower hydraulic conductivity values. However, the compacted soils from the current study plot consistently with the rest of the data, indicating that accounting for porosity could address the effect of compaction.

The equation developed by Terzaghi (1925), discussed previously and presented as Eq. 4, also includes porosity and therefore can consider the effects of compaction. The Terzaghi (1925) Equation predictions for all of the saturated hydraulic conductivity test data presented previously are shown in Figure 20. Based on this figure, the Terzaghi Equation tends to under-predict the K_{sat} values when the measured K_{sat} is less than 0.002 cm/s.

The equation developed by Chapuis (2004), discussed previously and presented as Eq. 6, includes the void ratio, e . Since void ratio is considered in this equation, it also can consider the effects of compaction. The Chapuis (2004) Equation predictions for all of the saturated hydraulic conductivity test data presented previously are shown in Figure 21. Figure 21(a) shows the relationship between the d_{10} -void ratio parameter and the measured K_{sat} value. Figure 21(b) shows the prediction trend between the measured K_{sat} and the predicted K_{sat} using the Chapuis Equation.

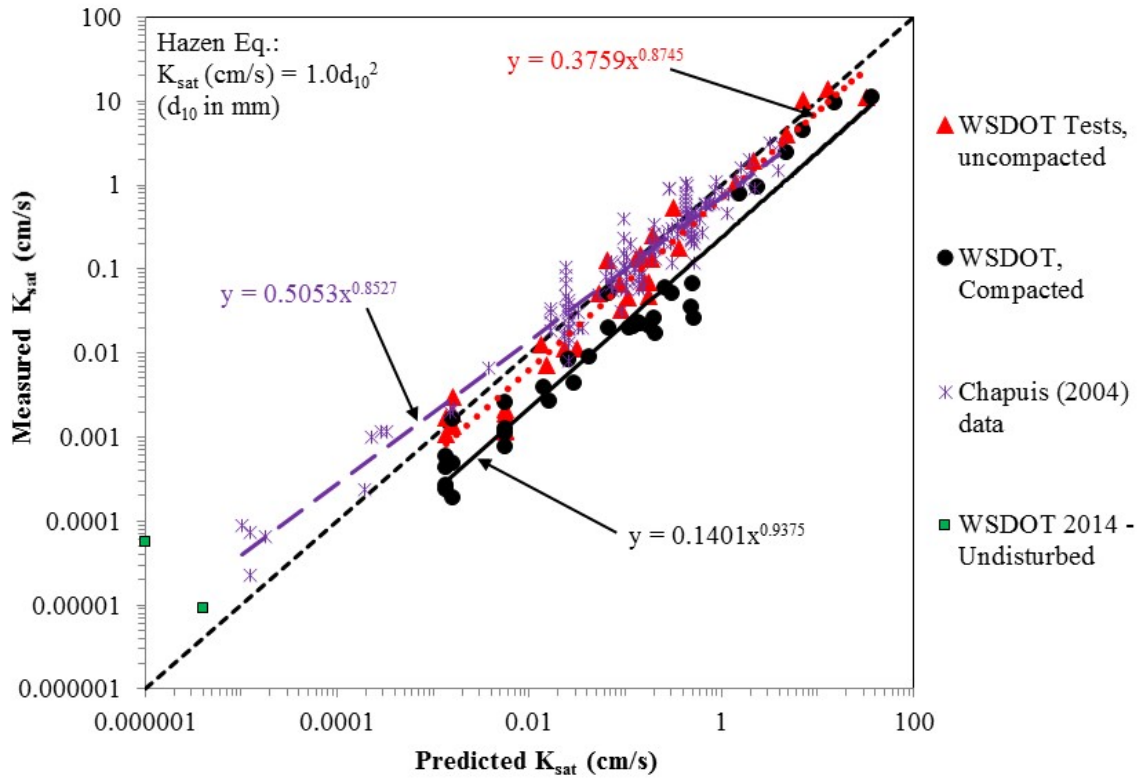


Figure 18. K_{sat} predictions using the Hazen Equation (with outliers removed).

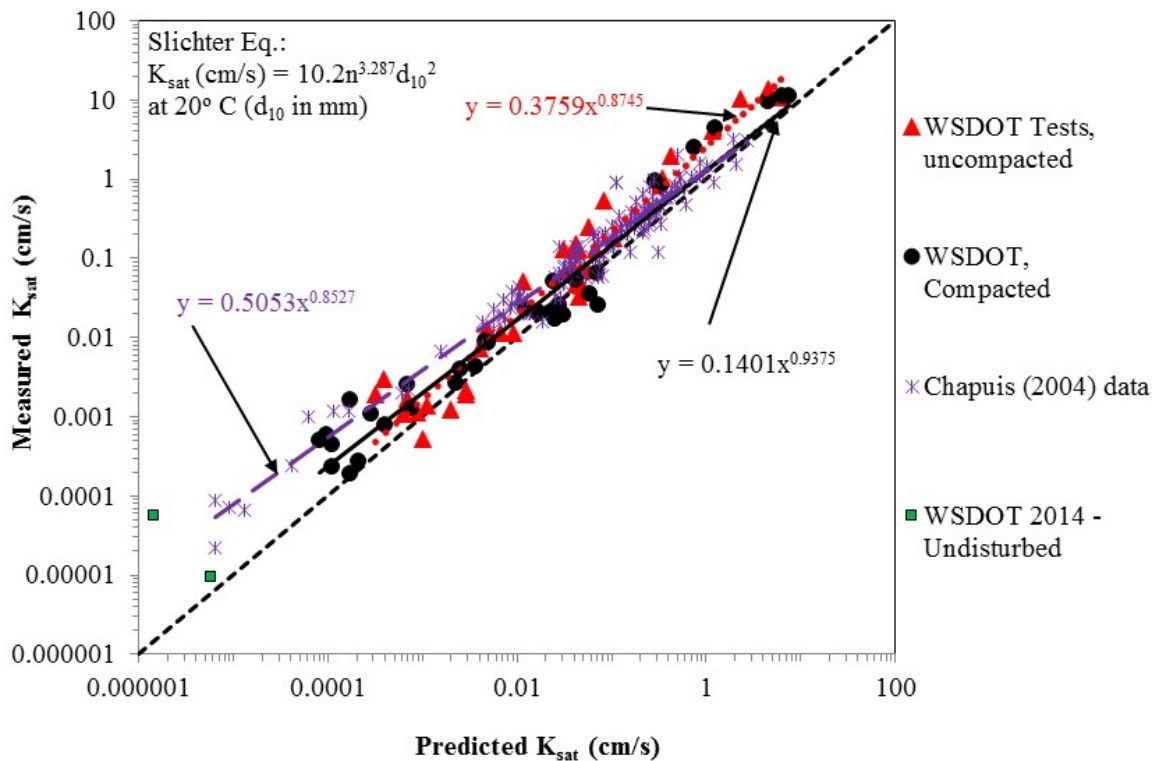


Figure 19. K_{sat} predictions using the Slichter Equation (with outliers removed).

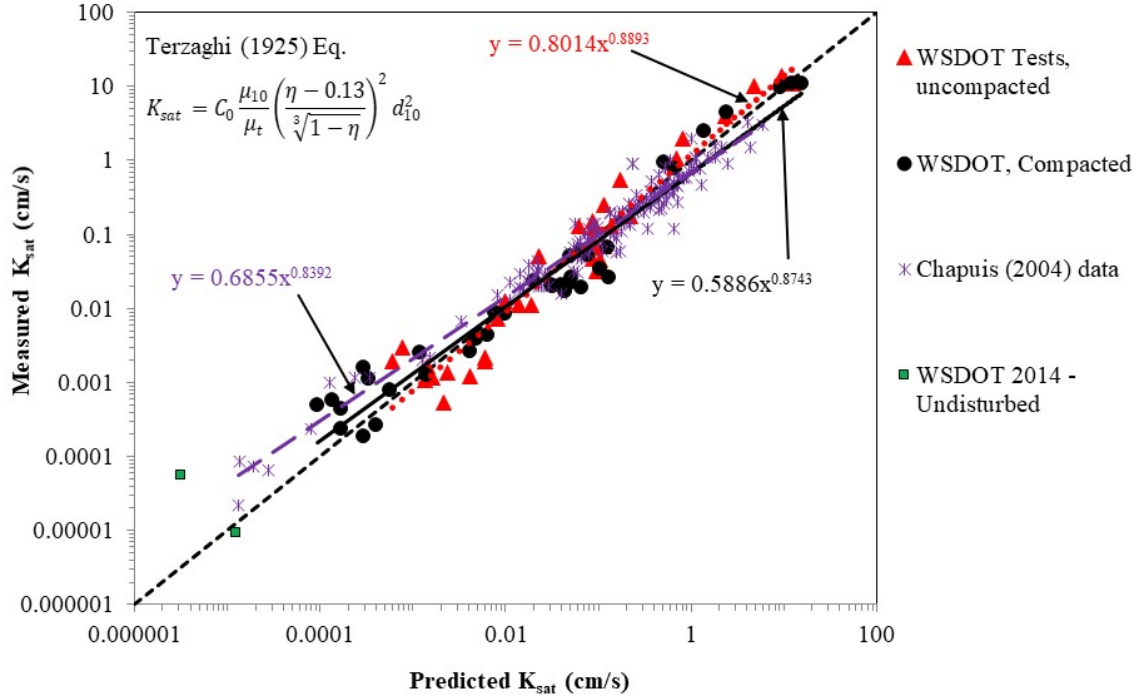


Figure 20. K_{sat} predictions using the Terzaghi Equation (with outliers removed).

For all the WSDOT data in Figure 21(b), the data trend does not follow the one-to-one correspondence line very well. Based on this figure, for the WSDOT tests, the Chapuis Equation tends to over-predict the K_{sat} values when the predicted K_{sat} is less than 0.01 cm/s and under-predict K_{sat} when the predicted K_{sat} is greater than about 0.5 cm/s. However, for the data published in Chapuis (2004), the Chapuis Equation provides a reasonably accurate prediction through most of the range in the data.

Regarding the two undisturbed Shelby Tube specimen test results, all of the methods (figures 18 through 21) had a poor prediction accuracy. However, for those two data points, the average of the two points generally followed the overall trend in the data.

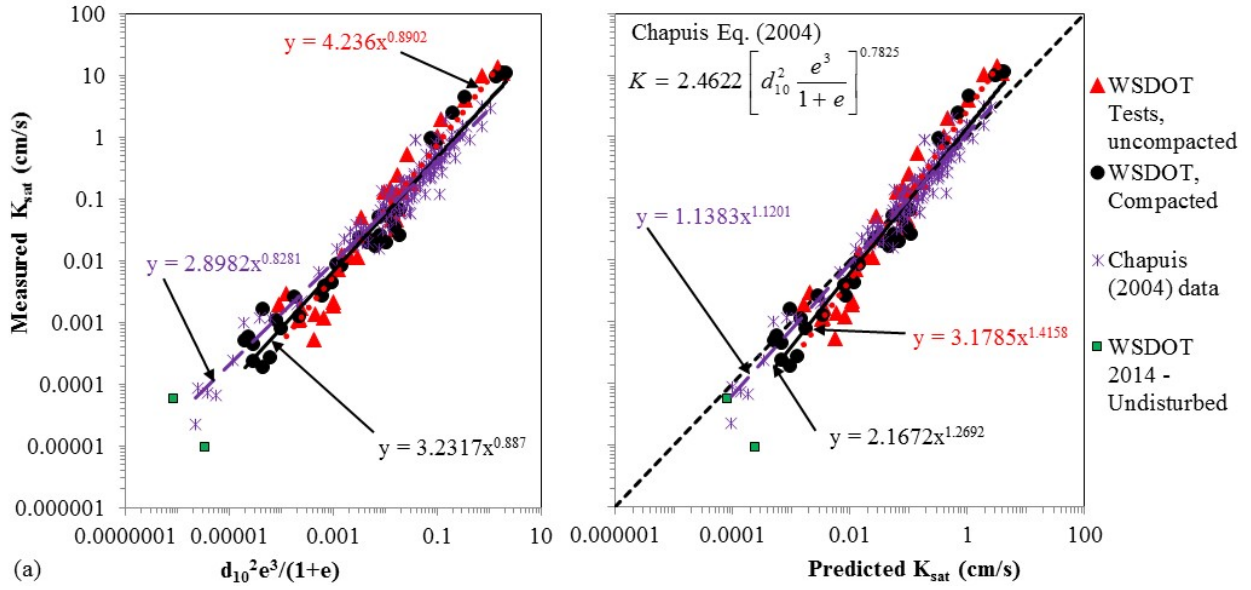


Figure 21. (a) Measured K_{sat} as a function of the Chapuis grain size – void ratio parameter, (b) K_{sat} predictions using the Chapuis (2004) equation (with outliers removed).

All of these prediction methods have some short-comings in accurately predicting the test results from the current study, some more minor than others, especially those that represent compacted soils. Minor empirical adjustments to these existing methods to provide the improvement needed are considered. However, before making these adjustments, assessment of the test results for possible outliers that could be removed is conducted, and outlier data removed.

The Slichter, Terzaghi and Chapuis methods can account for the effect of compaction through the soil porosity or void ratio. Therefore, these three methods are considered for further development, since the primary objective of this research is to account for the effect of compaction on K_{sat} .

Improvements to Existing Predictive Equations

Optimization of these historical methods was accomplished by using the Microsoft Excel function SOLVER, using the bias (defined as measured/predicted value of K_{sat}) statistics for the prediction method. The mean and coefficient of variation (COV) of the bias for the total measured hydraulic conductivity data set (i.e., all WSDOT tests conducted for the current study and the data from Chapuis 2004) as well as subsets within

this data were used to characterize the statistics of the data. The data from Massmann (2003) were excluded from the dataset used for optimization purposes, since those data were from air conductivity testing. Once the SOLVER optimized coefficients and exponents were obtained, they were further optimized by a trial and error process to obtain the lowest COV, considering the dataset as a whole and considering the various subsets of the data, as well as the trends in the data.

When using existing methods, it is important to identify the range of conditions for which the method is considered valid. Therefore, in addition to plotting the measured versus the predicted K_{sat} values for each method considered, the K_{sat} prediction method bias (Allen et al. 2005), defined as the measured/predicted K_{sat} value, as a function of the d_{10} size is also plotted to be able to more accurately see the range of applicability for the method and considered data. For a prediction method to be considered reasonably reliable, the “measured” prediction method bias should not exhibit significant dependency on the key input parameters that could affect the predicted value, in this case d_{10} , as well as the prediction itself (Bathurst et al. 2008, 2010). Therefore, in plots of prediction method bias versus the d_{10} size, for example, the regression should be approximately flat and as close to a bias of 1.0 as possible.

It should also be recognized that the range of applicability for these existing predictive equations reported in the literature only considers the data available at the time that were used to assess that range of applicability. The current study adds additional data not available previously that may require modification of the range of applicability.

Note that Chapuis (2012) defined “good predictions” for K_{sat} as predicted values that fall within one-half and twice the measured values. However, NAVFAC (1974) focused on a range of 0.33 to 3 times the mean of the measured values and indicated that two-thirds of the measured values fall within that range. Inevitably, there will be a small percentage of data points that fall outside these sets of ranges randomly distributed throughout the range of either predicted K_{sat} value or some soil parameter such as the d_{10} size. This is especially true when dealing with angular or irregularly shaped soil particles. This needs to be considered when establishing ranges of applicability for the various predictive equations. Chapuis (2012) used both ranges when assessing the acceptability of the predictions for the various K_{sat} prediction equations. Therefore, both

ranges are considered in this report (at least approximately) when assessing the range of applicability of the various K_{sat} equations.

Predictive equations considered to be good candidates in this study for optimization, considering the need to address the effects of compaction, include the Slichter, Terzaghi, and Chapuis methods. Other methods, such as the Hazen, Cozeny-Carmen, and Massmann methods, were also considered with regard to the soil conditions applicable to those methods. However, efforts to develop empirical improvements to those methods resulted in only very limited prediction accuracy improvement, if any.

With regard to the Slichter Method (Eq. 3), this optimization process resulted in the equation coefficient increasing from 10.2 to 21.2, the porosity exponent increasing from 3.287 to 3.5, and the d_{10} exponent decreasing from 2 to 1.75 as shown the following equation:

$$K_{sat} = 21.2 \eta^{3.5} d_{10}^{1.75} \quad (9)$$

Where K_{sat} is in cm/s and d_{10} is in mm, and all variables are as defined previously.

Figure 22 illustrates the prediction performance of the optimized equation. This optimization resulted in visually better alignment with the one-to-one correspondence line than the original equation (compare to Figure 19).

Regarding the trends in the prediction bias (i.e., measured/predicted value of K_{sat}), Figure 23 shows the bias as a function of the d_{10} size for both the original Slichter Equation and the optimized equation. For the original equation, the scatter in the bias is large. For the optimized equation, all the scatter in the bias is reduced and closer to 1.0. However, the scatter in the two undisturbed specimen test results remains significant. The range of applicability with regard to d_{10} size for this optimized equation, based on Figure 23, is from approximately 0.003 mm to 3 mm.

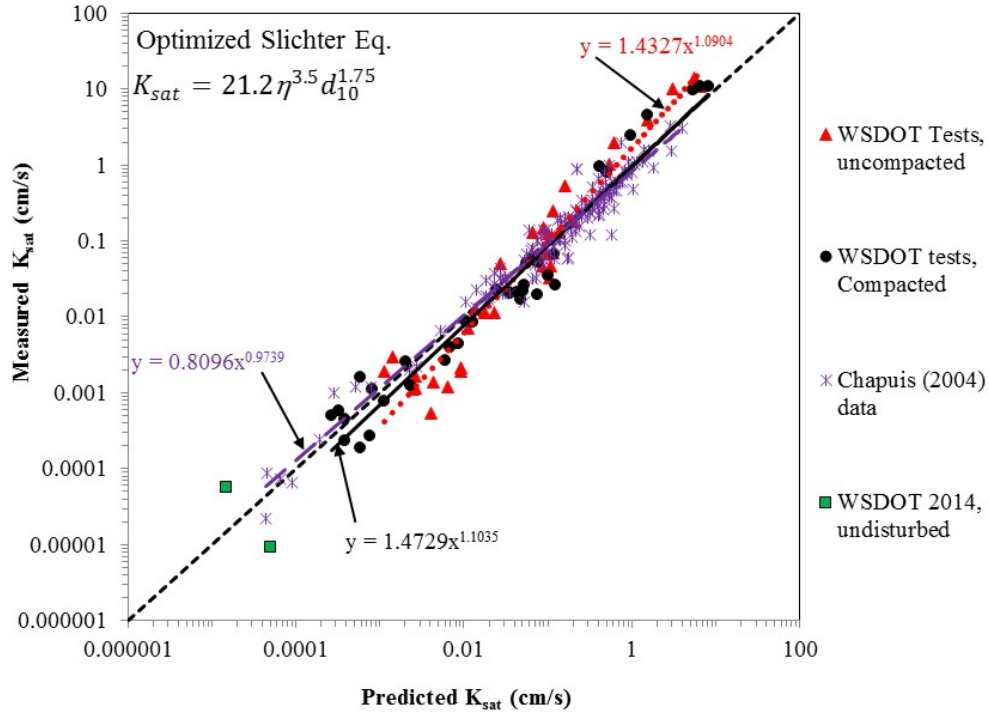


Figure 22. K_{sat} predictions using the optimized Slichter Equation, with outliers removed.

With regard to the Terzaghi Equation, through this optimization, the ratio of μ_{10}/μ_t was left unchanged at 1.3, the porosity constant and denominator exponent (i.e., the cube root) in the Terzaghi equation (Eq. 4) was left unchanged, C_0 is changed from 8.0 for smooth (rounded) grains and 4.6 (for irregular grains) to 4.6 (all soils), the overall exponent for the porosity expression is changed from 2 to 1.7, and the d_{10} exponent was changed from 2 to 1.75. The optimized Terzaghi Equation is therefore as follows:

$$K_{sat} = C_0 \frac{\mu_{10}}{\mu_t} \left(\frac{\eta - 0.13}{\sqrt[3]{1 - \eta}} \right)^{1.7} d_{10}^{1.75} \quad (10)$$

A minor differentiation in C_0 for smooth versus irregular/angular soil grains could be done, but the improvement is only very minor. Figure 24 illustrates the prediction performance of the optimized Terzaghi equation. This optimization resulted in visually better alignment with the one-to-one correspondence line than the original equation (compare to Figure 20).

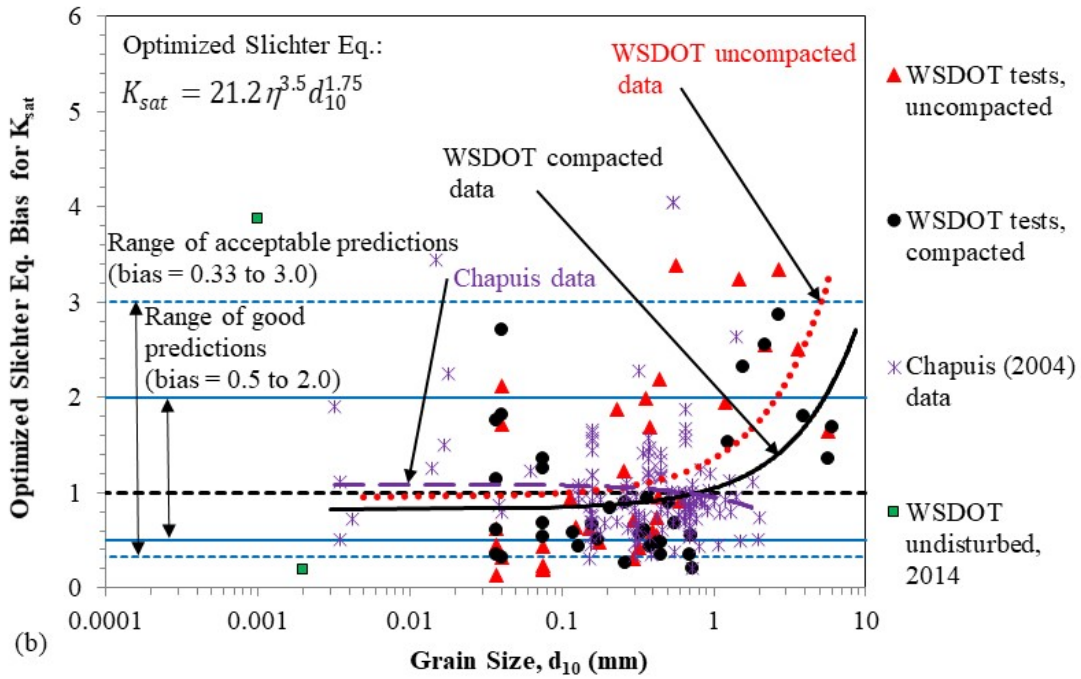
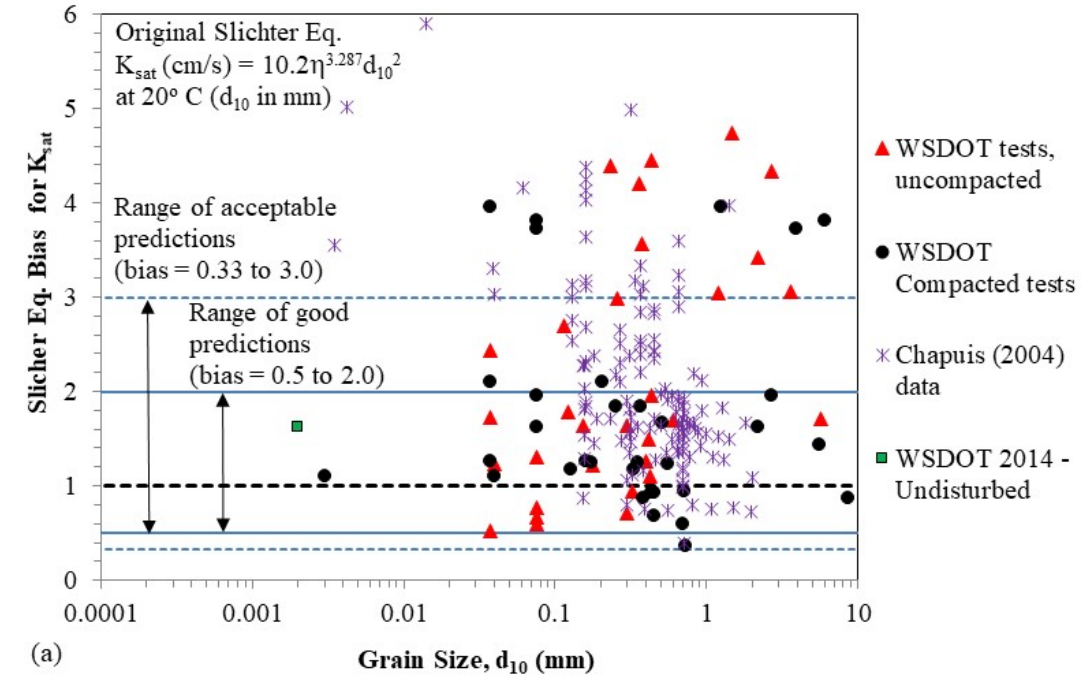


Figure 23. Method bias as a function of d_{10} size for (a) original Slichter Equation, but for 20° C, with outliers removed, and (b) optimized Slichter Equation at 20° C, with outliers removed (note: linear functions used for regressions).

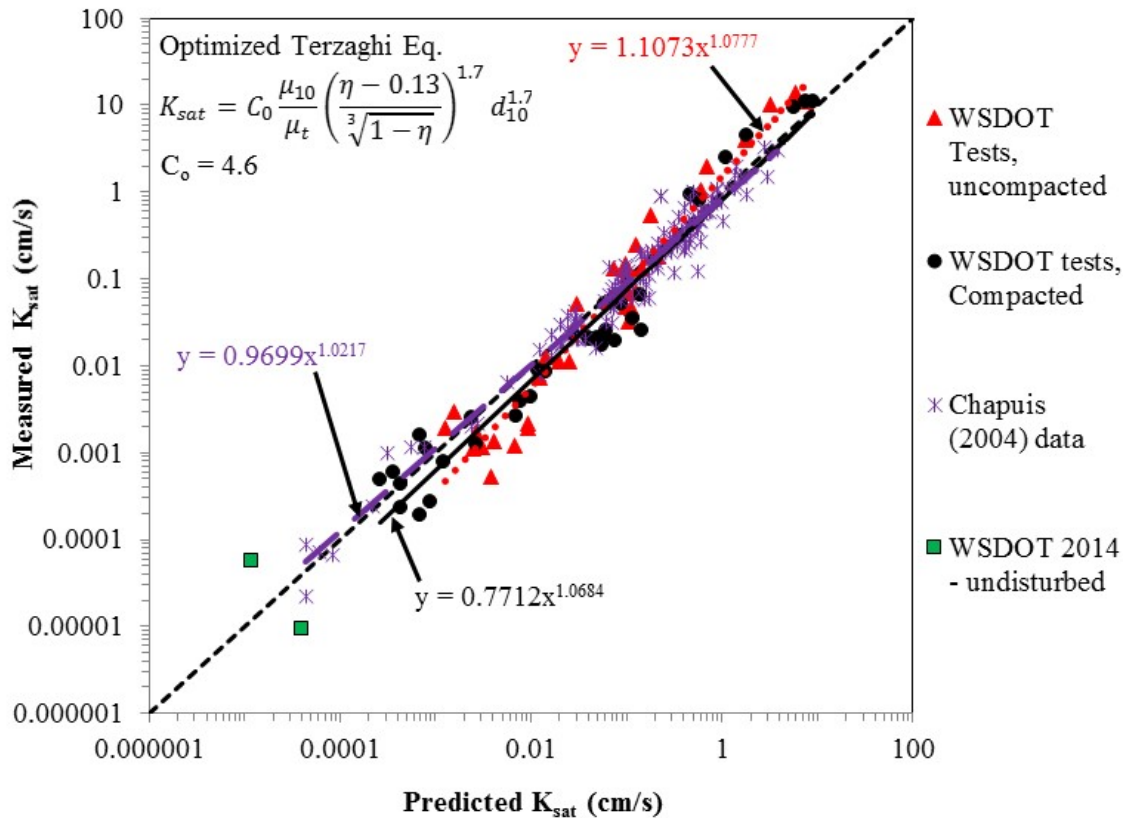


Figure 24. K_{sat} predictions using the optimized Terzaghi Equation, with outliers removed.

Figure 25 illustrates the trend in the bias as a function of the d_{10} size for both the original Terzaghi Equation and the optimized equation. For the original equation, there is an obvious trend of increasing bias as the d_{10} size decreases. This results in a rather restricted range of applicability regarding the d_{10} size of 0.1 mm to 5 mm. However, for the optimized equation, the scatter in the bias is reduced and closer to 1.0. The range of applicability, with regard to d_{10} size, increases to include finer grained soils, ranging from approximately 0.003 mm to 3 mm, similar to the Slichter Method.

It should be noted that the d_{10} exponent in both the Slichter and Terzaghi methods was optimal when the exponent was reduced from 2 to 1.75.

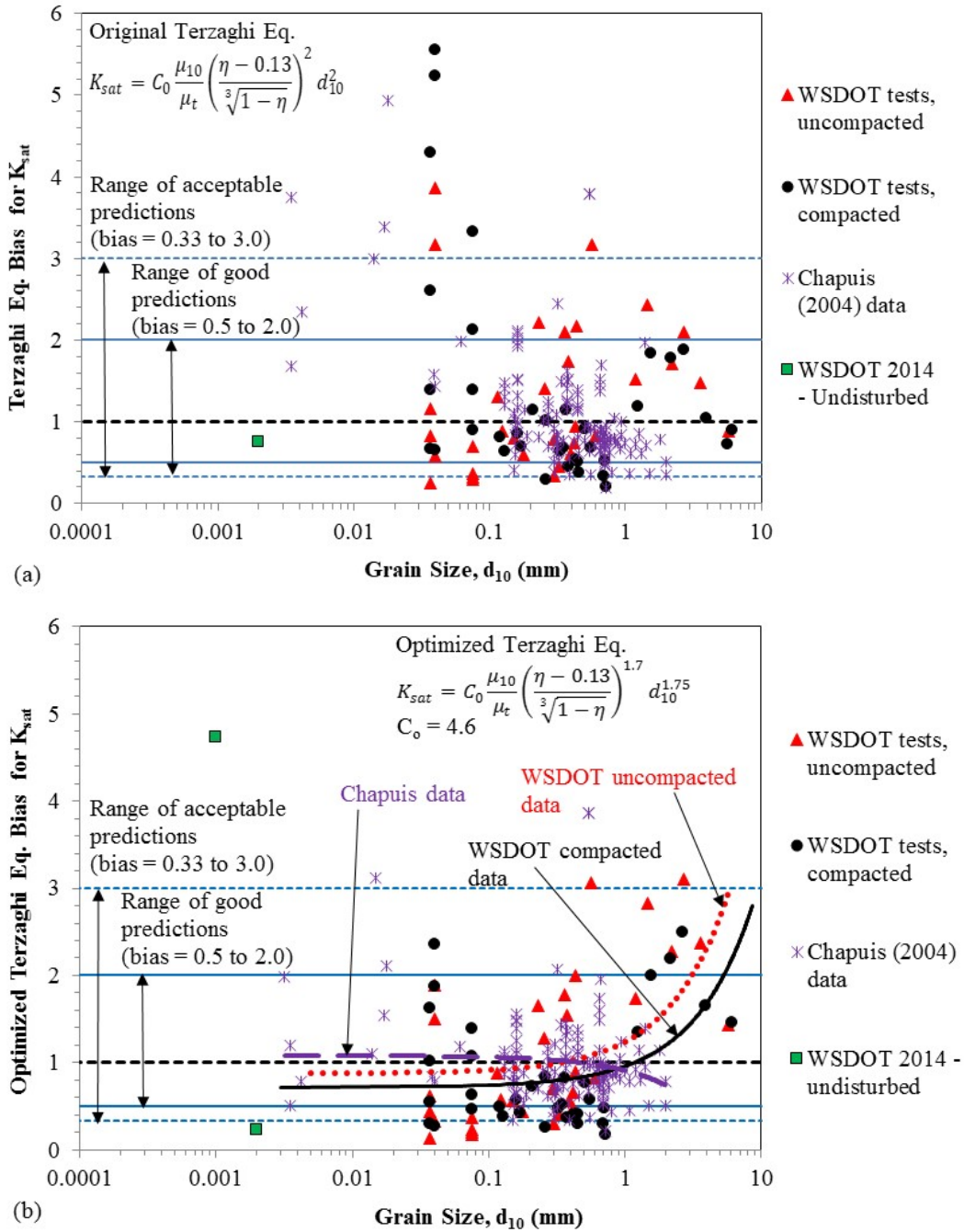


Figure 25. Method bias as a function of d_{10} size for (a) original Terzaghi Equation with outliers removed, and (b) optimized Terzaghi Equation with outliers removed (note: linear functions used for regressions).

With regard to the Chapuis Equation (Eq. 6), this optimization process resulted in the equation coefficient increasing from 2.4622 to 4.0, the equation exponent increasing

from 0.7825 to 1.25, the void ratio exponent decreasing from 3 to 1.9, and the d_{10} exponent decreasing from 2 to 1.4 as shown in Equation 11:

$$K_{sat} = 4.0 \left[d_{10}^{1.4} \frac{e^{1.9}}{1+e} \right]^{1.25} \quad (11)$$

It should be noted that the combined exponent for d_{10} is $1.4 \times 1.25 = 1.75$, which is consistent with the 1.75 d_{10} exponent in both the optimized Slichter and Terzaghi equations.

Figure 26 illustrates the prediction performance of the optimized Chapuis Equation. This optimization resulted in visually better alignment with the one-to-one correspondence line than the original equation (compare to Figure 21).

Figure 26 (b and c) illustrates the trend in the bias as a function of the d_{10} size for both the original Chapuis Equation and the optimized equation, respectively. For the original equation, there is an obvious trend of increasing bias as the d_{10} size increases, especially above 1 mm. This results in a range of applicability regarding the d_{10} size of approximately 0.005 mm to 0.7 mm. However, for the optimized equation, the scatter in the bias is reduced and closer to 1.0 on average. However, the scatter increases somewhat at the lower end of the d_{10} sizes, and for d_{10} sizes greater than 1.0 mm, there is still an upward trend in the data, though reduced from what it was for the original equation. The range of applicability, with regard to d_{10} size, increases to a range of approximately 0.003 mm to 3 mm, similar to the Slichter and Terzaghi optimized equations. However, the optimization process for the Chapuis equation did not bring the compacted and uncompacted WSDOT test data together as well as the optimized Slichter and Terzaghi equations.

Optimization of the Chapuis Equation to obtain the best fit of all the data sets resulted in improvement in the bias values similar to the Slichter and Terzaghi equations. The compacted soil sample bias values were more conservative (less than 1.0) relative to the optimized Slichter and Terzaghi equation predictions. For all three K_{sat} prediction equations, only modest improvements in the data scatter, especially within the d_{10} size range of applicability (i.e., 0.003 to 5 mm), could be obtained for the WSDOT data.

However, the improvements were still large enough to justify the empirical modifications made.

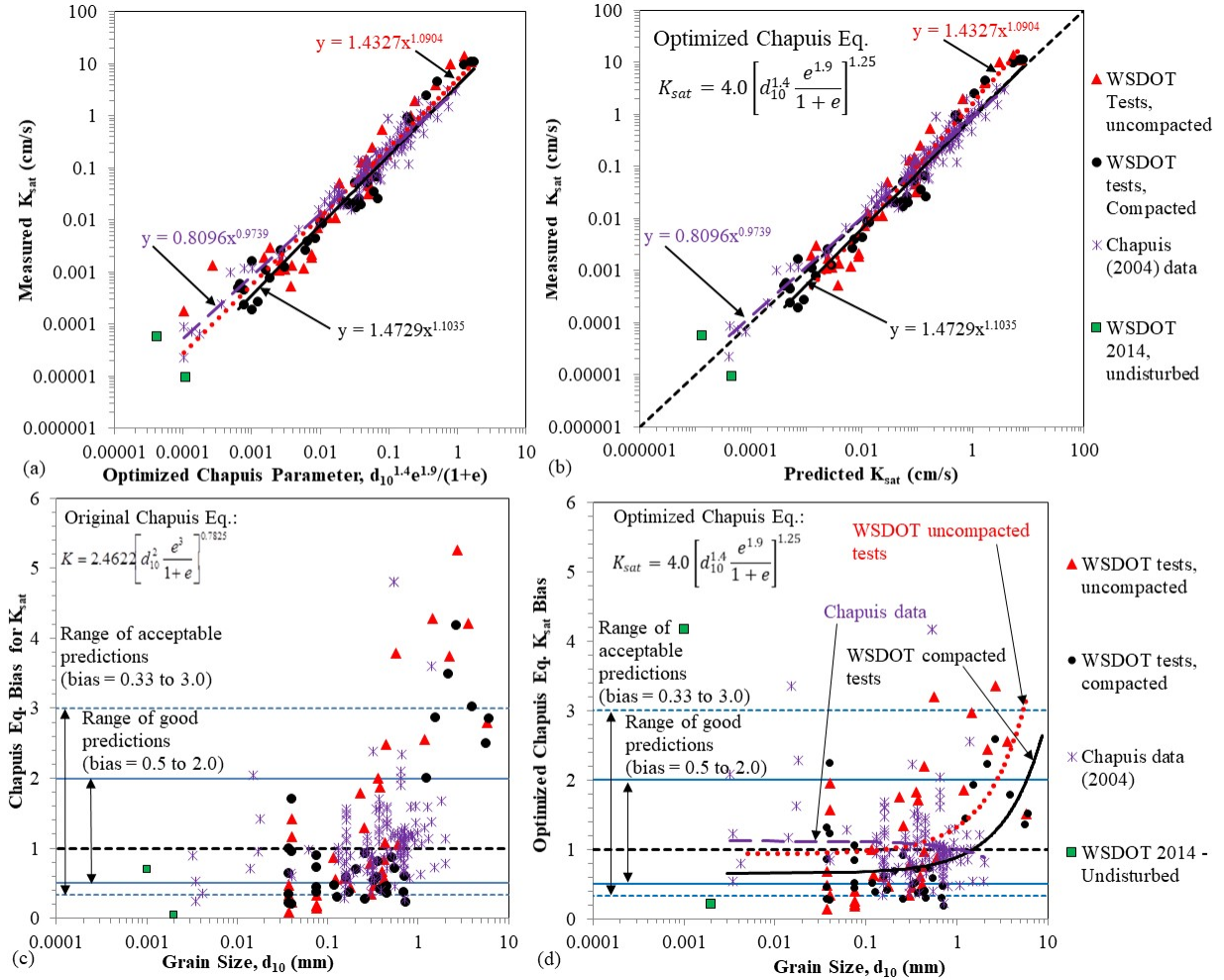


Figure 26. K_{sat} prediction for the optimized Chapuis Equation (i.e., Eq. 11), with outliers removed: (a) measured K_{sat} vs. optimized Chapuis parameter, (b) K_{sat} predictions using the optimized Chapuis Equation, (c) method bias as a function of d_{10} size for original Chapuis Equation, and (d) method bias as a function of d_{10} size for optimized Chapuis Equation (power functions used for regressions in parts a and b, and linear functions used in part d).

The inability to obtain more significant improvements with regard to prediction accuracy of the K_{sat} data obtained from the current study is likely due to the angularity and irregular shape of the soil particles tested. Chapuis (2004) specifically indicated that angular soils were troublesome with regard to prediction accuracy.

Since the focus of this study was on typical embankment soils in a compacted state, results for intermediate levels of compaction are not available. However, the data provided and the curve fitting conducted for all the K_{sat} prediction methods should represent the typical extremes of the compaction state of soils. This may not, however, represent the as compacted state of glacially consolidated soils such as is typical of glacial till in the state of Washington, since such soils were compacted under 3,000 ft (or more) of glacial ice.

Estimating Porosity Based on Grain Size Parameters and Compaction Level

This report section presents an investigation of the prediction of porosity from soil grain size data if a measured porosity is not available. The estimated porosity could be used with the Terzaghi (1925) or Slichter (1898) methods, for example, if the measured porosity is not available. To accomplish this, it was attempted to estimate the soil porosity, η , from grain size data. Vucovic and Soro (1992) attempted to estimate porosity using only the C_u value. Their prediction equation for soil porosity is as follows:

$$\eta = 0.255(1 + 0.83^{C_u}) \quad (12)$$

This equation was used to predict η for all the test results presented in this report in which the C_u could be determined. A plot of the results is provided in Figure 27. Based on this figure, the prediction bias trend lines for both the soil d_{10} size and the soil C_u , at least for “loose” (uncompacted) soil, are not horizontal. There is also an obvious difference between compacted and uncompacted soils except at large d_{10} sizes (i.e., gravels which also had low C_u values), which would be expected. This indicates that both the d_{10} size and C_u may not be formulated correctly in the equation – if they were, the trend lines would be horizontal or at least nearly so. Chapuis (2012) indicated that using grain size parameters without considering other parameters indicative of how densely packed the soil is will result in an inaccurate prediction of the porosity or void ratio.

To develop an improved predictive equation for porosity, the measured porosity values obtained from the K_{sat} laboratory tests are plotted against potential key soil parameters to assess whether or not these parameters have an influence on the porosity. These plots are shown in Figure 28.

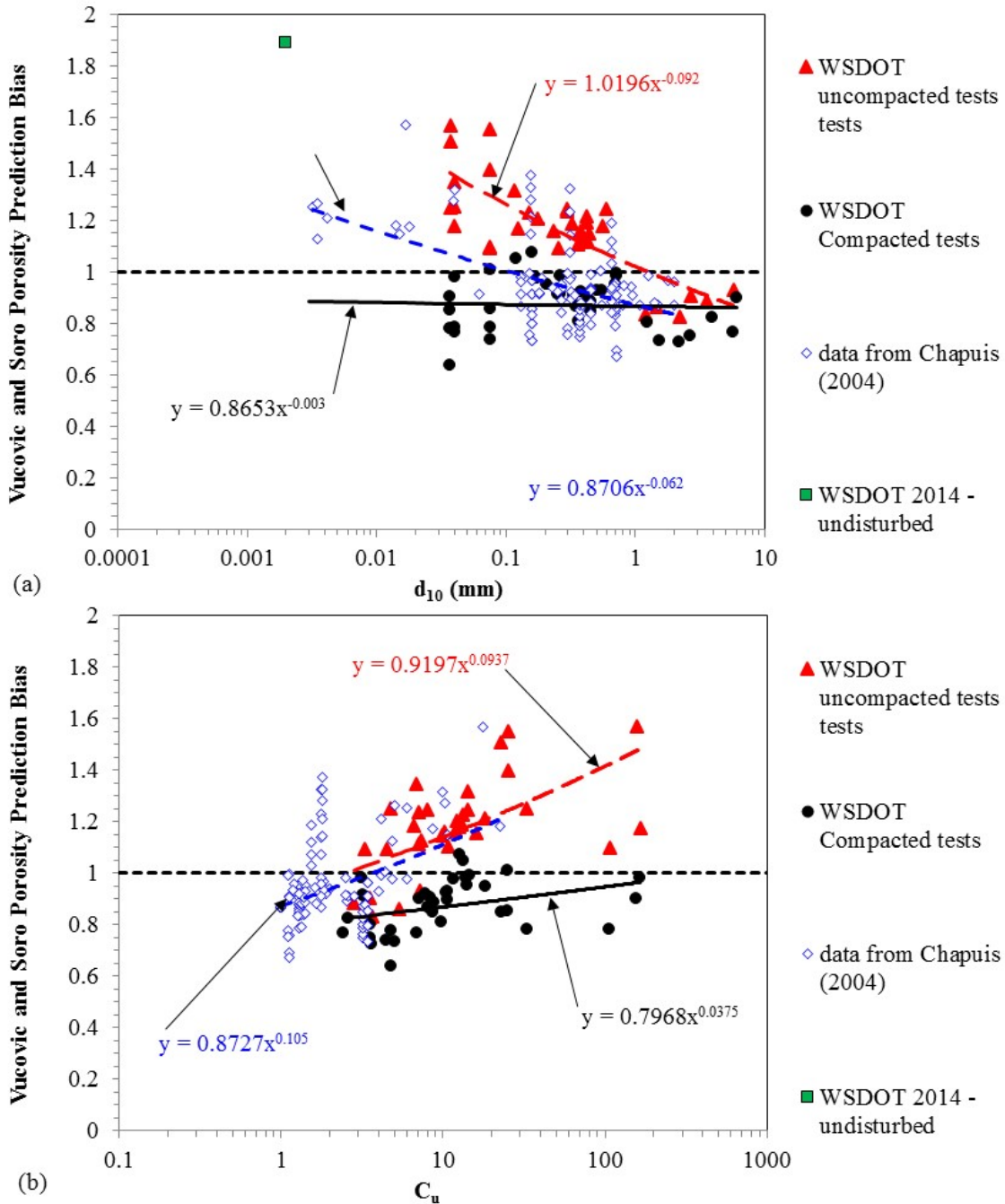


Figure 27. Porosity prediction bias for Vučović and Soro (1992) method as a function of: (a) d_{10} size, and (b) coefficient of uniformity, C_u (outliers removed).

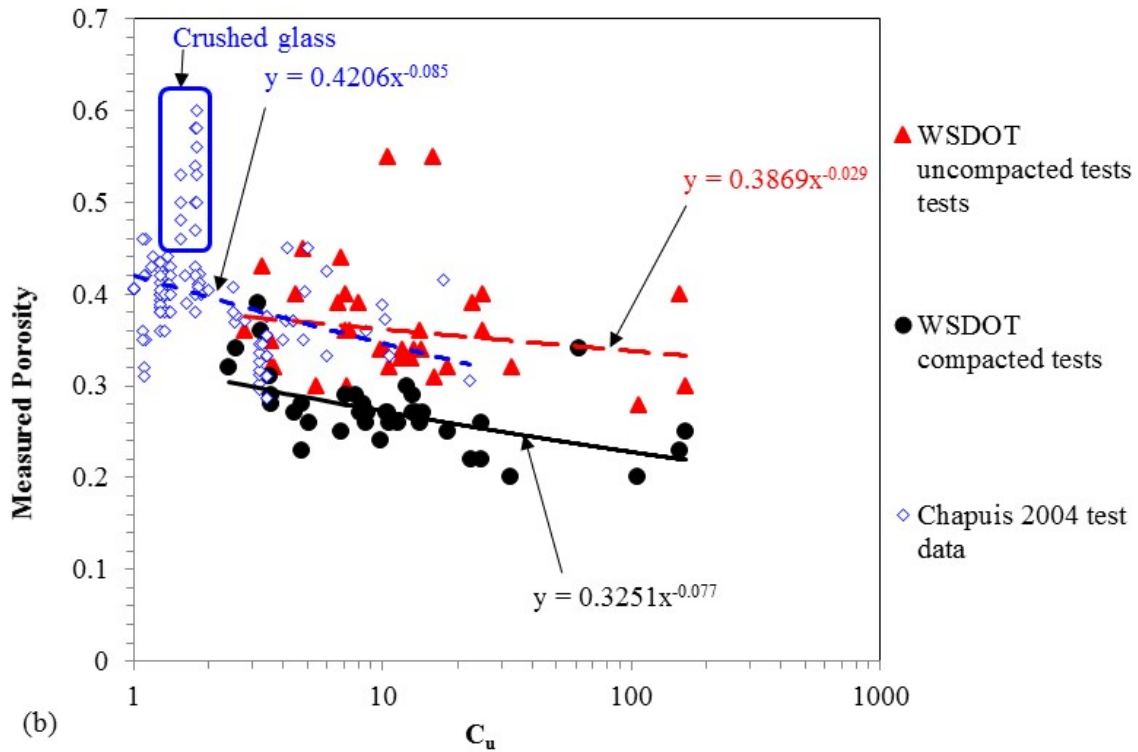
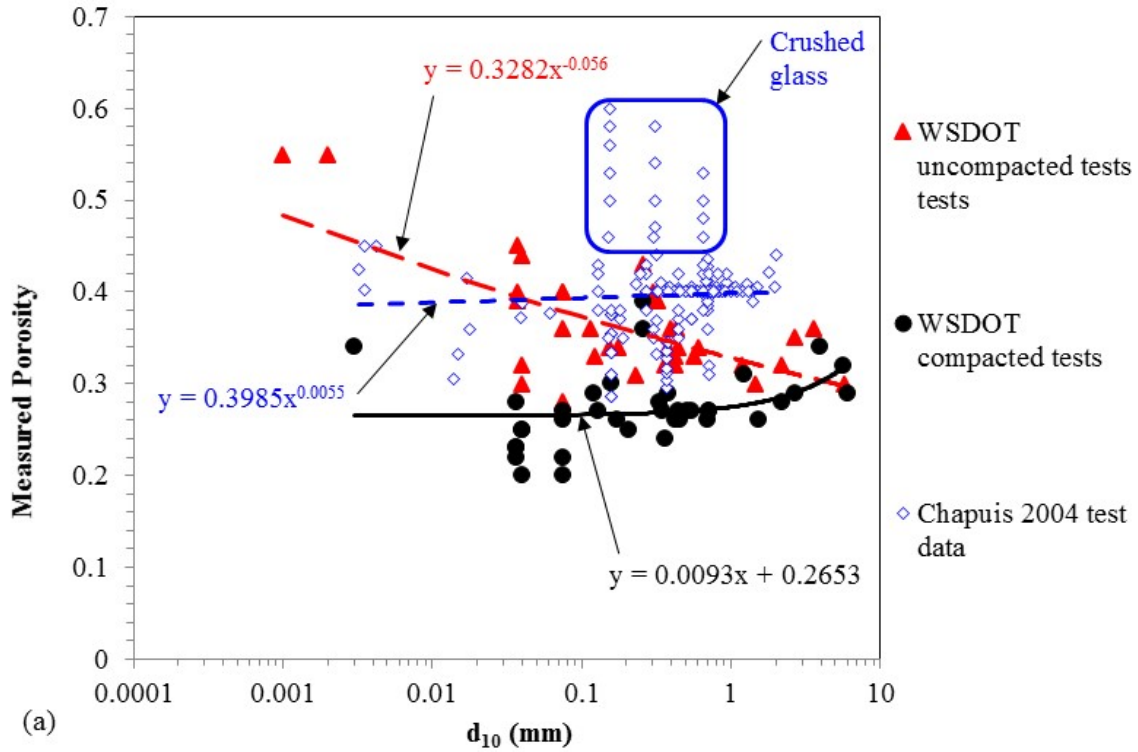


Figure 28. Effect of compaction on porosity as a function of: (a) the d_{10} size, and (b) the coefficient of uniformity, C_u (outliers removed).

It can be observed in Figure 28 that for uncompacted (i.e., loose) soils, there may be some dependency of porosity on the d_{10} size for the WSDOT soils. However, there is little d_{10} size dependency for the data gathered by Chapuis (2004). Furthermore, for both data sets, the scatter in the data is rather large. For the compacted soils, the bias trend line for the d_{10} size was approximately horizontal, indicating that the d_{10} size has little effect on the porosity if the soil is compacted. It should be noted that some of the data from Chapuis (2004) is crushed glass, and he indicated that predictions for the crushed glass were poor. If the crushed glass data are removed from the Chapuis dataset, the trend line for that data would line up better with the uncompacted WSDOT test data. Furthermore, the Chapuis (2004) data set included some test results for moderately compacted specimens. However, for C_u , all data sets have what appears to be a visual dependency between porosity and C_u , indicating that the soil C_u is an important factor in the determination of porosity, with or without compaction.

In the current study, it was attempted to consider both the soil d_{10} size and the coefficient of uniformity, C_u , with the objective of developing an improved correlation. This correlation would also need to consider how densely packed the soil is. Starting with the regressions made as shown in Figure 28, using the same optimization approach described earlier (i.e., using Solver in Excel as a starting point), coefficients and exponents applied to the variables d_{10} and C_u were adjusted to obtain the best visual fit of the data. This was attempted first considering only the uncompacted and lightly compacted (i.e., loose) soils. The coefficients and exponents were adjusted such that the COV of the bias (i.e., measured/predicted porosity value) was minimized and the mean bias was as close to 1.0 as possible. The form of the equation used to accomplish this is shown below:

$$\eta = P \times d_{10}^a \times C_u^b \times (F_{cp}) \quad (13)$$

where,

P = empirical porosity coefficient ($P = 0.4$)

a = empirical d_{10} exponent ($a = -0.08$)

b = empirical coefficient of uniformity coefficient ($b = -0.1$)

F_{cp} = compaction factor for porosity (set equal to 1.0 if not compacted or is loose)

However, it was first attempted to do this without considering the d_{10} size (i.e., “a” set equal to 0), since based in Figure 28 the trend with d_{10} appears to be marginal at best. To obtain the best fit of the data, it was determined that $P = 0.4$ and $b = -0.1$ should be used. The result of doing this is illustrated in Figure 29(a). Two observations can be made from this plot. The first observation is that both the WSDOT uncompact soil tests and the Chapuis (2004) soil test data sets (which primarily contains uncompact or lightly compacted specimens) appear to have a visual trend with the soil d_{10} value. Therefore, it appears that the soil d_{10} size should be considered when estimating the porosity for uncompact or lightly compacted (loose) soils. The second observation that can be made is that the compacted soil porosity is not affected by the soil d_{10} size, and that the compacted soil data trend line is on average about 85% of the measured soil porosity values (i.e., at a bias of 1.0). So if the d_{10} size is considered for the uncompact (loose) soil cases, the compaction factor F_{cp} will need to have a d_{10} component that in effect cancels out the d_{10} component used for the uncompact/loose soil case. Interestingly, all the data sets shown in this figure tend to converge at large (i.e., coarse sand/fine gravel sized) d_{10} sizes at a bias of slightly less than 1.0 in the plot. For such coarse soils, which for the testing conducted also tended to have low C_u values, compaction had little effect on the porosity, which was an expected outcome.

Figure 29(b) illustrates the effect of considering the d_{10} size for the uncompact soil tests, in which the exponent for d_{10} in Eq. 13 is set equal to -0.08 so that the prediction bias for the uncompact soils is near 1.0 for most of the range. However, doing so causes the compacted soil data set to have a dependency on the d_{10} size. F_{cp} must be developed to negate this effect, and also bring the prediction bias of the compacted soil data set close to 1.0 for its full range.

Eq. 14 provides the compaction factor formulation needed to address these issues.

$$F_{cp} = C_f d_{10}^c \tag{14}$$

where,

F_{cp} = porosity compaction factor

C_f = compaction factor coefficient ($C_f = 0.85$)

c = compaction factor exponent ($c = 0.08$)

Using this equation, for a range of d_{10} values from 0.001 mm to 1 mm, F_{cp} ranges from 0.49 to 0.85, respectively. The reduction in porosity due to compaction, therefore, is approximately 50% for silts, and once d_{10} is at 10 mm or more (coarse gravels), there is no effect of compaction on the porosity. F_{cp} should be set equal to 1.0 if the soil is not compacted, or for natural soils as deposited that are normally consolidated or lightly over-consolidated. For compacted soils, the combination of eq's. 13 and 14 simplifies to:

$$\eta = 0.34C_u^{-0.1} \quad (15)$$

Figure 30 illustrates the accuracy of the porosity predictions when using the combination of eq's. 13 and 14. Part (a) of Figure 30 shows all four data sets separately, but the regression line is for all the data together. The data scatter does seem to increase for the higher values of porosity (again, this is primarily due to the crushed glass data subset). However, the R^2 value for the data regression is moderately strong, and the accuracy of the predictions is judged visually to be acceptable. Part (b) of Figure 30 illustrates that there is little, if any, dependency between the porosity prediction bias and the d_{10} size, especially for test data obtained from the current study, indicating that the porosity prediction equation adequately addresses the most important variables for the data set considered. The minor dependency observed for the Chapuis (2004) data set is likely due to the crushed glass subset at d_{10} sizes 0.1 to 0.8 mm and bias values greater than 1.0, and the Polytechnique Hydrogeo Lab fine silty sand or till (Chapuis (2004) data subset at d_{10} sizes less than 0.02 mm in which the degree of compaction was not reported – if moderately compacted, the porosity prediction bias would be closer to 1.0 for this data subset, eliminating this minor dependency.

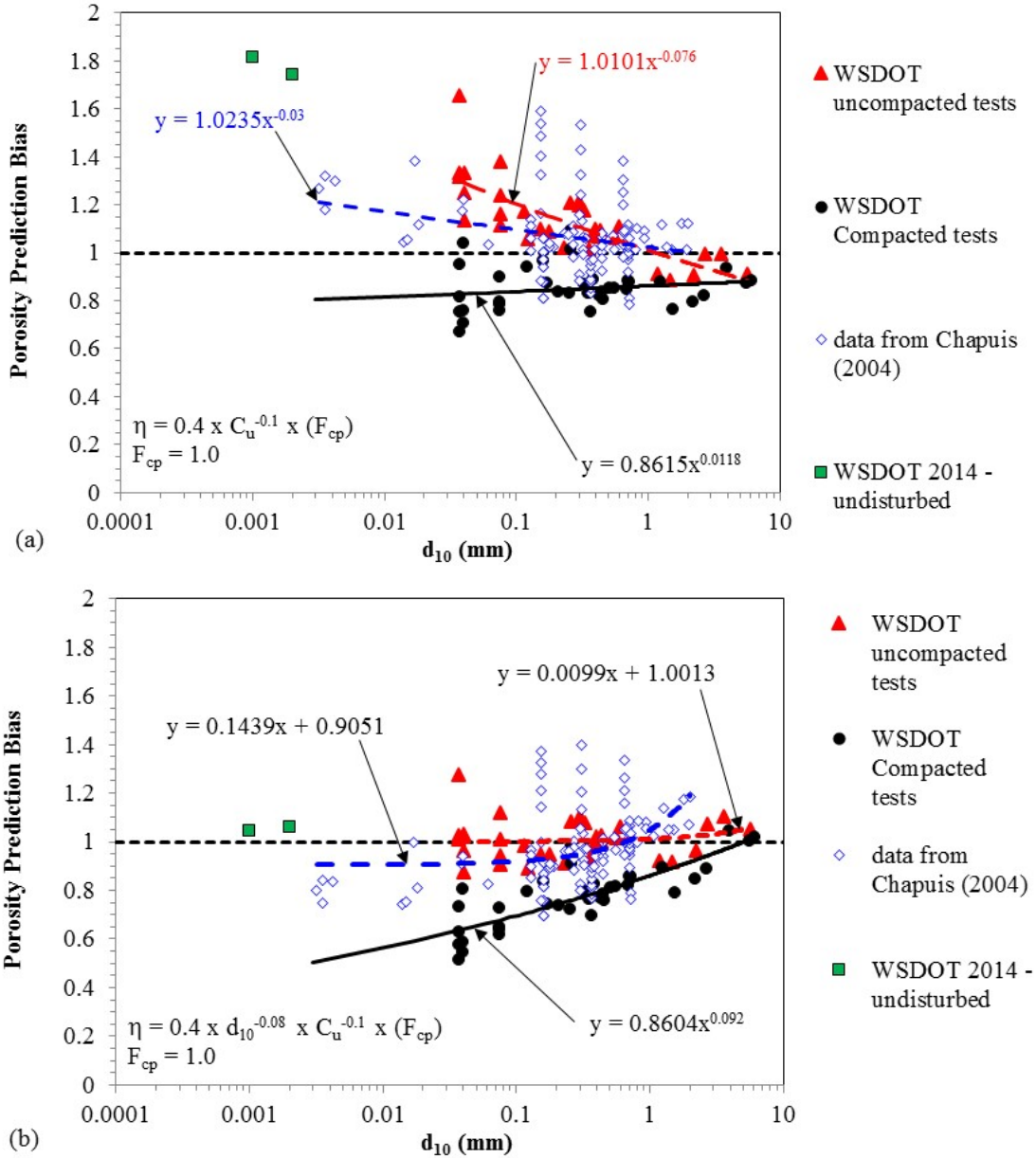


Figure 29. Porosity prediction bias as a function of the d_{10} size when: (a) the soil d_{10} size is not considered, and (b) the soil d_{10} size is considered.

Overall, the most data scatter for porosity prediction is in the data gathered by Chapuis (2004). However, these data were obtained for soils with a low coefficient of uniformity, C_u , as shown in Figure 31, and compaction may not affect soils with a low C_u as much as more well graded soils. Furthermore, much of the scatter appears to be due to the crushed glass data subset (i.e., as described regarding Figure 28).

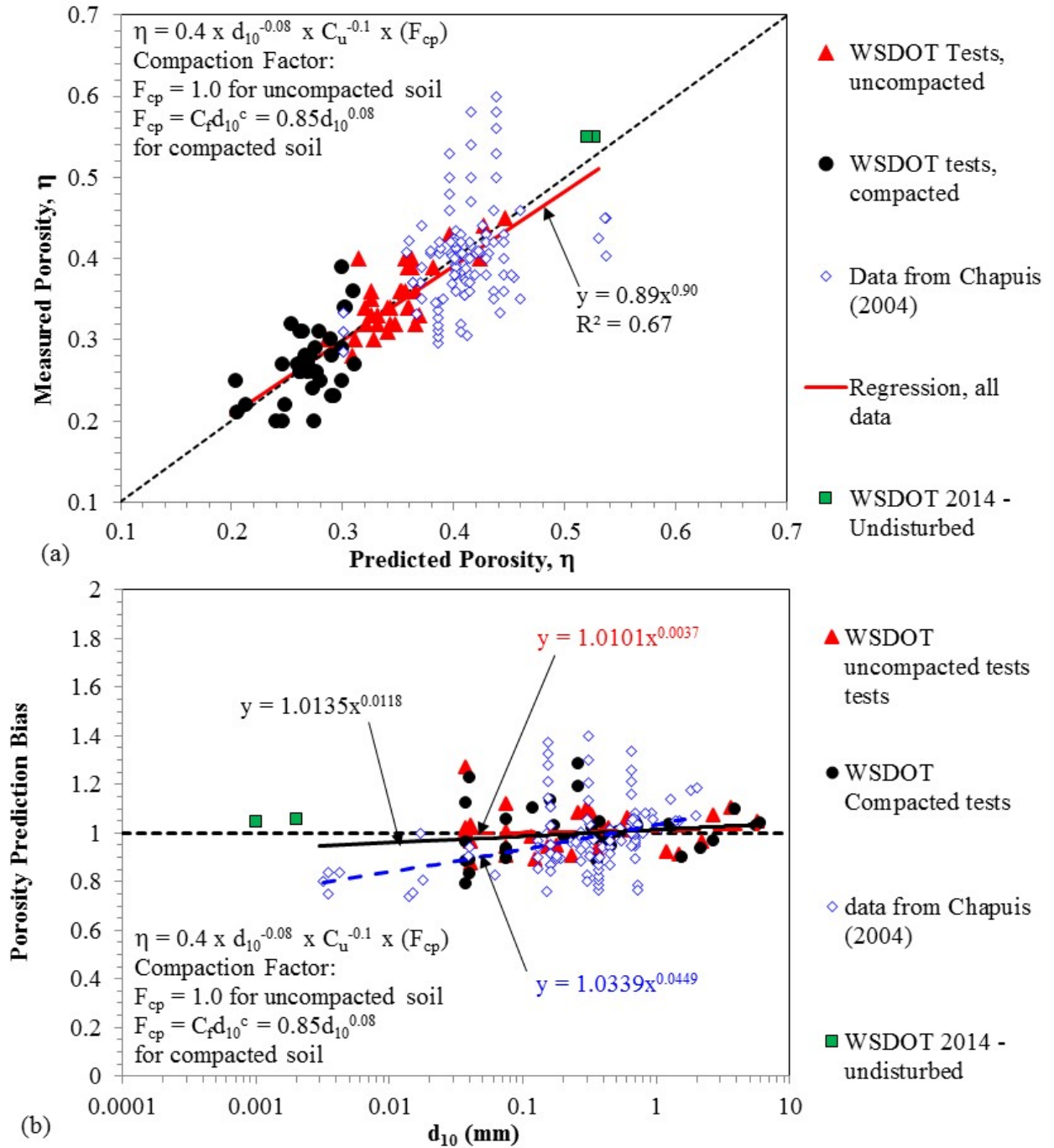


Figure 30. (a) Predicted versus measured porosity considering compaction effects (i.e., using equations 13 and 14), and (b) porosity prediction bias (i.e., measured/predicted value) as a function of the soil d_{10} size (outliers removed for both plots).

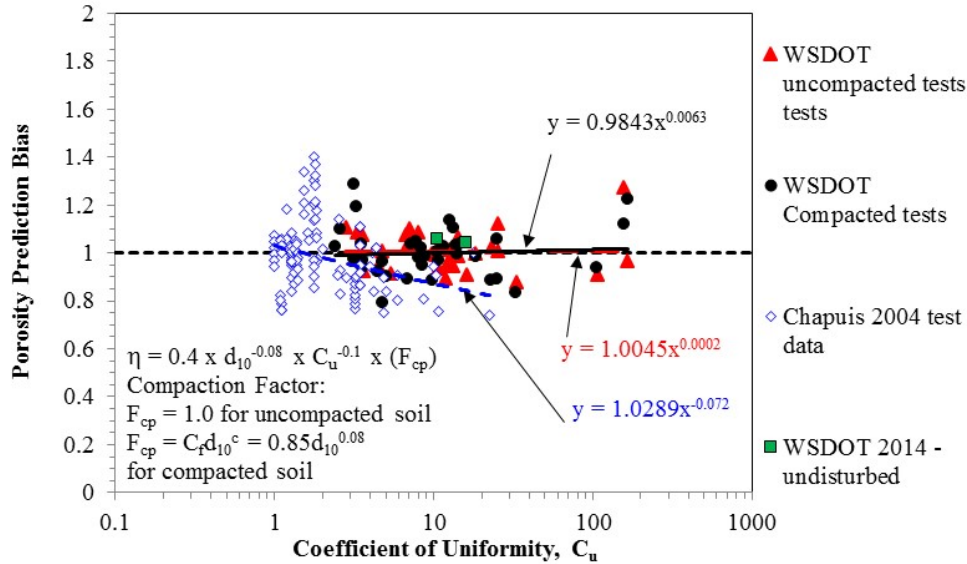


Figure 31. Porosity prediction bias versus the soil coefficient of uniformity, C_u (outliers removed).

Now that a reasonably accurate prediction method for soil porosity is available, it is possible to use the optimized Slichter and Terzaghi equations with just grain size data. However, it must be recognized that the porosity correction for compaction effects is rather crude in that it is either on or off, though it may be possible to interpolate for intermediate soil densities (both the compaction factor d_{10} exponent and coefficient may need to be interpolated between the two extremes).

Note that if this porosity compaction correction factor is applied to the estimated porosity in the optimized Slichter or Terzaghi equations, the effect of compaction on K_{sat} is as follows:

- At $d_{10} = 0.001$ mm, K_{sat} reduction is by a factor of 0.083.
- At $d_{10} = 1$ mm, K_{sat} reduction is by a factor of 0.57.

Comparing this to the factors currently in the WSDOT Highway Runoff Manual to account for compaction (WSDOT 2016a), the compaction reduction factors of 0.1 to 0.2 for sands and gravels are quite conservative relative to the findings in the current study, but the compaction reduction factor of 0.067 for fine grained (clayey soils) is only slightly conservative relative to the findings in the current study. Of course, if the

proposed methodology in the current study is used, there will no longer be a need for the compaction reduction factors in the WSDOT Highway Runoff Manual.

Using Estimated η and e with Optimized K_{sat} Prediction Methods

Using the porosity estimated from grain size data, and F_{cp} if the soil has been compacted, K_{sat} can be estimated based only on grain size data plus this empirically derived compaction factor F_{cp} . The prediction performance of the optimized Slichter, Terzaghi and Chapuis equations using the estimated porosity is illustrated in figures 32 through 34. For the optimized Chapuis Equation, the void ratio, e , was estimated from Eq. 16 below and the estimated porosity, η from eq's. 13 and 14.

$$e = \frac{\eta}{1-\eta} \tag{16}$$

In all cases, the effect of using a porosity or void ratio estimated from grain size parameters plus a compaction factor appears visually to be relatively small with regard to the K_{sat} prediction performance of these methods.

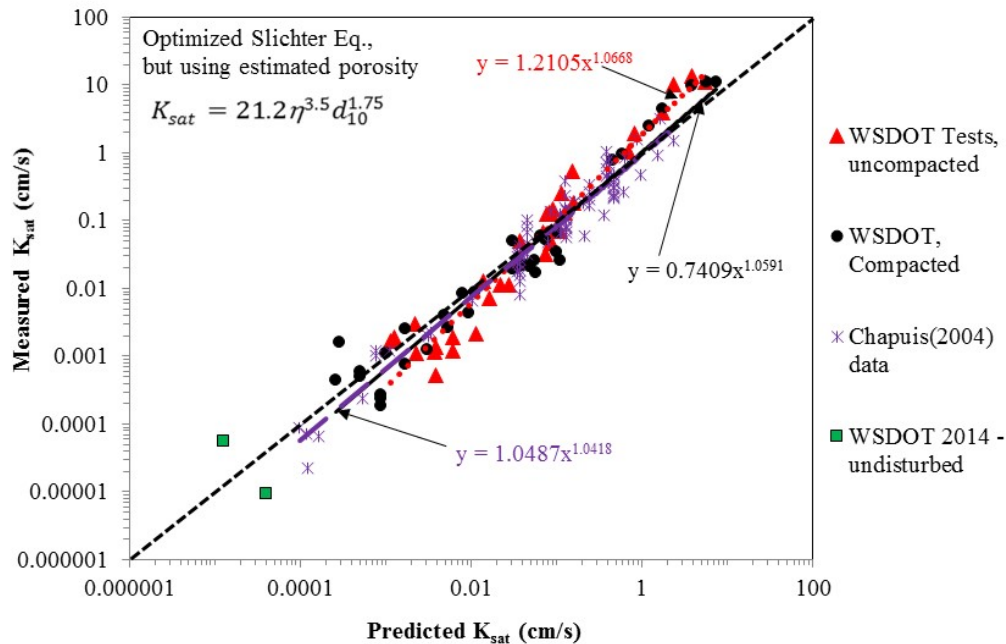


Figure 32. Optimized Slichter Equation, but using Eq's. 13 and 14 to estimate porosity (outliers removed).

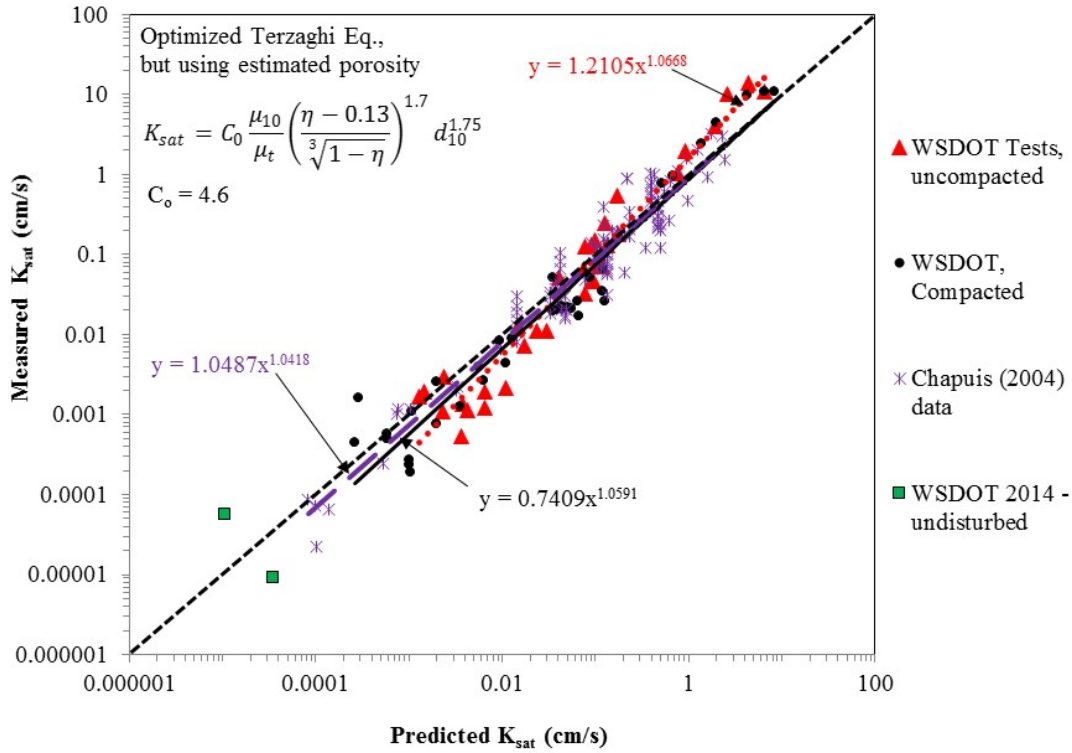


Figure 33. Optimized Terzaghi Equation, but using Eq's. 13 and 14 to estimate porosity (outliers removed).

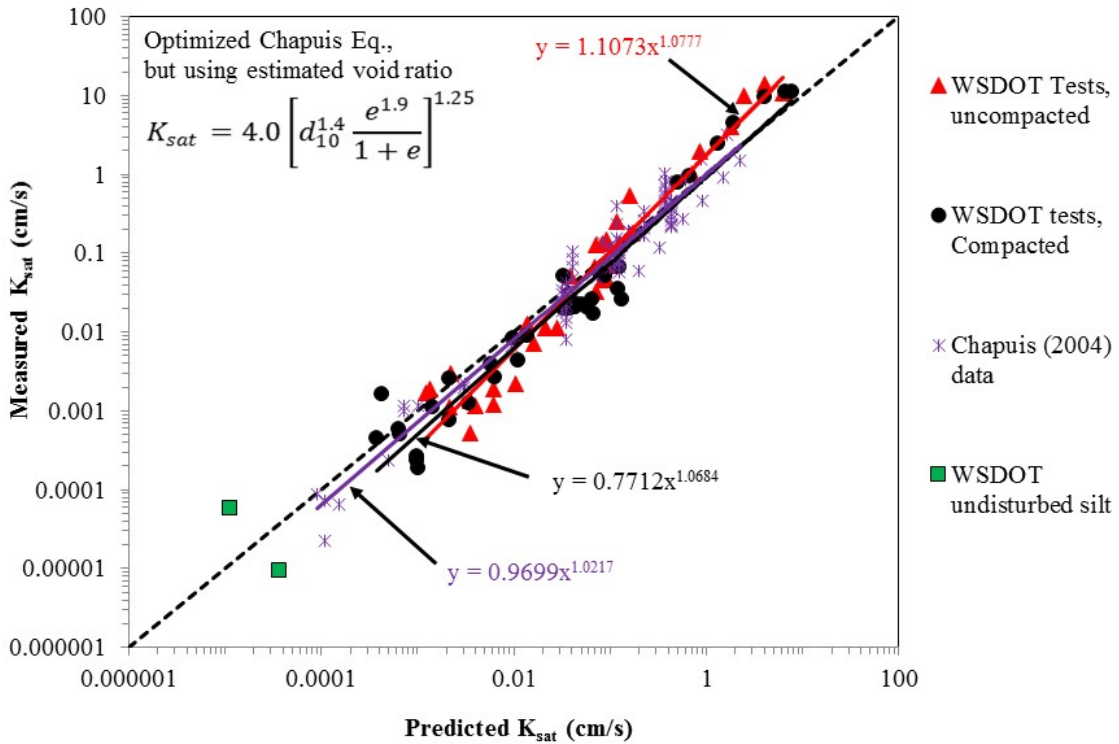


Figure 34. Optimized Chapuis Equation, but using Eq's. 13, 14, and 16 to estimate porosity and void ratio (outliers removed).

STATISTICAL ANALYSIS AND METHOD PERFORMANCE

This report section provides a statistical comparison of the various prediction methods investigated, to assist in identifying the best methods with regard to their performance. Table 5 summarizes the mean and COV for the original (i.e., not optimized) K_{sat} prediction methods investigated, using the prediction method bias, both for all the data and for the data subsets included (i.e., historical data from Chapuis 2004 and the current WSDOT study). All outliers identified previously have been removed to develop these statistics. Similarly, Table 6 provides the same information, but for the optimized methods using the measured porosity or void ratio. In both tables, the distribution (e.g., lognormal or normal) is not considered.

Comparison of the results summarized in these two tables demonstrates that the empirical adjustments made to the various K_{sat} prediction methods resulted in large improvements overall in the accuracy of the K_{sat} predictions. Based on this simple statistical analysis, the optimized Chapuis and Terzaghi equations had the lowest COV value (i.e., for all the data, the COV was reduced to 66%, a respectable value for K_{sat} prediction, especially considering the very large range of magnitudes that must be considered). The optimized Slichter Equation was not far behind with an overall COV of 67%. For all three prediction methods, mean bias values are just over 1.0. All of these equations also provide a significant improvement in the prediction accuracy relative to Eq. 1 (see Appendix G).

With regard to range of applicability of the various methods, in general, all of the methods, even after optimization, have an upper d_{10} size limit of about 2 to 3 mm. Above that, all the methods tend to under-predict the K_{sat} value (i.e., the bias is significantly greater than 1.0). At the finer grained end of the range, it is difficult to pick a lower limit as in general, the data are more sparse and data scatter increases; however, the trend in the regression of the bias values tends to stay near 1.0 even for soils with the smallest d_{10} sizes (i.e., down to a d_{10} size of about 0.003 mm).

Table 7 summarizes the statistics for the porosity prediction from the present study using the bias (i.e., measured/predicted porosity) for eq's. 13 and 14. Also shown are the statistics for the Vulkovic and Soro (1992) porosity prediction method. Based on

this table, the proposed porosity prediction method from the current study decreases the COV relative to the Vulcovic and Soro (1992) method COV by almost 50% when all the data subsets are combined. A COV for the combined data set of 13% for equations 13 and 14 is judged to be acceptable.

Table 5. Bias statistics for all historical methods investigated (outliers removed).

Data Set	No. of Meas., n	Simplified Hazen Method		Slichter Method		Terzaghi Method		Chapuis Method	
		Mean	COV	Mean	COV	Mean	COV	Mean	COV
WSDOT uncompacted tests	36	2.39	392%	3.59	180%	1.73	173%	1.38	101%
WSDOT compacted tests	37	--	--	2.20	83%	1.35	96%	1.04	100%
All WSDOT tests	73	--	--	2.89	164%	1.54	149%	1.21	102%
Chapuis (2004) tests	137	1.25	90%	2.50	86%	1.20	87%	1.11	58%
All Test data	210*	1.49*	294%*	2.64	125%	1.32	121%	1.14	78%

*For the Hazen Equation, all test data does not include compacted WSDOT tests (total n = 173).

Table 6. Bias statistics for all optimized methods investigated, using measured porosity or void ratio (outliers removed).

Data Set	No. of Meas., n	Slichter Method		Terzaghi Method		Chapuis Method	
		Mean	COV	Mean	COV	Mean	COV
WSDOT uncompacted tests	36	1.28	83%	1.20	88%	1.26	83%
WSDOT compacted tests	37	1.01	73%	0.90	73%	0.85	75%
All WSDOT tests	73	1.14	80%	1.05	84%	1.05	84%
Chapuis (2004) tests	137	1.02	57%	1.01	54%	1.06	55%
All Test data	210*	1.06	67%	1.02	66%	1.06	66%

Table 7. Summary of bias statistics (without consideration of data distribution) for prediction of soil porosity.

Data Set	No. of Meas., n	Statistical Parameter	Using Eq's 13 and 14	Vulkovic and Soro (1992)
Chapuis (2004) and WSDOT Tests	180	Mean	0.99	0.99
		COV	13%	21%
All WSDOT tests	73	Mean	1.01	1.05
		COV	9.1%	25%
Chapuis (2004) tests	107	Mean	0.99	0.96
		COV	15%	17%
All uncompacted WSDOT tests	36	Mean	1.01	1.22
		COV	7.9%	21%
All compacted WSDOT tests	37	Mean	1.00	0.88
		COV	10%	12%

The real proof regarding the impact of using an estimated porosity or void ratio rather than a measured one is the effect this has on the K_{sat} prediction accuracy. Table 8 presents a comparison of the mean bias and COV of the K_{sat} prediction equations with and without using an estimated porosity or void ratio. In this table, the distribution (e.g., lognormal or normal) is not considered.

Table 8. Bias statistics comparing the use of measured versus estimated porosity values as input for the optimized (a) Slichter, (b) Terzaghi, and (c) Chapuis methods.

(a)	Optimized Slichter Method			
	Measured η		Estimated η	
	Mean	COV	Mean	COV
Data Set				
WSDOT uncompacted tests	1.28	83%	1.31	88%
WSDOT compacted tests	1.01	73%	1.07	93%
All WSDOT tests	1.14	80%	1.19	91%
Chapuis (2004) tests	1.02	57%	1.03	70%
All Test data	1.06	67%	1.10	81%

(b)	Optimized Terzaghi Method			
	Measured η		Estimated η	
	Mean	COV	Mean	COV
Data Set				
WSDOT uncompacted tests	1.20	88%	1.23	94%
WSDOT compacted tests	0.90	73%	0.96	100%
All WSDOT tests	1.05	84%	1.09	97%
Chapuis (2004) tests	1.01	54%	1.03	67%
All Test data	1.02	66%	1.06	81%

(c)	Optimized Chapuis Method			
	Measured η		Estimated η	
	Mean	COV	Mean	COV
Data Set				
WSDOT uncompacted tests	1.26	83%	1.30	90%
WSDOT compacted tests	0.85	75%	0.90	85%
All WSDOT tests	1.05	84%	1.10	91%
Chapuis (2004) tests	1.06	55%	1.09	68%
All Test data	1.06	66%	1.09	78%

Based on this assessment as presented in Table 8, the Chapuis Method did slightly better overall when using an estimated void ratio, followed by the optimized Slichter and

Terzaghi methods when using an estimated porosity. The accuracy of estimating K_{sat} for test data from Chapuis (2004) was only slightly affected by the use of an estimated porosity rather than a measured one, whereas the K_{sat} estimate for the WSDOT test data was significantly affected by the use of an estimated porosity.

It should be noted that approximately 22% of the Chapuis (2004) dataset did not have adequate grain size data available (i.e., 30 K_{sat} measurements out of the 137 K_{sat} measurements in the Chapuis 2004 data set) to estimate the porosity from grain size data. However, the mean bias and COV of the smaller data set was about the same as for the full data set.

Bathurst et al. (2008, 2010) indicate that the prediction method bias should have no hidden dependency with the predicted value or a parameter considered in the prediction equation. This was considered in the optimized K_{sat} and porosity prediction equation development. Examples of this, considering dependency of the prediction method bias with the d_{10} size, are provided in figures 23, 25, and 26 for the original and optimized K_{sat} prediction equations. An assessment of the dependency between the K_{sat} prediction bias and the predicted K_{sat} values is summarized in Appendix I.

The original K_{sat} prediction methods do show visual dependencies with both the d_{10} size and the predicted K_{sat} values, in addition to having a mean bias that is significantly less or greater than 1.0. For the optimized Slichter, Terzaghi, and Chapuis equations, there is no dependency with both the d_{10} size and the predicted K_{sat} values, and the regression is nearly constant at 1.0 except near the upper end of the values (i.e., at d_{10} greater than 2 to 3 mm, and K_{sat} greater than 1 to 3 cm/s). This indicates that the primary variables that affect K_{sat} have been captured and formulated correctly.

For the porosity prediction bias, Figure 35 illustrates that there is little visual dependency between the porosity prediction bias and the predicted porosity values, with the possible exception of four data points from the Chapuis (2004) data set at the highest predicted porosity values. Likewise, figures 30 and 31 illustrate that there are no visual dependencies between the porosity prediction bias and the soil d_{10} size as well as the soil C_u , except at low values of C_u there appears to be greater scatter in the data. In spite of the potential dependency of the Chapuis (2004) data set with the porosity at small d_{10} sizes (Figure 30), and considering that this over-prediction may due to an unknown

degree of compaction in the specimens tested, the overall conclusion is that there are no apparent properties missing in the porosity prediction equation, nor are the properties addressed in the equation poorly formulated. Otherwise, there would be a dependency between the porosity prediction bias and the selected parameters.

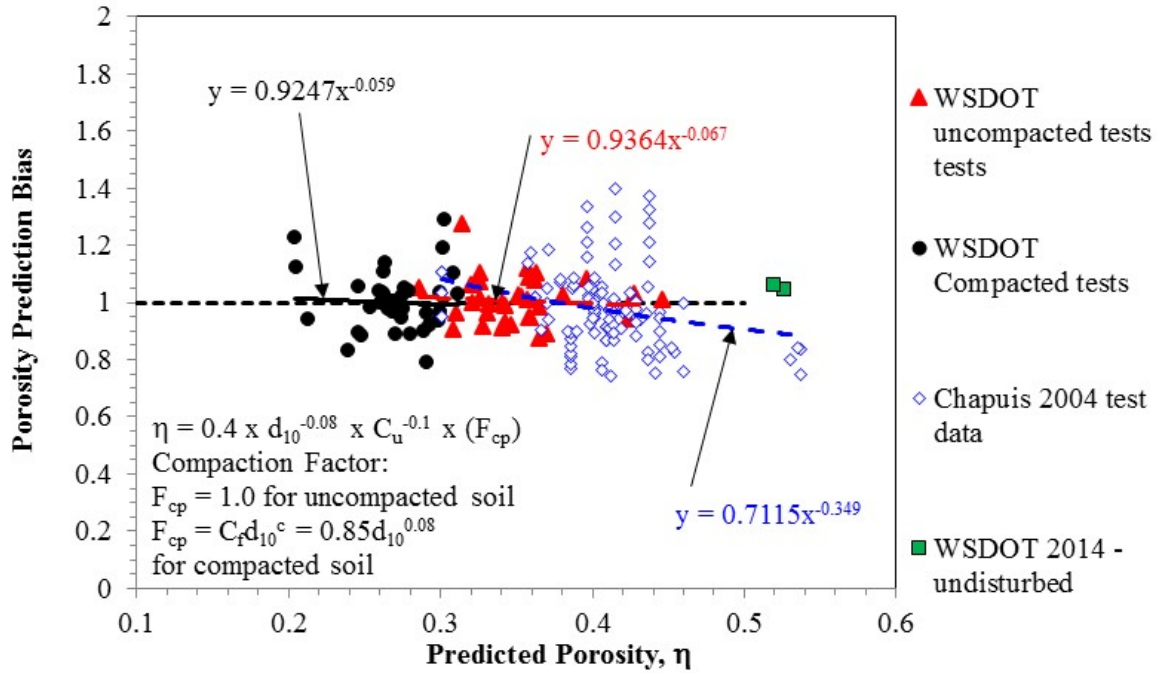


Figure 35. Porosity prediction bias as a function of porosity prediction value.

The shape of the statistical distributions for each prediction method is also important to consider (Allen et al. 2005). Figures 36 and 37 illustrate these distributions using the standard normal variable function in Excel to develop a Cumulative Distribution Function (CDF) for each K_{sat} estimation equation, using a measured porosity or void ratio. Essentially, this type of plot is the same as plotting the cumulative distribution data on probability paper. CDF's of normal distributions plot as a straight line on this type of plot, whereas CDF's of lognormal distributions plot as a curve (Allen et al. 2005). However, if a lognormal scale is used for the horizontal axis, lognormal distributions plot as a straight line. In this case, for lognormal distributions, the steeper the line, the smaller the variation and the lower the COV.

In most cases, the CDF's of the various subsets of the data were not perfectly lognormal, but deviated from a lognormal distribution, especially as data scatter

increased (especially true of the CDF's for the original equations). For statistical characterization purposes, the bias data mean and COV can be adjusted to better fit the tails of the distributions, since it is the tail region that can have the most effect on the probability that a failure criterion is exceeded (Allen et al. 2005). Usually, the fitting to tail approach is focused on one end of the distribution that is most important to assessing the probability that the failure criterion is exceeded (Allen et al., 2005). With regard to K_{sat} , if sizing an infiltration facility for a given design storm or series of storms, it is best to err on the side of under-estimating the K_{sat} value. Given the definition of bias (i.e., measured/predicted value), the bias should be greater than 1.0 (i.e., the predicted K_{sat} is lower than the measured value) so that a safe estimate is obtained. If the bias is less than 1.0, then the K_{sat} prediction is too high which could be unsafe with regard to meeting the design criteria for the infiltration facility. In this scenario, it would be most important to match the lower tail of the distribution as much as practical. In Load and Resistance Factor Design (LRFD) parlance (e.g., Allen et al. 2005), the storm water runoff volume that must be infiltrated is the load, and the ability of the soil to infiltrate that runoff is the resistance, in which case the lower tail must be matched. However, one must keep in mind that the more conservatively K_{sat} is estimated, the larger and more expensive the infiltration facility.

Figure 36 illustrates how well the prediction bias distributions are modeled using a lognormal fit to the data, both for the original and optimized equations. In this figure, it is in the upper tail CDF's that we see the most differentiation between the various methods assessed, at least for the Slichter and Terzaghi equations. For the Chapuis Equation, the biggest differentiation between the original and optimized equations is in the lower tail. The statistical parameters determined from matching the lower tail as much as practical are the ones to use to characterize the prediction method statistics for estimating infiltration, if a probability of exceedance is needed. Note that in Figure 36(a and b) for original Slichter and Terzaghi prediction equations, respectively, by fitting to the lower tail, the statistics are similar to the optimized Slichter and Terzaghi equations. For the Chapuis Equation (Figure 36(c)) however, fitting to the lower tail did not improve the statistics for the original equation. See Table 9 for a summary of the mean and COV values for the original K_{sat} equations.

Figure 37 and Table 10 illustrate the differences in the CDF's for the various data subsets for the optimized Slichter, Terzaghi, and Chapuis equations. All of the data set CDF's are reasonably close to lognormal throughout the range of bias values. However, only the lower tail lognormal fits are shown in the figure to keep the figure from becoming too cluttered. For all three K_{sat} prediction equations, the data set consisting of uncompacted sample test results obtained by WSDOT had the highest mean bias (i.e., just over 1.0) and the largest COV. The WSDOT compacted soil test dataset had a lower mean bias and a lower COV than the uncompacted WSDOT test data set for all three prediction equations. The Chapuis (2004) data set had the lowest COV of the three datasets.

An objective of the present study is to identify or develop a K_{sat} prediction equation that accounts for the effect of compaction on K_{sat} . Figure 37 and Table 10 illustrate how well this objective was accomplished. Visually, for all three optimized equations, there is a significant difference in the CDF's for the WSDOT uncompacted and compacted specimen datasets. The mean and COV of the bias values for the WSDOT compacted soil tests are lower than those of the uncompacted WSDOT soil tests. The relatively angular, irregular shape of the finer soil particles in the WSDOT test specimens may have contributed to poorer consistency in the K_{sat} test results for the “uncompacted” specimens that was not fully reflected in the measured porosity or void ratio for the test specimens, such as due to water flow path tortuosity through the specimens. This may also explain why the WSDOT uncompacted soil K_{sat} test statistical results were not consistent with the K_{sat} test statistical results gathered by Chapuis (2004), in that Chapuis (2004) indicated his K_{sat} equation did not do well with angular soils. However, compacting the specimens may have been sufficient to overcome the relatively angular sand particles from hanging up on one another, resulting in a more consistent soil structure. Overall, what can be said is that use of the soil porosity or void ratio significantly improved the consistency of the K_{sat} predictions for the compacted soils relative to K_{sat} equations based only on soil gradation (e.g., relative to the Hazen Equation – compare difference in WSDOT compacted and uncompacted datasets for the Hazen Equation to the difference between these two datasets for the other methods in Tables 9 and 10).

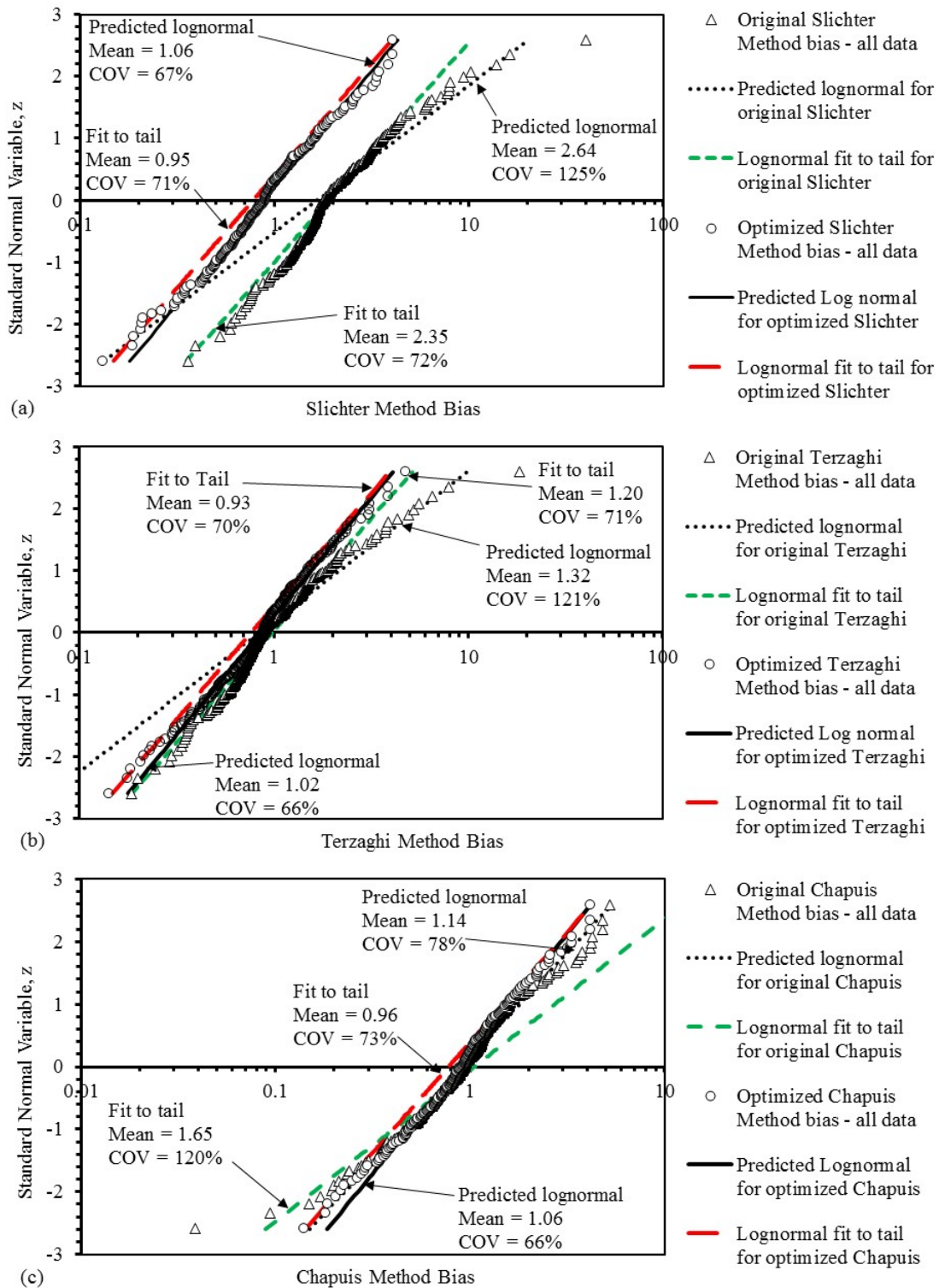


Figure 36. Bias distributions for the original and optimized equations with lognormal data fit and adjusted lognormal data fit to improve match the lower distribution tail (outliers removed): (a) Slichter Method, (b) Terzaghi Method, and (c) Chapuis Method.

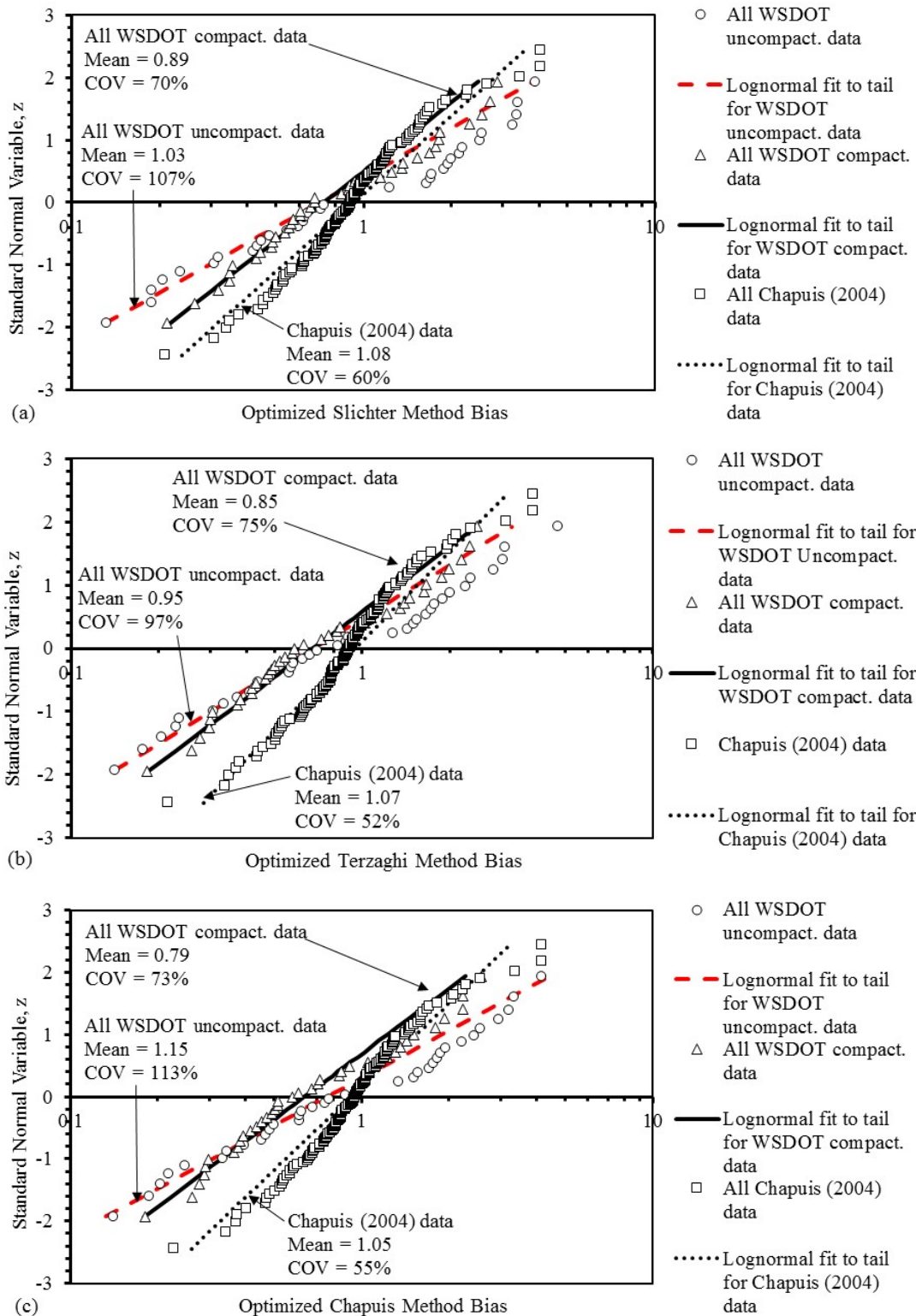


Figure 37. Bias distributions for datasets analyzed using the optimized K_{sat} equations with adjusted lognormal data fit to match the lower distribution tail (outliers removed): (a) Slichter Method, (b) Terzaghi Method, and (c) Chapuis Method.

Table 9. Bias statistics for all original K_{sat} prediction methods, using measured porosity or void ratio, comparing standard lognormal fit to lognormal fit adjusted to match lower distribution tail.

Original Equation	CDF Fit	WSDOT Uncompacted Tests		WSDOT Compacted Tests		Chapuis (2004) Tests		All Test Data	
		Mean	COV	Mean	COV	Mean	COV	Mean	COV
Slichter	Lognormal	3.59	180%	2.20	83%	2.50	86%	2.64	125%
	Fit to Tail	2.30	78%	2.20	82%	2.30	61%	2.10	67%
Terzaghi	Lognormal	1.73	173%	1.35	96%	1.20	87%	1.32	121%
	Fit to Tail	1.35	89%	1.32	91%	1.25	72%	1.35	74%
Chapuis	Lognormal	1.38	101%	1.04	100%	1.11	58%	1.14	78%
	Fit to Tail	1.70	206%	0.80	75%	1.12	61%	1.65	121%
Hazen	Lognormal	2.40	392%	0.29	72%	1.25	90%	N/A	N/A
	Fit to Tail	0.90	78%	0.28	79%	1.05	57%	N/A	N/A
Cozeny-Carmen	Lognormal	0.84	110%	1.00	131%	N/A	N/A	N/A	N/A
	Fit to Tail	0.60	100%	0.75	107%	N/A	N/A	N/A	N/A

*See Appendix H for details on the analysis of the Cozeny-Carmen Equation.

N/A – not available or applicable.

Table 10. Bias statistics for all optimized K_{sat} prediction methods, using measured porosity or void ratio, comparing standard lognormal fit to lognormal fit adjusted to match lower distribution tail.

Optimized Equation	CDF Fit	WSDOT Uncompacted Tests		WSDOT Compacted Tests		Chapuis (2004) Tests		All Test Data	
		Mean	COV	Mean	COV	Mean	COV	Mean	COV
Slichter	Lognormal	1.28	83%	1.01	73%	1.02	57%	1.06	67%
	Fit to Tail	1.03	107%	0.89	70%	1.08	60%	0.95	71%
Terzaghi	Lognormal	1.20	88%	0.90	73%	1.01	54%	1.02	66%
	Fit to Tail	0.95	97%	0.85	75%	1.07	52%	0.93	70%
Chapuis	Lognormal	1.26	83%	0.85	75%	1.06	55%	1.06	66%
	Fit to Tail	1.15	113%	0.79	73%	1.05	55%	0.96	73%

In summary, based on these analyses, the optimized Slichter, Terzaghi, and Chapuis equations are all similar with regard to their K_{sat} prediction accuracy and also have the widest range of applicability (i.e., all d_{10} sizes up to approximately 3 mm). Therefore, any of these three K_{sat} prediction equations can be recommended for use. If the d_{10} size is as much as 8 mm, all three equations tend to under-predict the K_{sat} value, but only by a half-order of magnitude, which may still be acceptable. Of these three K_{sat} equations, the optimized Slichter and Terzaghi equations provided the most consistent overall lognormal fit as well as fit to lower tail statistics for the WSDOT uncompacted and compacted datasets.

If a measured soil porosity is not available (which is likely to be true for new roadway fill, if needed for the project), the porosity can be estimated from grain size data and degree of compaction, making it possible to estimate K_{sat} from grain size data alone.

In this case, the optimized Slichter and Chapuis equations appear to be a little more accurate than the optimized Terzaghi Equation, especially for soils with irregular or angular soil particles, and are also a little simpler.

APPLICATION TO INFILTRATION DESIGN

To estimate infiltration rate for a given storm water Best Management Practice (BMP) installation, the K_{sat} value for each soil layer that can affect the infiltration rate must be determined, and an effective K_{sat} value determined considering the layer thicknesses. The geometric mean of the K_{sat} values for all the soil layers below the ground surface is used to determine the effective K_{sat} value for design (Massmann 2003 and WSDOT 2016a). It must also be recognized that predicting the K_{sat} value(s) to use for infiltration design is only part of what is needed to estimate infiltration and size the infiltration facility, with consideration to the runoff handled through natural dispersion, if that is being considered. Infiltration rate is a function of both the effective K_{sat} value and the hydraulic gradient (Massmann 2003, WSDOT 2016a). In addition, the storm water inflow to the facility or natural dispersion area must be determined. The determination of hydraulic gradient and storm water inflow are beyond the scope of this study. However, approaches to estimate the hydraulic gradient are provided in Massmann (2003) and WSDOT (2016a).

Once the effective K_{sat} value and hydraulic gradient are determined, there are other factors that can affect the infiltration rate, such as infiltration surface siltation or biofouling. This issue has been observed in infiltration ponds, but may not be as much of a factor on embankment side slopes. The focus of the work reported in Massmann (2003) was primarily on ponds. The reduction factors used to account for the siltation/biofouling issue were determined by relating infiltration rate observations in full-scale ponds to the estimated infiltration rate using the K_{sat} estimates determined from Eq. 1 multiplied by the estimated hydraulic gradient.

To determine the impact of using one of the optimized K_{sat} equations developed herein, estimates from Eq. 1 must be compared to estimates from the new optimized equations. Since the optimized Chapuis, Terzaghi and Slichter equations produce very similar K_{sat} estimates, this analysis will be carried out using just one of the optimized K_{sat} equations (i.e., the Slichter Equation). This comparison, presented as the ratio of the predicted K_{sat} value using the Slichter Equation to the K_{sat} value predicted by Eq. 1, is provided in Figure 38. Within a fairly narrow d_{10} range of 0.1 to 1.0 mm, both equations

provide a similar estimate of K_{sat} , though in general, the Slichter Equation is slightly more conservative than Eq. 1 even within this range, especially for the compacted soils. Outside this narrow range, however, the difference between Eq. 1 and the optimized Slichter Equation is much more obvious. When d_{10} is greater than 1.0 mm, the Eq. 1 K_{sat} prediction becomes orders of magnitude too large relative to the Slichter Equation prediction and the measured K_{sat} values from the saturated hydraulic conductivity testing. This is also true when the d_{10} value is significantly less than 0.1 mm (i.e., higher silt content soils).

The siltation/biofouling factors provided in the WSDOT Highway Runoff Manual (WSDOT 2016a) used to relate predicted infiltration rates from soil test data were developed considering K_{sat} predictions from Eq. 1. Considering that the optimized K_{sat} prediction equations recommended herein tend to predict smaller K_{sat} values than predicted by Eq. 1, it is logical to assume that these siltation/biofouling reduction factors could be overly conservative when used with the proposed K_{sat} prediction equations (i.e., optimized Slichter, Terzaghi, or Chapuis equations).

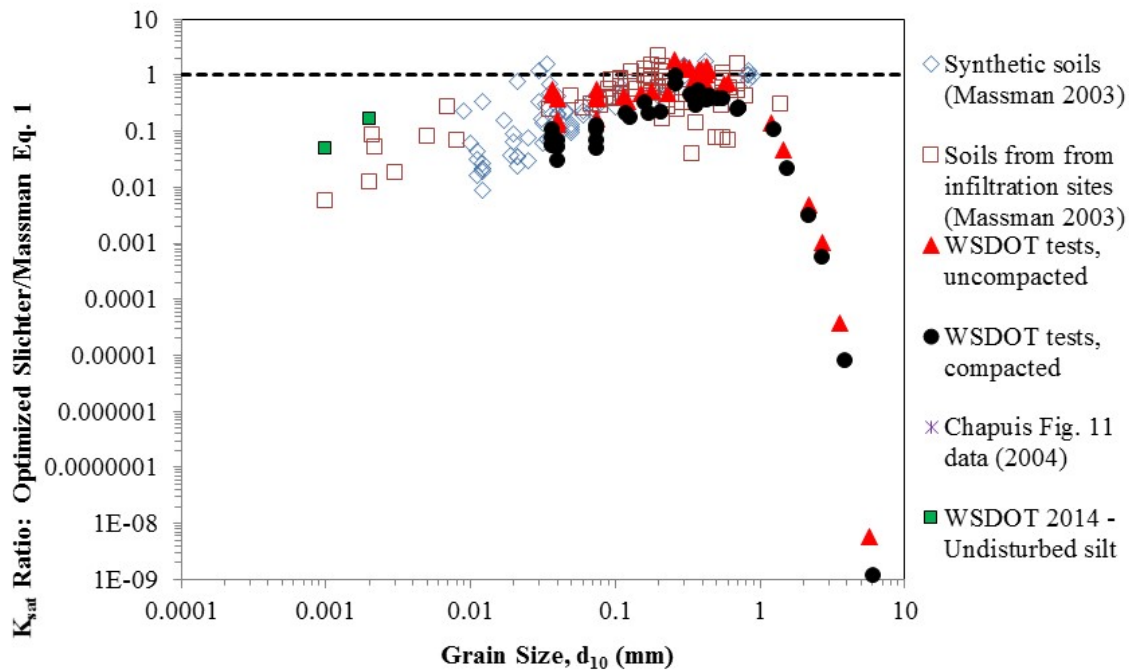


Figure 38. Ratio of optimized Slichter Equation (Eq. 9) to Massmann Equation (Eq. 1) K_{sat} predictions as a function of d_{10} size.

To test this assumption, Figure 39 presents a comparison of measured pond infiltration rates from Massmann (2003) and Wiltsie (1998) and the infiltration rates estimated using the optimized Slichter and Massmann (2003) equations to the “average” soil d_{10} size for each case history. An estimated porosity from grain size parameters and level of compaction/density (i.e., eq’s. 13 and 14) is used with the optimized Slichter Method to obtain K_{sat} for that method. The plots also separate the measured pond infiltration rates to those ponds that were well maintained and had little siltation or biofouling present from those measured infiltration rates for ponds that were poorly maintained (i.e., had siltation or biofouling). The predicted infiltration rates in the figure for both K_{sat} prediction equations assume a hydraulic gradient, i , of 1.0 and no reductions due to siltation and biofouling. Of course, the reality is that the hydraulic gradient is likely less than 1.0, but this is simply the first step in this evaluation process. Also shown in this plot are double-ring infiltrometer measurements taken in the pond bottom as reported by Wiltsie (1998).

The first observation that stands out in these plots is that trend lines for the measured full scale pond infiltration rates and the predicted “infiltration rates” are not consistent with each other, though this is strongly influenced by the measured infiltration rate in two ponds, and that there is a lot of data scatter. The second observation that can be made is that the double ring infiltrometer measurements in the pond bottoms are clearly indicating a higher infiltration rate than observed in the ponds, but are approximately consistent with the infiltration rates estimated using the K_{sat} prediction from the Optimized Slichter Equation, a hydraulic gradient of 1.0, and no reduction for pond bottom conditions. This indicates that the double-ring infiltrometer has a hydraulic gradient of approximately 1.0 and yields a value that is close to the K_{sat} for the soil tested. Also note that the infiltration rates estimated using the K_{sat} prediction from the Massmann (2003) Equation, a hydraulic gradient of 1.0, and no reduction for pond bottom conditions is generally higher than the double-ring infiltrometer measurements and the infiltration rate estimated using the Optimized Slichter Equation for K_{sat} .

The next step is to attempt to estimate the hydraulic gradient, the effect of the pond aspect ratio on infiltration rate, and the effect of the pond bottom conditions for the full scale pond case histories using the approach developed by Massmann (2003) and

which is provided in the WSDOT Highway Runoff Manual (WSDOT 2016a). Once that is completed, then these more accurate hydraulic gradients and additional corrections to account for the pond bottom conditions can be applied to the estimated K_{sat} values to obtain a more accurate infiltration rate estimate. The infiltration rate is then calculated as:

$$f = K_{sat} * i * CF_{silt/bio} * CF_{aspect} \tag{17}$$

Where, f = infiltration rate, i = hydraulic gradient, $CF_{silt/bio}$ = correction factor for siltation and biofouling, and CF_{aspect} = correction factor for the pond aspect ratio.

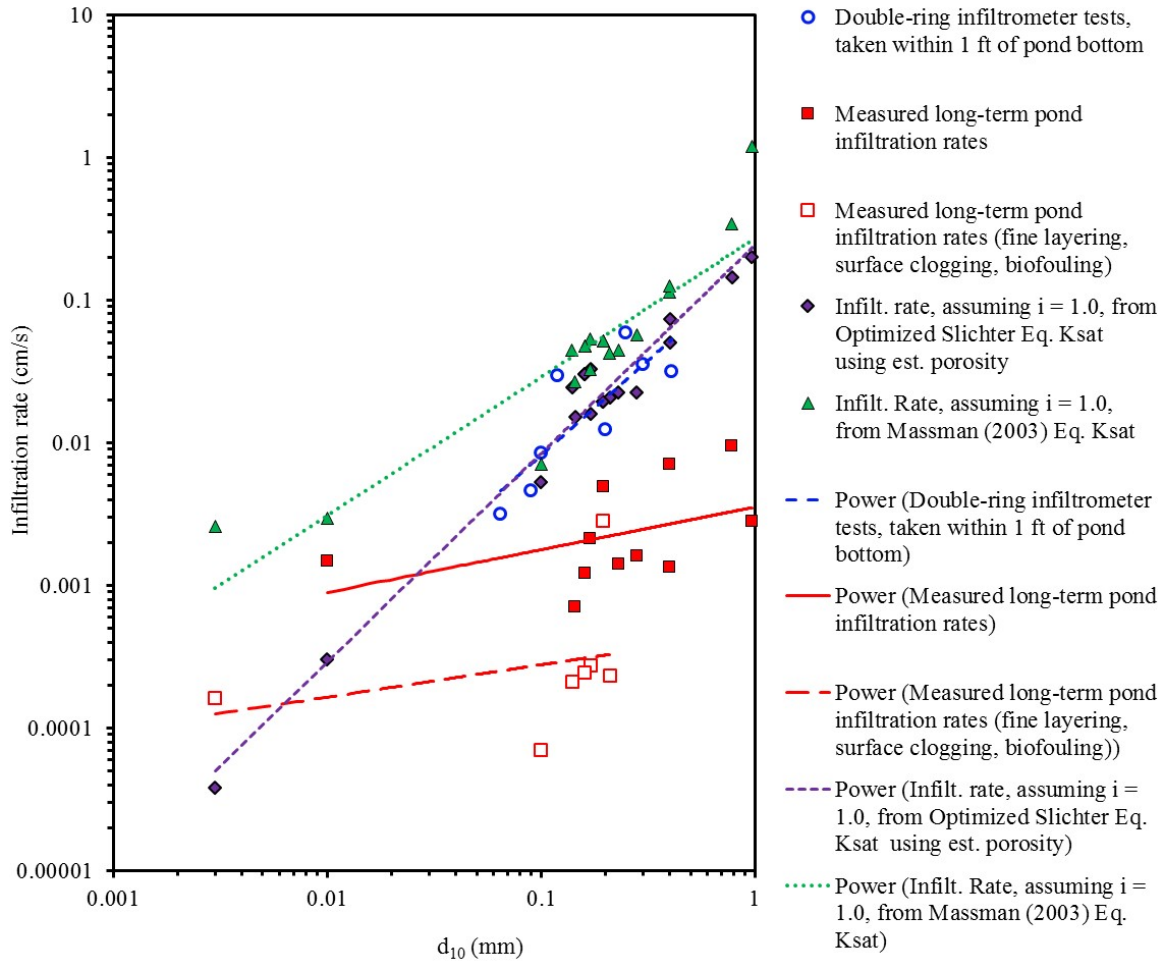


Figure 39. Comparison of full scale pond infiltration rates to infiltration rates from grain size analysis, assuming hydraulic gradient of 1.0, and from double-ring infiltrometer measurements just below pond bottoms for case histories in Western Washington.

Figure 40 presents a comparison between the estimated pond infiltration rates (i.e., “ f ” in Eq. 17) and measured full scale pond infiltration rates for several well documented ponds in the south Puget Sound area. Pond infiltration rates were estimated using the original Massmann (2003) equation (i.e., Eq. 1) and using the optimized Slichter Equation. Since the Slichter Equation requires a porosity value as input, an estimated porosity from grain size parameters and level of compaction/density was used, as a measured porosity from the undisturbed soil below the ponds was not available. Hydraulic gradients for these ponds were calculated as described in Massmann (2003) and as specified in the WSDOT Highway Runoff Manual (WSDOT 2016a). For the pond case histories considered here, the estimated hydraulic gradients ranged from 0.013 to 0.043 (Massmann 2003), all considerably less than 1.0.

The aspect ratio for the pond cases evaluated here is also considered in this analysis – see Massmann (2003) and WSDOT (2016a) for details on how to calculate the aspect ratio factor. In general, as the pond becomes more elongated, the aspect ratio factor increases, beginning at 1.0 for square ponds. For the cases evaluated, this aspect ratio factor ranged from 1.0 to near 1.1 for all cases except one, in which this factor was 1.3 (Massmann 2003).

The factor to account for site variability/number of measurements is not considered in these analyses. Essentially, it is assumed in these analyses that there are an adequate number of measurements to justify a factor close to 1.0. Additionally, the factor to account for the uncertainty of the method used to estimate K_{sat} (e.g., large-scale PIT versus small scale field test versus grain size based methods) specified in the DOE Stormwater Manual (DOE, 2014) is not considered in these analyses. The accuracy of the infiltration rate prediction will be assessed separately.

Consistent with Figure 39, the case histories in Figure 40, part (b) were separated into two groups: one for ponds in which the pond bottom conditions were good (i.e., well maintained), and a second group for ponds with poor pond bottom conditions. However, in part (a) of Figure 40, both pond groups are put together to be able to see trends as a function of d_{10} more clearly. The current recommended reduction factors for siltation/biofouling in both Massmann (2003) and WSDOT (2016a) were used to account for the condition of these ponds. For those ponds in the well maintained group, reduction

factors for pond bottom conditions ranged from 0.9 to 1.0. For pond bottom conditions that were poor, reduction factors ranged from 0.3 to 0.5 (see Massmann 2003 for details regarding these case histories and the reduction factors used).

As can be observed in Figure 40, there is a lot of scatter in the infiltration rate predictions with both K_{sat} prediction equations. In part (a), it can be observed that at the largest soil d_{10} values for the case histories evaluated, the estimated infiltration rates using both the optimized Slichter and Massmann (2003) equations to estimate K_{sat} , the predicted and measured infiltration rates are fairly close together. However, at smaller d_{10} values (i.e., high silt content soils), the scatter in the predictions increases, and infiltration estimates using the optimized Slichter Equation for K_{sat} are consistently lower (i.e., more conservative) than when the Massmann (2003) Equation is used to determine K_{sat} . In part (b), it can be observed that the predicted infiltration rates when using either K_{sat} method are mostly less than the measured rates. In one of the cases, when using the optimized Slichter Equation, the prediction is very conservative. In a couple of cases, when using the Massmann (2003) Equation, the prediction is slightly unconservative. Based on this figure, it appears that the siltation/biofouling reduction factor is overly conservative for finer grained soils (i.e., when the soil d_{10} is less than about 0.01 mm), especially when the optimized Slichter (or Terzaghi and Chapuis) Equation is used. This is consistent with the observation that the Massmann Equation tends to be unconservative for finer grained soils.

As discussed earlier in this report, the soil porosity (or void ratio) value needed in the optimized Slichter, Terzaghi, and Chapuis equations should be measured for the site soils if possible. For embankment fill materials, a measured soil porosity can be obtained from nuclear densometer readings conducted in accordance with WSDOT SOP 615 (WSDOT 2016c) obtained for the as compacted fill (or at least verified as the fill is placed). When using the nuclear densometer to obtain compaction information, the following equation can be used to determine the soil porosity:

$$\eta = [G_s(\gamma_w/\gamma_d) - 1]/(G_s(\gamma_w/\gamma_d)) \quad (18)$$

where,

G_s = specific gravity of solids

γ_w = unit weight of water, and

γ_d = dry unit weight of soil

Typically, G_s is 2.65 to 2.67 for sands and gravels, and for cohesive soil mixtures is 2.68 to 2.72 (see Table 2-1 in Bowles 1979).

It is also possible to use a laboratory compaction test of the proposed fill material to at least bracket the range of porosity of the fill material to be used if a sample of the fill material is available in advance. If the fill material is not available to evaluate, but the fill specifications to be used are known, then it is possible to use the test results obtained in this study to estimate the range of K_{sat} values that could be anticipated. For convenience, these values are summarized in Table 11 for typical as compacted WSDOT fill materials.

For existing subsurface soils, if it is possible to obtain undisturbed samples (i.e., for soils that are not too coarse), soil density, moisture content, and porosity values can be obtained in the laboratory. If undisturbed soil samples cannot be obtained, porosity can be estimated using soil grain size parameters as presented earlier. If the soil is normally consolidated, treat the soil as uncompacted to estimate the porosity. If the soil is known to be at least moderately over-consolidated, the soil should be treated as a compacted soil for the purpose of determining a porosity. A practical approach to assess the compactness of the in situ soil is to use the Standard Penetration Test (SPT) blow counts corrected for hammer efficiency and overburden stress, N_{160} (see Section 5.5 in the WSDOT Geotechnical Design Manual – WSDOT 2015). Typically, soils with a SPT N_{160} blow count of 30 blows/ft or more can be considered to be “compacted” soils when using Eq’s 13 and 14 to estimate porosity, and soils with a SPT N_{160} blow count of 10 or less can be considered “uncompacted.” Linear interpolation can be used for SPT N_{160} values in between these two values. If the soil is a glacially consolidated till, or if the soil is a clay, such soils are beyond the scope of this report. However, practically speaking, such soils should be considered as impermeable with regard to infiltration.

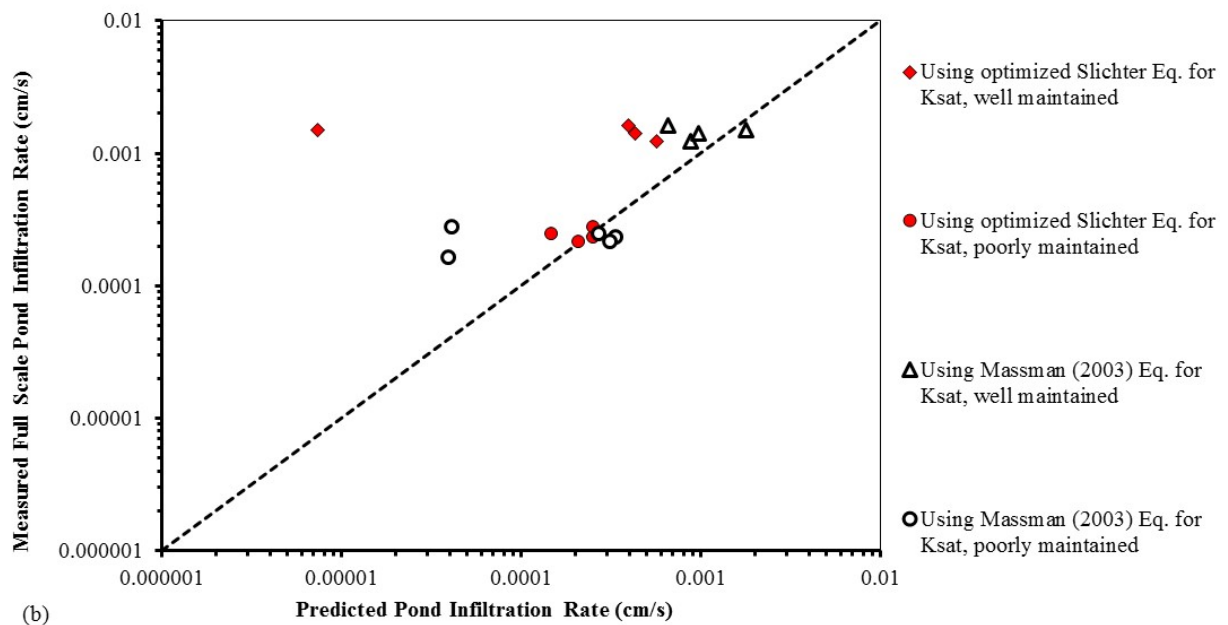
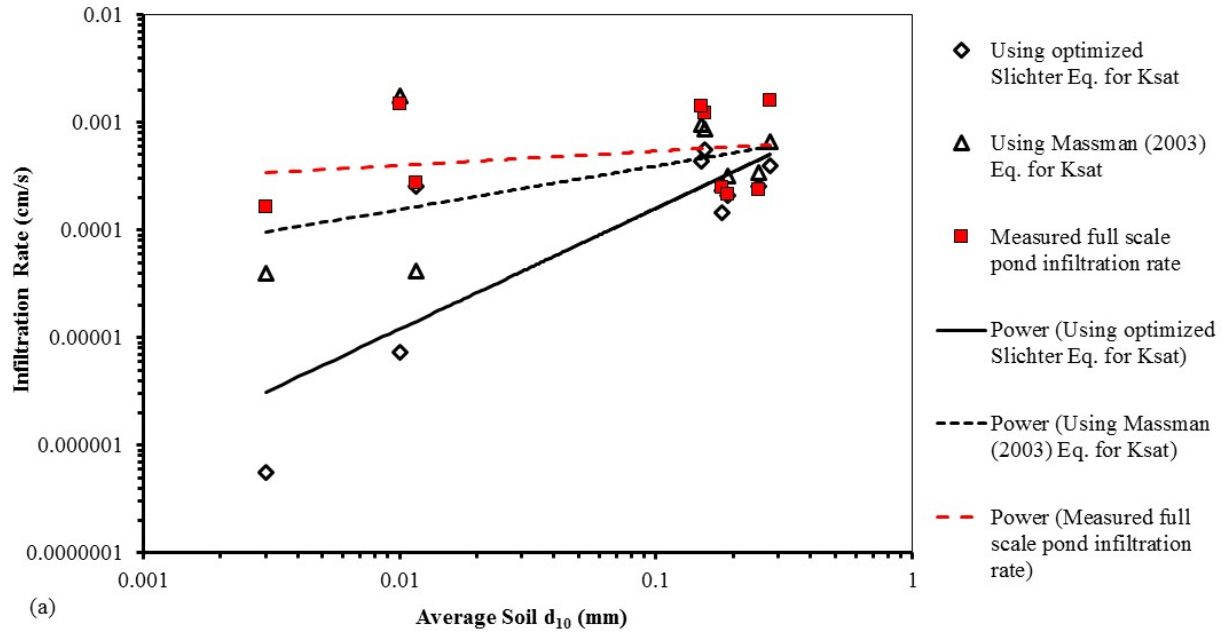


Figure 40. Comparison of estimated and measured full scale pond infiltration rates using the Massmann (2003) equation (Eq. 1) and the optimized Slichter Equation (Eq. 9) to estimate K_{sat} .

Table 11. Measured K_{sat} values for typical WSDOT fill materials.

Soil	Compacted K_{sat} (cm/s)
Fine End Gravel Borrow	0.02 to 0.022
Select Borrow	0.021 to 0.059
Common Borrow	0.017 to 0.026
Sandy Glacial Outwash	0.026 to 0.066
Course Gravel Borrow	11+

CONCLUDING REMARKS AND RECOMMENDATIONS

The estimation of hydraulic conductivity (K_{sat}) is a key step in the assessment of the rate of infiltration, whether that estimate is for an infiltration pond or trench, if it is for a highway embankment, or if it is for natural dispersion in general. The focus of this research is to assess available methods for estimating K_{sat} , especially with regard to the ability of various methods to assess K_{sat} in both a loose, uncompacted state as well as in a compacted state for embankments. K_{sat} prediction for natural soils is also considered.

The existing K_{sat} prediction equation in the WSDOT Highway Runoff Manual as well as other historical K_{sat} prediction equations were evaluated, especially with regard to their ability to account for the effects of compaction. To accomplish this, a series of relatively large diameter (i.e., 6 to 9 inch diameter) saturated hydraulic conductivity tests were conducted both in a loose state and in a compacted state. A total of 73 tests, after removal of outliers, were conducted to assess the effect of compaction. In addition, 137 saturated hydraulic conductivity tests were obtained from the literature as summarized by Chapuis (2004) to use as a basis for comparison to the tests from the current study, to make sure that the current test results are reasonably consistent with similar test results obtained by others.

For all of the data sets considered, including the ones developed specifically for this study, the measured K_{sat} is moderately to strongly correlated to the soil d_{10} size and moderately correlated to the soil uniformity coefficient, C_u .

Existing K_{sat} estimation equations evaluated include Eq. 1 (Massmann 2003 and WSDOT 2016a), Eq. 2 (Hazen 1892), Eq. 3 (Slichter 1898), Eq. 4 (Terzaghi 1925), and Eq. 6 (Chapuis 2004). A limited evaluation of the Kozeny-Carmen Equation (Eq. 5) was also conducted and included in an appendix. Of these, only the Slichter, Terzaghi, Kozeny-Carmen, and Chapuis equations are directly capable of addressing the effects of compaction or over-consolidation through the porosity or void ratio. All of these equations have, for the most part, been empirically developed, and their accuracy is dependent on the empirical data used to develop them. The soils used in the current study are characterized as consisting of irregular and subangular to angular particles, with the exception of the coarsest particles used which were more rounded. These soils are

also more well graded than soils used in previous studies, as the majority of the soils encountered by WSDOT, especially for embankments, are glacial in origin. Some of these historical K_{sat} equations were more affected by the difference in these soil characteristics than others. Of course, the simplified Hazen Equation is only a function of d_{10} , and it was clear that the measured K_{sat} values for the compacted soils were consistently smaller than predicted by that equation. All of the historical K_{sat} equations needed some empirical adjustment (i.e., optimization) to more accurately fit the measured K_{sat} measurements. After the historical equations were optimized, the optimized Slichter (Eq. 9), Terzaghi (Eq. 10) and Chapuis (Eq. 11) equations provided the most accurate K_{sat} predictions over the widest range for all the soils considered in this study.

Regarding the application of these results in infiltration design practice, the estimation of soil porosity can be a hindrance, especially for new compacted embankments, since even the specific soil characteristics of the embankment fill may not be known at design time. However, the fill material specifications are likely known, and the potential material sources that could be used for the fill may be known. Therefore, if the soil gradational property ranges can be determined, then the range in K_{sat} values for the proposed fill could be estimated, if the porosity of the compacted soil can be estimated using soil gradation parameters.

Porosity cannot be estimated with soil gradation properties alone. Using the data gathered in this study, as well as data gathered by others reported in the literature, the effect of soil gradation parameters on how well a given soil can be compacted was determined. While the effect of compaction on porosity, considering the soil gradational parameters, was only developed crudely (i.e., either the effect of compaction is either on or off), based on the available data, use of a porosity estimated from gradational parameters considering compaction effects in the optimized Slichter, Terzaghi and Chapuis equations had only a minimal effect on their prediction accuracy.

Full-scale infiltration pond examples provided in Wiltsie (1998) and Massmann (2003) are compared to infiltration estimates using the optimized Slichter (Eq. 9) and original (Eq. 1) Massmann (2003) K_{sat} equations combined with calculated hydraulic gradients for those ponds. For those cases where the soil d_{10} is greater than 0.1 mm, infiltration rate estimates using both methods were similar. However, both K_{sat}

prediction methods result in increasingly conservative infiltration rate predictions as the soil d_{10} decreases, with the optimized Slichter Equation producing more conservative estimates than the Massmann (2003) Equation. This means that infiltration rates estimated using the new, more accurate K_{sat} equations may be smaller when the soil d_{10} size is less than 0.1 mm, if adjustments are not made to the empirically developed siltation/biofouling correction factors recommended by Massmann (2003).

It is recommended that the current K_{sat} prediction equation in the WSDOT Highway Runoff Manual (WSDOT 2016a) be replaced with the optimized Slichter, Terzaghi, and/or Chapuis equations (Eq's. 9, 10, and/or 11, respectively). If only grain size data are available for estimation of K_{sat} for an embankment soil or for subsurface natural soil strata, the porosity can be estimated using eq's. 13 and 14, which use the soil d_{10} size, C_u , and the degree of compaction or over-consolidation (i.e., either it is compacted or loose, or for natural subsurface soil strata it is either over-consolidated or normally consolidated) as input parameters. Interpolation between the uncompacted and compacted conditions when estimating porosity could be done if desired. With regard to application of these findings to infiltration design, the current reduction factors for siltation/biofouling are acceptable if the soil d_{10} size is 0.1 mm or more, but may be overly conservative for smaller soil d_{10} sizes. This is especially true when using the optimized K_{sat} prediction methods recommended in this report.

Regarding the test method uncertainty factor in the DOE Stormwater Manual (DOE 2014), the greater accuracy of the optimized Slichter, Terzaghi, and Chapuis equations, and the comparison to full scale pond infiltration rate measurements, indicates that the test method uncertainty factor should be much closer to 1.0.

ACKNOWLEDGMENTS

The author wishes to acknowledge the support provided by the WSDOT Environmental Services Office during this study to promote the funding needs and for general guidance to develop this study. The author also wishes to acknowledge the contributions by Bob Grandorff and Sam Wade in developing and conducting the laboratory testing which were key in being able to carry out this study. Finally, the author wishes to acknowledge the data provided by Dr. R. P. Chapuis that were used in the analyses he conducted in his 2004 paper in the Canadian Geotechnical Journal cited in this report. His help in supplying that data is much appreciated.

REFERENCES

- AASHTO, 2014, *Standard Test Method for Permeability of Granular Soils (Constant Head), Rigid Wall, T215*, Washington DC, 15 pp.
- AASHTO, 2015, *Standard Method of Test Moisture-Density Relations of Soils Using a 4.54-kg (10-lb) Rammer and a 457-mm (18-in.) Drop, T180-15*, AASHTO, Washington DC, 14 pp.
- AASHTO, 2017, *Standard Test Method for Moisture-Density Relations of Soils Using a 2.5-kg (5.5-lb) Rammer and a 305-mm (12 in.) Drop, T99-17*, Washington DC, 13 pp.
- Allen, T.M., Nowak, A.S. and Bathurst, R.J., 2005, *Calibration to Determine Load and Resistance Factors for Geotechnical and Structural Design*, Transportation Research Board Circular E-C079, Washington, DC, 93 p.
- ASTM, 2014, *Standard Test Method for Sieve Analysis of Fine and Coarse Aggregates, C-136-06*, ASTM, West Conshohocken PA, 5 pp.
- ASTM, 2009, *Standard Test Methods for Laboratory Determination of Density (Unit Weight) of Soil Specimens, D7263-09*, ASTM, West Conshohocken PA, 7 pp.
- ASTM, 2016, *Measurement of Hydraulic Conductivity of Saturated Porous Materials Using a Flexible Wall Permeameter, Method C – Falling Head, Rising Tailwater, D5084-16a*, ASTM, West Conshohocken PA, 24 pp.
- Bathurst, R.J., Allen, T.M., and Nowak, A.S., 2008, “Calibration Concepts for Load and Resistance Factor Design (LRFD) of Reinforced Soil Walls,” *Canadian Geotechnical Journal*, Vol. 45, pp. 1377-1392.
- Bathurst, R.J., Huang, B., and Allen, T.M., 2010, Load and resistance factor design (LRFD) calibration for steel grid reinforced soil walls, *GeoRisk*, Vol. 5, N’s 3-4, pp. 218-228.
- Blackwell, P.S., A.J. Ringrose-Voase, N.S. Jayawardane, K.A. Olsson, D.C. McKenzie, and W.K. Mason, 1990, “The use of air-filled porosity and intrinsic permeability to air to characterize structure of macropore space and saturated hydraulic conductivity of clay soil,” *Journal of Soil Science*, 41, pp. 215-228.

- Bowles, J. E., 1979, *Physical and Geotechnical Properties of Soils*, McGraw-Hill, 478 pp.
- Carman, P. C., 1937, "Fluid flow through granular beds," *Trans Inst Chem Eng*, London, 15, pp. 150–166.
- Carman, P. C., 1939, "Permeability of saturated sands, soils and clays," *Journal of Agriculture Science*, 29, pp. 263–273.
- Carrier, W.D., 2003, "Goodbye, Hazen, Hello, Kozeny-Carman," *ASCE Journal of Geotechnical and Geoenvironmental Engineering*, 129, pp.1054–1056.
- Chapuis, R. P., 2004, "Predicting the Saturated Hydraulic Conductivity of Sand and Gravel Using Effective Diameter and Void Ratio," *Canadian Geotechnical Journal*, Vol. 41, pp. 787-795, DOI: 10.1139/T04-022.
- Chapuis, R. P., 2012, "Predicting the Saturated Hydraulic Conductivity of Soils: A Review," *Bull. Eng. Geol. Environ.*, 71, pp. 401-434, DOI: 10.1007/s10064-012-0418-7.
- Hazen, A., 1892, *Some physical properties of sand and gravel, with special reference to their use in filtration*, Massachusetts State Board of Health, 24th annual report, Boston, pp. 539–556.
- Holtz. R. D., and Kovaks, W. D., 1981, *An Introduction to Geotechnical Engineering*, Prentice-Hall, p. 119.
- Iversen B., P. Moldrup, P. Schjonning, and P.Loll. 2001, "Air and water permeability in differently textured soils at two measurement scales," *Soil Science*, 166(10), pp. 643-659.
- Kozeny, J., 1927, "Ueber kapillare Leitung des Wassers in Boden." *Sitzungsber Akad, Wiss., Wien Math. Naturwiss. Kl. Abt.2a* 13:271–306 (in German)
- Leroueil, S., J.-P. Le Bihan, S. Sebaihi, and V. Alicescu, 2002, "Hydraulic conductivity of compacted tills from northern Quebec," *Canadian Geotechnical Journal*, 39(5).
- Loll, P., Moldrup P., Schjonning P., and Riley H., 1999, "Predicting Saturated Hydraulic Conductivity from Air Permeability: Application in Stochastic Water Infiltration Modeling," *Water Resources*, 35(8), pp. 2387-2400.

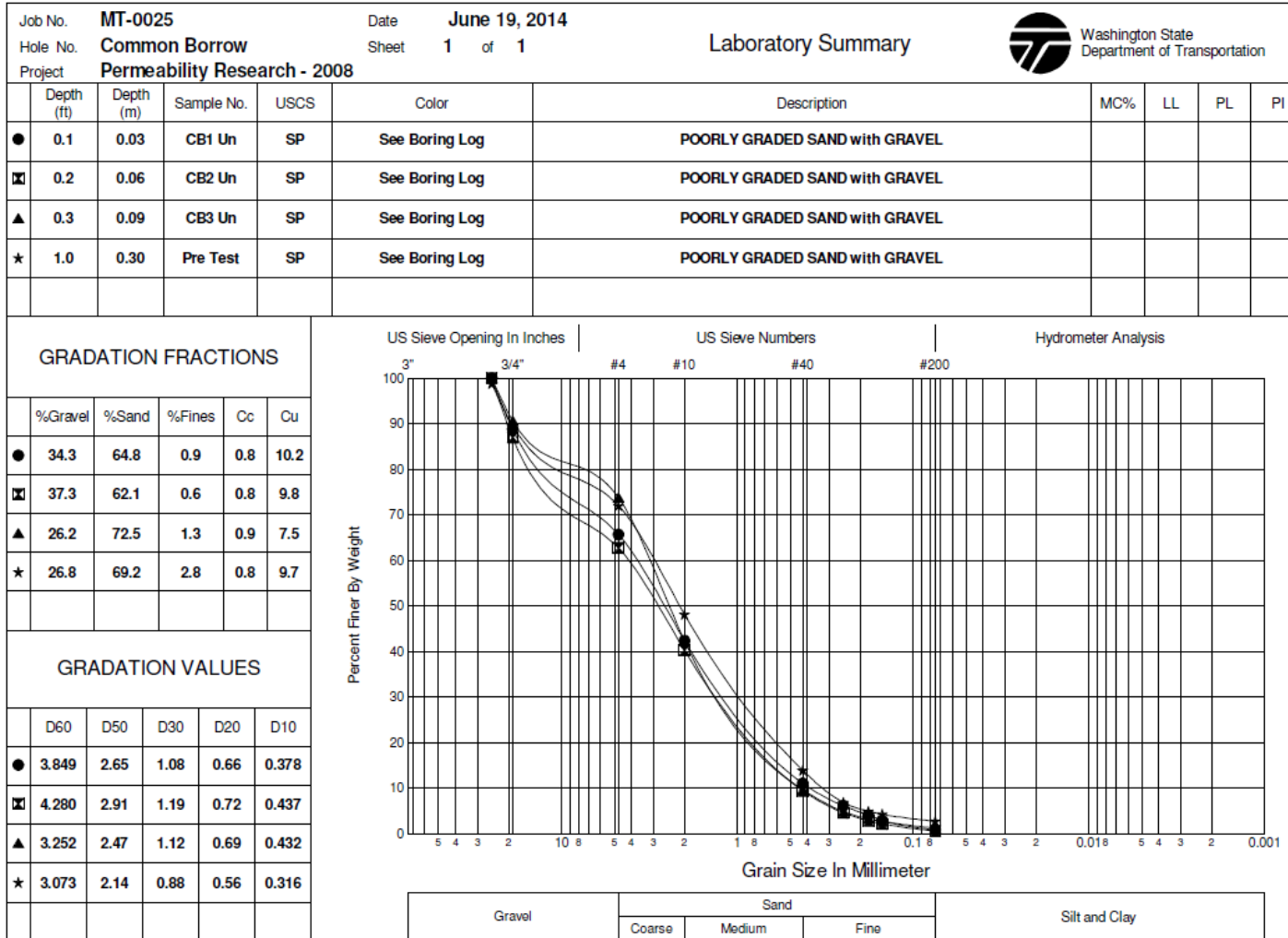
- Massmann, J. W., 2003, Implementation of Infiltration Ponds Research, WA-RD 578.1, 218 pp.
- Massmann, J. W., 2008, Infiltration Pond Research Extension, Keta Waters LLC, unpublished report for WSDOT, 57 pp.
- NAVFAC, 1974, *Soil Mechanics, Foundations, and Earth Structures, Naval Facilities Engineering Command (NAVFAC) Design Manual DM7*. U.S. Government Printing Office, Washington, D.C.
- Slichter C. S., 1898, *Theoretical investigation of the motion of ground waters*. US Geological Survey, 19th Annual Report, 2:295–384.
- Taylor, D.W., 1948, *Fundamentals of Soil Mechanics*, John Wiley & Sons, New York.
- Terzaghi, C., 1925, “Principles of soil mechanics: III. Determination of permeability of clay,” *Engineering News Record*, 95(21), pp. 832–836.
- Vukovic, M. and Soro, A., 1992, *Determination of Hydraulic Conductivity of Porous Media from Grain Size Composition*, Water Resources Publications, Littleton, CO, 84 pp.
- Watabe, Y., S. Leroueil, and J-P. Le Bihan, 2000, “Influence of compaction conditions on pore-size distribution and saturated hydraulic conductivity,” *Canadian Geotechnical Journal*, Vol. 37(6), p. 1184.
- Weeks, E.P., 1978, “Field Determination of Vertical Permeability to Air in the Unsaturated Zone,” USGS professional paper 1051, Washington, D.C.
- Wiltsie, E.A., 1998, *Stormwater Facilities Performance Study, Infiltration Pond Testing and Data Evaluation*, Thurston County, Washington.
- Washington State Dept. of Ecology (WSDOE), 2014, *Stormwater Management Manual for Western Washington*, Publication Number 14-10-055, 1192 pp. (specifically Vol. III, Chapter 3).
- WSDOT, 2008, *Standard Specifications for Road, Bridge, and Municipal Construction*, M 41-10.
- WSDOT, 2015, *WSDOT Geotechnical Design Manual*, M 46-03, 868 pp.
- WSDOT, 2016a, *WSDOT Highway Runoff Manual*, M31-16, 522 pp. (specifically Appendix 4D).

WSDOT, 2016b, “Method of Test for Compaction Control of Granular Materials,” T606,
WSDOT Materials Manual, M46-01, 12 pp.

WSDOT, 2016c, “Determination of the % Compaction for Embankment & Untreated
Surfacing Materials Using the Nuclear Moisture-Density Gauge,” SOP 615,
WSDOT Materials Manual, M46-01, 6 pp.

APPENDIX A

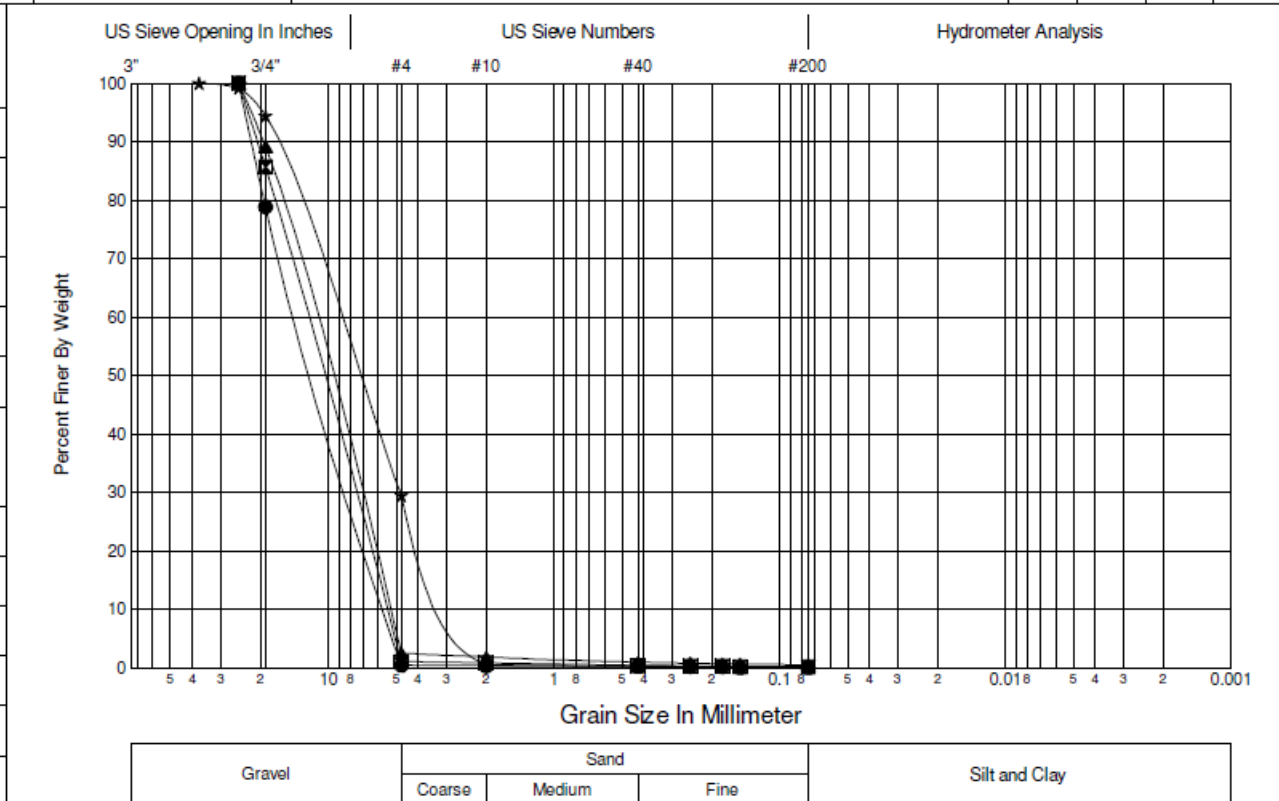
LABORATORY SUMMARIES OF SOILS USED FOR 2008 TESTING



	Depth (ft)	Depth (m)	Sample No.	USCS	Color	Description	MC%	LL	PL	PI
●	0.4	0.12	CGB1 Com	GP	See Boring Log	POORLY GRADED GRAVEL				
☒	0.5	0.15	CGB2 Com	GP	See Boring Log	POORLY GRADED GRAVEL				
▲	0.6	0.18	CGB3 Com	GP	See Boring Log	POORLY GRADED GRAVEL				
★	1.0	0.30	Pre Test	GP	See Boring Log	POORLY GRADED GRAVEL with SAND				

GRADATION FRACTIONS					
	%Gravel	%Sand	%Fines	Cc	Cu
●	99.5	0.4	0.1	0.8	2.4
☒	98.9	0.9	0.2	0.8	2.3
▲	97.5	2.0	0.5	0.9	2.2
★	70.5	29.5	0.1	1.0	3.4

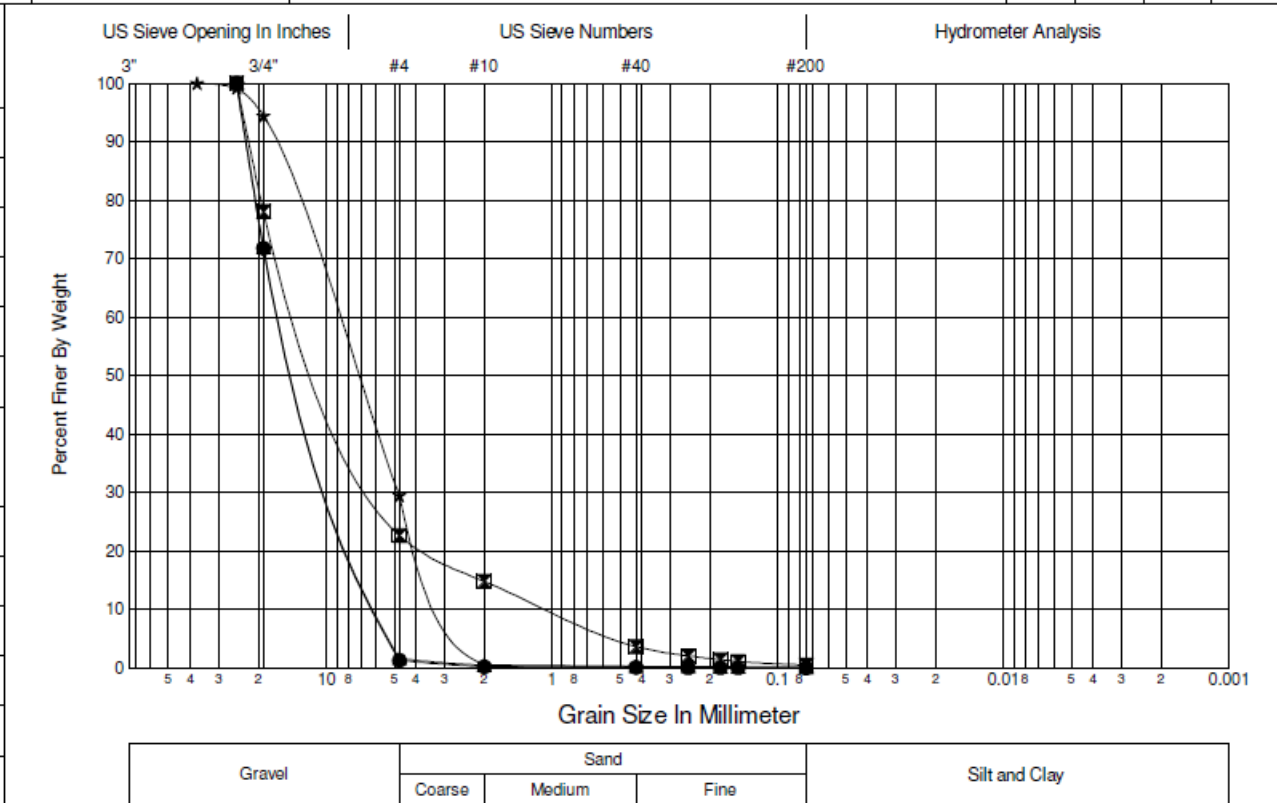
GRADATION VALUES					
	D60	D50	D30	D20	D10
●	13.614	11.41	8.01	6.71	5.623
☒	12.477	10.59	7.63	6.48	5.498
▲	11.914	10.15	7.37	6.28	5.354
★	9.106	7.36	4.80	3.58	2.655




	Depth (ft)	Depth (m)	Sample No.	USCS	Color	Description	MC%	LL	PL	PI
●	0.1	0.03	CGB1 Un	GP	See Boring Log	POORLY GRADED GRAVEL				
☒	0.2	0.06	CGB2 Un	GW	See Boring Log	WELL-GRADED GRAVEL with SAND				
▲	0.3	0.09	CGB3 Un	GP	See Boring Log	POORLY GRADED GRAVEL				
★	1.0	0.30	Pre Test	GP	See Boring Log	POORLY GRADED GRAVEL with SAND				

GRADATION FRACTIONS					
	%Gravel	%Sand	%Fines	Cc	Cu
●	98.7	1.3	0.0	0.8	2.7
☒	77.4	22.2	0.5	2.6	11.8
▲	98.4	1.6	0.0	0.8	2.7
★	70.5	29.5	0.1	1.0	3.4

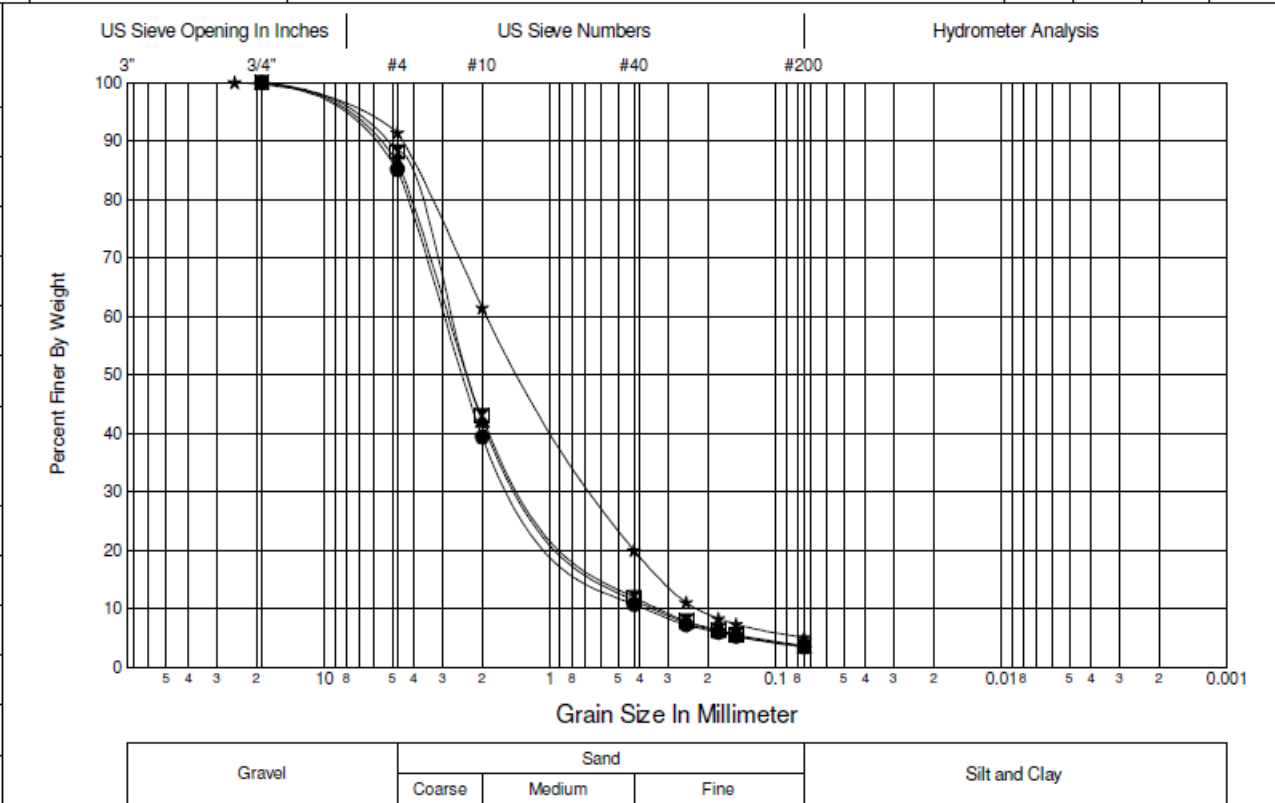
GRADATION VALUES					
	D60	D50	D30	D20	D10
●	15.073	12.38	8.35	6.86	5.637
☒	12.103	9.42	5.71	3.55	1.029
▲	15.037	12.34	8.32	6.83	5.607
★	9.106	7.36	4.80	3.58	2.655




Job No.	MT-0025		Date	June 19, 2014		 Washington State Department of Transportation				
Hole No.	Fine Gravel Borrow		Sheet	1 of 1						
Project	Permeability Research - 2008		Laboratory Summary							
	Depth (ft)	Depth (m)	Sample No.	USCS	Color	Description	MC%	LL	PL	PI
●	0.4	0.12	FGB1 Com	SW	See Boring Log	WELL-GRADED SAND				
☒	0.5	0.15	FGB2 Com	SW	See Boring Log	WELL-GRADED SAND				
▲	0.6	0.18	FGB3 Com	SW	See Boring Log	WELL-GRADED SAND				
★	1.0	0.30	Pre Test	SP-SM	See Boring Log	POORLY GRADED SAND with SILT				

GRADATION FRACTIONS					
	%Gravel	%Sand	%Fines	Cc	Cu
●	14.9	81.6	3.5	1.3	7.8
☒	11.9	84.4	3.7	1.2	8.4
▲	13.6	82.8	3.6	1.2	8.2
★	8.6	86.3	5.1	0.9	8.6

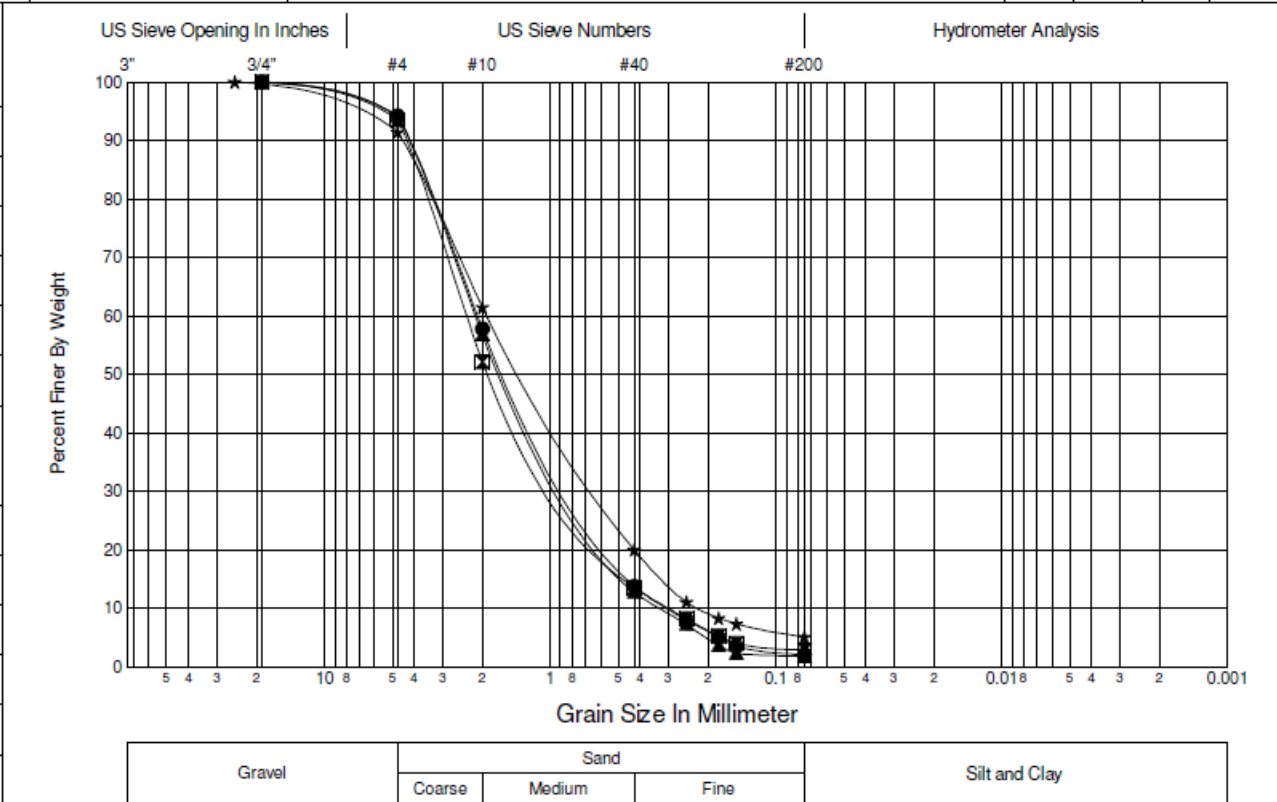
GRADATION VALUES					
	D60	D50	D30	D20	D10
●	2.955	2.45	1.20	0.70	0.379
☒	2.768	2.28	1.04	0.63	0.328
▲	2.838	2.33	1.09	0.66	0.347
★	1.893	1.30	0.62	0.42	0.219




Job No.	MT-0025		Date	June 19, 2014		 Washington State Department of Transportation				
Hole No.	Fine Gravel Borrow		Sheet	1 of 1						
Project	Permeability Research - 2008		Laboratory Summary							
	Depth (ft)	Depth (m)	Sample No.	USCS	Color	Description	MC%	LL	PL	PI
●	0.1	0.03	FGB1 Un	SP	See Boring Log	POORLY GRADED SAND				
☒	0.2	0.06	FGB2 Un	SP	See Boring Log	POORLY GRADED SAND				
▲	0.3	0.09	FGB3 Un	SP	See Boring Log	POORLY GRADED SAND				
★	1.0	0.30	Pre Test	SP-SM	See Boring Log	POORLY GRADED SAND with SILT				

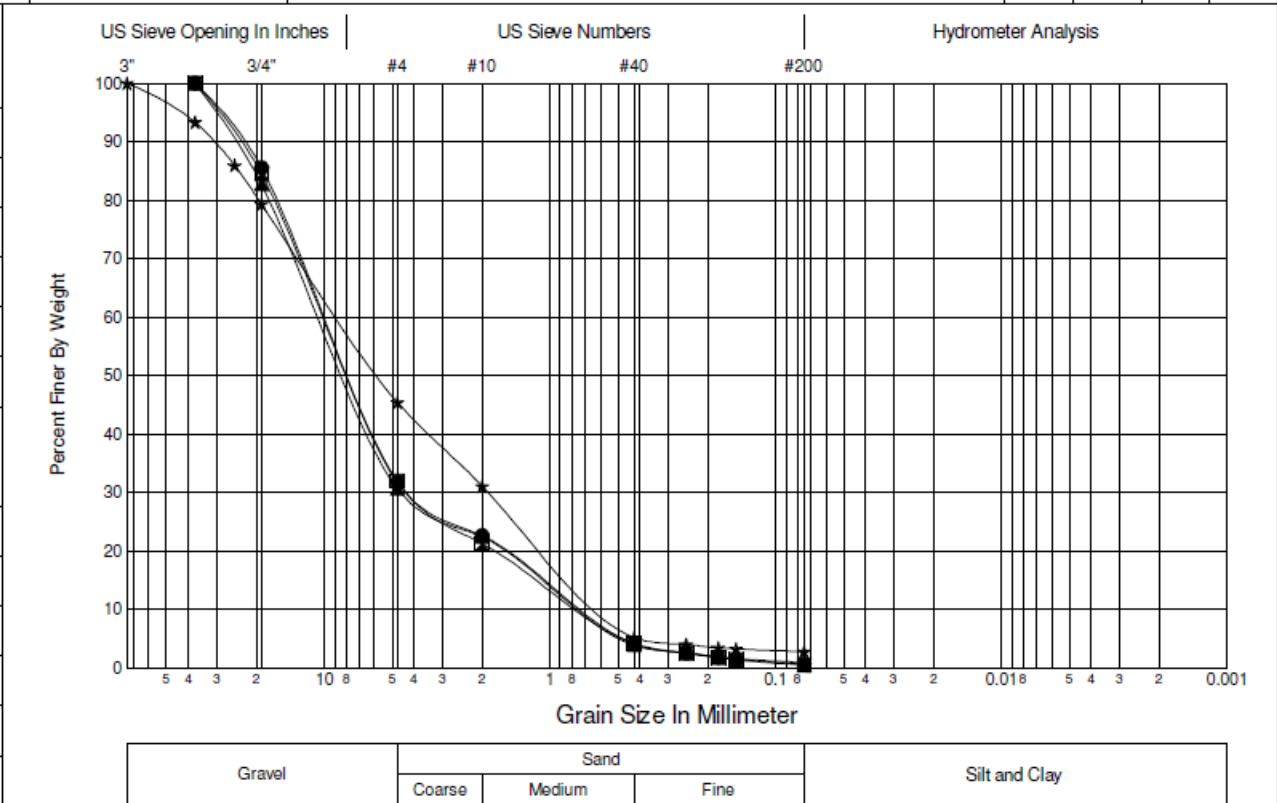
GRADATION FRACTIONS					
	%Gravel	%Sand	%Fines	Cc	Cu
●	5.8	92.1	2.1	0.9	7.1
☒	6.4	90.7	2.9	1.0	7.9
▲	5.9	92.3	1.8	0.9	6.6
★	8.6	86.3	5.1	0.9	8.6


GRADATION VALUES					
	D60	D50	D30	D20	D10
●	2.108	1.52	0.75	0.53	0.299
☒	2.355	1.83	0.82	0.55	0.297
▲	2.156	1.58	0.78	0.55	0.325
★	1.893	1.30	0.62	0.42	0.219



Job No.	MT-0025		Date	June 19, 2014		 Washington State Department of Transportation				
Hole No.	Sandy Glacial Outwash		Sheet	1 of 1						
Project	Permeability Research - 2008		Laboratory Summary							
	Depth (ft)	Depth (m)	Sample No.	USCS	Color	Description	MC%	LL	PL	PI
●	0.4	0.12	SGO1 Com	GW	See Boring Log	WELL-GRADED GRAVEL with SAND				
☒	0.5	0.15	SGO2 Com	GW	See Boring Log	WELL-GRADED GRAVEL with SAND				
▲	0.6	0.18	SGO3 Com	GW	See Boring Log	WELL-GRADED GRAVEL with SAND				
★	1.0	0.30	Pre Test	GP	See Boring Log	POORLY GRADED GRAVEL with SAND				

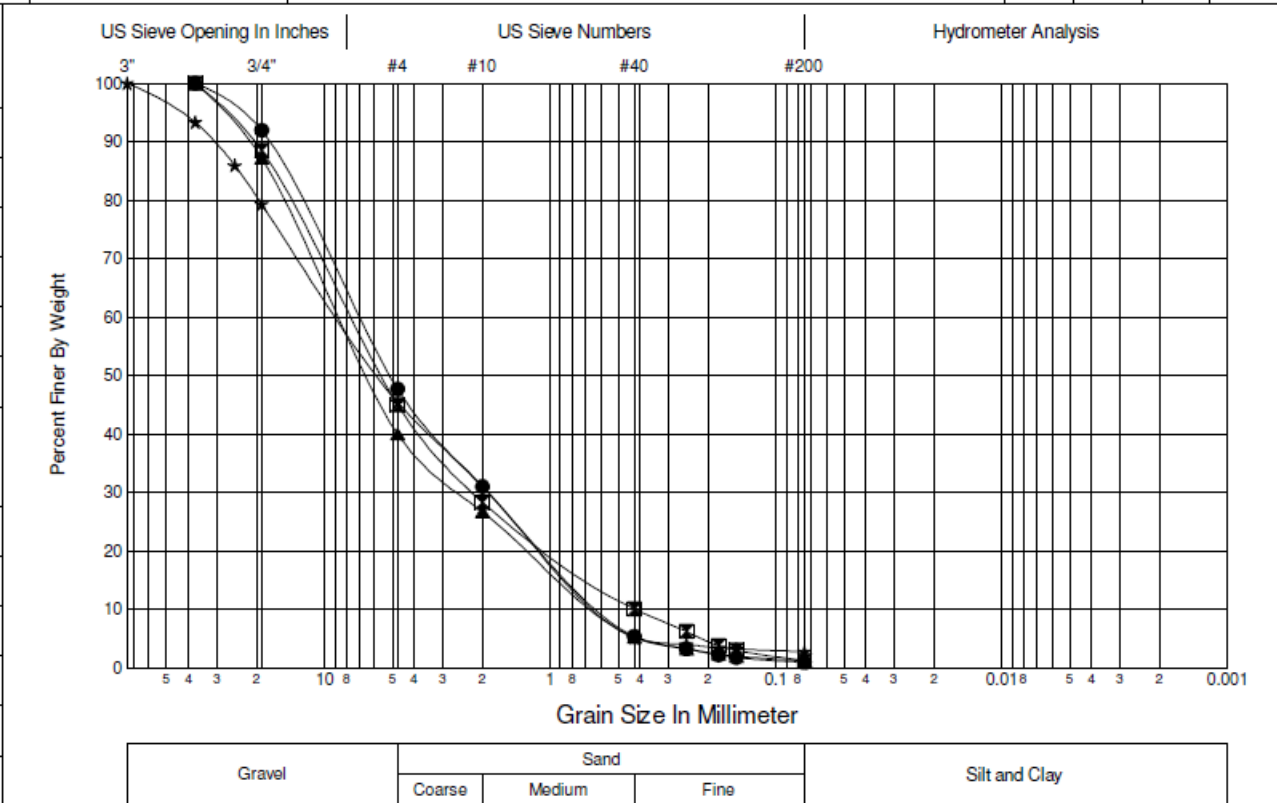
GRADATION FRACTIONS					
	%Gravel	%Sand	%Fines	Cc	Cu
●	68.2	31.1	0.6	2.4	14.1
☒	68.1	31.4	0.5	2.3	13.8
▲	69.3	29.7	0.9	2.7	14.6
★	54.6	42.6	2.8	0.7	15.2
GRADATION VALUES					
	D60	D50	D30	D20	D10
●	9.836	7.60	4.02	1.61	0.695
☒	9.957	7.65	4.06	1.78	0.722
▲	10.382	7.95	4.43	1.64	0.710
★	8.619	5.73	1.88	1.03	0.567




Job No.	MT-0025		Date	June 19, 2014		 Washington State Department of Transportation				
Hole No.	Sandy Glacial Outwash		Sheet	1 of 1						
Project	Permeability Research - 2008		Laboratory Summary							
	Depth (ft)	Depth (m)	Sample No.	USCS	Color	Description	MC%	LL	PL	PI
●	0.1	0.03	SGO1 Un	GP	See Boring Log	POORLY GRADED GRAVEL with SAND				
☒	0.2	0.06	SGO2 Un	GW	See Boring Log	WELL-GRADED GRAVEL with SAND				
▲	0.3	0.09	SGO3 Un	GW	See Boring Log	WELL-GRADED GRAVEL with SAND				
★	1.0	0.30	Pre Test	GP	See Boring Log	POORLY GRADED GRAVEL with SAND				

GRADATION FRACTIONS					
	%Gravel	%Sand	%Fines	Cc	Cu
●	52.3	46.8	0.9	0.9	12.4
☒	55.0	43.7	1.3	1.5	18.2
▲	60.0	38.8	1.2	1.2	14.2
★	54.6	42.6	2.8	0.7	15.2

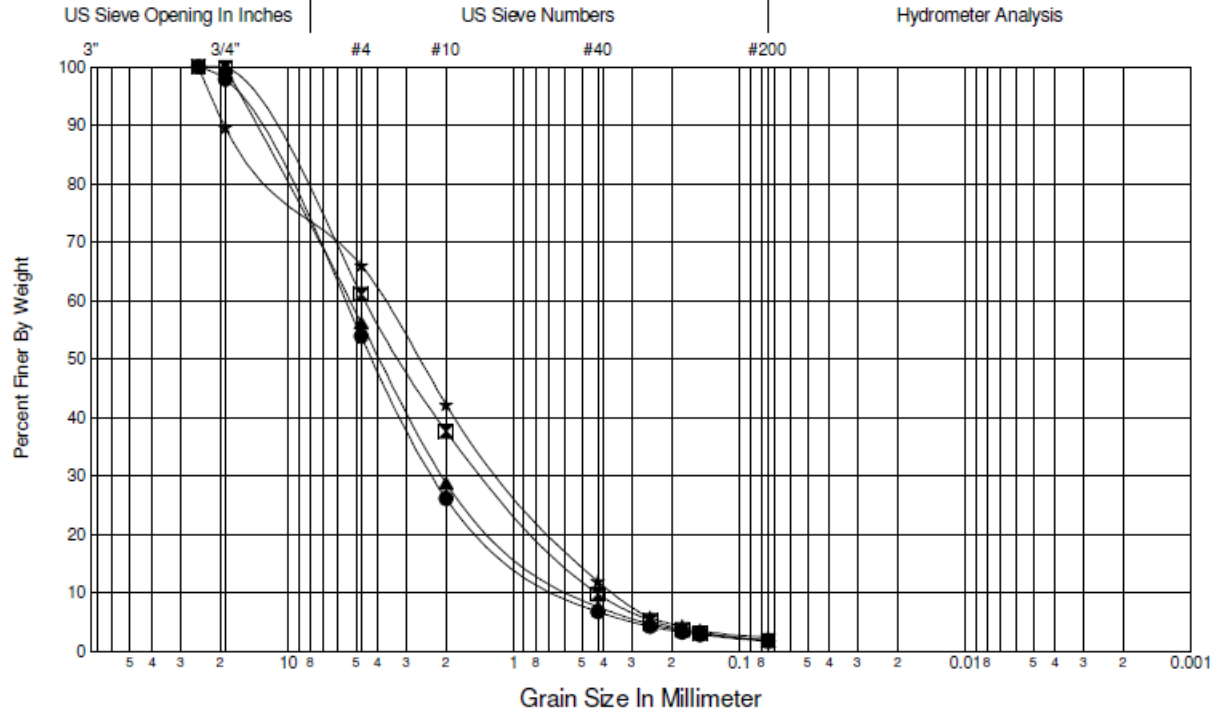
GRADATION VALUES					
	D60	D50	D30	D20	D10
●	6.983	5.10	1.88	1.03	0.561
☒	7.658	5.57	2.18	0.99	0.420
▲	8.545	6.37	2.48	1.23	0.600
★	8.619	5.73	1.88	1.03	0.567




Job No.	MT-0025		Date	June 19, 2014		 Washington State Department of Transportation				
Hole No.	Select Borrow		Sheet	1 of 1						
Project	Permeability Research - 2008		Laboratory Summary							
	Depth (ft)	Depth (m)	Sample No.	USCS	Color	Description	MC%	LL	PL	PI
●	0.4	0.12	SB1 Com	SW	See Boring Log	WELL-GRADED SAND with GRAVEL				
☒	0.5	0.15	SB2 Com	SP	See Boring Log	POORLY GRADED SAND with GRAVEL				
▲	0.6	0.18	SB3 Com	SW	See Boring Log	WELL-GRADED SAND with GRAVEL				
★	1.0	0.30	Pre Test	SP	See Boring Log	POORLY GRADED SAND with GRAVEL				

GRADATION FRACTIONS					
	%Gravel	%Sand	%Fines	Cc	Cu
●	46.1	52.2	1.7	1.6	10.5
☒	38.9	59.3	1.8	0.9	10.6
▲	43.8	54.3	1.8	1.6	10.6
★	34.0	63.6	2.4	0.8	10.7

GRADATION VALUES					
	D60	D50	D30	D20	D10
●	5.758	4.21	2.26	1.22	0.551
☒	4.559	3.15	1.31	0.75	0.429
▲	5.358	3.91	2.08	1.05	0.507
★	3.815	2.65	1.07	0.64	0.358

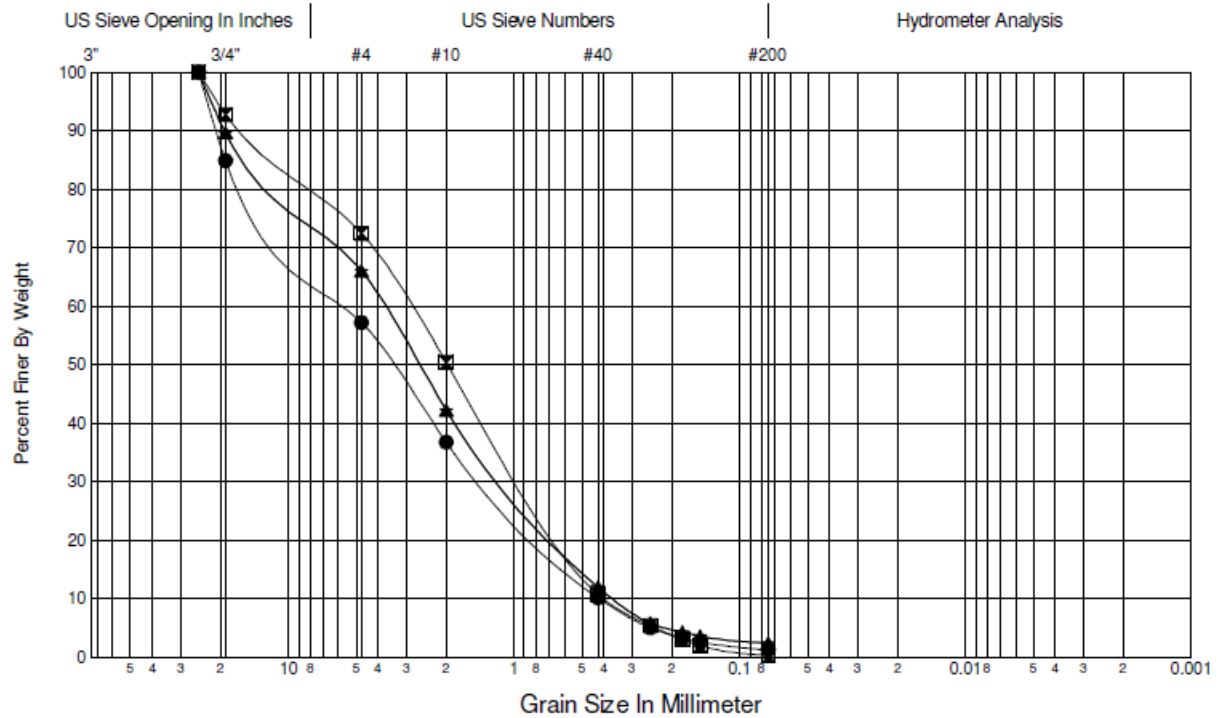


Gravel	Sand			Silt and Clay
	Coarse	Medium	Fine	

Job No.	MT-0025		Date	June 19, 2014		 Washington State Department of Transportation				
Hole No.	Select Borrow		Sheet	1 of 1						
Project	Permeability Research - 2008		Laboratory Summary							
	Depth (ft)	Depth (m)	Sample No.	USCS	Color	Description	MC%	LL	PL	PI
●	0.1	0.03	SB1 Un	SP	See Boring Log	POORLY GRADED SAND with GRAVEL				
☒	0.2	0.06	SB2 Un	SP	See Boring Log	POORLY GRADED SAND with GRAVEL				
▲	0.3	0.09	SB3 Un	SP	See Boring Log	POORLY GRADED SAND with GRAVEL				
★	1.0	0.30	Pre Test	SP	See Boring Log	POORLY GRADED SAND with GRAVEL				

GRADATION FRACTIONS					
	%Gravel	%Sand	%Fines	Cc	Cu
●	42.8	56.0	1.2	0.8	13.0
☒	27.6	72.1	0.3	0.7	7.4
▲	34.0	63.6	2.4	0.8	10.7
★	34.0	63.6	2.4	0.8	10.7

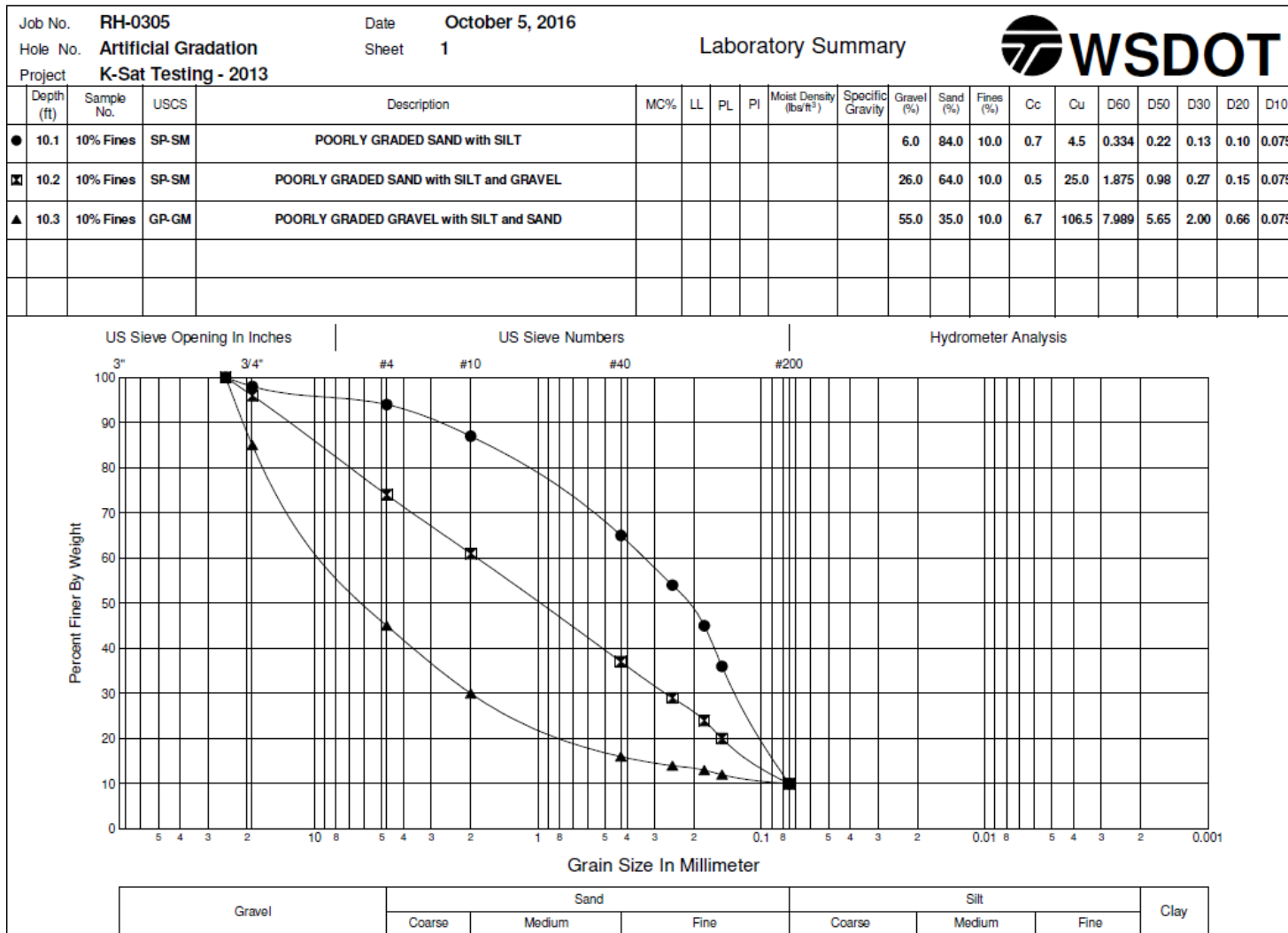
GRADATION VALUES					
	D60	D50	D30	D20	D10
●	5.466	3.50	1.35	0.75	0.419
☒	2.918	1.97	0.90	0.61	0.396
▲	3.815	2.65	1.07	0.64	0.358
★	3.815	2.65	1.07	0.64	0.358



Gravel	Sand			Silt and Clay
	Coarse	Medium	Fine	

APPENDIX B

LABORATORY SUMMARIES AND CLOSE-UP PHOTOS OF SOILS USED FOR 2013 TESTING

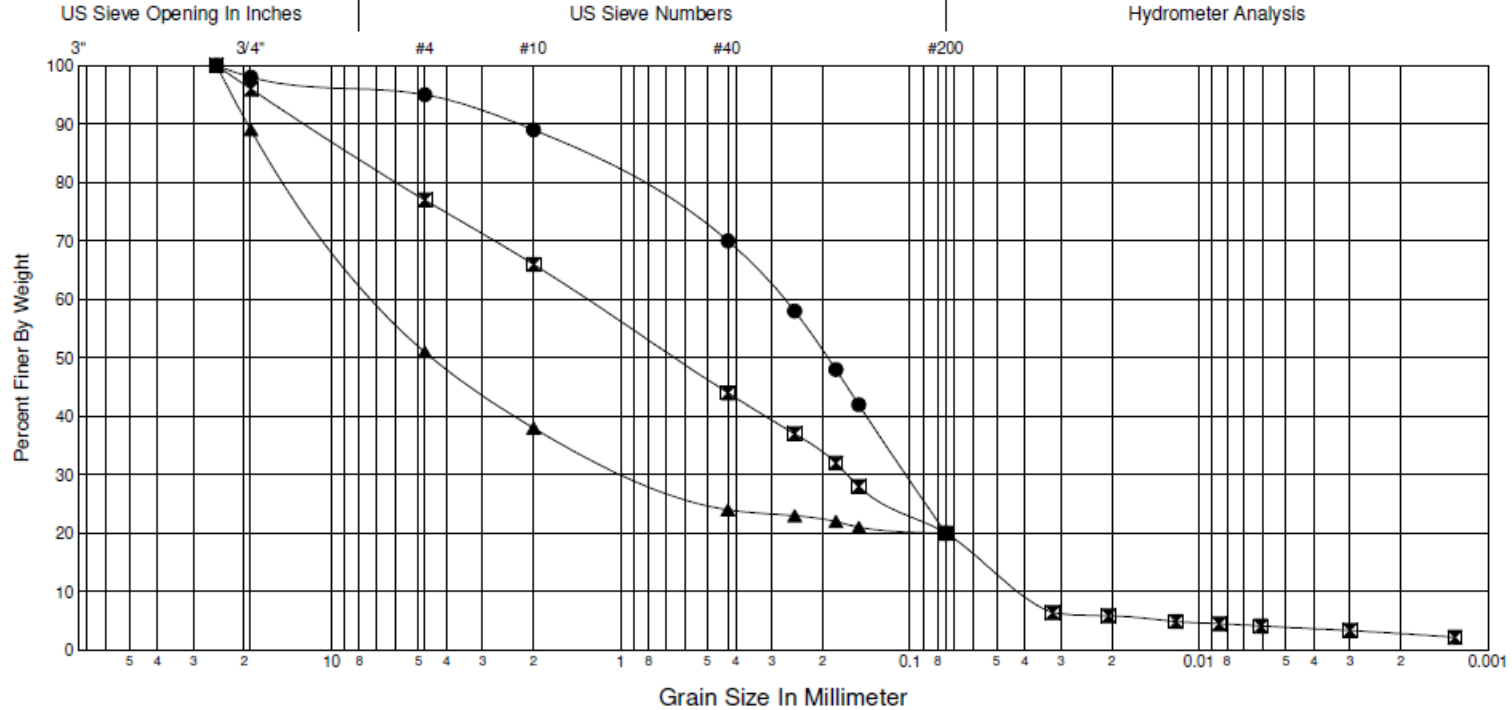


Job No. **RH-0305** Date **October 5, 2016**
 Hole No. **Artificial Gradation** Sheet **1**
 Project **K-Sat Testing - 2013**

Laboratory Summary



Depth (ft)	Sample No.	USCS	Description	MC%	LL	PL	PI	Moist Density (lb/ft ³)	Specific Gravity	Gravel (%)	Sand (%)	Fines (%)	Cc	Cu	D60	D50	D30	D20	D10
● 20.1	20% Fines	SM	SILTY SAND							5.0	75.0	20.0			0.273	0.19	0.10	0.08	
☒ 20.2	20% Fines	SM	SILTY SAND with GRAVEL						2.79	23.0	57.0	20.0	0.5	32.8	1.311	0.65	0.16	0.08	0.040
▲ 20.3	20% Fines	GM	SILTY GRAVEL with SAND							49.0	31.0	20.0			6.596	4.44	0.83	0.08	



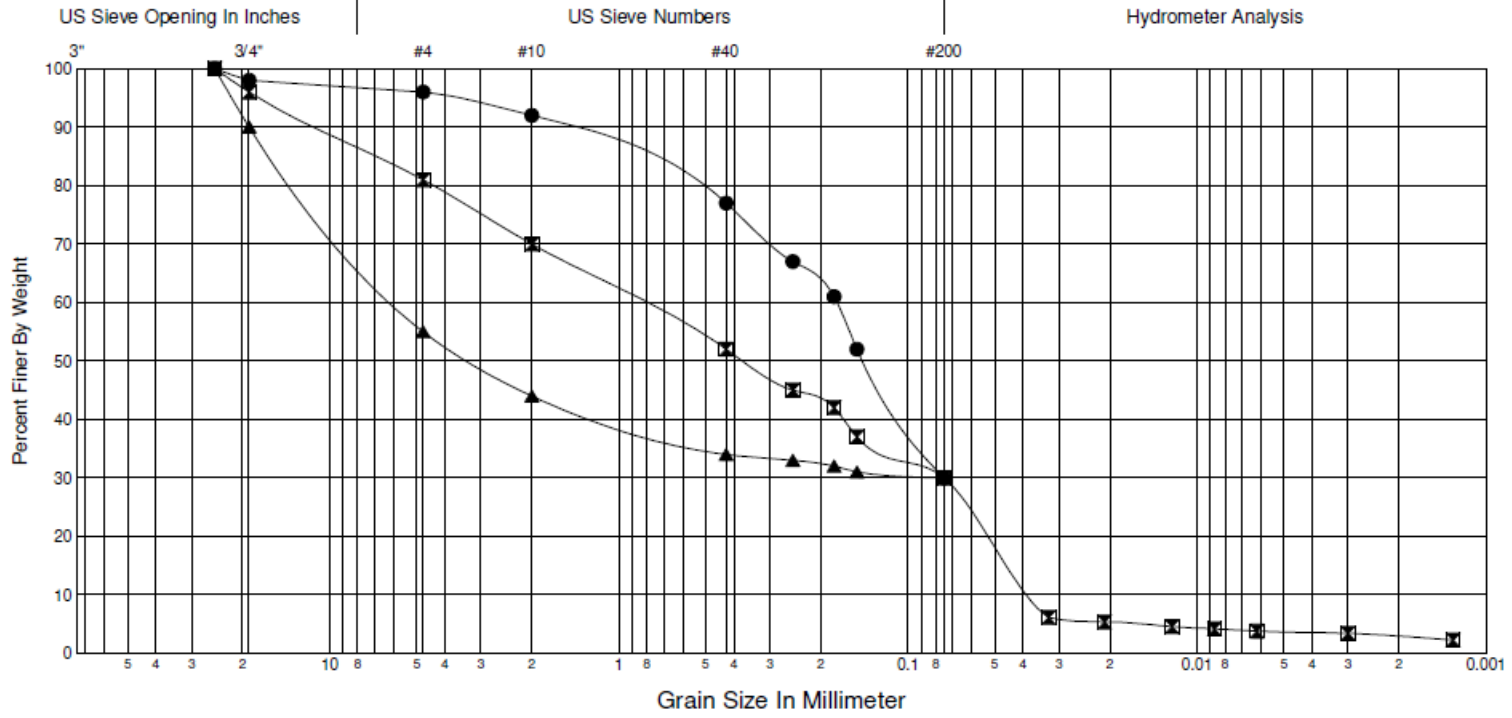
Gravel	Sand			Silt			Clay
	Coarse	Medium	Fine	Coarse	Medium	Fine	

Job No. **RH-0305** Date **October 5, 2016**
 Hole No. **Artificial Gradation** Sheet **1**
 Project **K-Sat Testing - 2013**

Laboratory Summary



Depth (ft)	Sample No.	USCS	Description	MC%	LL	PL	PI	Moist Density (lb/ft ³)	Specific Gravity	Gravel (%)	Sand (%)	Fines (%)	Cc	Cu	D60	D50	D30	D20	D10
● 30.1	30% Fines	SM	SILTY SAND							4.0	66.0	30.0			0.176	0.14	0.08		
☒ 30.2	30% Fines	SM	SILTY SAND with GRAVEL						2.75	19.0	51.0	30.0	0.2	22.7	0.846	0.37	0.08	0.05	0.037
▲ 30.3	30% Fines	GM	SILTY GRAVEL with SAND							45.0	25.0	30.0			5.790	3.21	0.08		



Gravel	Sand			Silt			Clay
	Coarse	Medium	Fine	Coarse	Medium	Fine	

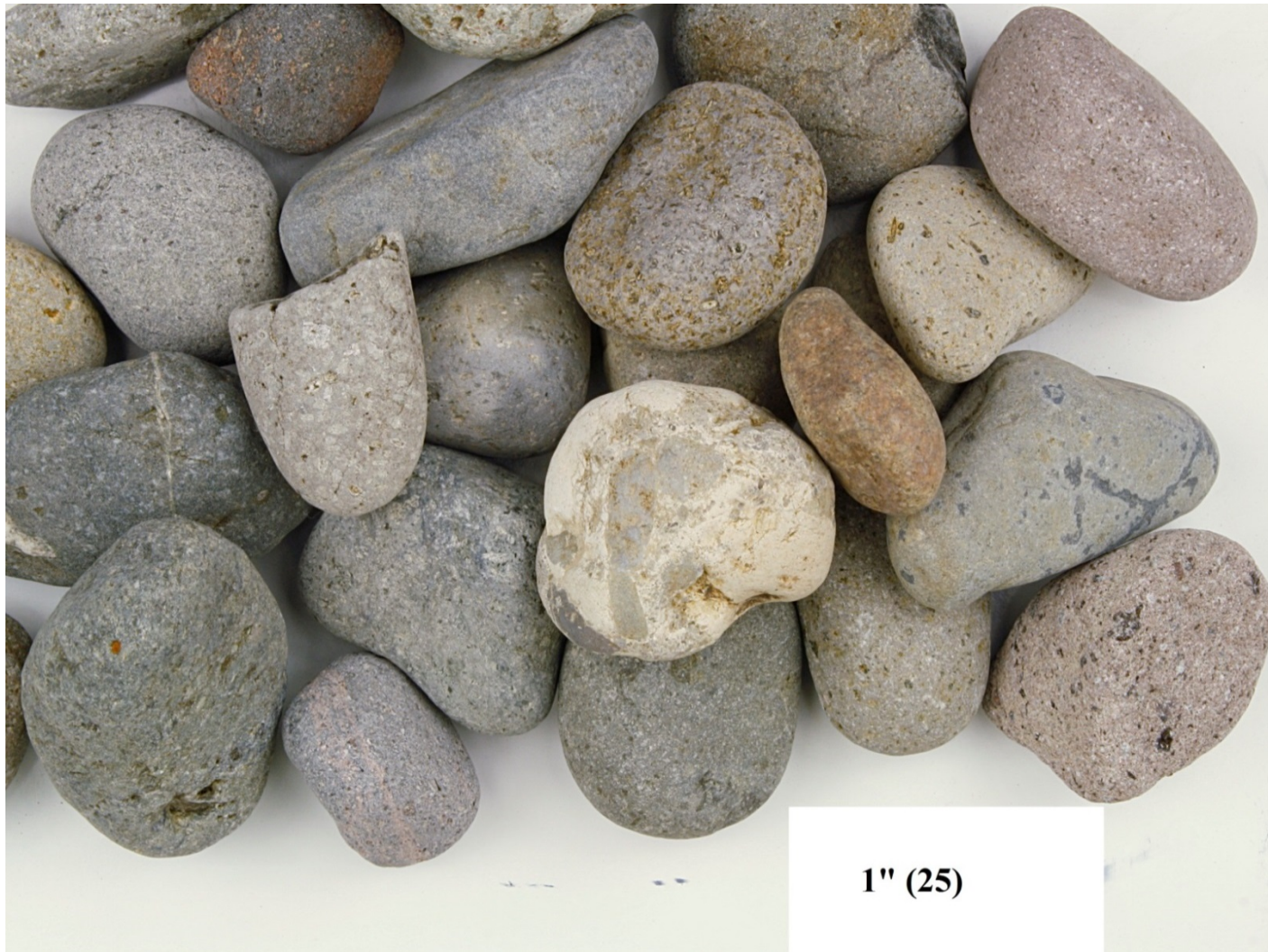


Figure B.1. Close-up of 1.0 in. (25 mm) soil particles used in 2013 and 2014 K_{sat} testing.



Figure B.2. Close-up of 0.75 in. (19 mm) soil particles used in 2013 and 2014 K_{sat} testing.



Figure B.3. Close-up of 0.0167 in. (0.425 mm) soil particles used in 2013 and 2014 K_{sat} testing.



Figure B.4. Close-up of 0.0098 in. (0.25 mm) soil particles used in 2013 and 2014 K_{sat} testing.



Figure B.5. Close-up of 0.0071 in. (0.18 mm) soil particles used in 2013 and 2014 K_{sat} testing.



Figure B.6. Close-up of 0.0059 in. (0.15 mm) soil particles used in 2013 and 2014 K_{sat} testing.



Figure B.7. Close-up of 0.003 in. (0.075 mm) soil particles used in 2013 and 2014 K_{sat} testing.

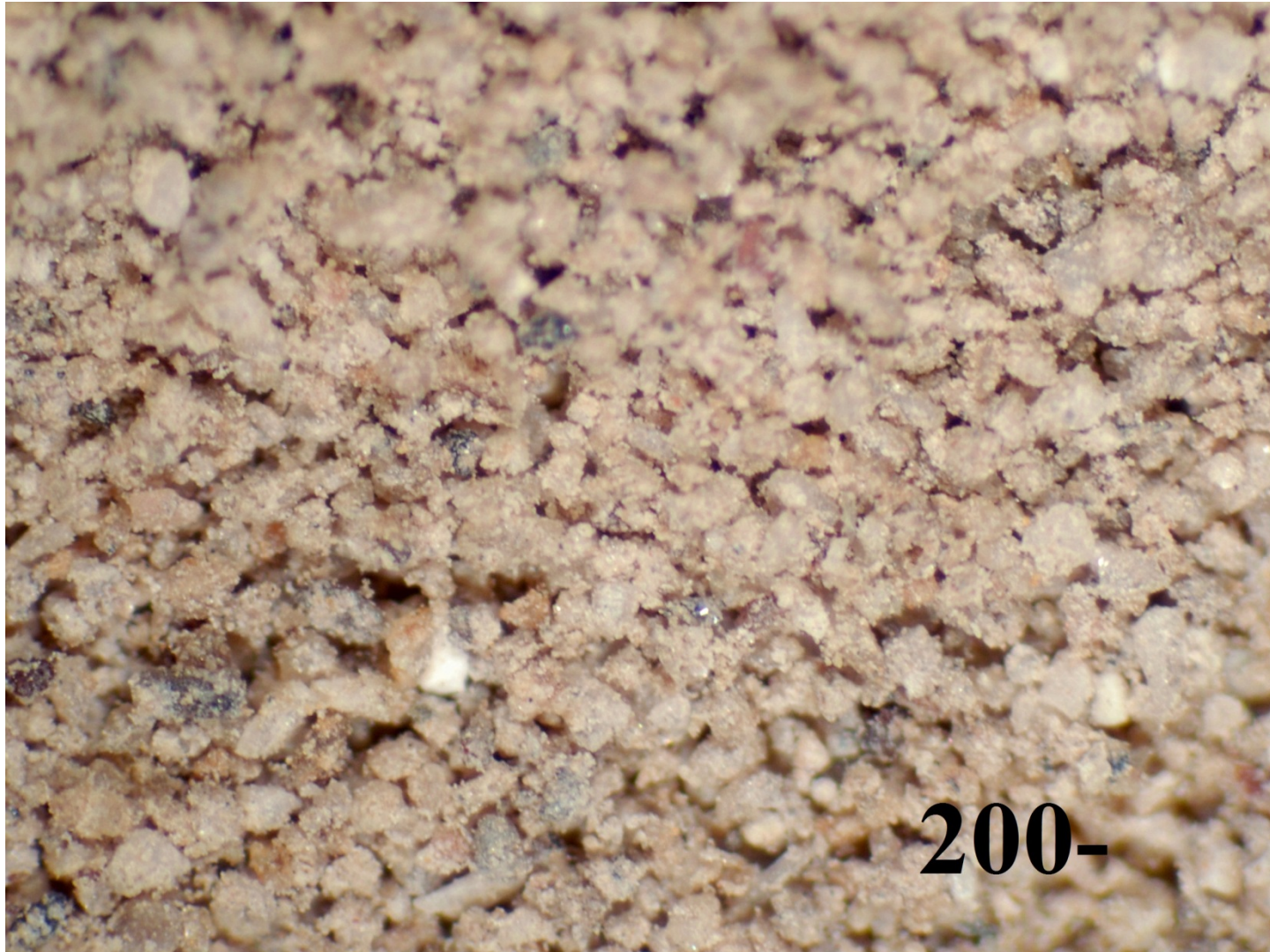
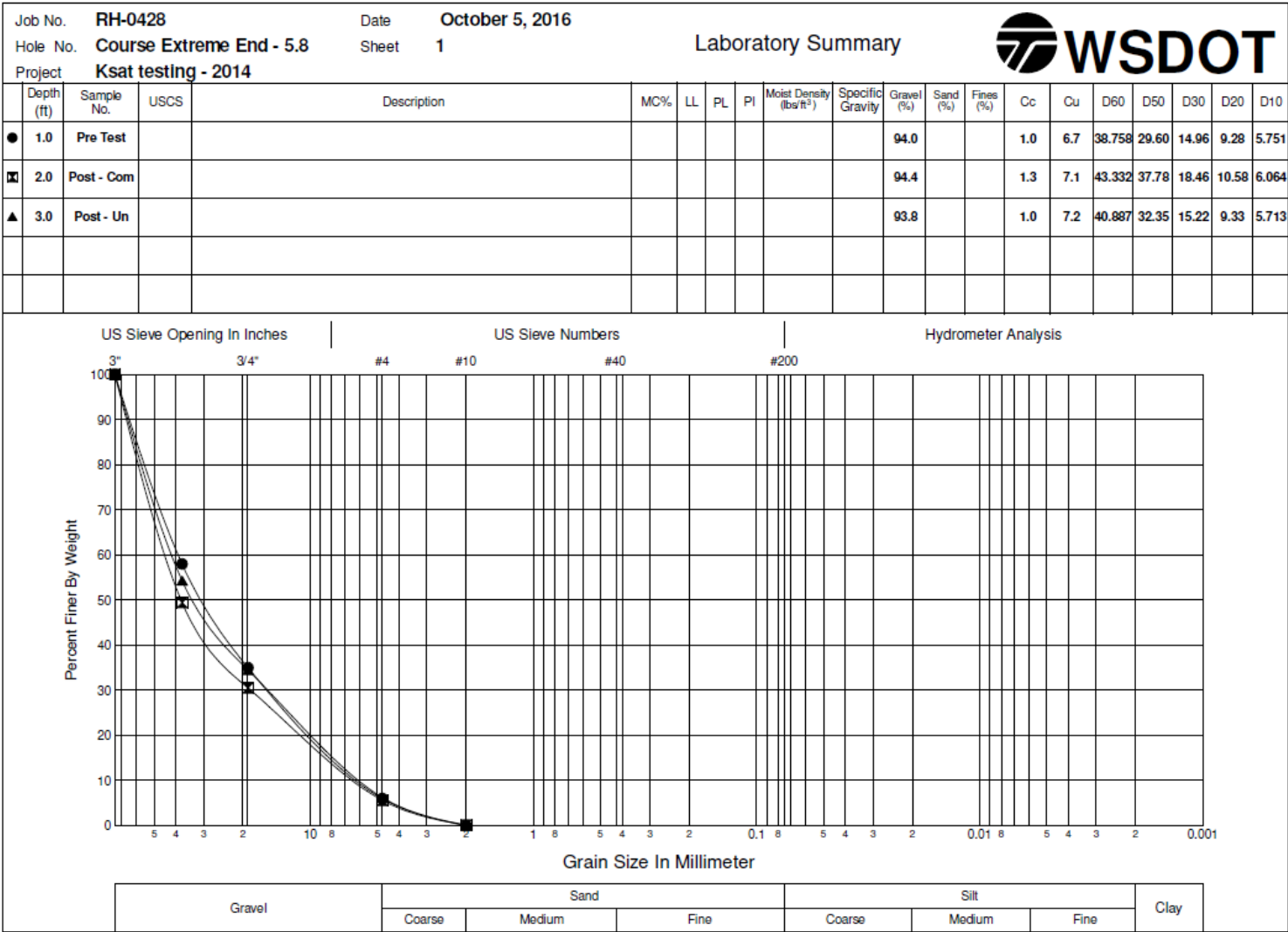


Figure B.8. Close-up of 0.003 in. (0.075 mm) minus soil particles used in 2013 and 2014 K_{sat} testing.

APPENDIX C

LABORATORY SUMMARIES OF SOILS USED FOR 2014 TESTING

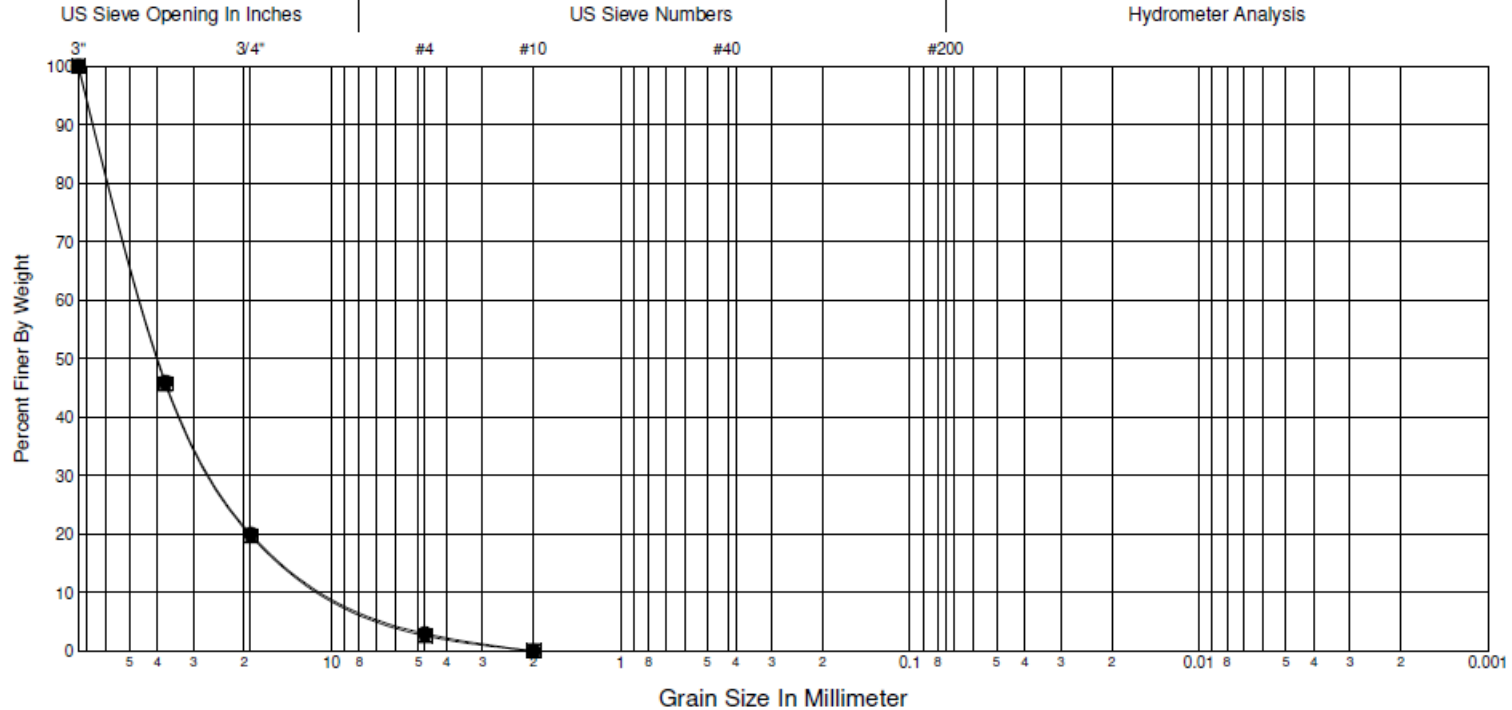


Job No. **RH-0428** Date **October 5, 2016**
 Hole No. **Course Extreme End - 8.4** Sheet **1**
 Project **Ksat testing - 2014**

Laboratory Summary



Depth (ft)	Sample No.	USCS	Description	MC%	LL	PL	PI	Moist Density (lb/ft ³)	Specific Gravity	Gravel (%)	Sand (%)	Fines (%)	Cc	Cu	D60	D50	D30	D20	D10
1.0	Pre Test									97.0			1.6	5.3	44.882	39.48	24.68	19.00	8.406
2.0	Post - Com									97.3			1.6	5.2	45.012	39.62	24.87	19.14	8.627



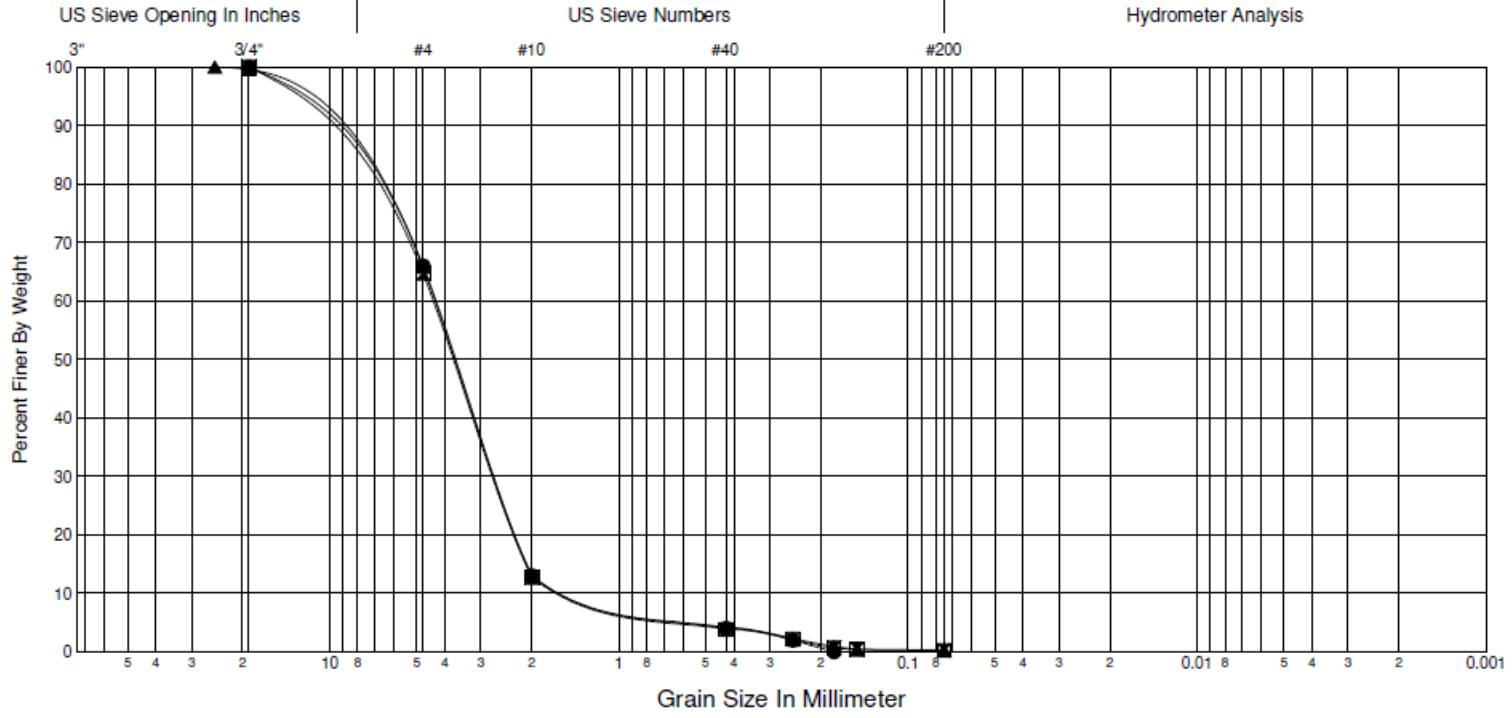
Gravel	Sand			Silt			Clay
	Coarse	Medium	Fine	Coarse	Medium	Fine	

Job No. **RH-0428** Date **October 5, 2016**
 Hole No. **Fine Sand/Gravel - 1.2** Sheet **1**
 Project **Ksat testing - 2014**

Laboratory Summary



Depth (ft)	Sample No.	USCS	Description	MC%	LL	PL	PI	Moist Density (lbs/ft ³)	Specific Gravity	Gravel (%)	Sand (%)	Fines (%)	Cc	Cu	D60	D50	D30	D20	D10	
● 1.0	Pre Test									34.0			1.4	3.6	4.307	3.66	2.64	2.24	1.193	
☒ 2.0	Post - Com	SP	POORLY GRADED SAND with GRAVEL							35.3	64.5	0.2	1.3	3.5	4.390	3.72	2.67	2.26	1.241	
▲ 3.0	Post - Un	SP	POORLY GRADED SAND with GRAVEL							34.2	65.5	0.3	1.4	3.6	4.320	3.67	2.64	2.24	1.191	



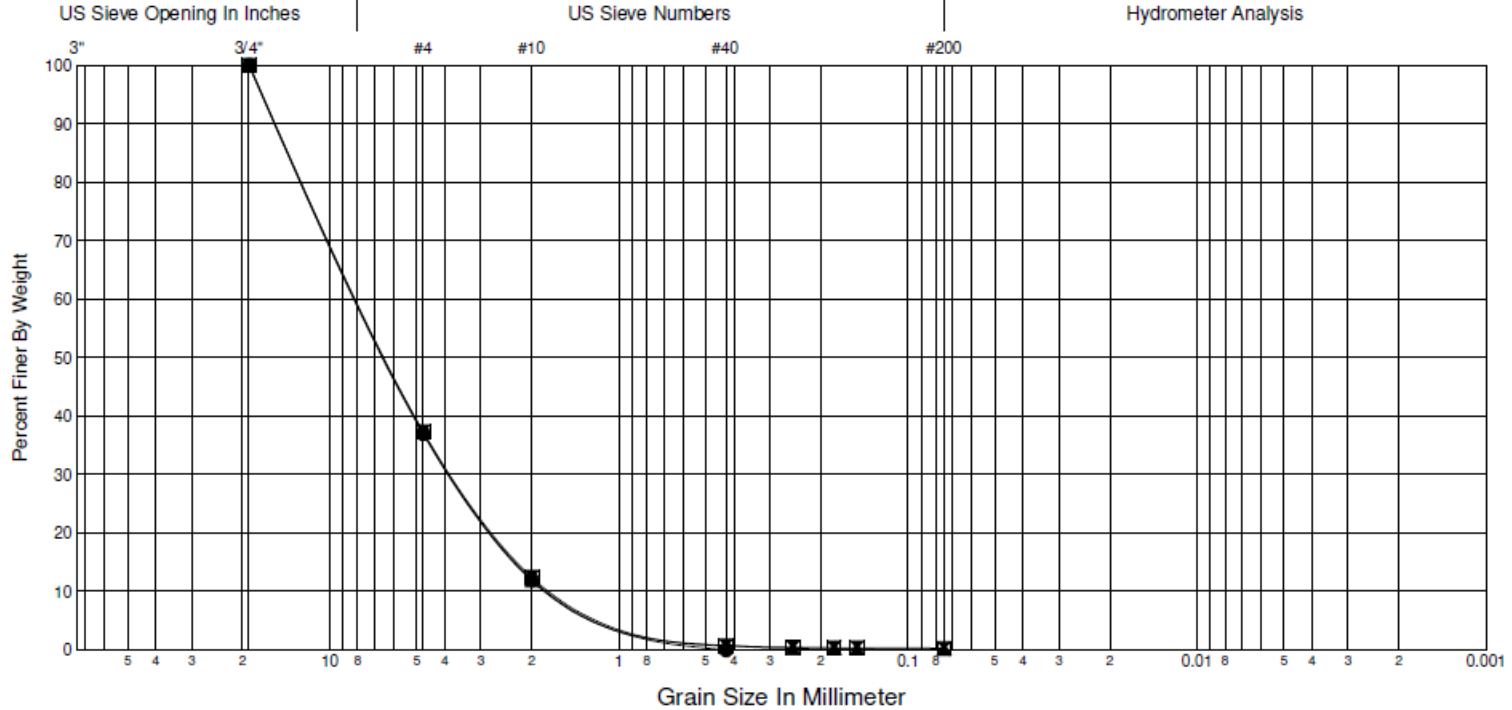
Gravel	Sand			Silt			Clay
	Coarse	Medium	Fine	Coarse	Medium	Fine	

Job No. **RH-0428** Date **October 5, 2016**
 Hole No. **Course Sand/Gravel - 1.55** Sheet **1**
 Project **Ksat testing - 2014**

Laboratory Summary



Depth (ft)	Sample No.	USCS	Description	MC%	LL	PL	PI	Moist Density (lb/ft ³)	Specific Gravity	Gravel (%)	Sand (%)	Fines (%)	Cc	Cu	D60	D50	D30	D20	D10
● 1.0	Pre Test							135	2.67	63.0			1.1	5.1	7.879	6.32	3.73	2.64	1.545
■ 2.0	Post - Un	GW	WELL-GRADED GRAVEL with SAND							62.7	37.0	0.3	1.2	5.4	7.846	6.29	3.69	2.61	1.460
▲ 3.0	Post - Com	GW	WELL-GRADED GRAVEL with SAND							62.7	37.1	0.1	1.1	5.1	7.851	6.29	3.71	2.64	1.550



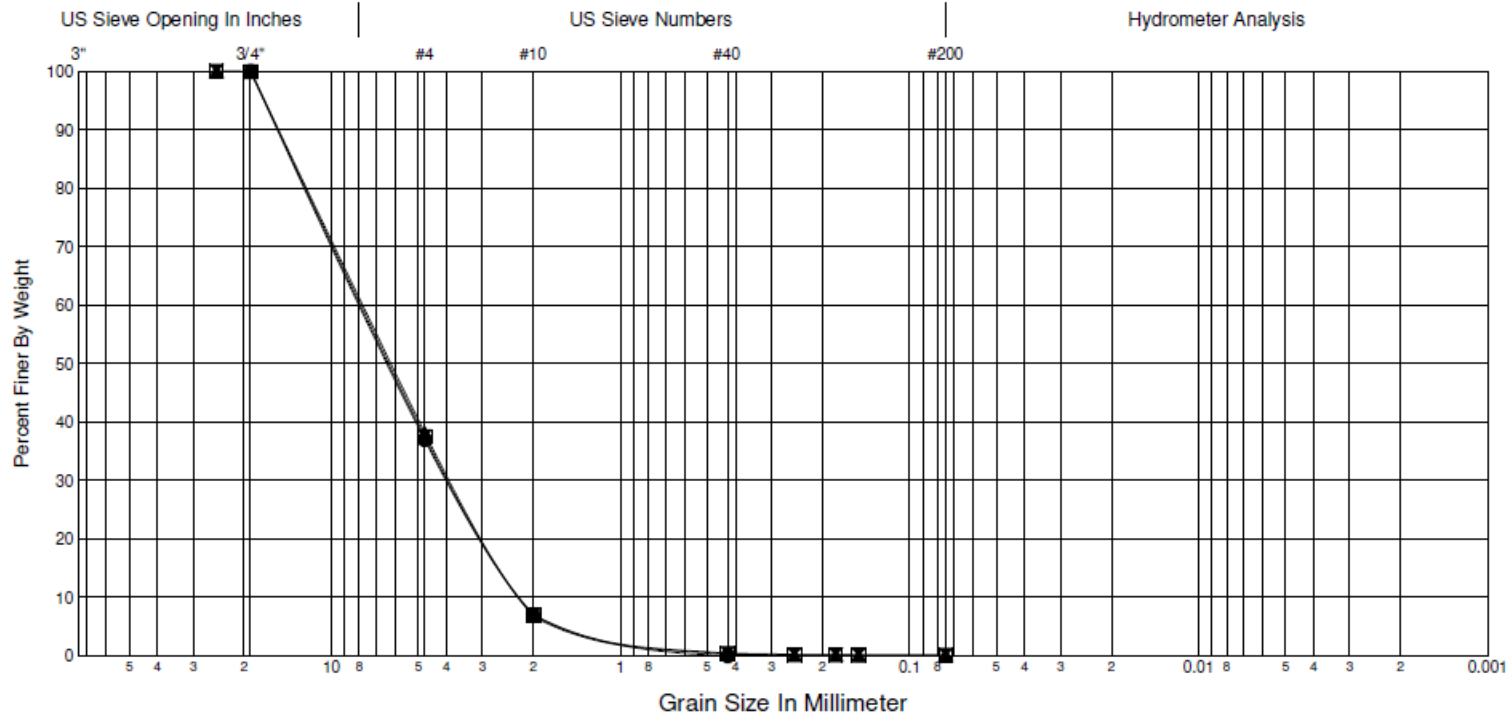
Gravel	Sand			Silt			Clay
	Coarse	Medium	Fine	Coarse	Medium	Fine	

Job No. **RH-0428** Date **October 5, 2016**
 Hole No. **Course Sand/Gravel - 2.18** Sheet **1**
 Project **Ksat testing - 2014**

Laboratory Summary



Depth (ft)	Sample No.	USCS	Description	MC%	LL	PL	PI	Moist Density (lb/ft ³)	Specific Gravity	Gravel (%)	Sand (%)	Fines (%)	Cc	Cu	D60	D50	D30	D20	D10
● 1.0	Pre Test									63.0			0.9	3.6	7.879	6.32	3.88	2.91	2.181
■ 2.0	Post - Com	GP	POORLY GRADED GRAVEL with SAND							62.5	37.4	0.1	0.9	3.6	7.829	6.27	3.84	2.89	2.178
▲ 3.0	Post - Un	GP	POORLY GRADED GRAVEL with SAND							61.8	38.1	0.1	0.8	3.5	7.748	6.19	3.79	2.88	2.186



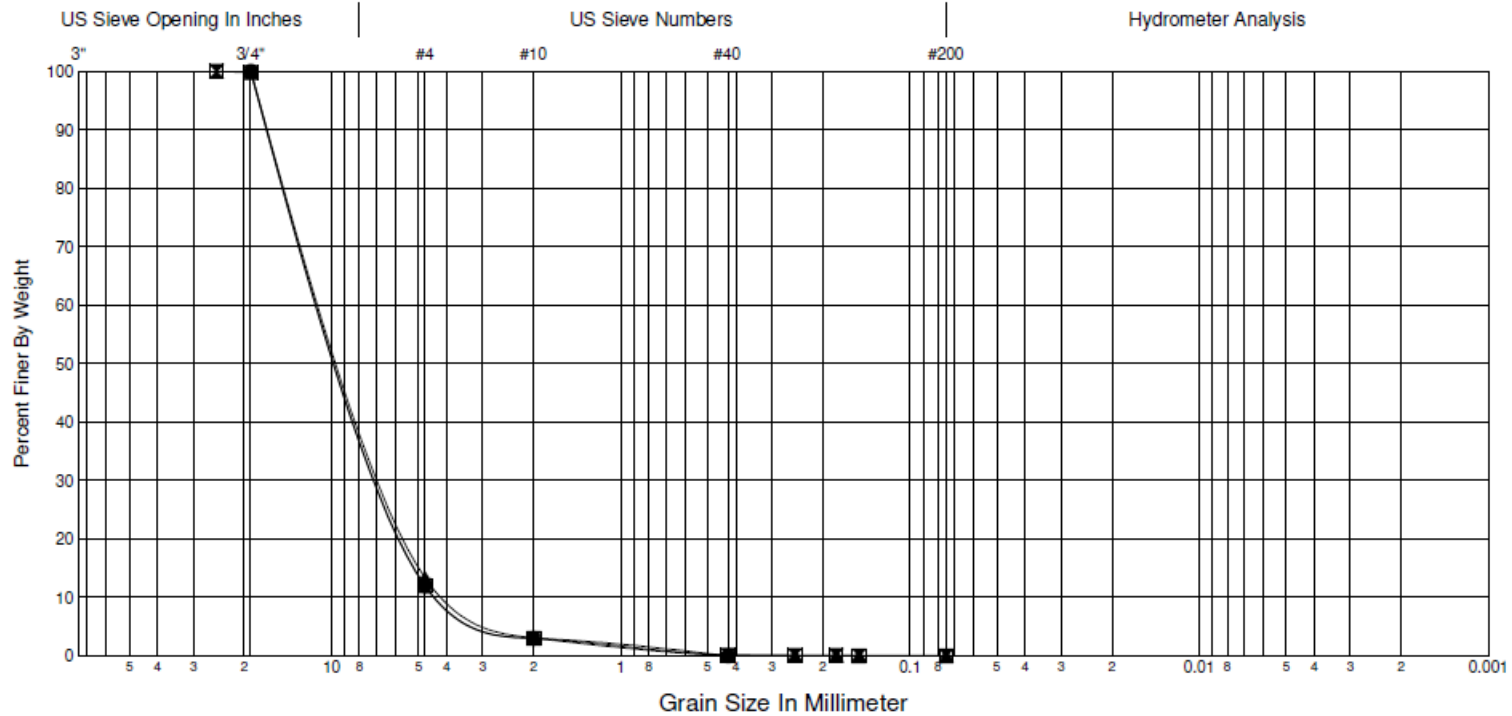
Gravel	Sand			Silt			Clay
	Coarse	Medium	Fine	Coarse	Medium	Fine	

Job No. **RH-0428** Date **October 5, 2016**
 Hole No. **Course Sand/Gravel - 3.9** Sheet **1**
 Project **Ksat testing - 2014**

Laboratory Summary



Depth (ft)	Sample No.	USCS	Description	MC%	LL	PL	PI	Moist Density (lb/ft ³)	Specific Gravity	Gravel (%)	Sand (%)	Fines (%)	Cc	Cu	D60	D50	D30	D20	D10
● 1.0	Pre Test									88.0			1.0	2.6	10.118	8.64	6.31	5.39	3.919
■ 2.0	Post - Com	GP	POORLY GRADED GRAVEL							88.0	12.0	0.0	1.0	2.6	10.133	8.65	6.31	5.39	3.918
▲ 3.0	Post - Un	GP	POORLY GRADED GRAVEL							86.6	13.3	0.0	1.1	2.8	10.016	8.53	6.20	5.28	3.577



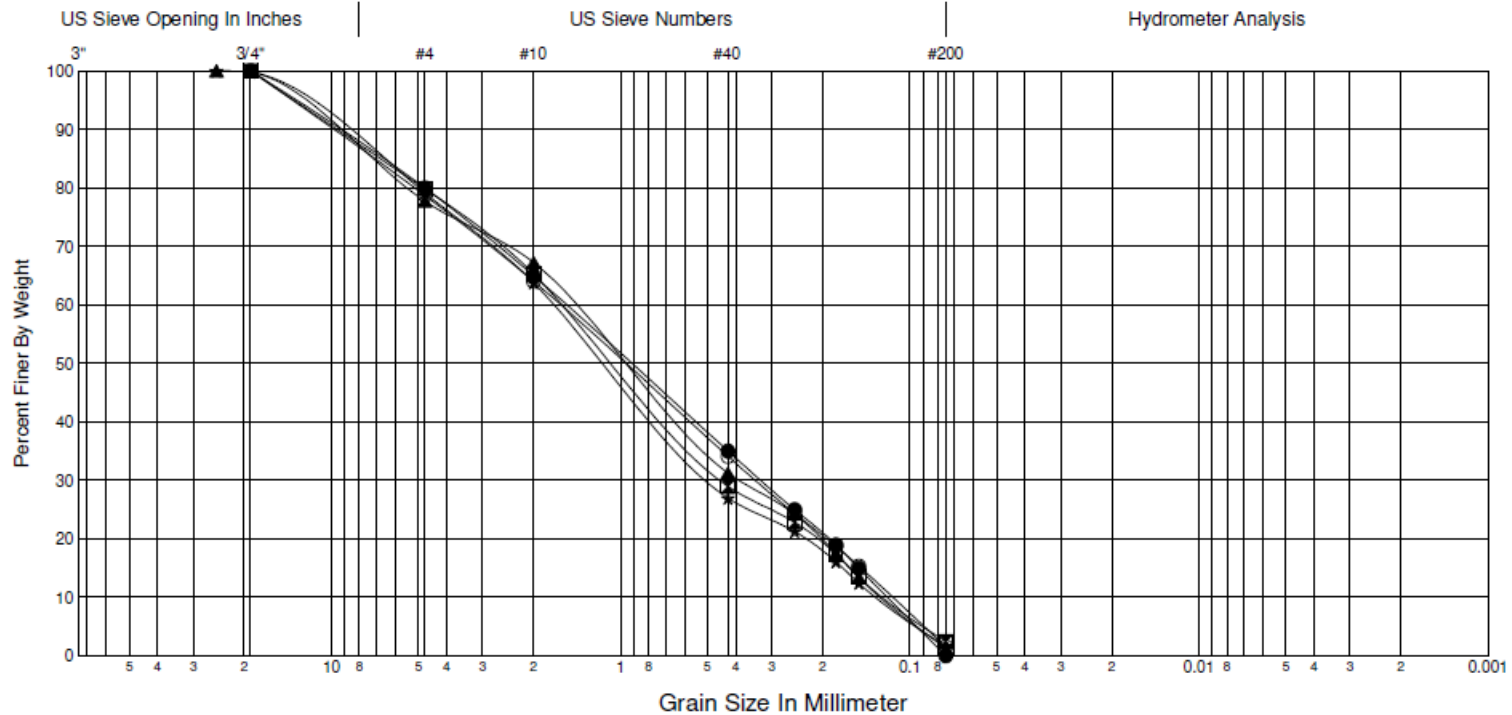
Gravel	Sand			Silt			Clay
	Coarse	Medium	Fine	Coarse	Medium	Fine	

Job No. **RH-0428** Date **October 5, 2016**
 Hole No. **Fine Sand/Gravel - 0.12** Sheet **1**
 Project **Ksat testing - 2014**

Laboratory Summary



Depth (ft)	Sample No.	USCS	Description	MC%	LL	PL	PI	Moist Density (lb/ft ³)	Specific Gravity	Gravel (%)	Sand (%)	Fines (%)	Cc	Cu	D60	D50	D30	D20	D10
● 1.0	Pre Test	SP	POORLY GRADED SAND with GRAVEL							20.0	80.0	0.0	0.6	13.0	1.545	0.92	0.33	0.19	0.119
■ 2.0	Post - Com	SW	WELL-GRADED SAND with GRAVEL							20.1	77.4	2.4	1.0	13.3	1.596	1.04	0.44	0.21	0.120
▲ 3.0	Post - Un	SP	POORLY GRADED SAND with GRAVEL							22.3	76.4	1.3	0.8	11.9	1.464	0.95	0.39	0.20	0.123
★ 4.0	PostF - Com	SW	WELL-GRADED SAND with GRAVEL							20.8	77.6	1.6	1.1	13.3	1.704	1.12	0.48	0.23	0.128
⊙ 5.0	Post - Un3	SP	POORLY GRADED SAND with GRAVEL							21.3	77.2	1.5	0.6	14.1	1.621	0.97	0.34	0.19	0.115



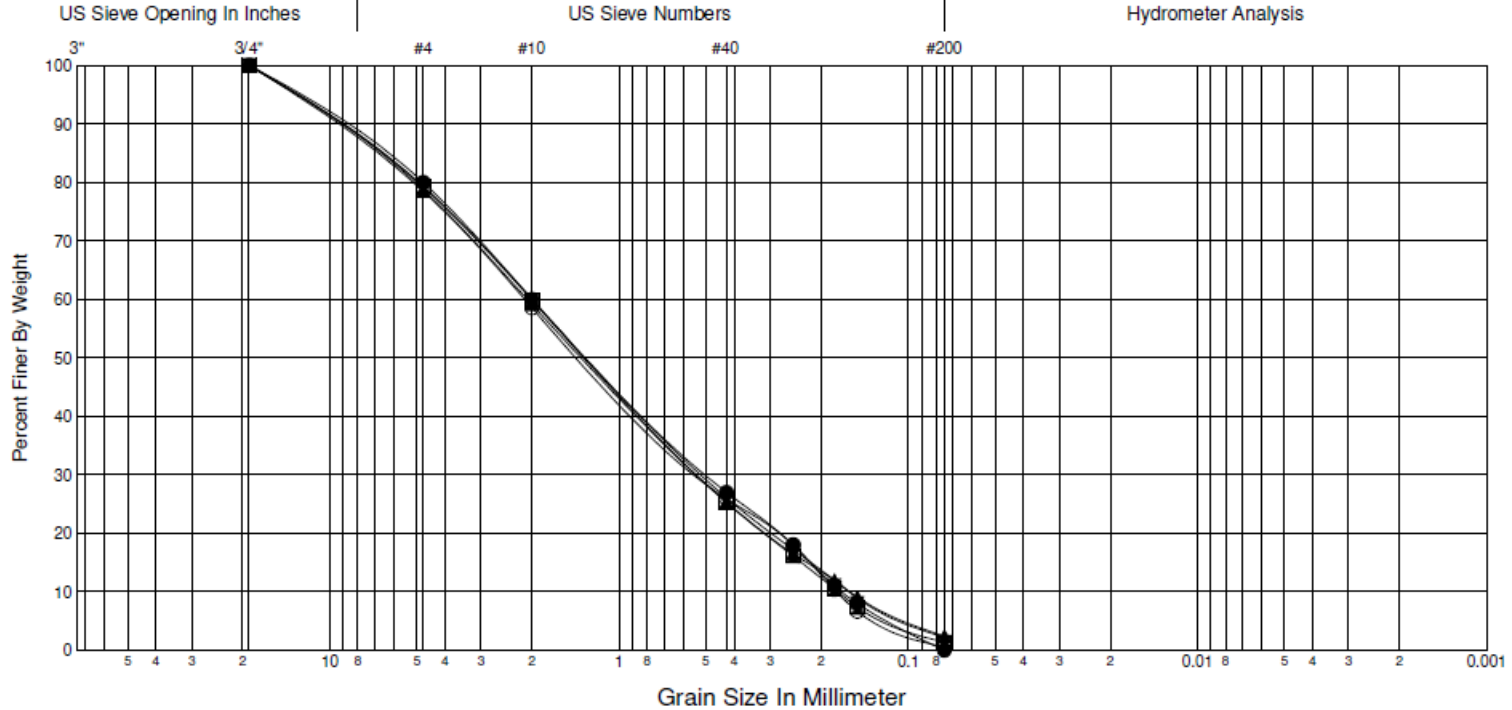
Gravel	Sand			Silt			Clay
	Coarse	Medium	Fine	Coarse	Medium	Fine	

Job No. **RH-0428** Date **October 5, 2016**
 Hole No. **Fine Sand/Gravel - 0.17** Sheet **1**
 Project **Ksat testing - 2014**

Laboratory Summary



Depth (ft)	Sample No.	USCS	Description	MC%	LL	PL	PI	Moist Density (lbs/ft ³)	Specific Gravity	Gravel (%)	Sand (%)	Fines (%)	Cc	Cu	D60	D50	D30	D20	D10
● 1.0	Pre Test	SP	POORLY GRADED SAND with GRAVEL							20.0	80.0	0.0	0.7	11.8	2.000	1.25	0.49	0.28	0.169
■ 2.0	Post - Un	SP	POORLY GRADED SAND with GRAVEL							20.7	77.9	1.4	0.8	11.5	2.008	1.28	0.53	0.31	0.175
▲ 3.0	Post - Com	SP	POORLY GRADED SAND with GRAVEL							21.5	76.1	2.4	0.8	13.1	2.078	1.32	0.53	0.31	0.159
★ 4.0	Post - Com2	SP	POORLY GRADED SAND with GRAVEL							20.7	77.1	2.2	0.8	12.5	2.001	1.27	0.51	0.30	0.160
◎ 5.0	Post - Un2	SP	POORLY GRADED SAND with GRAVEL							21.2	78.2	0.6	0.7	12.0	2.127	1.33	0.52	0.29	0.177



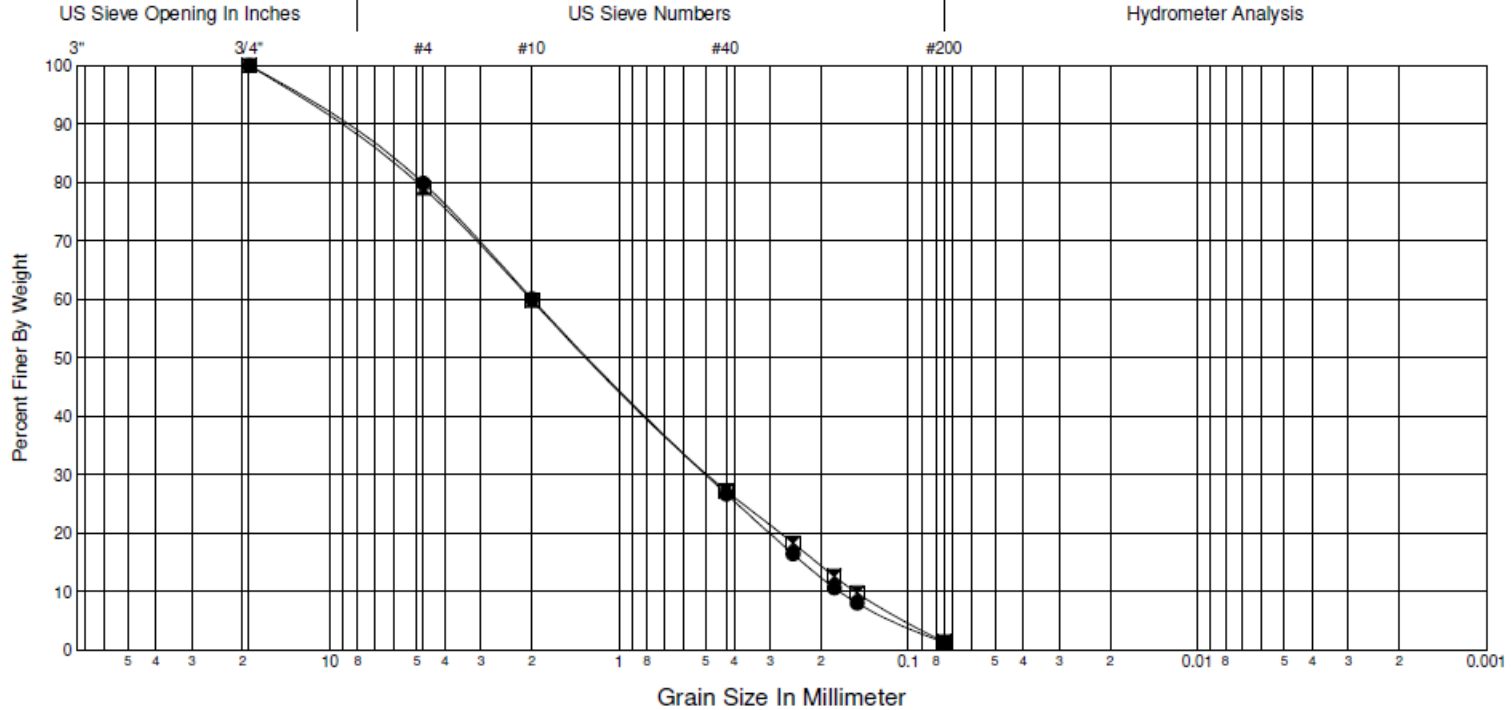
Gravel	Sand			Silt			Clay
	Coarse	Medium	Fine	Coarse	Medium	Fine	

Job No. **RH-0428** Date **October 5, 2016**
 Hole No. **Fine Sand/Gravel - 0.17** Sheet **2**
 Project **Ksat testing - 2014**

Laboratory Summary



Depth (ft)	Sample No.	USCS	Description	MC%	LL	PL	PI	Moist Density (lb/ft ³)	Specific Gravity	Gravel (%)	Sand (%)	Fines (%)	Cc	Cu	D60	D50	D30	D20	D10	
6.0	Post - ComF	SP	POORLY GRADED SAND with GRAVEL							20.1	78.6	1.3	0.7	11.6	1.991	1.25	0.50	0.30	0.172	
7.0	Post - Un4	SP	POORLY GRADED SAND with GRAVEL							20.9	77.7	1.4	0.8	13.2	2.014	1.25	0.48	0.28	0.152	



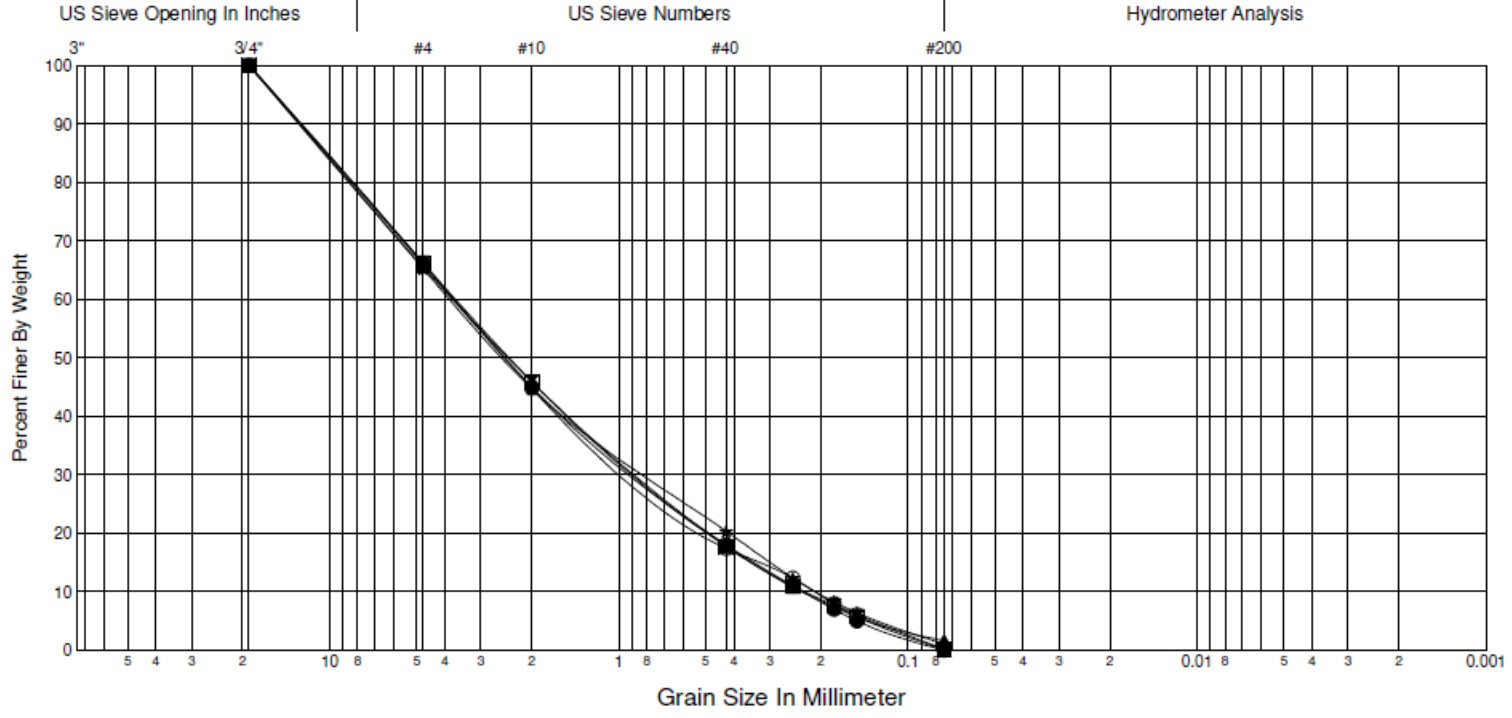
Gravel	Sand			Silt			Clay
	Coarse	Medium	Fine	Coarse	Medium	Fine	

Job No. **RH-0428** Date **October 5, 2016**
 Hole No. **Fine Sand/Gravel - 0.23** Sheet **1**
 Project **Ksat testing - 2014**

Laboratory Summary



Depth (ft)	Sample No.	USCS	Description	MC%	LL	PL	PI	Moist Density (lbs/ft ³)	Specific Gravity	Gravel (%)	Sand (%)	Fines (%)	Cc	Cu	D60	D50	D30	D20	D10
● 1.0	Pre Test	SP	POORLY GRADED SAND with GRAVEL							34.0	66.0	0.0	0.8	16.1	3.710	2.46	0.85	0.48	0.230
■ 2.0	Post - Com	SP	POORLY GRADED SAND with GRAVEL							33.8	66.1	0.1	0.8	16.0	3.645	2.38	0.83	0.48	0.227
▲ 3.0	Post - Un	SP	POORLY GRADED SAND with GRAVEL							34.5	63.9	1.6	0.8	16.1	3.722	2.40	0.83	0.48	0.231
★ 4.0	Post - Com3	SP	POORLY GRADED SAND with GRAVEL							34.7	64.2	1.0	0.8	18.4	3.805	2.50	0.78	0.42	0.207
⊙ 5.0	Post - Un2	SP	POORLY GRADED SAND with GRAVEL							33.8	66.0	0.2	1.0	17.6	3.693	2.47	0.87	0.49	0.210



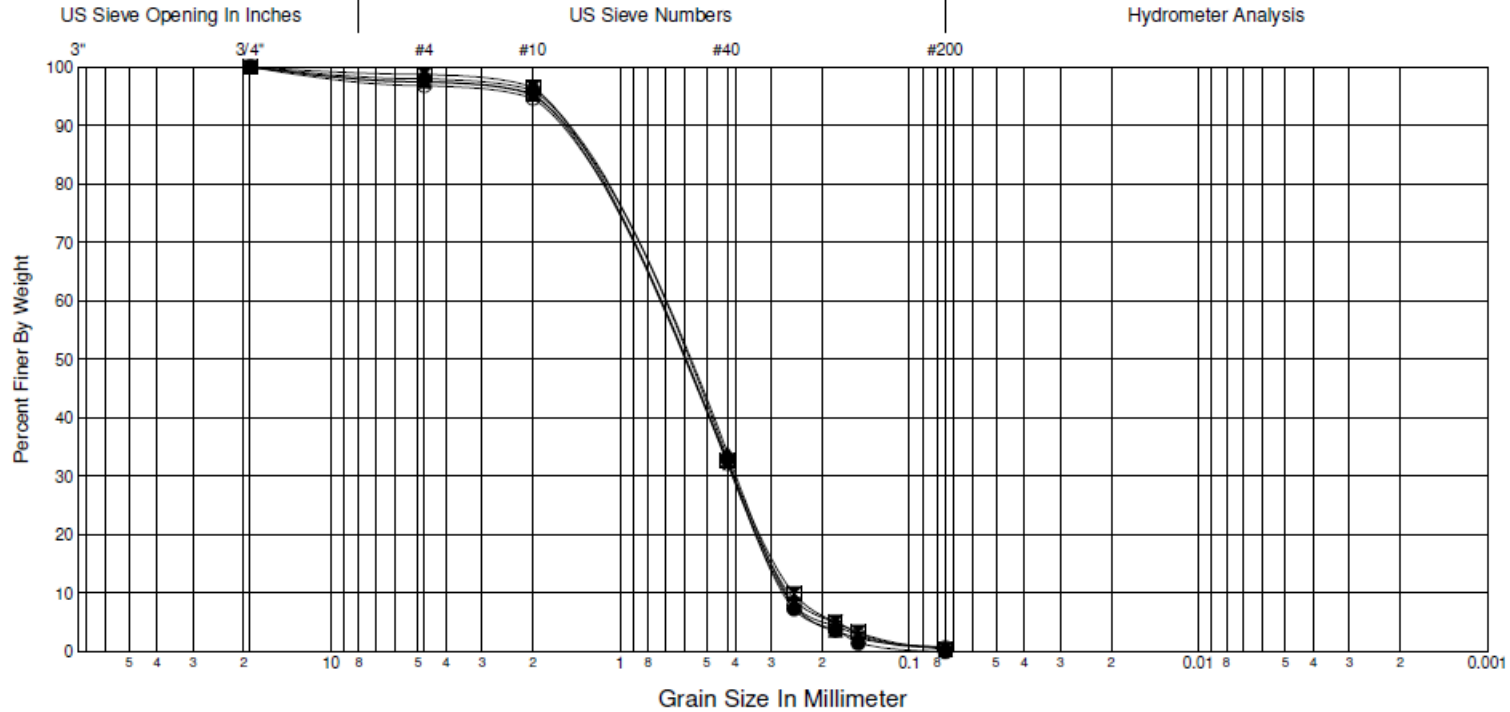
Gravel	Sand			Silt			Clay
	Coarse	Medium	Fine	Coarse	Medium	Fine	

Job No. **RH-0428** Date **October 5, 2016**
 Hole No. **Fine Sand/Gravel - 0.26** Sheet **1**
 Project **Ksat testing - 2014**

Laboratory Summary



Depth (ft)	Sample No.	USCS	Description	MC%	LL	PL	PI	Moist Density (lb/ft ³)	Specific Gravity	Gravel (%)	Sand (%)	Fines (%)	Cc	Cu	D60	D50	D30	D20	D10
● 1.0	Pre Test	SP	POORLY GRADED SAND							2.0	98.0	0.0	0.7	3.1	0.825	0.65	0.40	0.32	0.264
☒ 2.0	Post - Un	SP	POORLY GRADED SAND							1.2	98.4	0.4	0.8	3.3	0.825	0.65	0.40	0.32	0.251
▲ 3.0	Post - Com	SP	POORLY GRADED SAND							2.5	96.7	0.8	0.7	3.2	0.821	0.64	0.39	0.32	0.260
★ 4.0	Post - Un-3	SP	POORLY GRADED SAND							2.5	96.7	0.8	0.8	3.3	0.840	0.66	0.40	0.32	0.256
◎ 5.0	Post - Com2	SP	POORLY GRADED SAND							3.2	96.2	0.7	0.7	3.2	0.846	0.66	0.40	0.33	0.261



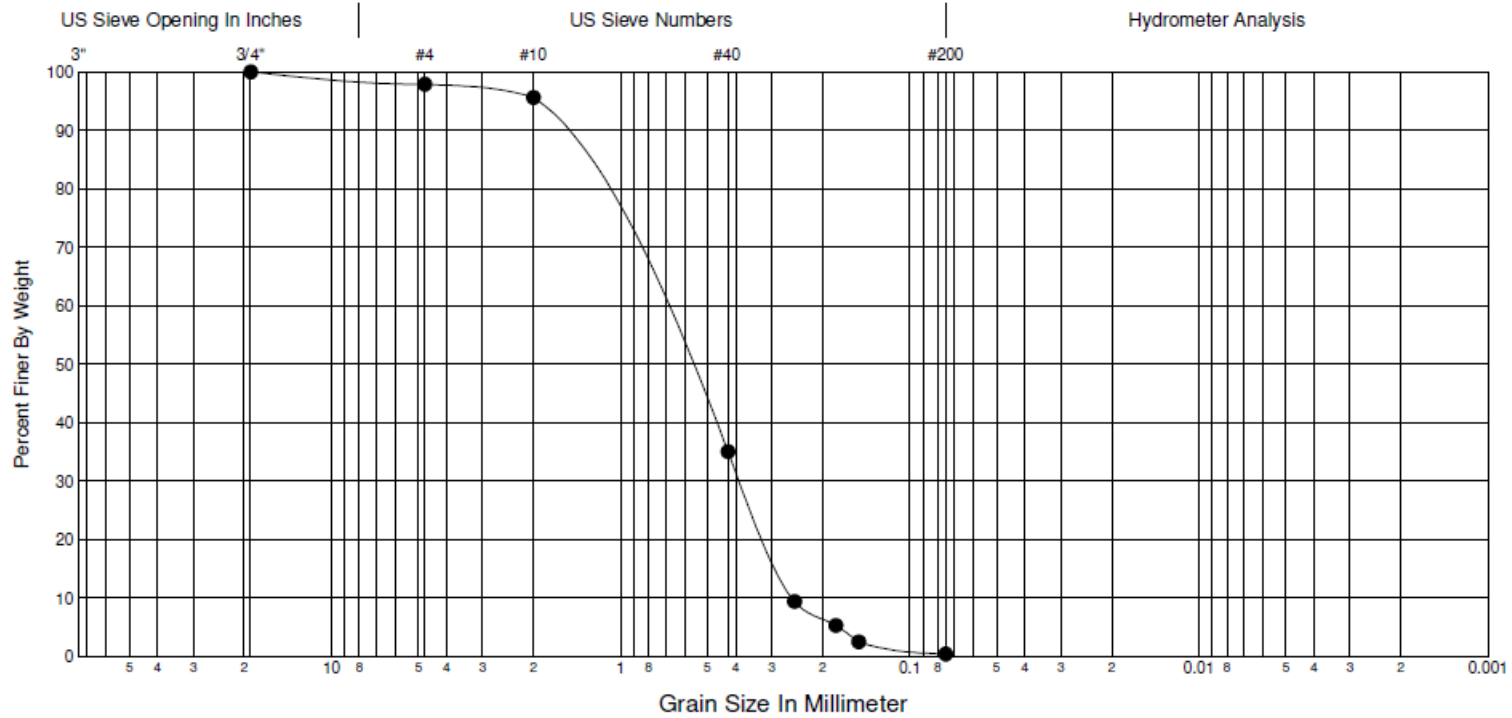
Gravel	Sand			Silt			Clay
	Coarse	Medium	Fine	Coarse	Medium	Fine	

Job No. **RH-0428** Date **October 5, 2016**
 Hole No. **Fine Sand/Gravel - 0.26** Sheet **2**
 Project **Ksat testing - 2014**

Laboratory Summary



Depth (ft)	Sample No.	USCS	Description	MC%	LL	PL	PI	Moist Density (lb/ft ³)	Specific Gravity	Gravel (%)	Sand (%)	Fines (%)	Cc	Cu	D60	D50	D30	D20	D10		
6.0	Post - ComF	SP	POORLY GRADED SAND						2.77	2.1	97.5	0.4	0.7	3.2	0.804	0.62	0.38	0.31	0.253		



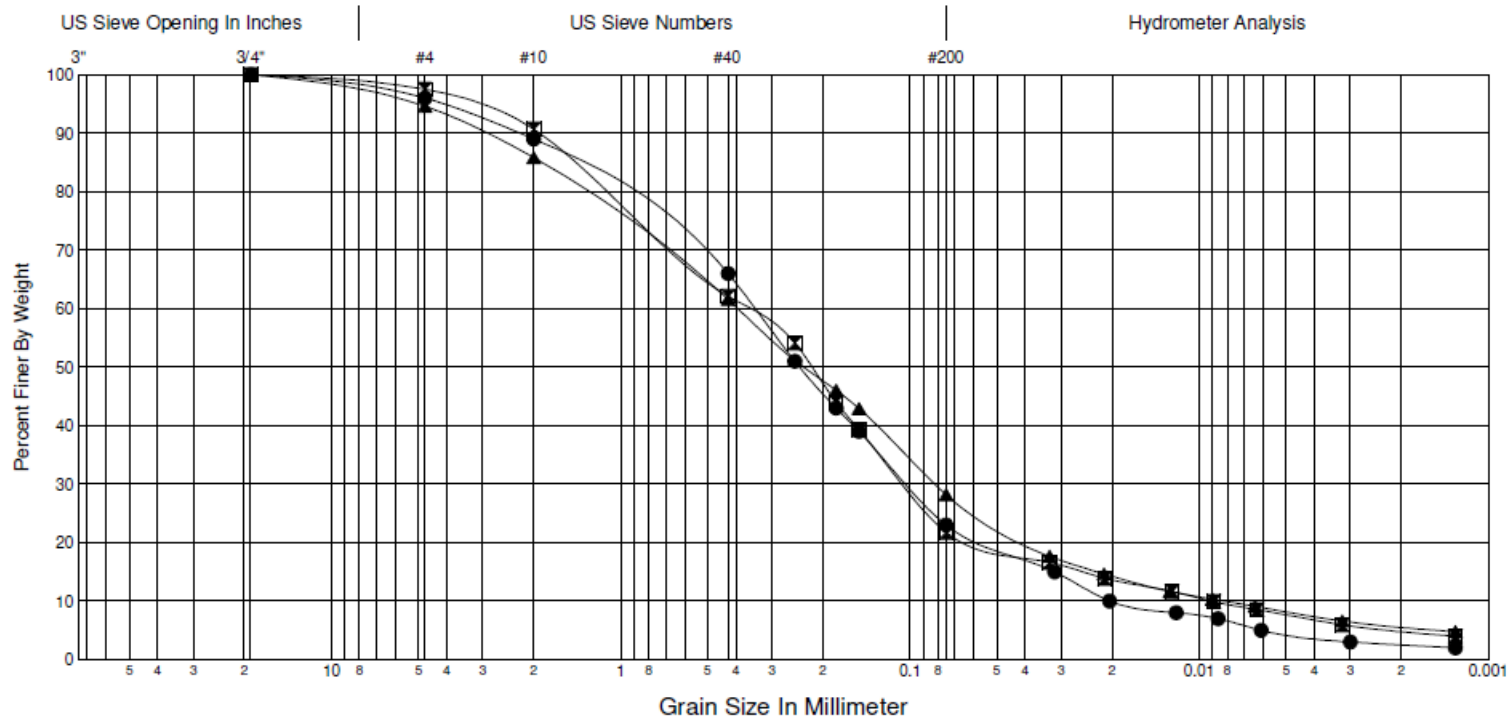
Gravel	Sand			Silt			Clay
	Coarse	Medium	Fine	Coarse	Medium	Fine	

Job No. **RH-0428** Date **October 5, 2016**
 Hole No. **Fine Extreme End - 0.02** Sheet **1**
 Project **Ksat testing - 2014**

Laboratory Summary



Depth (ft)	Sample No.	USCS	Description	MC%	LL	PL	PI	Moist Density (lb/ft ³)	Specific Gravity	Gravel (%)	Sand (%)	Fines (%)	Cc	Cu	D60	D50	D30	D20	D10
1.0										4.0	73.0	23.0	1.5	16.8	0.344	0.24	0.10	0.05	0.020
2.0	Post - COM	SM	SILTY SAND	10	NA	NP	NA		2.67	2.5	75.7	21.8	3.2	40.6	0.370	0.22	0.10	0.06	0.009
3.0	Post - UN	SM	SILTY SAND	10	NA	NP	NA		2.63	5.4	66.4	28.2	2.1	47.8	0.393	0.23	0.08	0.04	0.008



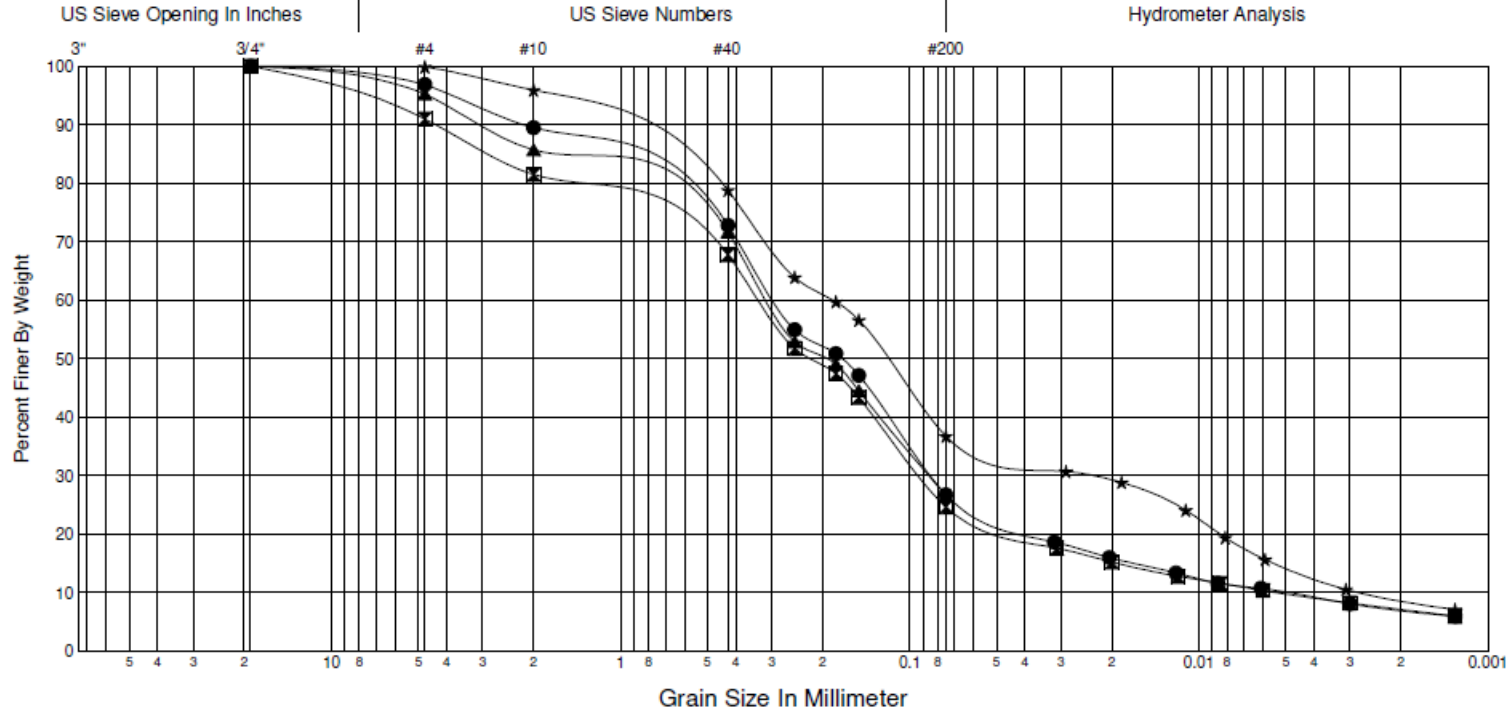
Gravel	Sand			Silt			Clay
	Coarse	Medium	Fine	Coarse	Medium	Fine	

Job No. **RH-0428** Date **October 5, 2016**
 Hole No. **Fine Extreme End - 0.005** Sheet **1**
 Project **Ksat testing - 2014**

Laboratory Summary



Depth (ft)	Sample No.	USCS	Description	MC%	LL	PL	PI	Moist Density (lb/ft ³)	Specific Gravity	Gravel (%)	Sand (%)	Fines (%)	Cc	Cu	D60	D50	D30	D20	D10
● 0.0	Pre Test	SM	SILTY SAND						2.71	3.1	70.1	26.7	4.8	58.0	0.290	0.17	0.08	0.04	0.005
■ 1.0	Post - Com	SM	SILTY SAND	60	NA	NP	NA		2.73	9.0	66.3	24.7	4.8	61.7	0.328	0.22	0.09	0.04	0.005
▲ 2.0	Post - Un									4.7	68.6	26.6			0.306	0.20	0.09		
★ 3.0	Post-0.005-2	SM	SILTY SAND	21	20	NP	NA		2.76	0.1	63.1	36.8	1.2	68.1	0.184	0.12	0.02	0.01	0.003



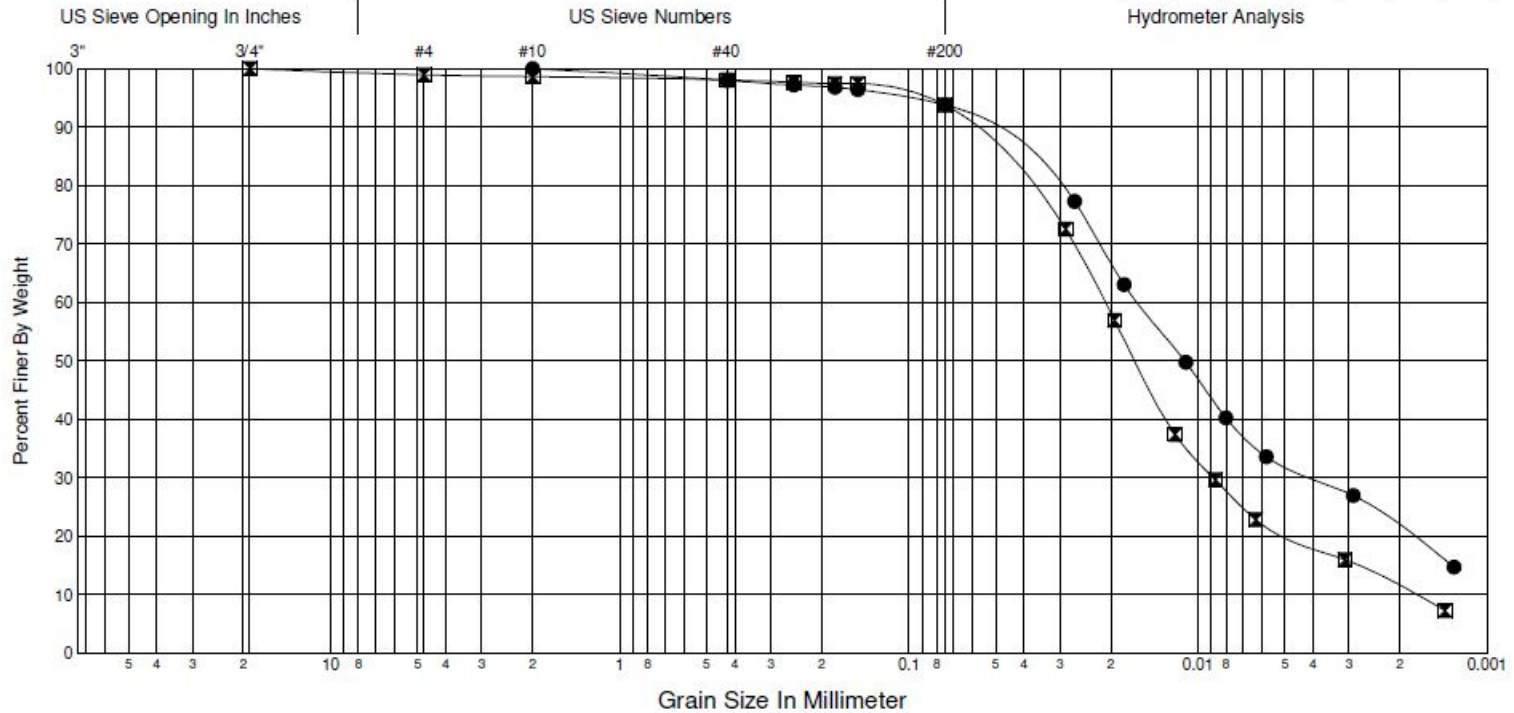
Gravel	Sand			Silt			Clay
	Coarse	Medium	Fine	Coarse	Medium	Fine	

Job No. **MS-7119** Date **November 22, 2016**
 Hole No. **FC-5-14** Sheet **1**
 Project **I-5 Chehalis Flood Control Study**

Laboratory Summary



Depth (ft)	Sample No.	USCS	Description	MC%	LL	PL	PI	Moist Density (lbs/ft ³)	Specific Gravity	Gravel (%)	Sand (%)	Fines (%)	Cc	Cu	D60	D50	D30	D20	D10	
● 10.0	S-5	ML	SILT	35	37	26	11	118	2.76	0.0	6.2	93.8			0.016	0.01	0.00	0.00		
☒ 16.0	S-9	ML	SILT	40	34	30	4	114	2.62	1.1	5.1	93.8	2.1	11.7	0.021	0.02	0.01	0.00	0.002	



Gravel	Sand			Silt			Clay
	Coarse	Medium	Fine	Coarse	Medium	Fine	

APPENDIX D

COMPACTION TEST LABORATORY SUMMARIES FOR SOILS USED FOR 2013 TESTING



Moisture - Density Relationship Report

Field Sample Number		Lab Number		Transmittal Number		Control Number		Federal Aid Number	
Project Number RH-0428		SR	Org. Code	Project Description (or section) K-SAT Testing 2014					
Source of Materials 10.2		Type of Material SILTY SAND with Gravel		Sample Weight 20lbs	Date Sampled 3/9/15	Date Tested 3/10/15	Tested By JTT01	% Passing 3/4 100	% Passing #4 96
T-99 or T-180 T-180	Method D	Mold Size (in) 6"	Specific Gravity 2.77	Comments					
Can Number	1	2	3	4	5	6	7	8	
Specimen Wt. + Mold	10480.0	10650.0	10560.0	10490.0	10570.0				
Wt. of Mold:	5750.0	5750.0	5750.0	5750.0	5750.0				
Vol. Factor:	0.075	0.075000	0.075000	0.075000	0.075000				
Wet Sample + Can	859.9	648.6	705.0	769.3	5220.0				
Dry Sample + Can	823.1	613.8	659.5	714.4	4900.0				
Wt. Comp. Soil	10.4279	10.8026	10.6042	10.4499	10.6263				
Tare Wt.	221.2	182.3	215.1	214.7	269.9				
Net Dry Wt.	601.9	431.5	444.4	499.7	4630.1				
Wt. of Water	36.8	34.8	45.5	54.9	320.0				
Wet Density	139.0	144.0	141.4	139.3	141.7				
Water Content	0.0611	0.0806	0.1024	0.1099	0.0691				
Water Content %	6.11%	8.06%	10.24%	10.99%	6.91%				
Dry Density	131.0	133.3	128.3	125.5	132.5				

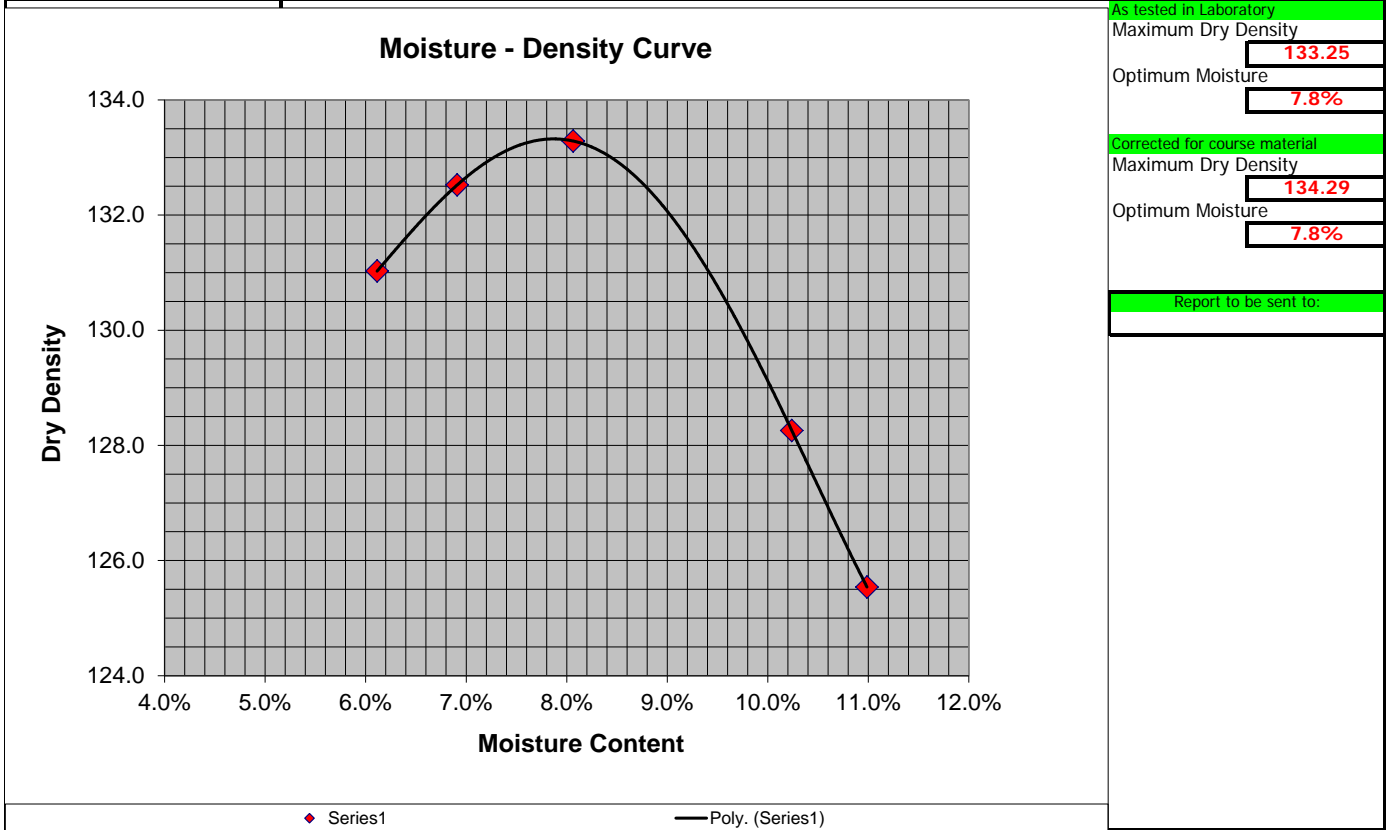


Figure D.1. Compaction test for 2013 WSDOT manufactured soil with 26% Gravel, 64%, Sand, and 10% fines.

Moisture - Density Relationship Report

Field Sample Number		Lab Number		Transmittal Number		Control Number		Federal Aid Number	
Project Number RH-0428		SR	Org. Code	Project Description (or section) K-SAT Testing 2014					
Source of Materials 20.2		Type of Material SILTY SAND with Gravel		Sample Weight 20lbs	Date Sampled 3/22/15	Date Tested 3/23/15	Tested By JTT01	% Passing 3/4 100	% Passing #4 96
T-99 or T-180 T-180	Method D	Mold Size (in) 6"	Specific Gravity 2.76	Comments					
Can Number	1	2	3	4	5	6	7	8	
Specimen Wt. + Mold	10566.0	10480.0	10247.0	10675.0	10696.0				
Wt. of Mold:	5750.0	5750.0	5750.0	5750.0	5750.0				
Vol. Factor:	0.075	0.075000	0.075000	0.075000	0.075000				
Wet Sample + Can	992.1	1305.0	875.5	819.2	765.5				
Dry Sample + Can	945.0	1248.6	848.5	771.8	727.4				
Wt. Comp. Soil	10.6174	10.4279	9.9142	10.8578	10.9041				
Tare Wt.	227.6	731.4	228	228.2	232.2				
Net Dry Wt.	717.4	517.2	620.5	543.6	495.2				
Wt. of Water	47.1	56.4	27.0	47.4	38.1				
Wet Density	141.6	139.0	132.2	144.8	145.4				
Water Content	0.0657	0.1090	0.0435	0.0872	0.0769				
Water Content %	6.57%	10.90%	4.35%	8.72%	7.69%				
Dry Density	132.8	125.4	126.7	133.2	135.0				

As tested in Laboratory

Maximum Dry Density	135
Optimum Moisture	7.7%

Corrected for course material

Maximum Dry Density	135.9
Optimum Moisture	7.7%

Report to be sent to:

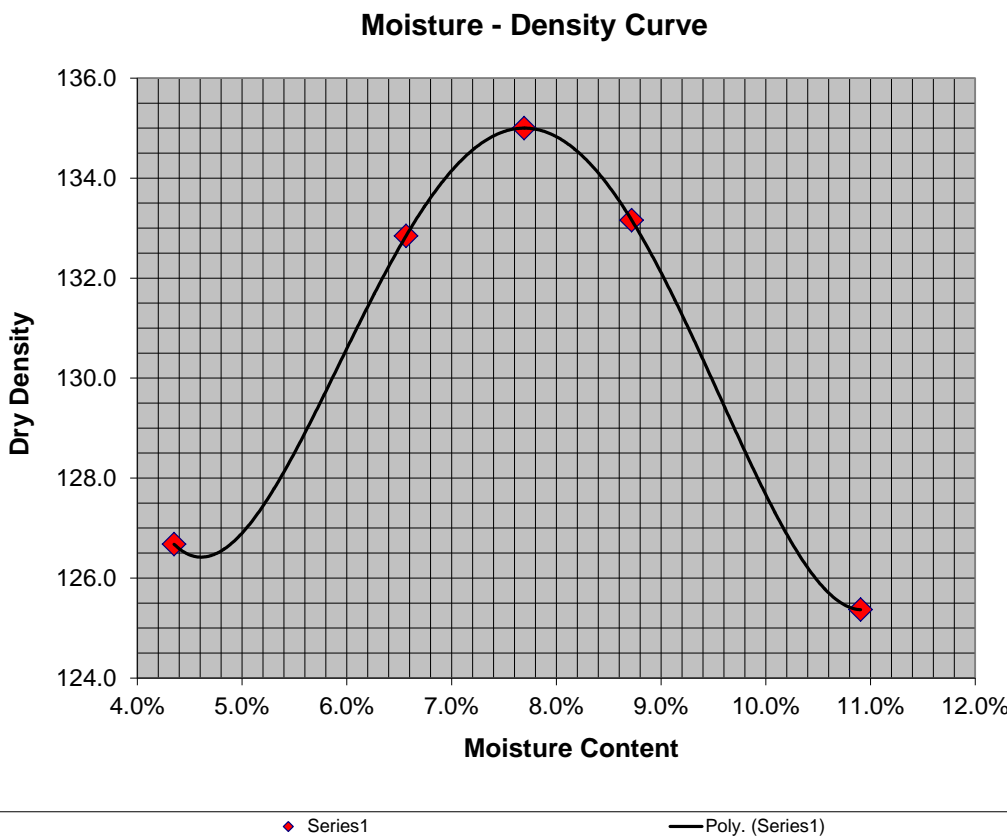


Figure D.2. Compaction test for 2013 WSDOT manufactured soil with 23% Gravel, 57%, Sand, and 20% fines.

Moisture - Density Relationship Report

Field Sample Number		Lab Number		Transmittal Number		Control Number		Federal Aid Number	
Project Number RH-0428		SR	Org. Code	Project Description (or section) K-SAT Testing 2014					
Source of Materials 30.2		Type of Material SILTY SAND with Gravel		Sample Weight 20lbs	Date Sampled 4/1/15	Date Tested 4/2/15	Tested By JTT01	% Passing 3/4 100	% Passing #4 76
T-99 or T-180	Method	Mold Size (in)	Specific Gravity	Comments					
Can Number		1	2	3	4	5	6	7	8
Specimen Wt. + Mold		10437.0	10314.0	10533.0	10564.0	10280.0			
Wt. of Mold:		5750.0	5750.0	5750.0	5750.0	5750.0			
Vol. Factor:		0.075000	0.075000	0.075000	0.075000	0.075000			
Wet Sample + Can		916.0	837.3	1226.7	914.0	1294.3			
Dry Sample + Can		865.0	766.1	1132.5	853.0	1222.3			
Wt. Comp. Soil		10.3331	10.0619	10.5447	10.6130	9.9869			
Tare Wt.		236.1	215.9	232	229.5	231.9			
Net Dry Wt.		628.9	550.2	900.5	623.5	990.4			
Wt. of Water		51.0	71.2	94.2	61.0	72.0			
Wet Density		137.8	134.2	140.6	141.5	133.2			
Water Content		0.0811	0.1294	0.1046	0.0978	0.0727			
Water Content %		8.11%	12.94%	10.46%	9.78%	7.27%			
Dry Density		127.4	118.8	127.3	128.9	124.1			

As tested in Laboratory

Maximum Dry Density

129.3

Optimum Moisture

9.2%

Corrected for course material

Maximum Dry Density

130.43

Optimum Moisture

9.1%

Report to be sent to:

Moisture - Density Curve

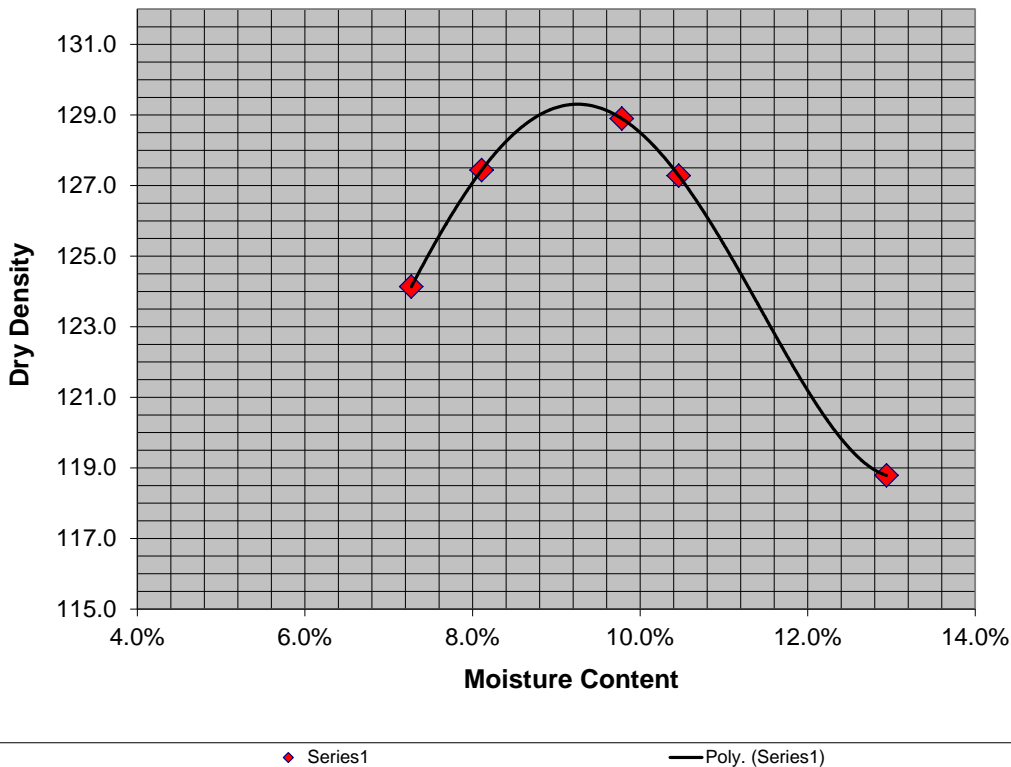


Figure D.3. Compaction test for 2013 WSDOT manufactured soil with 19% Gravel, 51%, Sand, and 30% fines.

APPENDIX E

COMPACTION TEST LABORATORY SUMMARIES FOR SOILS USED FOR 2014 TESTING



Moisture - Density Relationship Report

Field Sample Number		Lab Number		Transmittal Number		Control Number		Federal Aid Number	
Project Number RH-0428		SR	Org. Code	Project Description (or section) K-SAT Testing 2014					
Source of Materials 0.02		Type of Material Extreme Fine End		Sample Weight 7.5lbs	Date Sampled 1/23/15	Date Tested 1/28/15	Tested By JJT01	% Passing 3/4 100%	% Passing #4 98%
T-99 or T-180 T-99	Method B	Mold Size (in) 4"	Specific Gravity 2.67	Comments					
Can Number	1	2	3	4	5	6	7	8	
Specimen Wt. + Mold	5372.0	5446.0	5564.0	5560.0	5572.0				
Wt. of Mold:	3564.0	3564.0	3564.0	3564.0	3564.0				
Vol. Factor:	0.075	0.033200	0.033200	0.033200	0.033200				
Wet Sample + Can	350.0	370.9	478.4	282.7	263.0				
Dry Sample + Can	325.0	340.7	445.5	257.0	237.4				
Wt. Comp. Soil	3.9860	4.1491	4.4092	4.4004	4.4269				
Tare Wt.	82	81.6	201.3	87.8	84.5				
Net Dry Wt.	243.0	259.1	244.2	169.2	152.9				
Wt. of Water	25.0	30.2	32.9	25.7	25.6				
Wet Density	120.1	125.0	132.8	132.5	133.3				
Water Content	0.1029	0.1166	0.1347	0.1519	0.1674				
Water Content %	10.29%	11.66%	13.47%	15.19%	16.74%				
Dry Density	108.9	111.9	117.0	115.1	114.2				

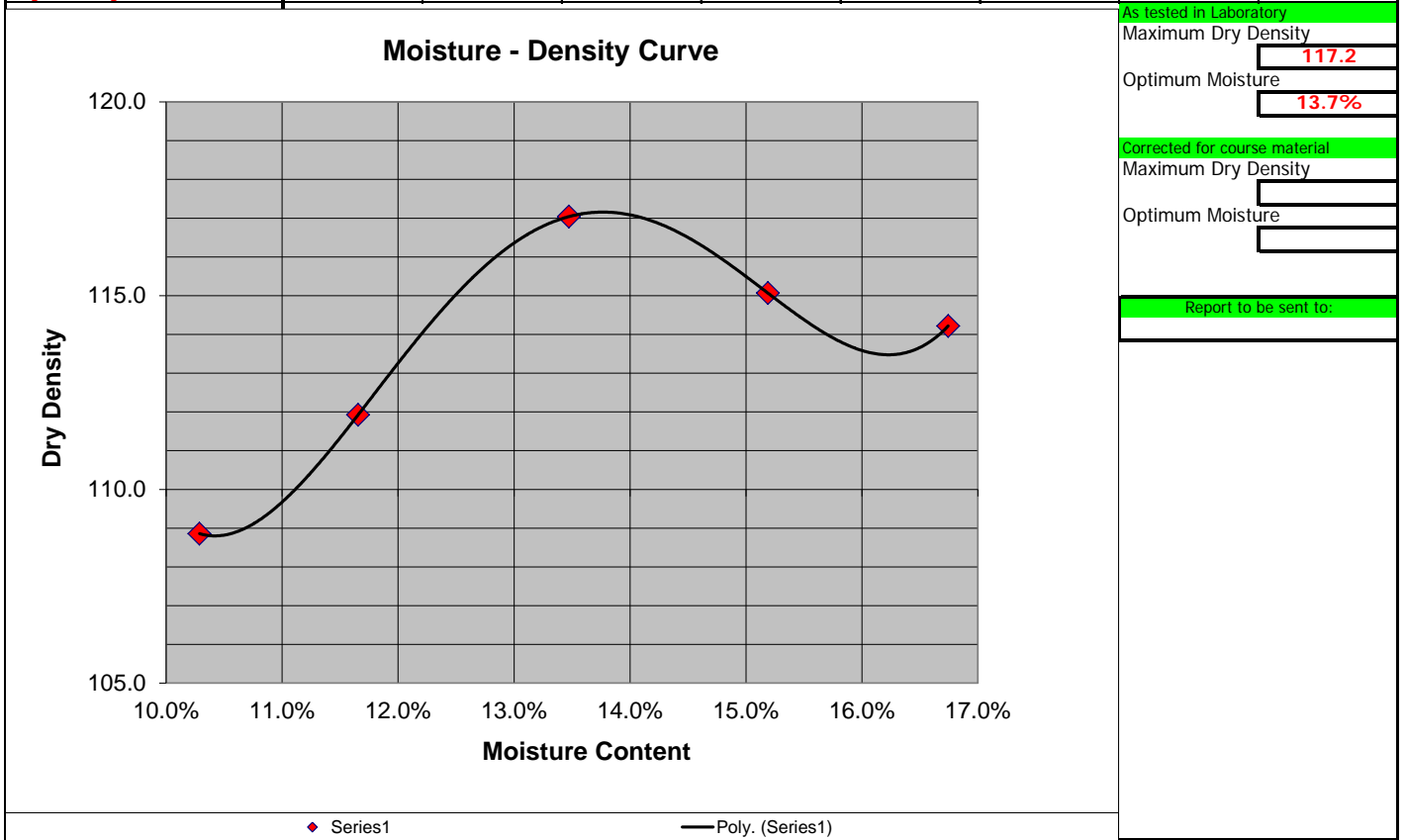


Figure E.1. Compaction test for 2014 WSDOT manufactured soil – extreme fine end with target d₁₀ of 0.02 mm.

Moisture - Density Relationship Report

Field Sample Number		Lab Number		Transmittal Number		Control Number		Federal Aid Number	
Project Number RH-0428		SR	Org. Code	Project Description (or section) K-SAT Testing 2014					
Source of Materials 0.26		Type of Material Fine End Sand		Sample Weight 20 lbs	Date Sampled 1/27/15	Date Tested 1/28/15	Tested By JTT01	% Passing 3/4 100	% Passing #4 98
T-99 or T-180 T-180	Method D	Mold Size (in) 6"	Specific Gravity 2.77	Comments					
Can Number	1	2	3	4	5	6	7	8	
Specimen Wt. + Mold	10040.0	10386.0	10500.0	10500.0	10380.0	10460.0			
Wt. of Mold:	5747.9	5747.9	5747.9	5747.9	5747.9	5747.9			
Vol. Factor:	0.075	0.075000	0.075000	0.075000	0.075000	0.075000			
Wet Sample + Can	634.7	512.7	588.5	524.5	527.2	628.4			
Dry Sample + Can	610.5	490.0	551.1	493.0	495.0	593.5			
Wt. Comp. Soil	9.4624	10.2252	10.4766	10.4766	10.2120	10.3884			
Tare Wt.	216	228	201.6	214.6	234.6	228			
Net Dry Wt.	394.5	262.0	349.5	278.4	260.4	365.5			
Wt. of Water	24.2	22.7	37.4	31.5	32.2	34.9			
Wet Density	126.2	136.3	139.7	139.7	136.2	138.5			
Water Content	0.0613	0.0866	0.1070	0.1131	0.1237	0.0955			
Water Content %	6.13%	8.66%	10.70%	11.31%	12.37%	9.55%			
Dry Density	118.9	125.5	126.2	125.5	121.2	126.4			

As tested in Laboratory	
Maximum Dry Density	126.5
Optimum Moisture	10.2%
Corrected for course material	
Maximum Dry Density	
Optimum Moisture	
Report to be sent to:	

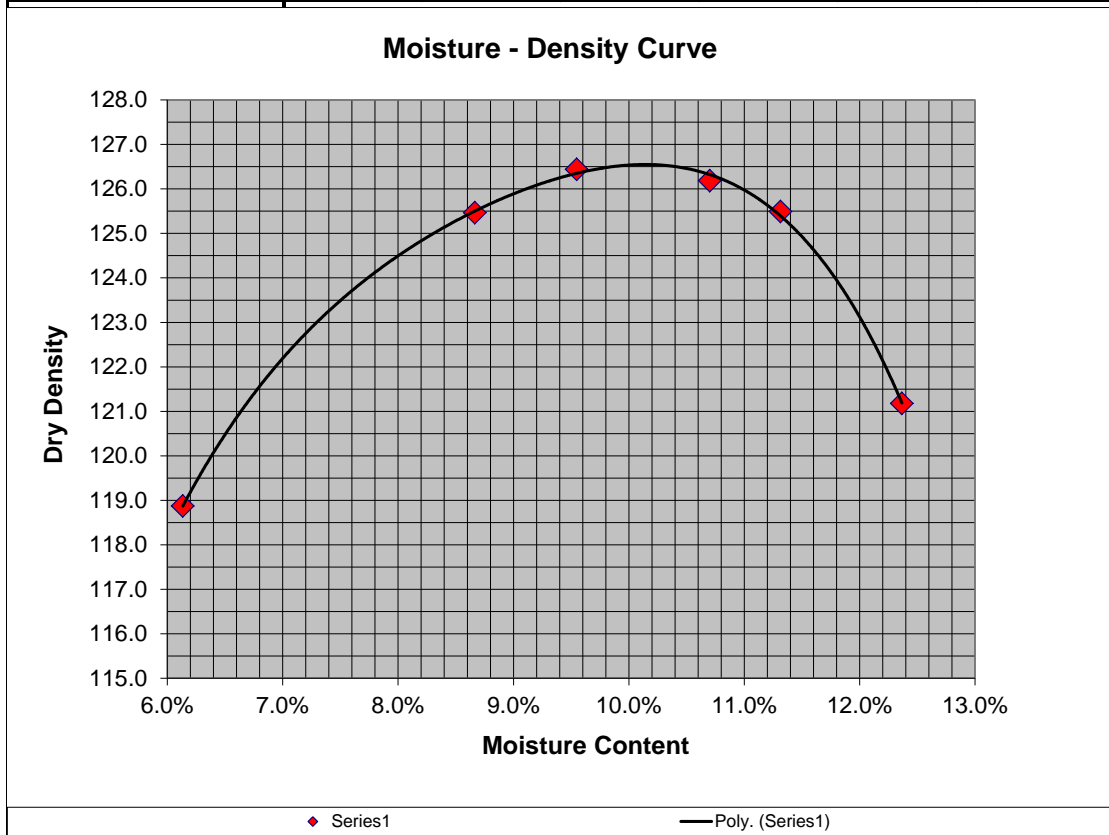


Figure E.2. Compaction test for 2014 WSDOT manufactured soil –fine end sand with target d₁₀ of 0.26 mm.

APPENDIX F

GRAIN SIZE PARAMETERS OF SOILS TESTED

Table F.1. Measured index properties for soils tested in current study, sorted by degree of compaction and then by the d₁₀ size.

Source of Soil	Test Year	Soil Case	Com-pacted?	Permea-meter Type	d ₁₀ (mm)	d ₃₀ (mm)	d ₆₀ (mm)	d ₉₀ (mm)	Fines Fraction, by Weight	Coeff. of Uniformity, C _u	Coeff. of Curvature, C _c
MS-7119, FC-5-14, S-5, SR5 near Chehalis (Shelby tube, undisturbed sample)	2014	Natural alluvial soil (silt)	No	Flexible	0.001	0.004	0.016	0.059	0.938	16.0	1.00
MS-7119, FC-5-14, S-5, SR5 near Chehalis (Shelby tube, undisturbed sample)	2014	Natural alluvial soil (silt)	No	Flexible	0.002	0.009	0.021	0.063	0.938	10.5	1.93
Manufactured by WSDOT	2014	Extreme Fine End - 0.005 mm	No	Flexible	0.005	0.09	0.306	3.0	0.37	61.2	5.29
Manufactured by WSDOT	2014	Extreme Fine End - 0.01 mm	No	Flexible	0.008	0.082	0.393	3.021	0.38	49.1	2.14
Manufactured by WSDOT	2013	Gravel = 4%, Sand = 66%, Silt = 30%	No	Flexible	0.037	0.075	0.176	1.63	0.300	4.76	0.86
Manufactured by WSDOT	2013	Gravel = 19%, Sand = 51%, Silt = 30%	No	Flexible	0.037	0.075	0.846	10.91	0.300	22.9	0.18
Manufactured by WSDOT	2013	Gravel = 45%, Sand = 25%, Silt = 30%	No	Flexible	0.037	0.075	5.79	19.0	0.300	156	0.03
Manufactured by WSDOT	2013	Gravel = 5%, Sand = 75%, Silt = 20%	No	Flexible	0.040 ¹	0.103	0.273	2.31	0.200	6.83	0.97
Manufactured by WSDOT	2013	Gravel = 49%, Sand = 31%, Silt = 20%	No	Flexible	0.040	0.825	6.596	19.48	0.200	165	2.58
Manufactured by WSDOT	2013	Gravel = 23%, Sand = 57%, Silt = 20%	No	Flexible	0.040	0.164	1.311	12.26	0.200	32.8	0.51
Manufactured by WSDOT	2013	Gravel = 55%, Sand = 35%, Silt = 10%	No	Flexible	0.075	2.00	7.989	20.82	0.100	107	6.68
Manufactured by WSDOT	2013	Gravel = 26%, Sand = 64%, Silt = 10%	No	Flexible	0.075	0.267	1.875	13.02	0.100	25.00	0.51
Manufactured by WSDOT	2013	Gravel = 26%, Sand = 64%, Silt = 10%	No	Flexible	0.075	0.267	1.875	13.02	0.100	25.00	0.51
Manufactured by WSDOT	2013	Gravel = 6%, Sand = 84%, Silt = 10%	No	Flexible	0.075	0.128	0.334	2.90	0.100	4.45	0.65
Manufactured by WSDOT	2014	Fine End Sand - 0.12 mm	No	Rigid	0.115	0.34	1.621	9.9	0.015	14.1	0.62
Manufactured by WSDOT	2014	Fine End Sand - 0.12 mm	No	Rigid	0.123	0.387	1.46	10.25	0.013	11.87	0.83
Manufactured by WSDOT	2014	Fine End Sand - 0.17 mm	No	Rigid	0.152	0.485	2.014	9.794	0.006	13.25	0.77
Manufactured by WSDOT	2014	Fine End Sand - 0.17 mm	No	Rigid	0.177	0.517	2.127	9.88	0.010	12.02	0.71
Manufactured by WSDOT	2014	Fine End Sand - 0.23 mm	No	Rigid	0.231	0.83	3.722	11.0	0.010	16.11	0.80
Manufactured by WSDOT	2014	Fine End Sand - 0.26 mm	No	Rigid	0.256	0.404	0.84	1.751	0.080	3.28	0.76
Manufactured by Glacier NW Inc.	2008	Fine End Gravel Borrow	No	Rigid	0.297	0.822	2.355	4.41	0.056	7.93	0.97
Manufactured by Glacier NW Inc.	2008	Fine End Gravel Borrow	No	Rigid	0.299	0.752	2.108	4.30	0.056	7.05	0.90

Source of Soil	Test Year	Soil Case	Com-pacted?	Permea-meter Type	d ₁₀ (mm)	d ₃₀ (mm)	d ₆₀ (mm)	d ₉₀ (mm)	Fines Fraction, by Weight	Coeff. of Uniformity, C _u	Coeff. of Curvature, C _c
Manufactured by Glacier NW Inc.	2008	Fine End Gravel Borrow	No	Rigid	0.325	0.781	2.157	4.32	0.056	6.64	0.87
Pit J149 (Grand Mound)	2008	Select Borrow	No	Rigid	0.358	1.069	3.815	19.0	0.028	10.66	0.84
Manufactured by Glacier NW Inc.	2008	Common Borrow	No	Rigid	0.378	1.084	3.849	19.57	0.038	10.18	0.81
Pit J149 (Grand Mound)	2008	Select Borrow	No	Rigid	0.396	0.903	2.918	15.73	0.028	7.37	0.71
Pit J149 (Grand Mound)	2008	Select Borrow	No	Rigid	0.419	1.35	5.466	20.85	0.028	13.05	0.80
Pit J149 (Grand Mound)	2008	Sandy Glacial Outwash	No	Rigid	0.42	2.178	7.658	19.6	0.007	18.23	1.47
Manufactured by Glacier NW Inc.	2008	Common Borrow	No	Rigid	0.437	1.195	4.28	20.26	0.038	9.79	0.76
Manufactured by Glacier NW Inc.	2008	Common Borrow	No	Rigid	0.432	1.12	3.073	18.04	0.038	7.41	0.90
Pit J149 (Grand Mound)	2008	Sandy Glacial Outwash	No	Rigid	0.561	1.882	6.983	17.88	0.007	12.45	0.90
Pit J149 (Grand Mound)	2008	Sandy Glacial Outwash	No	Rigid	0.6	2.478	8.545	19.6	0.007	14.24	1.20
Manufactured by Glacier NW Inc.	2008	Course Gravel Borrow	No	Rigid	1.029	5.711	12.10	22.07	0.032	11.76	2.62
Manufactured by WSDOT	2014	Coarse Sand and Gravel – 1.2 mm	No	Rigid	1.19	2.64	4.32	12.82	0.003	3.63	1.36
Manufactured by WSDOT	2014	Coarse Sand and Gravel – 1.55 mm	No	Rigid	1.46	3.69	7.846	15.23	0.001	5.06	1.13
Manufactured by WSDOT	2014	Coarse Sand and Gravel – 2.18 mm	No	Rigid	2.19	3.79	7.75	15.2	0.001	3.54	0.85
Manufactured by WSDOT	2014	Coarse Sand and Gravel – 2.9 mm	No	Rigid	2.68	5.61	9.47	15.98	0.00	3.53	1.24
Manufactured by WSDOT	2014	Coarse Sand and Gravel – 3.9 mm	No	Rigid	3.577	6.2	10.02	16.27	0.00	2.80	1.07
Manufactured by Glacier NW Inc.	2008	Course Gravel Borrow	No	Rigid	5.607	8.32	15.04	22.68	0.032	2.68	0.82
Manufactured by Glacier NW Inc.	2008	Course Gravel Borrow	No	Rigid	5.637	8.355	15.07	22.68	0.032	2.67	0.82
Manufactured by WSDOT	2014	Coarse Sand and Gravel – 5.8 mm	No	Rigid	5.713	15.22	40.89	64.45	0.00	7.16	0.99
Manufactured by WSDOT	2014	Extreme Fine End - 0.005 mm	Yes	Flexible	0.003	0.024	0.184	0.78	0.37	61.33	1.04
Manufactured by WSDOT	2014	Extreme Fine End - 0.01 mm	Yes	Flexible	0.009	0.104	0.37	1.928	0.218	41.11	3.25
Manufactured by WSDOT	2013	Gravel = 4%, Sand = 66%, Silt = 30%	Yes	Flexible	0.037	0.075	0.176	1.63	0.30	4.76	0.86
Manufactured by WSDOT	2013	Gravel = 4%, Sand = 66%, Silt = 30%	Yes	Flexible	0.037	0.075	0.176	1.63	0.30	4.76	0.86
Manufactured by WSDOT	2013	Gravel = 19%, Sand = 51%, Silt = 30%,	Yes	Flexible	0.037	0.075	0.846	10.91	0.300	22.86	0.18
Manufactured by WSDOT	2013	Gravel = 19%, Sand = 51%, Silt = 30%	Yes	Flexible	0.037	0.075	0.846	10.91	0.300	22.86	0.18
Manufactured by WSDOT	2013	Gravel = 45%, Sand = 25%, Silt = 30%	Yes	Flexible	0.037	0.075	5.79	19.0	0.300	156.5	0.026
Manufactured by WSDOT	2013	Gravel = 45%, Sand = 25%, Silt = 30%	Yes	Flexible	0.037	0.075	5.79	19.0	0.300	156.8	0.026
Manufactured by WSDOT	2013	Gravel = 5%, Sand = 75%, Silt = 20%	Yes	Flexible	0.040	0.103	0.273	2.31	0.200	6.83	0.97
Manufactured by WSDOT	2013	Gravel = 49%, Sand = 31%, Silt = 20%	Yes	Flexible	0.040 ¹	0.825	6.596	19.48	0.200	164.9	2.58
Manufactured by WSDOT	2013	Gravel = 23%, Sand = 57%, Silt = 20%	Yes	Flexible	0.040	0.164	1.311	12.26	0.200	32.78	0.51

Source of Soil	Test Year	Soil Case	Com-pacted?	Permea-meter Type	d ₁₀ (mm)	d ₃₀ (mm)	d ₆₀ (mm)	d ₉₀ (mm)	Fines Fraction, by Weight	Coeff. of Uniformity, C _u	Coeff. of Curvature, C _c
Manufactured by WSDOT	2013	Gravel = 55%, Sand = 35%, Silt = 10%	Yes	Flexible	0.075	2.00	7.989	20.82	0.100	106.52	6.68
Manufactured by WSDOT	2013	Gravel = 26%, Sand = 64%, Silt = 10%	Yes	Flexible	0.075	0.267	1.875	13.02	0.100	25.00	0.51
Manufactured by WSDOT	2013	Gravel = 26%, Sand = 64%, Silt = 10%	Yes	Flexible	0.075	0.267	1.875	13.02	0.100	25.00	0.51
Manufactured by WSDOT	2013	Gravel = 6%, Sand = 84%, Silt = 10%	Yes	Flexible	0.075	0.128	0.334	2.90	0.100	4.45	0.65
Manufactured by WSDOT	2014	Fine End Sand - 0.12 mm	Yes	Rigid	0.120	0.444	1.6	9.55	0.024	13.33	1.03
Manufactured by WSDOT	2014	Fine End Sand - 0.12 mm	Yes	Flexible	0.128	0.483	1.7	9.82	0.016	13.28	0.81
Manufactured by WSDOT	2014	Fine End Sand - 0.17 mm	Yes	Rigid	0.160	0.509	2.01	9.737	0.022	12.56	0.81
Manufactured by WSDOT	2014	Fine End Sand - 0.17 mm	Yes	Flexible	0.172	0.495	1.99	9.54	0.013	11.57	0.72
Manufactured by WSDOT	2014	Fine End Sand - 0.23 mm	Yes	Rigid	0.207	0.785	3.81	12.75	0.010	18.41	0.78
Manufactured by WSDOT	2014	Fine End Sand - 0.26 mm	Yes	Rigid	0.260	0.39	0.821	1.50	0.015	3.16	0.71
Manufactured by WSDOT	2014	Fine End Sand - 0.26 mm	Yes	Flexible	0.253	0.383	0.804	1.732	0.004	3.18	0.72
Manufactured by WSDOT	2014	Fine End Sand - 0.26 mm	Yes	Rigid	0.261	0.405	0.846	1.781	0.007	3.24	0.74
Manufactured by Glacier NW Inc.	2008	Fine End Gravel Borrow	Yes	Rigid	0.33	1.043	2.768	5.93	0.056	8.39	1.19
Manufactured by Glacier NW Inc.	2008	Fine End Gravel Borrow	Yes	Rigid	0.35	1.086	2.838	6.854	0.056	8.11	1.19
Manufactured by Glacier NW Inc.	2008	Common Borrow	Yes	Rigid	0.365	1.291	3.571	11.77	0.038	9.78	1.28
Manufactured by Glacier NW Inc.	2008	Fine End Gravel Borrow	Yes	Rigid	0.38	1.204	2.955	7.51	0.056	7.78	1.29
Pit J149 (Grand Mound)	2008	Select Borrow	Yes	Rigid	0.429	1.307	4.559	13.32	0.028	10.63	0.87
Manufactured by Glacier NW Inc.	2008	Common Borrow	Yes	Rigid	0.449	1.532	3.939	12.88	0.038	8.77	1.33
Manufactured by Glacier NW Inc.	2008	Common Borrow	Yes	Rigid	0.454	1.655	3.881	12.81	0.038	8.55	1.55
Pit J149 (Grand Mound)	2008	Select Borrow	Yes	Rigid	0.507	2.078	5.358	13.85	0.028	10.57	1.59
Pit J149 (Grand Mound)	2008	Select Borrow	Yes	Rigid	0.551	2.255	5.758	14.83	0.028	10.45	1.60
Pit J149 (Grand Mound)	2008	Sandy Glacial Outwash	Yes	Rigid	0.695	4.017	9.84	19.6	0.007	14.15	2.36
Pit J149 (Grand Mound)	2008	Sandy Glacial Outwash	Yes	Rigid	0.71	4.429	10.38	19.6	0.007	14.62	2.66
Pit J149 (Grand Mound)	2008	Sandy Glacial Outwash	Yes	Rigid	0.722	4.055	9.96	19.6	0.007	13.79	2.29
Manufactured by WSDOT	2014	Coarse Sand/Gravel – 1.2 mm	Yes	Rigid	1.24	2.67	4.39	12.82	0.002	3.54	1.31
Manufactured by WSDOT	2014	Coarse Sand/Gravel – 1.55 mm	Yes	Rigid	1.55	3.71	7.85	15.2	0.003	5.38	1.19
Manufactured by WSDOT	2014	Coarse Sand/Gravel – 2.18 mm	Yes	Rigid	2.18	3.84	7.83	15.24	0.001	3.59	0.86
Manufactured by WSDOT	2014	Coarse Sand/Gravel – 2.9 mm	Yes	Rigid	2.67	5.61	9.5	16.08	0.000	3.56	1.24
Manufactured by WSDOT	2014	Coarse Sand/Gravel – 3.9 mm	Yes	Rigid	3.92	6.31	10.12	16.23	0.000	2.58	1.00
Manufactured by Glacier NW Inc.	2008	Course Gravel Borrow	Yes	Rigid	5.354	7.373	11.91	19.4	0.032	2.23	0.85

Source of Soil	Test Year	Soil Case	Compacted?	Permea-meter Type	d ₁₀ (mm)	d ₃₀ (mm)	d ₆₀ (mm)	d ₉₀ (mm)	Fines Fraction, by Weight	Coeff. of Uniformity, C _u	Coeff. of Curvature, C _c
Manufactured by Glacier NW Inc.	2008	Course Gravel Borrow	Yes	Rigid	5.498	7.63	12.48	20.65	0.032	2.27	0.85
Manufactured by Glacier NW Inc.	2008	Course Gravel Borrow	Yes	Rigid	5.623	8.009	13.61	21.96	0.032	2.42	0.84
Manufactured by WSDOT	2014	Coarse Sand/Gravel – 5.8 mm	Yes	Rigid	6.06	18.46	43.33	65.39	0.000	7.15	1.30
Manufactured by WSDOT	2014	Coarse Sand/Gravel – 8.4 mm	Yes	Rigid	8.63	24.87	45.01	66.01	0.000	5.22	1.59

¹Extrapolated below No. 200 sieve size to obtain value.

APPENDIX G

ADDITIONAL ANALYSES FOR THE DATA AND EQUATION BY MASSMAN (2003)

This appendix provides additional analyses of the Massmann (2003) data and K_{sat} equation (Eq. 1 in main report). The purposes for the appendix include:

- assessment the differences between the converted air permeability data gathered by Massmann (2003) and the saturated hydraulic conductivity data gathered in the current study as well as by Chapuis (2004), and
- statistical assessment of the K_{sat} equation developed by Massmann (2003).

Regarding the air permeability data converted to K_{sat} , since the Massmann (2003) equation does not address compacted soils, the Chapuis Equation (Eq. 6) is used for comparing the air permeability data to the saturated hydraulic conductivity data. This comparison is illustrated in Figure G.1. In this figure, it is obvious that the Massmann (2003) converted air permeability data have values that are an order of magnitude or more higher than the saturated hydraulic conductivity data gathered by Chapuis (2004) and in the present study.

Figure G.2 shows the Massmann (2003) Equation prediction bias as a function of the d_{10} size. A logarithmic scale for the Y-axis is necessary due to the very wide range in the bias values. The Chapuis (2004) data could not be included in this plot due to the lack of adequate soil gradation data. This figure illustrates that with the exception of a narrow range in d_{10} size of 0.1 to 0.6 mm and only for the uncompacted WSDOT test data, all the rest of the data is well out of range regarding prediction accuracy.

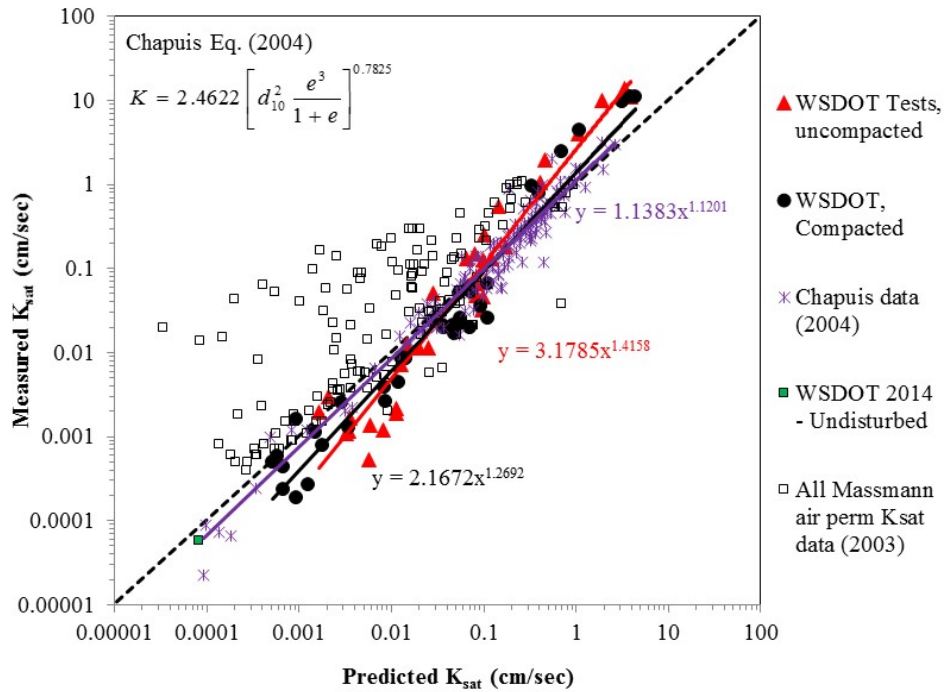


Figure G.1. K_{sat} prediction bias for equation by Chapuis (2004) – all data, including converted air permeability data gathered by Massmann (2003).

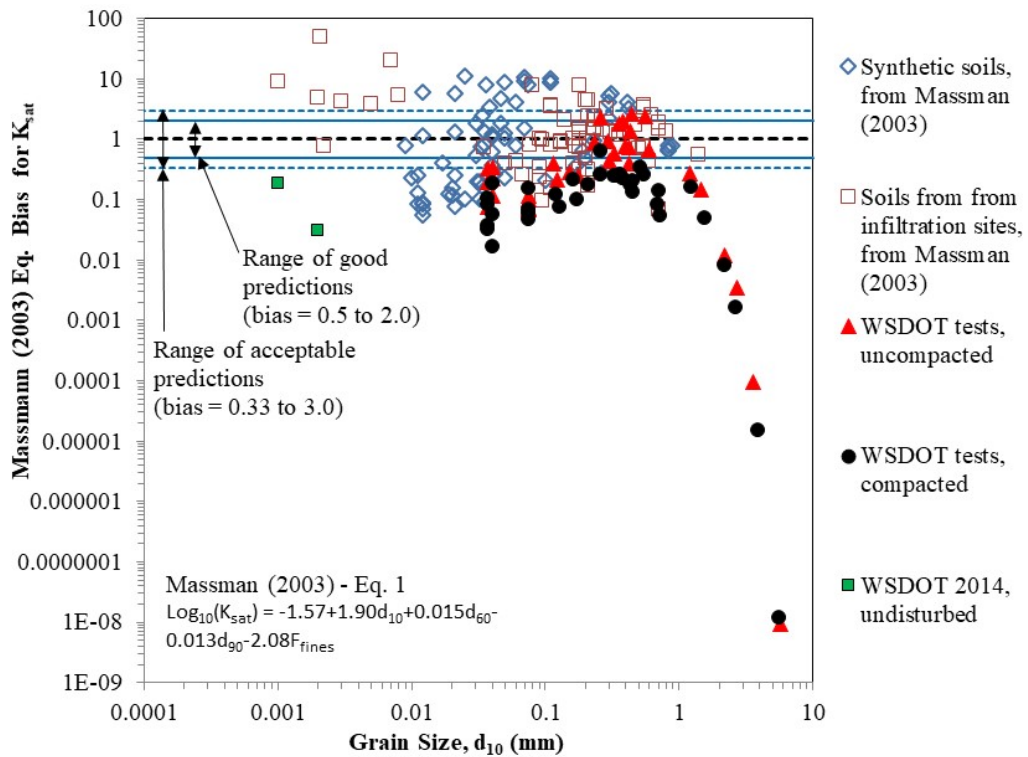


Figure G.2. K_{sat} prediction bias for equation by Massman (2003) – all data except data from Chapuis (2004).

Figure G.3 through G.6 provide CDF plots of various subsets of the WSDOT data for the Massmann (2003) Equation bias. If all of the data are considered, it is obvious that the distribution is not lognormal, and the COV is unreasonably high. If the data corresponding to a d_{10} of greater than 1.0 mm are removed, the distribution is reasonably close to lognormal, but a general lognormal fit of the data is still not very representative of the distribution, requiring as fit to the lower tail. Even when doing this, the statistics are poor, with the mean value significantly less than 1.0 and the COV still too high.

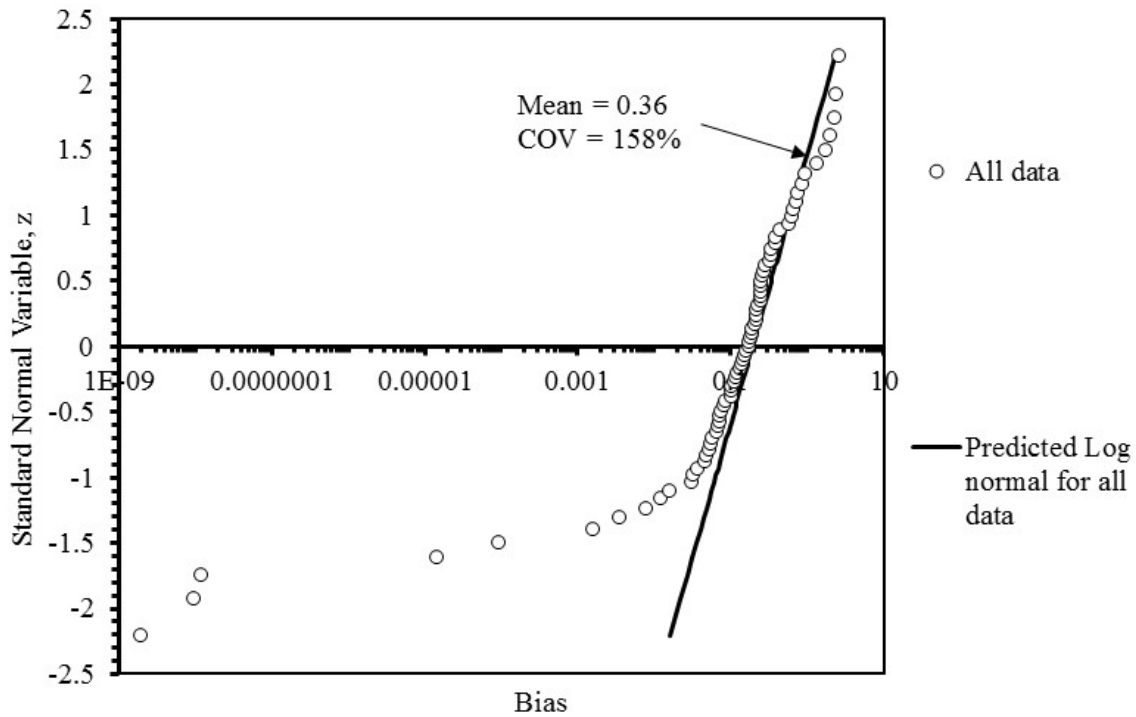


Figure G.3. CDF of K_{sat} prediction bias for equation by Massman (2003) – all WSDOT specimen data.

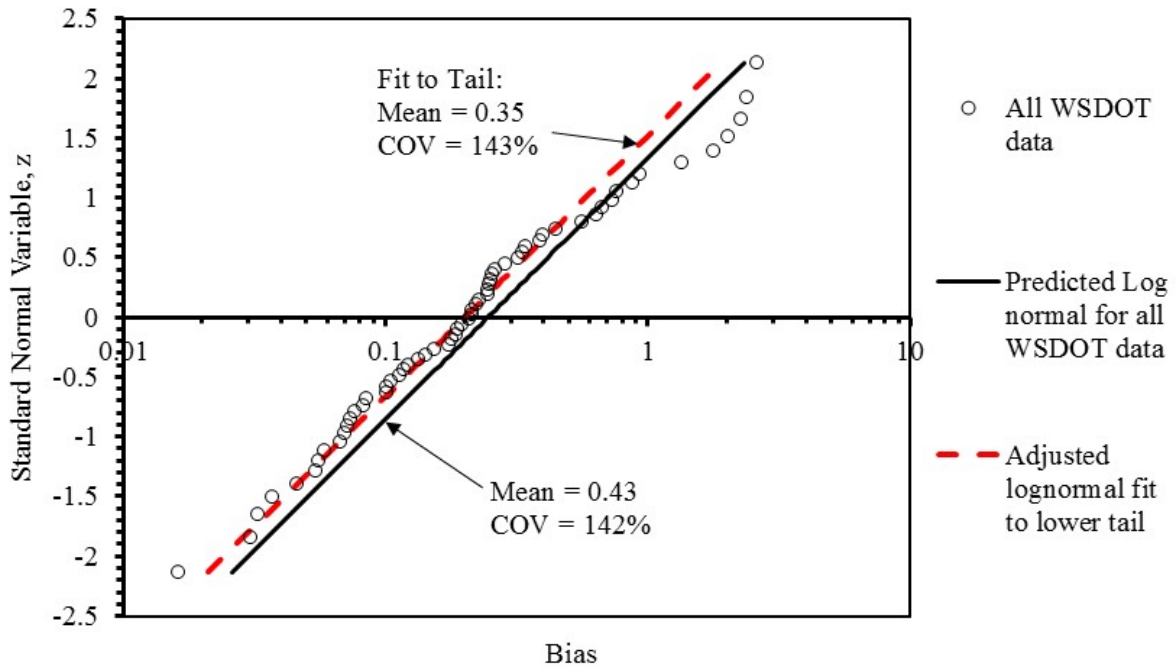


Figure G.4. CDF of K_{sat} prediction bias for equation by Massman (2003) – all WSDOT specimen data with $d_{10} \leq 1.0$ mm.

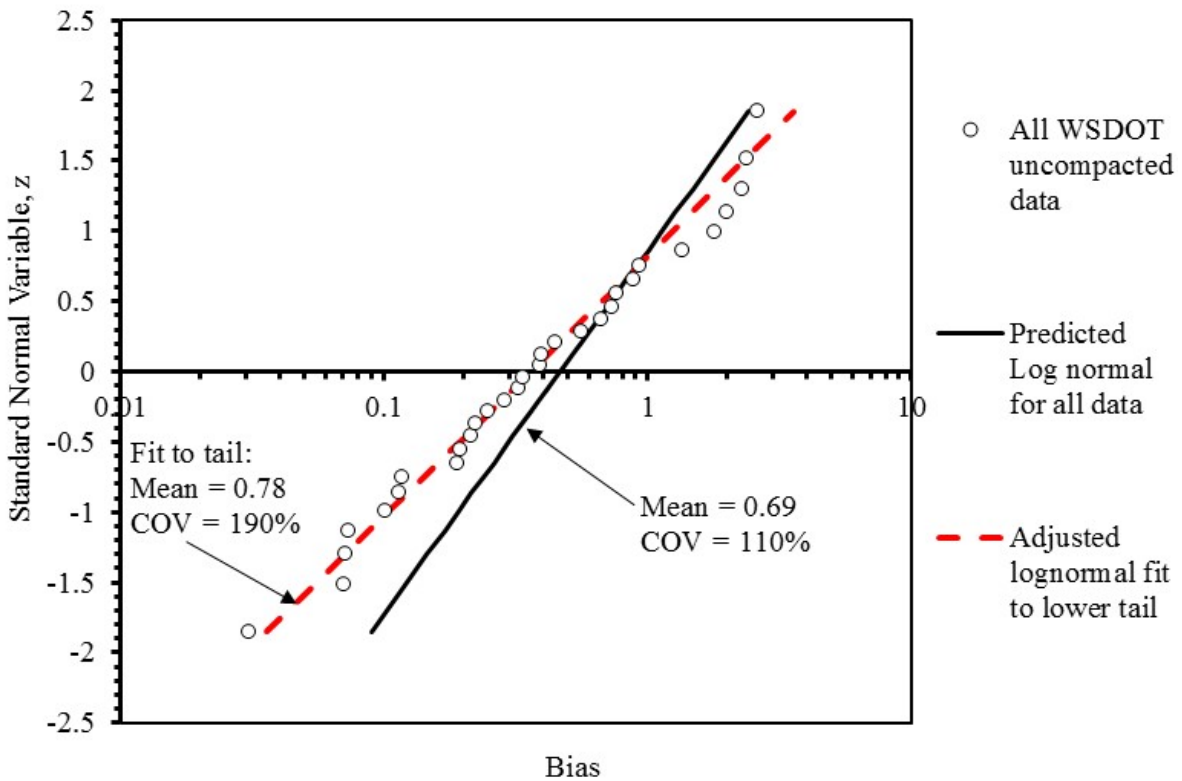


Figure G.5. CDF of K_{sat} prediction bias for equation by Massman (2003) – all uncompacted WSDOT specimen data with $d_{10} \leq 1.0$ mm.

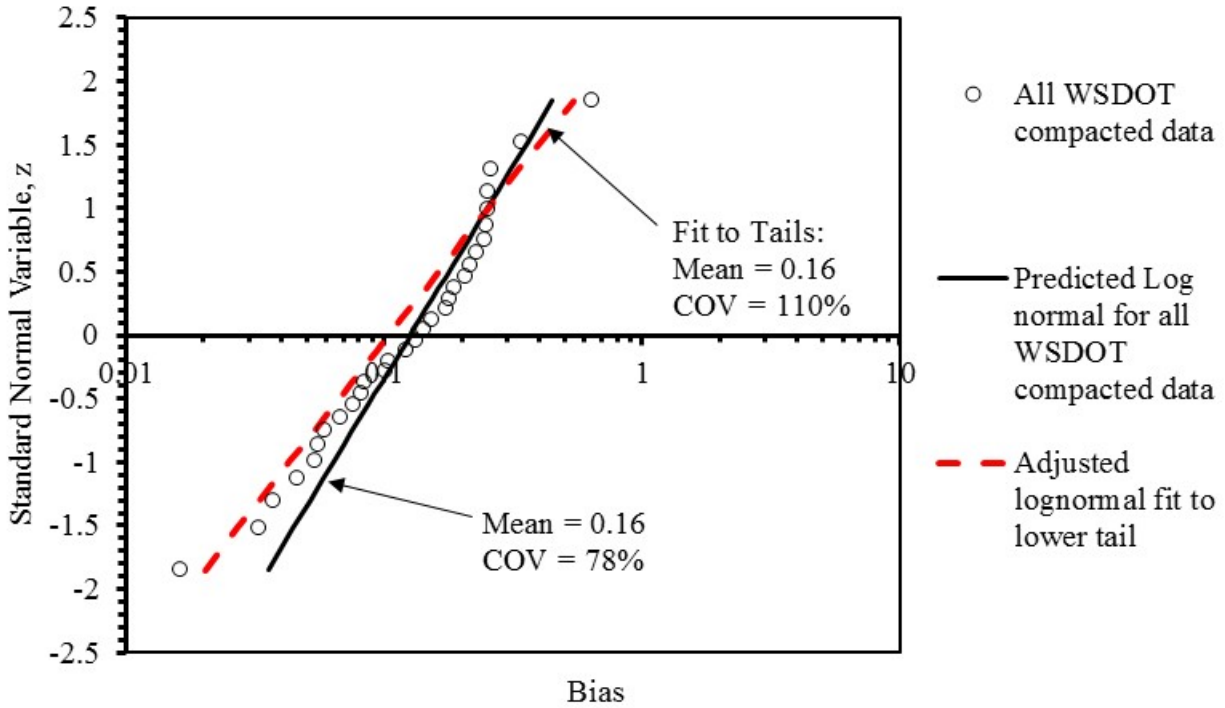


Figure G.6. CDF of K_{sat} prediction bias for equation by Massman (2003) – all compacted WSDOT specimen data with $d_{10} \leq 1.0$ mm.

APPENDIX H

ASSESSMENT OF THE COZENY-CARMEN EQUATION

The Cozeny-Carmen Method, shown in the report as Eq. 5, is repeated below for convenience:

$$K_{sat} = C \frac{g}{\mu_w \rho_w} \left(\frac{e^3}{S_s^2 G_s^2 (1+e)} \right) \quad (\text{H.1 - Eq. 5})$$

where,

C = a constant that depends on the porous space geometry

g = gravitational constant (m/s²)

μ_w = dynamic viscosity of water (Pa-s)

ρ_w = density of water (kg/m³)

G_s = specific gravity of solids

S_s = specific surface of solids (m²/mass of solids in kg)

e = void ratio

Carrier (2003) further developed this equation to apply directly to soil grain size distribution data as follows:

$$K_{sat} = 19,900 \left\{ \frac{100\%}{\left[\sum \left(\frac{f_i}{(d_{li}^{0.404} \times d_{si}^{0.595})} \right) \right]} \right\}^2 \frac{1}{SF^2} \left[\frac{e^3}{1+e} \right] \quad (\text{H.2})$$

where,

f_i = increment of % passing by weight from grain size distribution (%)

d_{li} = grain size at upper end of considered grain size increment (mm)

d_{si} = grain size at lower end of considered grain size increment (mm)

e = void ratio

SF = soil particle shape factor (equals 6.1 to 6.6 for rounded particles, 6.4 to 7.5 for subangular particles, and 7.7 to 8.4 for angular particles)

This form of the equation is used in this appendix. To calculate the values within the summation in Eq. H.2, the following soil grain sizes are used: d_{60} , d_{50} , d_{30} , d_{20} , d_{10} , and d_0 . Due to the need for the full grain size curve to complete this calculation, only the test results from the current study could be used (i.e., there was not enough grain size information to do this for the data gathered in Chapuis 2004).

Figure H.1 shows how well the Cozeny-Carmen Equation predicted the measured K_{sat} values. The void ratio helped to bring the uncompacted and compacted test results together, similar to the original and optimized Slichter, Terzaghi, and Chapuis equations. The overall trend in the data is off the one-to-one correspondence line in the plot. Figure H.2 illustrates the prediction bias trend and overall scatter in the data as a function of the d_{10} size. Figure H.3 shows the statistical distribution of the two data sets that could be evaluated, and the resulting statistics. The distributions are close to lognormal, but the COV values are high.

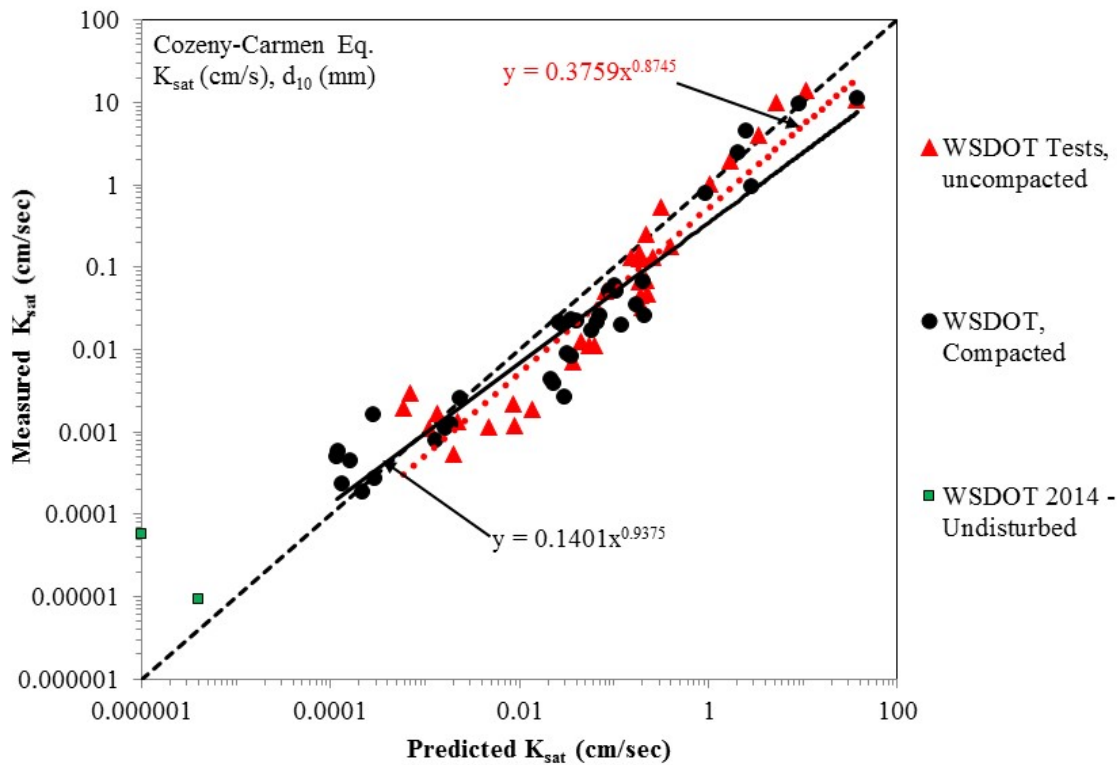


Figure H.1. K_{sat} predictions using the Cozeny-Carmen Equation, with outliers removed.

Attempts to optimize this equation in a similar manner as was done for the other three equations was not successful, in that while an improvement in the overall trend in the data in Figure H.1 could be obtained, the data statistics were not improved.

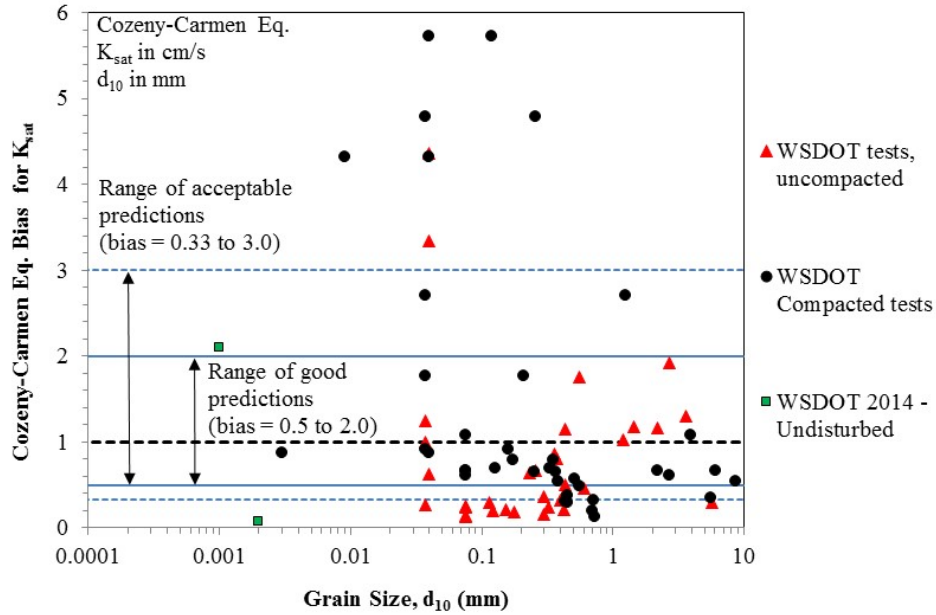


Figure H.2. Method bias as a function of d_{10} size for the Cozeny-Carmen Equation with outliers removed.

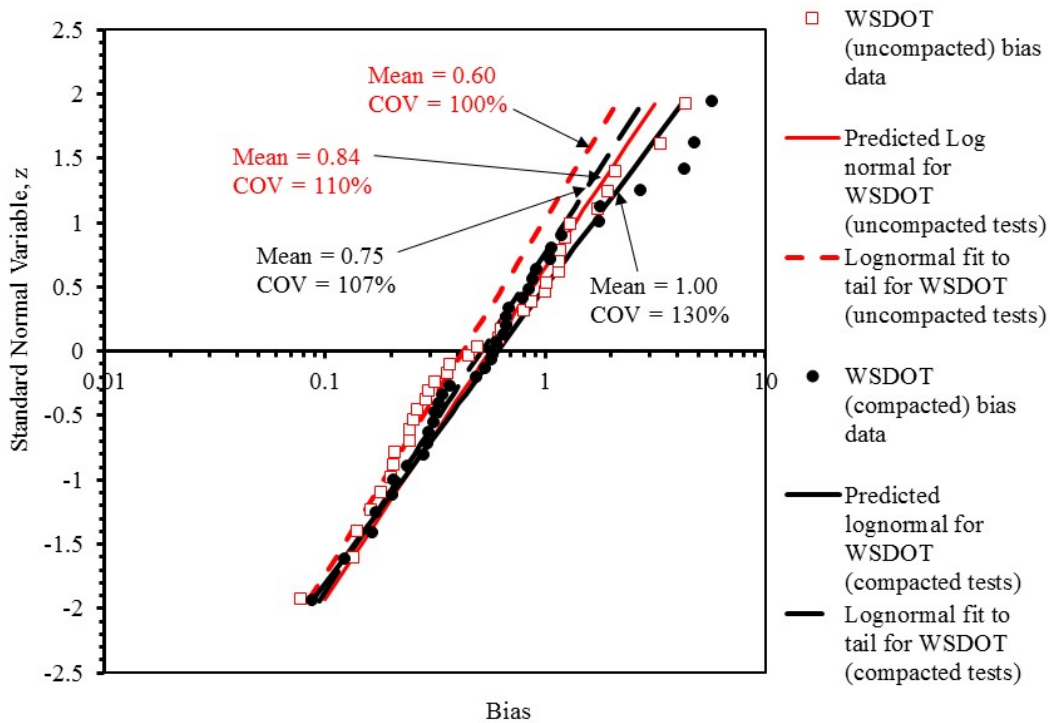


Figure H.3. Bias distributions for datasets analyzed using the Cozeny-Carmen equation with lognormal fit to data and adjusted lognormal data fit to match the lower distribution tail (outliers removed).

APPENDIX I

DEPENDENCE OF THE K_{SAT} PREDICTION BIAS ON THE PREDICTED K_{SAT} VALUE

Figures I-1 through I-3 illustrate the potential dependency between the K_{sat} prediction bias and the predicted K_{sat} values for the optimized Slichter, Terzaghi, and Chapuis equations. In general, there appears to be little, if any, dependency for all three equations, except possibly at the upper end of the K_{sat} range (i.e., predicted K_{sat} greater than approximately 1 to 3 cm/s).

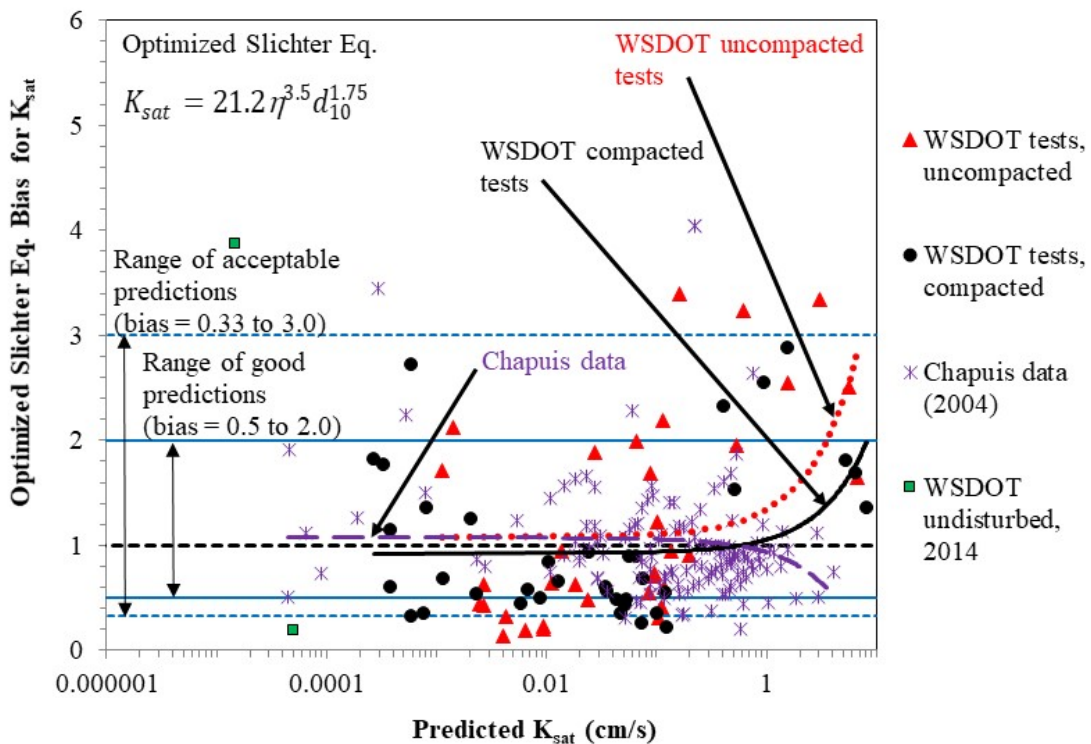


Figure I.1. K_{sat} method bias as a function of predicted K_{sat} value for the Optimized Slichter Equation (outliers removed); linear functions used for regressions.

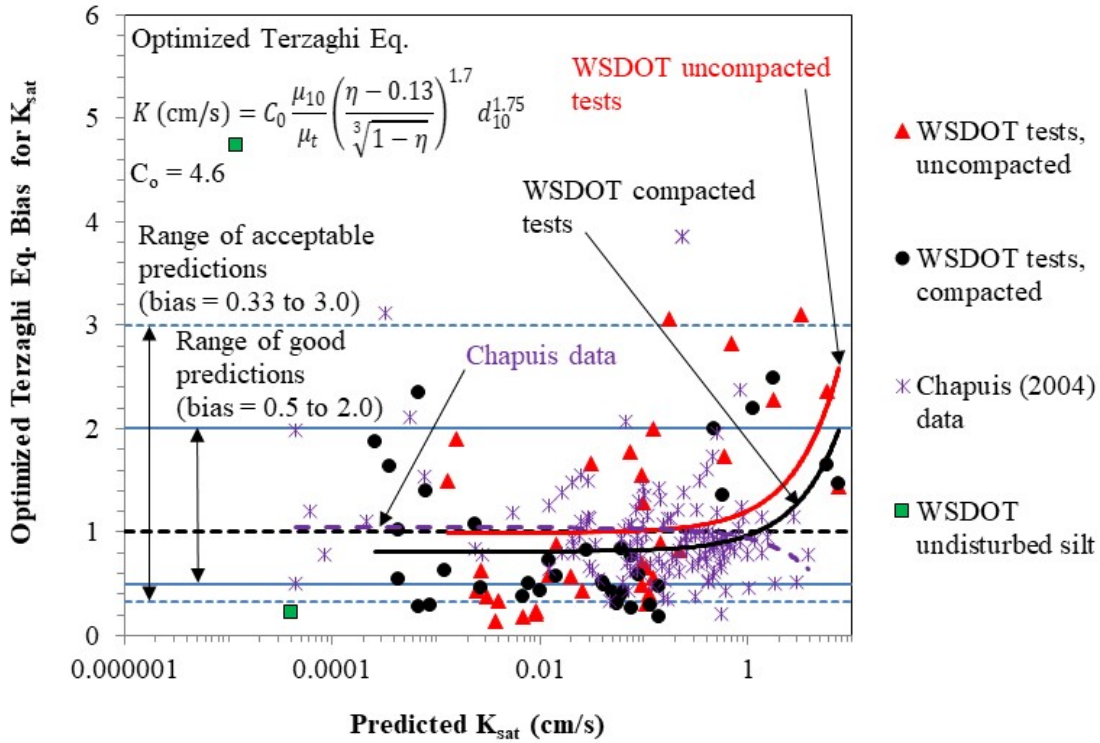


Figure I.2. K_{sat} method bias as a function of predicted K_{sat} value for the Optimized Terzaghi Equation (outliers removed); linear functions used for regressions.

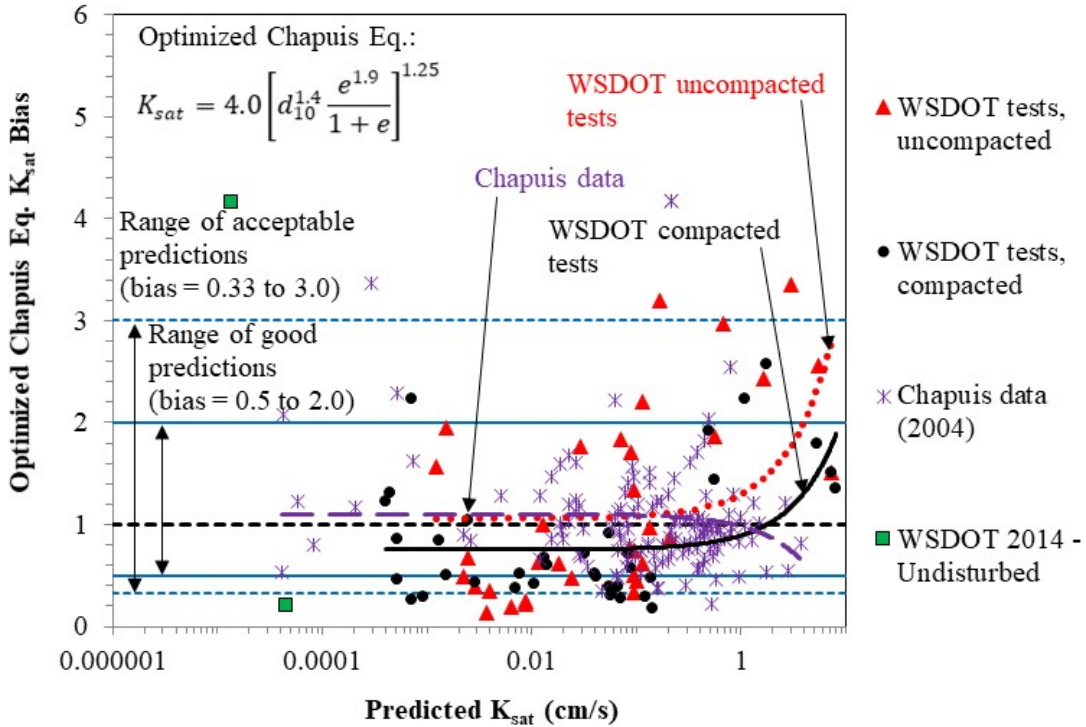


Figure I.3. K_{sat} method bias as a function of predicted K_{sat} value for the Optimized Chapuis Equation (outliers removed); linear functions used for regressions.

Americans with Disabilities Act (ADA) Information

This material can be made available in an alternate format by emailing the Office of Equal Opportunity at wsdotada@wsdot.wa.gov or by calling toll free, 855-362-4ADA (4232). Persons who are deaf or hard of hearing may make a request by calling the Washington State Relay at 711.

Title VI Notice to Public

It is the Washington State Department of Transportation's policy to assure that no person shall, on the grounds of race, color, national origin or sex, as provided by Title VI of the Civil Rights Act of 1964, be excluded from participation in, be denied the benefits of, or be otherwise discriminated against under any of its federally funded programs and activities. Any person who believes his/her Title VI protection has been violated, may file a complaint with WSDOT's Office of Equal Opportunity. For additional information regarding Title VI complaint procedures and/or information regarding our non-discrimination obligations, please contact OEO's Title VI Coordinator at 360-705-7082.

Americans with Disabilities Act (ADA) Information:

This material can be made available in an alternate format by emailing the Office of Equal Opportunity at wsdotada@wsdot.wa.gov or by calling toll free, 855-362-4ADA(4232). Persons who are deaf or hard of hearing may make a request by calling the Washington State Relay at 711.

Title VI Statement to Public:

It is the Washington State Department of Transportation's (WSDOT) policy to assure that no person shall, on the grounds of race, color, national origin or sex, as provided by Title VI of the Civil Rights Act of 1964, be excluded from participation in, be denied the benefits of, or be otherwise discriminated against under any of its federally funded programs and activities. Any person who believes his/her Title VI protection has been violated, may file a complaint with WSDOT's Office of Equal Opportunity (OEO). For additional information regarding Title VI complaint procedures and/or information regarding our non-discrimination obligations, please contact OEO's Title VI Coordinator at (360) 705-7082.
